



**TEHNIČKI GLASNIK - TECHNICAL JOURNAL**

Scientific-professional journal of University North

Volume 17

Varaždin, December 2023

Issue 4

Pages 479-635

**Editorial Office:**

Sveučilište Sjever / University North – Tehnički glasnik / Technical journal  
 Sveučilišni centar Varaždin / University Center Varaždin  
 Jurja Križanića 31b, 42000 Varaždin, Croatia  
 Tel. ++385 42 493 338, Fax. ++385 42 493 336  
 E-mail: tehnickiglasnik@unin.hr  
<https://tehnickiglasnik.unin.hr>  
<https://www.unin.hr/djelatnost/izdavastvo/tehnicki-glasnik/>  
<https://hrcak.srce.hr/tehnickiglasnik>

**Founder and Publisher:**

Sveučilište Sjever / University North

**Council of Journal:**

Marin MILKOVIĆ, Chairman; Anica HUNJET, Member; Goran KOZINA, Member; Mario TOMIŠA, Member;  
 Vlado TROPŠA, Member; Damir VUSIĆ, Member; Milan KLJAJIN, Member; Anatolii KOVROV, Member; Petar MIŠEVIĆ, Member

**Editorial Board:****Domestic Members:**

Chairman Damir VUSIĆ (1), Milan KLJAJIN (1), Marin MILKOVIĆ (1), Krešimir BUNTAK (1), Anica HUNJET (1), Živko KONDIĆ (1), Goran KOZINA (1), Ljudevit KRPAN (1), Krunoslav HAJDEK (1), Marko STOJČIĆ (1), Božo SOLDO (1), Mario TOMIŠA (1), Vlado TROPŠA (1), Vinko VIŠNJIĆ (1), Sanja ŠOLIĆ (1), Dean VALDEC (1), Predrag PUTNIK (1), Petar MIŠEVIĆ (1), Duško PAVLETIĆ (5), Branimir PAVKOVIĆ (5), Mile MATIJEVIĆ (3), Damir MODRIĆ (3), Nikola MRVAC (3), Klaudio PAP (3), Ivana ŽILJAK STANIMIROVIĆ (3), Krešimir GRILEC (6), Biserka RUNJE (6), Sara HAVRLIŠAN (2), Dražan KOZAK (2), Roberto LUJIĆ (2), Leon MAGLIĆ (2), Ivan SAMARDŽIĆ (2), Antun STOIC (2), Katica ŠIMUNOVIĆ (2), Goran ŠIMUNOVIĆ (2), Ladislav LAZIĆ (7), Ante ČIKIĆ (1), Darko DUKIĆ (9), Gordana DUKIĆ (10), Srđan MEDIĆ (11), Sanja KALAMBURA (12), Marko DUNDER (13), Zlata DOLAČEK-ALDUK (4), Dina STOBER (4)

**International Members:**

Boris TOVORNIK (14), Milan KUHTA (15), Nenad INJAC (16), Marin PETROVIĆ (18), Salim IBRAHIMEFENDIĆ (19), Zoran LOVREKOVIĆ (20), Igor BUDAK (21), Darko BAJIĆ (22), Tomáš HANÁK (23), Evgenij KLIMENKO (24), Oleg POPOV (24), Ivo ČOLAK (25), Katarina MONKOVA (26), Berenika HAUSNEROVA (8), Nenad GUBELJAK (27), Stefaniya KLARIC (28), Bertrand MARESCHAL (29), Sachin R. SAKHARE (30), Suresh LIMKAR (31), Mandeep KAUR (32), Aleksandar SEDMAK (33), Han-Chieh CHAO (34), Sergej HLOCH (26), Grzegorz M. KRÓLCZYK (35), Djordje VUKELIC (21), Stanislaw LEGUTKO (17), Valentin POPOV (36), Dragan MARINKOVIC (36), Hamid M. SEDIGHI (37), Cristiano FRAGASSA (38), Dragan PAMUČAR (39)

**Editor-in-Chief:**

Milan KLJAJIN

**Technical Editor:**

Goran KOZINA

**Graphics Editor:**

Snježana IVANČIĆ VALENKO

**IT support:**

Tomislav HORVAT

**Print:**

Centar za digitalno nakladništvo, Sveučilište Sjever

**All manuscripts published in journal have been reviewed.****Manuscripts are not returned.****The journal is free of charge and four issues per year are published**

(In March, June, September and December)

**Circulation:** 100 copies**Journal is indexed and abstracted in:**

Web of Science Core Collection (Emerging Sources Citation Index - ESCI), Scopus, EBSCOhost Academic Search Complete, EBSCOhost – One Belt, One Road Reference Source Product, ERIH PLUS, CITEFACTOR – Academic Scientific Journals, DOAJ – Directory of Open Access Journals, Hrcak – Portal znanstvenih časopisa RH

**Registration of journal:**The journal "Tehnički glasnik" is listed in the HGK Register on the issuance and distribution of printed editions on the 18<sup>th</sup> October 2007 under number 825.**Preparation ended:**

October 2, 2023

**Published (online):**

October 10, 2023

**Published (print):**

December 15, 2023

**Legend:**

(1) University North, (2) University of Slavonki Brod, (3) Faculty of Graphic Arts Zagreb, (4) Faculty of Civil Engineering Osijek, (5) Faculty of Engineering Rijeka, (6) Faculty of Mechanical Engineering and Naval Architecture Zagreb, (7) Faculty of Metallurgy Sisak, (8) Tomas Bata University in Zlin, (9) Department of Physics of the University of Josip Juraj Strossmayer in Osijek, (10) Faculty of Humanities and Social Sciences Osijek, (11) Karlovac University of Applied Sciences, (12) University of Applied Sciences Velika Gorica, (13) Department of Polytechnics - Faculty of Humanities and Social Sciences Rijeka, (14) Faculty of Electrical Engineering and Computer Science - University of Maribor, (15) Faculty of Civil Engineering - University of Maribor, (16) University College of Teacher Education of Christian Churches Vienna/Krems, (17) Faculty of Mechanical Engineering - Poznan University of Technology (Poland), (18) Mechanical Engineering Faculty Sarajevo, (19) University of Travnik - Faculty of Technical Studies, (20) Higher Education Technical School of Professional Studies in Novi Sad, (21) University of Novi Sad - Faculty of Technical Sciences, (22) Faculty of Mechanical Engineering - University of Montenegro, (23) Brno University of Technology, (24) Odessa State Academy of Civil Engineering and Architecture, (25) Faculty of Civil Engineering - University of Mostar, (26) Faculty of Manufacturing Technologies with the seat in Prešov - Technical University in Košice, (27) Faculty of Mechanical Engineering - University of Maribor, (28) College of Engineering, IT & Environment - Charles Darwin University, (29) Université Libre de Bruxelles, (30) Vishwakarma Institute of Information Technology (Pune, India), (31) AISSMS Institute of Information Technology (Pune, India), (32) Permtech Research Solutions (India), (33) University of Belgrade, (34) National Dong Hwa University - Taiwan, (35) Faculty of Mechanical Engineering - Opole University of Technology (Poland), (36) TU Berlin - Germany, (37) Shahid Chamran University of Ahvaz - Iran, (38) University of Bologna - Italy, (39) University of Defence in Belgrade - Military Academy - Serbia

<b>CONTENT</b>	<b>I</b>
Josip Nad*, Dunja Srpak, Antonija Šumiga, Branko Tomičić <b>Applying the ERP Business Software in the Analysis of Electric Drives Steady State</b>	479
Tanja Tomić*, Lidija Tepeš Golubić, Jana Žiljak Gršić, Matija Bušić <b>Application of Response Surface Methodology in the Analysis of Weldability Test Results on X80 Steel</b>	486
Mustapha Dlimi <b>Touchard Series for Solving Volterra Integral Equations Form of the Lane-Emdan Equations</b>	493
Maosheng Zheng*, Jie Yu <b>A Novel Method for Solving Multi-objective Shortest Path Problem in Respect of Probability Theory</b>	497
Abdelhakim Walid Makhoulfi*, Samira Louafi <b>Parametric Study for Optimising Building Form and Height: An Approach toward Net Zero Energy &amp; Carbon in Buildings</b>	501
Maryam Sabaroo, Abazar Mehrali* <b>Designing a Desirable House with consideration of Strengthening the Sense of Peace of the Residents: A Case of District 6 of Tehran</b>	508
Erfan Mehregan*, Somayeh Sanaei, Mohsen Manna, Hamed Bozorgkhoo, Shahin Heidari <b>The Role of SCM practices in Competitive Advantage and Firm Performance: A Mediating Role of Supply Chain Innovation and TQM</b>	516
Jeon-Ho Lee, Woo-Jun Hwang, Chang-Woo Lee, Sang-Soo Lee* <b>Properties of Magnesia Composites According to Replacement Ratio of Perlite</b>	524
Hyekwon Kim, Yejin Jeong, Sangwon Seo, Jongyoung Youn, Donghoon Lee* <b>A Study on Radiant Heat Application to the Curing Process for Improvement of Free-form Concrete Panel Productivity</b>	529
Yong-Gu Kim, Chang-Woo Lee, Woo-Jun Hwang, Sang-Soo Lee* <b>Properties of CLC According to Replacement Ratio of Cao-CSA Expansive Additive</b>	535
Suzana Pasanec Preprotić*, Gorana Petković, Mario Bracić, Ana Marošević Dolovski <b>Comprehensive Principles for Enhancing the Adhesive Bound Book Performances</b>	543
Mirko Karakašić*, Ilija Svalina, Daniel Novoselović, Iva Samardžić, Hrvoje Glavaš, Radomir Đokić <b>Application of the Functional Flow Diagrams in a Design of the Level Crossing Hydraulic Barrier Drive</b>	554
Nikolina Stanić Loknar*, Tajana Koren Ivančević, Mateo Bekavac, Snježana Ivančić Valenko <b>Technologies for Web Animations and their Positive and Negative Sides Regarding Web Page Metrics</b>	566
Dorja Hatlak, Andrija Bernik*, Igor Tomičić <b>Influence of Video Games on Cognitive Abilities and Intelligence</b>	572
İsmail Akgül*, Ömer Çağrı Yavuz, Uğur Yavuz <b>Deep Learning Based Models for Detection of Diabetic Retinopathy</b>	581
Nino Krznar, Petar Piljek*, Zdenka Keran <b>Multicopter UAV Design and Development – Case Study</b>	588
Yong-woo Kim, Sangchul Kim* <b>Allocating Safety Cost using in Construction Site</b>	594
Seng-Phil Hong, Debnath Bhattacharyya* <b>A Study on the Improvement of Security Image Analysis Capability Using Artificial Intelligence</b>	598
Marinko Stojkov, Goran Delija, Ivan Đuračić*, Tomislav Alinjak <b>Air Quality Supervision System using the IoT Platform</b>	605
Anica Hunjet*, Marin Milković, Nikolina Topolko Špoljar <b>Rewarding Scientific Productivity of University North Employees</b>	614
Emre Deniz Yalçın*, Aykut Çanakçı <b>Investigation of Tribological Applications and Mechanical Properties of Zinc-Aluminium (ZA40)/Multi-Wall Carbon Nanotube (MWCNT) Composite Alloys</b>	620
Domagoj Nakić*, Ines Belalov Dovečer, Dražen Vouk, Bojan Đurin <b>Analysis of Sewage Sludge Disposal Routes – Varazdin and Medimurje County</b>	628
<b>INSTRUCTIONS FOR AUTHORS</b>	<b>III</b>

# ICCAML2024

## VIRTUAL MODE

### 1ST INTERNATIONAL CONFERENCE ON CURRENT ADVANCEMENTS IN MACHINE LEARNING

Symbiosis Institute of Computer Studies  
and Research, Symbiosis International  
(Deemed University), Pune India

## 28 & 29 FEB 2024

- MODERNIZATION IN MACHINE LEARNING
- MACHINE LEARNING FOR DATA ANALYTICS
- MACHINE LEARNING FOR AUTOMATION

## SPRINGER (CCIS)

**Web URL:**

<https://iccaml2024.sicsr.ac.in>

**Email ID:**

[iccaml2024@sicsr.ac.in](mailto:iccaml2024@sicsr.ac.in)



वसुधैव कुटुम्बकम्

**SYMBIOSIS**  
**INSTITUTE OF COMPUTER STUDIES  
AND RESEARCH, PUNE**

[A CONSTITUENT OF  
SYMBIOSIS INTERNATIONAL (DEEMED UNIVERSITY), PUNE]

# Applying the ERP Business Software in the Analysis of Electric Drives Steady State

Josip Nad\*, Dunja Srpak, Antonija Šumiga, Branko Tomičić

**Abstract:** The paper presents the possibility of using ERP business software for the purpose of analyzing steady states of electric drives. A centrifugal pump is used as an example of active load. After reviewing previous research and presenting the basic principles of using the ERP model, the analysis of the operation of the centrifugal pump and the processing of the results of the propulsion measurements were approached. Two flow control options are considered and both methods are compared regarding energy consumption. After that, the method of calculating energy saving using the ERP model is shown. The calculation results provide data on different costs depending on the type of flow control. Since an induction motor with a frequency converter is provided for flow control by changing the speed, the final step is rough profitability estimate of the investment in frequency converter, which was also done directly in the ERP model.

**Keywords:** electric drives; energy saving; ERP model; induction machine

## 1 INTRODUCTION

Intense changes at the political and business levels require managers to make faster decisions. A particularly important area is energy saving, which has been a very current topic of research in all branches of industry for a long time.

Previous research on the possible use of Enterprise Resource Planning systems (ERP) for technical calculations and analysis has shown that the ERP system is able to give the desired results for the managerial level of consideration of technical problems. The authors in [1] especially point out that process is principally quicker the lesser the number of involved people and if the main protagonists use the corresponding tool familiar to them. In doing so, managers are recognized as natural ERP users, and as people who cannot afford to search for data on several different systems, as well as excessive dependence on assistants who should do the necessary research instead and prepare all the data for their managers. Nowadays, managers are looking for all the necessary information in one place. This thinking is confirmed by more and more research, especially [2], which states that top managers understand that they must not wait for perfect information - after receiving 65% information security, they make a decision.

The ERP model used in this paper is based on the principles presented in the literature [3-5]. It is a standard SAP ERP solution (SAP stands for Systems, Applications and Products in Data Processing), where with the functionality of Production Planning (PP module), Controlling (CO module) and Variant Configuration (LO-VC module) it is possible to achieve a complete simulation picture of the production part of the business with the necessary elements of technical calculations [6].

The basis for this paper is research presented in [7-9]. In [7], SAP ERP was used for the analysis of induction machines. It has been shown that by setting the so-called analytical ERP model, all parameters of the equivalent circuit can be reached, as well as the static torque characteristic, both based on the measurement results.

The paper [8] presents the idea of using the ERP model in order to improve the decision - making process in the production of power transformers. The principles of calculating the basic dimensions of transformers are shown, and it is pointed out that the obtained results can make three basic business estimates necessary for the decision to enter a new project: estimating the availability of production capacity, estimating the availability of production materials and estimating production costs.

In [9] it is shown in detail how the ERP model can be used to calculate the basic dimensions of an electrical machine based on the initial requirements, using standard principles of variant configuration.

The efficiency of electric drives is the topic of the review [10], because of great energy consumption for electric drives in the world. It presents the state of art in electrical machine modeling and analysis using electrical machine electrical equivalent circuit models, to define the high-frequency behavior of the machine. For the analysis of machine operation, the finite element method (FEM) method is often used as in [11], or the traditional analytical method as in [12], while a hybrid calculation method of radial electromagnetic force based on FEM and analytical method is proposed in [13]. A new analytic-numeric method for permanent magnet synchronous machines (PMSM) is presented in [14] and validated by experimental results. The importance of accurate modeling of the machine in the development phase of an electrical drive system, as well as in the designing of the electrical machines is highlighted in [15, 16]. An extended synchronous machine model that includes dynamic iron losses and their temperature dependence is presented in [15], while a design approach of the Bearingless Induction Motor is proposed in [16].

This paper deals with the possibility of using ERP models for the purpose of analyzing steady states of variable frequency electric drives. It shows the new and different method for calculation of energy saving and calculation of repayment time on investment in electric drives modernization or improvement. Both calculations are done by applying the ERP model.

After this introduction and the overview of related researches, the second chapter is providing the information about basic methods applied in this research. Third chapter describes the calculation of energy savings using the ERP model, and one of the possible ways to calculate the repayment time of the investment in a variable frequency electric drive. Conclusions are given at the end of paper.

## 2 CENTRIFUGAL PUMPS AND ENERGY CONSUMPTION

Fig. 1 shows the guiding idea of the whole research, obtained by comparing the dynamic (blue line) and static (red line) characteristics of the induction machine. Namely, just as the study of static characteristics is sufficient for a large part of the analysis of the behavior and driving capabilities of electrical machines, in the same way it is sufficient for managerial decision making to have the results of rough technical calculations available. In a time of unexpected and highly intense changes, decision making needs to be simplified and accelerated as much as possible.

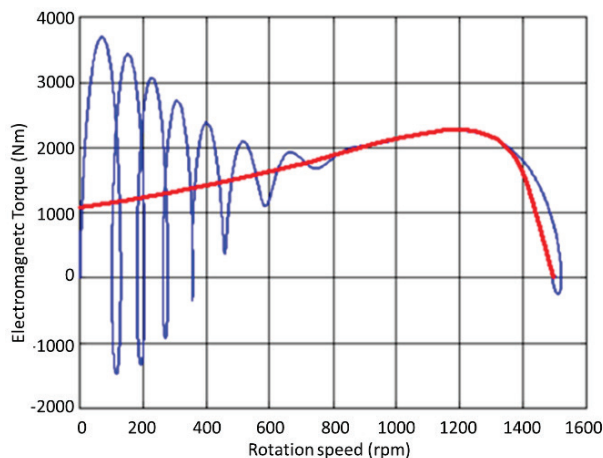


Figure 1 Static and dynamic characteristics of an induction motor [6]

Whether it is about companies that manufacture electrical machinery or companies that use electrical machinery, using a simplified method of analysis of machine operation, calculation of parameters and calculation of dimensions can achieve good enough results needed for managerial decision making.

### 2.1 Description of ERP Software Customization for Application in Technical Analyzes and Calculations

When customizing SAP ERP software for possible applications for technical analysis and calculations, two options were used. One consisted of the use of a LO-VC module and the other of a PP module. In both options, only the adjustment of system parameters was made, without additional programming.

Thus, for example, the standard SAP functionality of the Variant Configuration with additionally created dependencies and formulas was used to calculate the parameters of the equivalent circuit of an induction machine. The second method was then used to obtain the torque

characteristic as a function of speed. The equivalent circuit parameters in SAP are defined as constants in the PP work center formula. Because of high level integration of PP work centers and CO cost centers (including CO activity types and CO cost elements), it was possible to use the standard form of CO cost calculation formulas to calculate basic technical parameters: slip, torque and current.

The torque characteristic is obtained as a result of the Kloss equation, which shows the dependence of the speed of rotation, i.e. slip, and on the torque developed by the induction motor:

$$\frac{T}{T_b} = \frac{2}{\frac{s}{s_b} + \frac{s_b}{s}} \quad (1)$$

Labels of variables used in an Eq. (1):  $T$  – torque,  $T_b$  – breakdown (maximum) torque,  $s$  – slip,  $s_b$  – breakdown slip.

In the ERP software, the method of simulating the functionality of confirming production orders, which is an integral part of the PP module, was used to obtain the steady state characteristic of a specific induction machine. All calculated dots can then be linked by additional programming in ABAP (Advanced Business Application Programming) to obtain a graphical representation (Fig. 2).

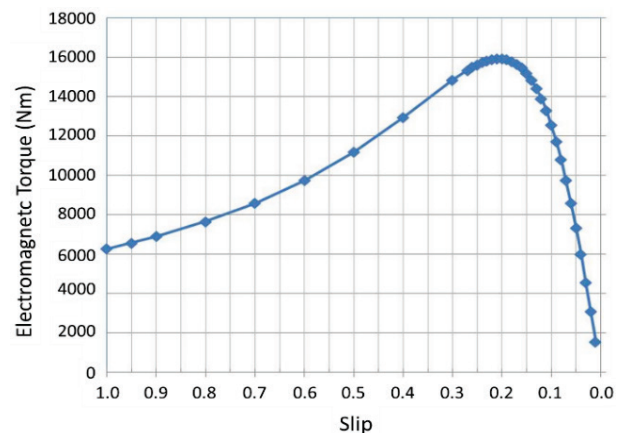


Figure 2 Induction machine torque curve obtained by ERP model [6]

In addition to the analysis of machine operation, the ERP model can also be used for dimensional calculations and cost estimate. Thus, in [9], the calculation of the basic dimensions of the power transformer is presented (made according to the adopted procedure [17, 18] defined in 19 steps). After defining the necessary specifications, by calculating all the elements of the core and winding, the final collection of data is obtained based on three results: the amount of copper, the amount of magnetic sheet metal and the amount of transformer oil.

Fig. 3 shows an example of using dimensional calculations in an ERP model for business decision making in the case of a large electrical machinery manufacturer.

From the dimension calculation, procedure moves to calculating the required resources, after which material

availability check and cost estimates are automatically performed as necessary information for decision making.

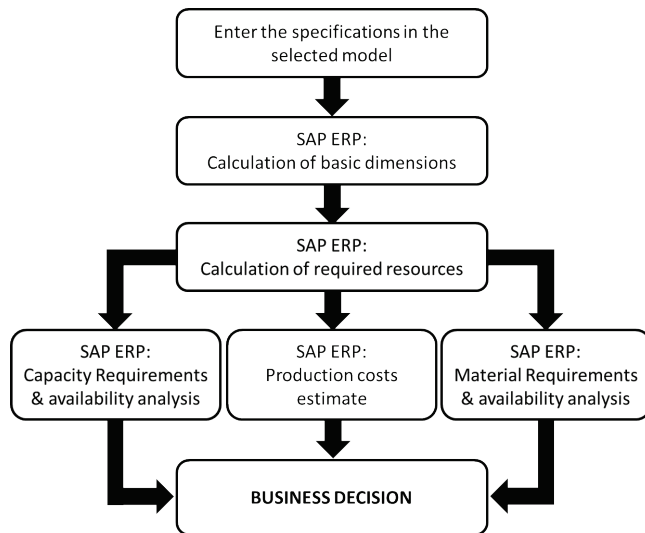


Figure 3 Using ERP models for business decision making [8]

Fig. 4 shows a more detailed presentation of the steps in the ERP model for obtaining data on the required quantities of materials and the required production times. Immediately after entering the desired specifications of the electrical machine, it starts with the calculation of dimensions and in parallel analyzes of historical records of production times by types of electrical machines. By including historical data in the ERP model, the calculation of the required working capacities for the production of the desired electrical machine was obtained.

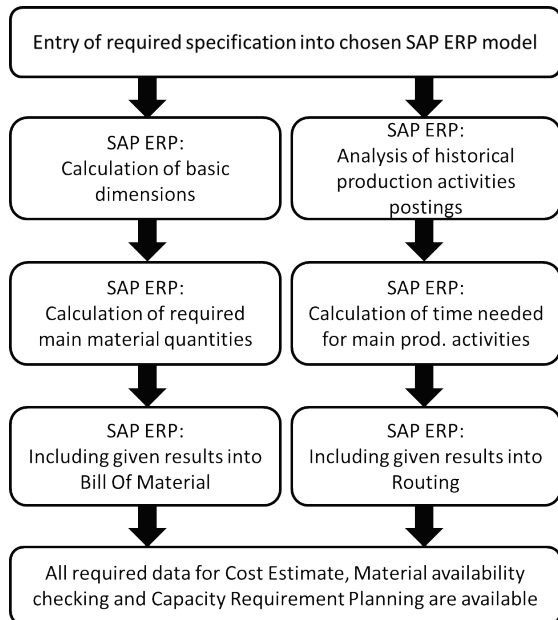


Figure 4 Key data preparation process [9]

Based on the cost of materials and production activities, the application of standard financial rules leads to an estimate

of the total production price, or COGS (Costs of Goods Sold) in business language.

## 2.2 Application of ERP Model for Calculation of Energy Savings in Controlled Electric Drives

Variable frequency electric drives provide several significant options for possible savings. One possibility is seen in the control of fluid flow by varying the speed of rotation instead of damping. A centrifugal pump was used as an example of induction machine load in this study. Based on the results of operational measurements, the static characteristics of the pump and pipeline are obtained, which is then included in the ERP model, and further simulation calculations are approached.

Fig. 5 shows the process within the ERP model that aims to calculate energy savings and in the end return on investment.

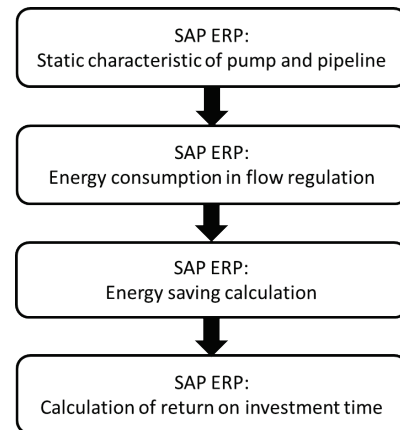


Figure 5 The procedure for calculating energy savings and return on investment

## 2.3 Centrifugal Pump Performance Characteristics

In the flow of incompressible fluids, the active force that allows flow through the pipelines is dependent on the pressure drop and the difference in geodetic height between the centers of the two pipelines.

Flow pressure drop in case of liquids is done by Eq. (2):

$$\Delta p = p_1 - p_2 = \left( \lambda_{tr} \frac{L}{d} + \sum \zeta \right) \rho w^2 + \rho g (h_2 - h_1). \quad (2)$$

List of variables used in an Eq. (2):  $\lambda_{tr}$  – friction coefficient,  $\zeta$  – loss coefficient,  $w$  – flow rate (m/s),  $\rho$  – fluid density (kg/m<sup>3</sup>),  $L$  – length (m),  $d$  – diameter (m),  $h$  – geodetic height (m),  $g$  – gravity acceleration (m/s<sup>2</sup>).

The active force for the transmission of liquids is obtained by the operation of the pumps and the corresponding height distribution of the pipeline. It can be seen from Eq. (2) that the pressure drop can be changed in two ways: by adding resistance to the system or by changing the fluid flow rate. Thus, the two basic options for fluid flow control are damping control and pump speed control, i.e. control via device that allows fluid transfer.

The basic quantities that characterize the operation of the pumps are the flow rate, the rotational speed and the delivery height. Since the flow rate is proportional to the speed of the pump, it follows that in order to control the speed, it is necessary to know the dependence of the flow and the delivery height of the pump on the speed. The flow rate is proportional to the speed of rotation of the pump (3), while the pressure, i.e. the delivery height and the speed of rotation are related by the square law (4).

$$Q = k_1 \cdot n, \quad (3)$$

$$H = k_2 \cdot n^2. \quad (4)$$

List of variables used in an Eqs. (3) and (4):  $Q$  – flow ( $\text{m}^3$ ),  $H$  – delivery high (mWC),  $k_1$ ,  $k_2$  – coefficients of proportionality,  $n$  – rotation speed (rpm).

The power of the pumps delivered to the liquid is obtained from Eq. (5):

$$P = \rho \cdot g \cdot H \cdot Q. \quad (5)$$

List of variables used in an Eqs. (3) and (4):  $P$  – Power (W),  $\rho$  – fluid density ( $\text{kg}/\text{m}^3$ ),  $g$  – gravity acceleration ( $\text{m}/\text{s}^2$ ),  $H$  – delivery height (mWC),  $Q$  – flow ( $\text{m}^3$ ).

A general presentation of the dependence of the delivery height on the flow is given in Fig. 6. The characteristic of the pipeline and the characteristic of the pump are shown. The intersection of these two characteristics gives the operating point of the pump.

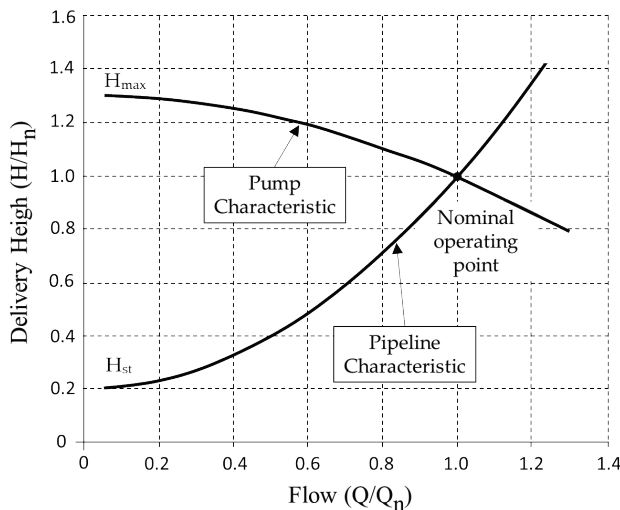


Figure 6 Static characteristic of pipeline and centrifugal pump [19]

Figs. 7 and 8 show two different ways of flow reduction, control by damping and control by speed. When using the flow control by damping (Fig. 7), the characteristic of the pipeline changes. Control is done by valves in the outlet line, by placing the valve in Position B instead of Position A, which adds new resistance to the flow line and thus reduces (dampens) the flow. With this method of control, it is moving along the pump curve at speed  $n_1$  from the A system curve to the B system curve. The delivery height increases from  $H$  to

$H_2$ . This way of control, reducing the flow does not reduce the energy required for the operation of the pump, but is spent on overcoming additional increased hydraulic frictional resistances, due to the damping of the valves.

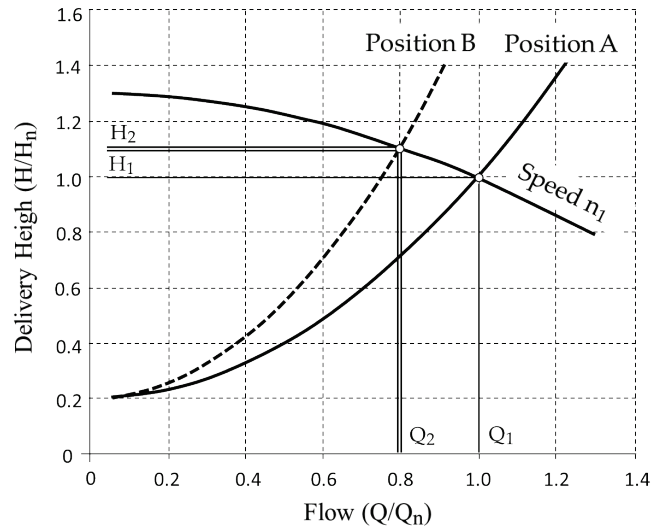


Figure 7 Flow control by damping

By changing the pump speed of rotation (Fig. 8), the characteristic of the pump changes, and thus the amount of fluid supply, while the characteristic of the pipeline remains the same.

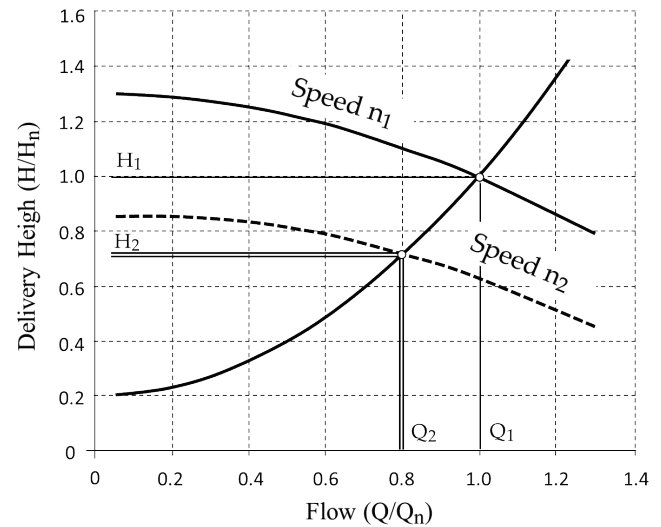


Figure 8 Flow control by changing the rotation speed

For a known pump characteristic at a certain speed, a new characteristic for a different speed, higher or lower than the nominal one, can be obtained on the basis of the law of similarity. The operating point will be at the intersection of the new pump characteristics and the pipeline characteristics. By lowering the vertical from this intersection, a flow corresponding to the new speed of rotation,  $n_2$ , is obtained. The delivery height decreases from  $H$  to  $H_1$ .

This method of control (reducing the speed of the pump to reduce the flow) reduces the energy required to operate the

pump at a lower motor speed, thus achieving the desired energy savings: if the Eq. (5) for power on the pump blades is multiplied by time, energy is obtained.

### 3 CALCULATION OF ENERGY SAVING USING ERP MODEL

In this central part of the article, two basic calculations using the ERP model will be presented: energy saving and investment repayment time.

#### 3.1 Centrifugal Pump Performance Characteristics

An example of the calculation will be an electric drive with an induction motor and a centrifugal pump with the following data [19]:

- nominal rotation speed 1485 rpm,
- flow at nominal speed 2500 m<sup>3</sup>/h,
- delivery high at nominal speed 140 mVS.

From the measured static characteristics that show the dependence of the delivery height on the flow, the full "name" of the function representing a specific curve can be easily obtained via excel, with "Format Trendline" option. The resulting function name is then used in the ERP model, where a formula is created using a variant configuration. As an example of switching the formula from excel to the ERP model, the calculation of the delivery height value in the case of flow control by damping can be given. After loading the measured values into excel, the formula "given" by excel, using second order polynomial for having trendline, looks as shown in the Eq. (6):

$$y = -0.3 \cdot x^2 + 0.02 \cdot x + 1.30. \quad (6)$$

In order for Eq. (6) to be used in the ERP model, the following preparatory steps need to be done:

- creating characteristics for entering initial values (density, flow rate and time)
- creation of characteristics for calculation of derived values (delivery height at constant speed, delivery height at change of speed, energy consumption in control by damping, energy consumption in control by speed and energy saving)
- creating a configuration class and assigning the created characteristics to the configuration class
- creating dependencies with formulas for calculation of delivery height and energy saving
- assignment of created dependencies to characteristics
- creating a master record of the material that will serve as a simulation object
- assignment of material as simulation object to the class
- creating a configuration profile
- assigning a configuration class to the configuration profile
- assigning all defined dependencies to the configuration profile

Fig. 9 shows eight created characteristics. All characteristics are numerical format and all of them are grouped together for easier searching and finding.

Chars / Values	Desc.	Group	Char. St.	Format
UNIN_101	Density	UNIN_JN	Released	Numeric Format
UNIN_102	Heigh	UNIN_JN	Released	Numeric Format
UNIN_103	Flow	UNIN_JN	Released	Numeric Format
UNIN_104	Time	UNIN_JN	Released	Numeric Format
UNIN_105	Heigh 2	UNIN_JN	Released	Numeric Format
UNIN_111	Energy 1	UNIN_JN	Released	Numeric Format
UNIN_112	Energy 2	UNIN_JN	Released	Numeric Format
UNIN_113	Energy 3	UNIN_JN	Released	Numeric Format

Figure 9 Characteristics created in ERP model

Fig. 10 shows the five dependencies created.

Dep.	Description	S Dep. Type
UNIN_102	Pipeline	1 Procedure
UNIN_105	Constant speed	1 Procedure
UNIN_111	Energy 1 (valve)	1 Procedure
UNIN_112	Energy 2 (speed)	1 Procedure
UNIN_113	Energy - delta	1 Procedure

Figure 10 Dependencies created in ERP model

With the system prepared in this way, it is possible to include Eq. (6) in the ERP model (Fig. 11).

Procedure	UNIN_105	Constant speed
Editor		
$\$self.UNIN_105 = -0.3 * \$self.UNIN_103 * \$self.UNIN_103 + 0.02 * \$self.UNIN_103 + 1.3$		

Figure 11 Eq. (6) after inclusion in the ERP model

Once the system is fully prepared, simulation calculations can be started. In order to calculate the energy consumption, it is enough to enter the relative value of the flow (amount of flow in relation to the nominal flow) and the desired length (time) of observation in the configuration table. As a result, the system provides the delivery height and the required power that must be delivered to the liquid, for both control modes. To facilitate the process, it can be assumed in the preparation of the model that it will work, for example, with water as a liquid, so the specific density is predefined. By entering the desired value of flow and the observed length of time, the value for the delivery height in both methods of flow control, the amount of energy consumed, and the savings themselves are reached.

Fig. 12 shows the result for 80% of the nominal flow for 10 hours. There is a difference in energy consumption. In the case of flow control by damping, the energy consumption for 10 hours of operation is 87 kWh, and in the case of flow control by rotation speed only 55 kWh. The difference in consumption is 32 kWh, or more than 35%.

With a system prepared in this way, it is possible to make quick checks for any other example based on the same physical basis. It is enough to make a correction of several

parameters of the previously prepared system on the basis of operational measurements.

Characteristic Value Assignment	
Char. description	Char. Value
<input type="checkbox"/> Density	1,000.00 kg/m3
<input type="checkbox"/> Flow	0.80 m3
<input type="checkbox"/> Time	10 h
<input type="checkbox"/> Heigh	0.70 m
<input type="checkbox"/> Heigh 2	1.10 m
<input type="checkbox"/> Energy 1	55 kW.h
<input type="checkbox"/> Energy 2	87 kW.h
<input type="checkbox"/> Energy 3	32 kW.h

Figure 12 Simulation calculation of energy savings

### 3.2 Calculation of Investment Repayment Time

Frequency converters can be a significant investment, and managers want a quick calculation of profitability and investment payback time. Without going into more detail about economic regularities, it is enough to know that the profitability of an investment depends significantly on the interest rate on borrowed money. According to the methodology discussed in [19], the Eq. (7) is used for rough calculation of repayment time on investment:

$$T = \frac{\log\left(1 - \frac{IV}{YS} \cdot k\right)}{\log(1 - k)} \quad (7)$$

List of variables used in an Eq. (7):  $T$  – repayment time (years),  $IV$  – investment value (EUR),  $YS$  – annual savings (EUR),  $k$  – annual interest rate (%).

To calculate the repayment time, as in the previous calculations, an appropriate characteristic is created in the ERP model to which the previous formula is linked.

In the simulation calculation, the resulting repayment time is obtained by simply entering the interest rate and the value of the investment (assuming that the value of the annual savings is calculated in the previous step). The required characteristics in the ERP model are shown in Fig. 13 and Eq. (7) is presented in ERP model as in Fig. 14.

Char. Name	Description	Group	Format
UNIN_201	Investment	UNIN_JN	CURR
UNIN_202	Yearly savings	UNIN_JN	CURR
UNIN_203	Interest rate	UNIN_JN	NUM
UNIN_210	Repayment time	UNIN_JN	NUM

Figure 13 Characteristics created for the purpose of calculating the repayment time

The final result, i.e. the required payback time of the investment (Fig. 15) is obtained using the simulation procedure (standard functionality of the SAP variant configuration). Fig. 15 shows that for an investment value of EUR 80,000, with an annual saving of EUR 12,000 and an

interest rate of 8%, a total of 9 years is required to repay the investment.

Procedure	UNIN_210	Repayment time
Editor		
$\$self.UNIN_210 = \frac{\log10(1 - (\$self.UNIN_201 / \$self.UNIN_202 * \$self.UNIN_203 / 100))}{\log10(1 - \$self.UNIN_203 / 100)}$		

Figure 14 Formula for calculating repayment time

Characteristic Value Assignment	
Char. description	Char. Value
<input type="checkbox"/> Investment	80,000.00 EUR
<input type="checkbox"/> Yearly savings	12,000.00 EUR
<input type="checkbox"/> Interest rate	8.00 %
<input type="checkbox"/> Repayment time	9.1 yr

Figure 15 Simulation calculation of investment repayment time

In general, the longer the pump would run in reduced flow mode, the annual savings would increase and the repayment time would be shortened.

## 4 CONCLUSION

This paper presents the current state of research in the field of possible applications of ERP models for the purpose of rough technical calculations and analyzes. The goal of creating an ERP model is to enable managers as natural users of the ERP system to more easily access the key data needed for quick decision making. In this step of the research, it was shown that with the help of a well prepared ERP model, managers can easily get a static analysis of electric drives, with an emphasis on possible savings in the case of variable frequency drives.

An electric drive with an induction motor and a centrifugal pump is analyzed here, but a similar methodology can be applied to other systems, e.g. in monitoring the development and installation of advanced systems in electric vehicles.

The results of rough calculations using the ERP model provide data on different energy consumption depending on whether flow control by damping or speed change is used. Since, in general, all types of savings usually require additional investments, the ERP model also enables a rough calculation of the investment repayment time. All the important steps that need to be taken in order to prepare an ERP model are presented. In future work, it is possible to consider what effect would have failures in electric drives on Recovery of Investment.

The authors estimate that the whole process could be a great help to managers in considering existing alternatives in decision making.

Future work will be focused on further improvements of ERP model, making it even more easy to use by managers.

## 5 REFERENCES

- [1] Hruška, D. (2015). *Radical Decision Making*. Palgrave MacMillan, New York. <https://doi.org/10.1057/9781137492319>
- [2] Lytkina Botelho, E., Rosenkoetter Powel, K., Kincaid, S., & Wang, D. (2017). *What sets successful CEOs apart?* Harvard Business Review, May-June.
- [3] Akhtar, J. (2013). *Production Planning and Control with SAP ERP*. Galileo Press, Boston.
- [4] Blumohr, U., Munch, M., & Ukalovic, M. (2012). *Variant Configuration with SAP*. Galileo Press, Boston.
- [5] Jordan, J. (2012). *Product Cost Controlling with SAP*. Galileo Press, Boston.
- [6] Nađ, J. (2017). Improvement of business decision making process using analytical model of transformer in ERP software. *PhD thesis*, University of Zagreb.
- [7] Nađ, J. & Vražić, M. (2018). Analytical model of electrical machines in business software. *Tehnički vjesnik*, 25 (2), 582-586. <https://doi.org/10.17559/TV-20160626125528>
- [8] Nađ, J. & Vražić, M. (2017). Decision making in transformer manufacturing companies with help of ERP Business software. *Proceedings of the 15<sup>th</sup> International Conference on Electrical Machines, Drives and Power Systems ELMA2017*, 379-382. <https://doi.org/10.1109/ELMA.2017.7955468>
- [9] Nađ, J. (2018). *Analytical model of electrical machines in business software – quick and powerful electrical calculations by ERP*. Lambert Academic Publishing
- [10] Moreno, Y., Almandoz, G., Egea, A., Arribas, B., & Urdangarin, A. (2021). Analysis of Permanent Magnet Motors in High Frequency-A Review. *Applied Sciences-Basel*, 11(14), Art. No. 6334. <https://doi.org/10.3390/app11146334>
- [11] Jung, J. & Cebulski, B. (2018). Analytic Design of Multi-Phase Electric Machines with Independent H-Bridge Supply. *IEEE 2018 XIII International Conference on Electrical Machines (ICEM)*, Alexandroupoli, Greece, 2037-2043. <https://doi.org/10.1109/ICELMACH.2018.8507031>
- [12] Tomićić B., Havaš L., & Srpak D. (2018) Influence of strands transposition on current distribution and power losses in windings of AC machines. *Tehnički glasnik*, 12(2), 86-92. <https://doi.org/10.31803/tg-20180301185613>
- [13] Dai, T. Y., Li, H., Li, J. F., Yuan, B., & Liu, X. Y. (2019). A Hybrid Calculation Method of Radial Electromagnetic Force Based on Finite Element Method and Analytic Method in A Permanent Magnet Synchronous Machine. *International Conference on Electrical Machines and Systems ICEMS*, Harbin, Peoples R of China, 2081-2084. <https://doi.org/10.1109/ICEMS.2019.8921891>
- [14] Urbanek, S., Quattrone, F., & Ponick, B. (2017) Implementation and Validation of a New Analytic-Numeric Method for Dynamic Core Loss Calculation. *IEEE International Electric Machines and Drives Conference (IEMDC)*, Miami, FL. <https://doi.org/10.1109/IEMDC.2017.8002073>
- [15] Lange, T., Qi, F., Dehn, J., & De Doncker, R. W. (2015) Synchronous machine model considering dynamic losses and lumped parameter thermal network. *IEEE International Electric Machines and Drives Conference*, Coeur d'Alene, ID, 536-542. <https://doi.org/10.1109/IEMDC.2015.7409110>
- [16] Chen, J. H., Fujii, Y., Johnson, M. W., Farhan, A., & Severson, E. L. (2019). Optimal design of the Bearingless Induction motor. *IEEE Transactions on Industry Applications*, 57(2), 1375-1388. <https://doi.org/10.1109/TIA.2020.3044970>
- [17] Deshpande, M. V. (2011). *Design and testing of Electrical Machines*. PHI Learning, New Delhi.
- [18] Georgilakis, P. S. (2009). *Spotlight on Modern Transformer Design*. Springer-Verlag, London. <https://doi.org/10.1007/978-1-84882-667-0>
- [19] Nađ, J. (1998). Energy saving and reliability increasing by controlling of electrical drives. *Master thesis*, University of Zagreb.

## Authors' contacts:

**Josip Nađ**, PhD, MBA

(Corresponding author)

Department of Electrical Engineering, University North,

42 000 Varaždin, Croatia

jnad@unin.hr

+385-91-61-000-15

**Dunja Srpak**, PhD, Assistant Professor

Department of Electrical Engineering, University North,

42 000 Varaždin, Croatia

dsrpak@unin.hr

**Antonija Šumiga**, Assistant

Department of Electrical Engineering, University North,

42 000 Varaždin, Croatia

asumiga@unin.hr

**Branko Tomićić**, PhD, Senior lecturer

Department of Electrical Engineering, University North,

42 000 Varaždin, Croatia

btomicic@unin.hr

# Application of Response Surface Methodology in the Analysis of Weldability Test Results on X80 Steel

Tanja Tomić\*, Lidija Tepeš Golubić, Jana Žiljak Gršić, Matija Bušić

**Abstract:** Engineering research is based on experiments that give answers how different influential process factors can impact an outcome. Therefore, the research plot has to be designed in order to capture a valid analysis of the results. Many research projects use research methodologies as a help to reach the answers in a technical point of view and to determine the laws of the controlled input variables on the experimental outcome. This paper will show a realistic usage of the response surface methodology with an CCD experimental plan for 2 influence factors on a welding example using FCAW welding process in order to investigate the hydrogen input and the critical implant stress upon changing the heat input and preheat temperature and to define the weldability of API 5L X80 steel welds.

**Keywords:** central composite design; diffused hydrogen content; heat input; implant test; preheating; response surface methodology; Weldability X80 steel; welding

## 1 INTRODUCTION

Experimental tests are conducted in order to determine the laws, whereby certain input variables are intentionally modified to determine the output result of the change and draw valid, systematic, and objective conclusions. In order to reach a valid conclusion, it is necessary to conduct valid research, a valid experiment, and valid analysis of the test results, which is achieved by applying the appropriate methodology.

The methodology of scientific research and the technology of scientific and development research represent the intellectual logistics of modern educational and scientific industries [1]. In this paper, the methodology of the scientific research paper will be approached from a technical point of view, which includes data collection by conducting a standardized experiment and analysis of the obtained results varied in the experiment as independent influencing variables.

product development, production improvement, and production technologies. The general model of the processing system is based on input data that change within the process due to the action of controlled and uncontrolled variables and output data, as shown in Fig. 1.

For a meaningful design of experimental research, it is necessary to define the relationship between the observed phenomenon and influential factors through the determination of the strategy of the experimental paper.

The scientific approach to the research paper requires the use of appropriate models of the experimental plan in order to be able to determine as precisely as possible the regularity that appears in the observed model and which excludes the occurrence of noise or error. Since financial resources must be planned for each new scientific research paper, a scientific research paper is in most cases a large risky investment. Well-developed plans and models of experimental research in a scientific research paper can also achieve great savings.

### 1.1 Influence of Hydrogen Content on the Weldability of Steel

In this paper, the weldability of API 5L X80 steel was tested with respect to the occurrence of diffuse hydrogen according to the following influential parameters: preheating temperature and heat input.

API 5L X80 steel mainly finds application in pipeline construction. According to literature, statistics showed that API 5L X80 steel has been used in global pipelines exceeding 300 000.00 km because modern TMCP technology makes it possible to produce an excellent combination of strength, toughness and weldability combining the proper alloying [3]. The pipeline for transporting, for example, the gaseous medium is installed in the ground, whereby during the service life the pipeline may be exposed to hydrogen absorption from localized corrosion mechanisms and as a by-product of cathodic protection. Although API 5L X80 steels are characterized by good toughness in the event that a larger amount of hydrogen is absorbed under certain conditions, there may be a loss of toughness and hardening of the material. In this case, hydrogen fragility occurs. The

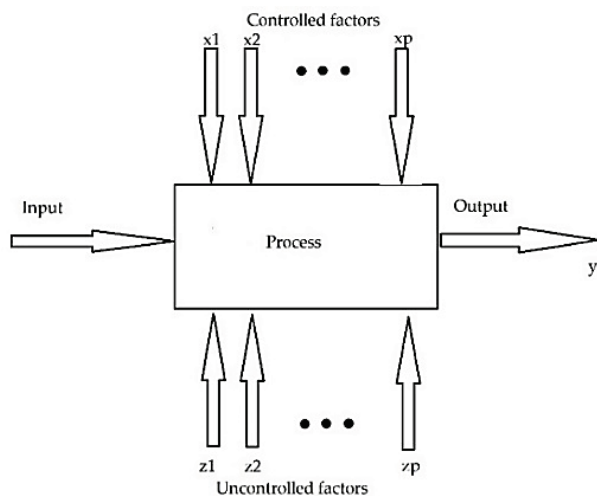


Figure 1 The general model of the processing system [2]

In the engineering profession, research is based on experimental testing of great importance for the field of

literature indicates that during the service life of the pipeline was observed a sixfold increase in the hydrogen content on the outer walls of the pipeline in the first two years of operation, while tenfold higher amounts of hydrogen were estimated for 15 years of operation [4]. Namely, one of the common phenomena that can occur as a manufacturing error with welding technology is the appearance of cold cracks. Cold cracks occur at temperatures below 300 °C and can appear immediately, after several hours or even days after welding. Cold cracks correlate with material microstructure, material stress, and hydrogen content.

During the service life, the appearance of cold cracks on a welded pipeline or other welded steel structure could result in great material damage and damage dangerous to man and his environment.

Numerous literature sources mention different methods of preventing such material degradation or controlling the conditions in which cold cracks can occur [4-7].

The biggest obstacle is the lack of a universally applicable model for determining the amount of hydrogen sufficient to initiate a cold crack and that this model applies to all steels. Namely, all phenomena that occur as a consequence of the action of hydrogen on the degradation of materials are confirmed or not confirmed by the so far proposed theories on the mechanisms of action of hydrogen.

This paper presents one method determined through a scientific research paper with which the amount of hydrogen at which cold cracks can occur can be determined. In this paper, the tests were performed on steel supplied in the form of a plate produced by a Thermo Mechanical Controlled Process (TMCP).

The welding technology used was Flux Cored Arc Welding (FCAW). During welding, two flux-filled wires were used, which differ in flux content and composition. Both types of flux can be found in practical applications. The composition of the flux in the wires was of rutile and basic character.

The centrally composite experimental plan was used as the selected experimental plan. Therefore, for each wire, 14 experiment states were determined, of which 6 repetitions were in the centre.

The following were chosen as influential independent variables: heat input ( $E$ , kJ/cm) and preheating temperature ( $T_p$ , °C). Since these two variables impact the amount of diffused hydrogen, the goal of this paper was to show how the amount of diffused hydrogen is generated in the base material through this chosen welding procedure.

For the purposes of the research, test tubes for measuring the amount of diffused hydrogen and for the Implant test were made.

The obtained results were subjected to detailed analysis and statistical processing that determined the prediction of the action of individual independent variables, and a mathematical model for predicting the amount of diffused hydrogen and critical Implant stress was developed.

Based on all experimental data, the critical amount of diffused hydrogen expressed in ml H<sub>2</sub>/100 g of welds was determined, as well as the optimal welding parameters in

which the probability of cold cracks as a result of hydrogen action is lower.

## 2 DESIGN OF THE EXPERIMENT AND THE EXPERIMENTAL PLAN

For successful process optimization, it is necessary to define the relationship between the observed phenomenon and the influencing factors. The starting point of the experiment in this paper was the choice of approach in defining the experimental plan, with the aim of controlling the influencing factors in the researched process. Since it is a nonlinear system, the statistical method of the response surface was used.

Response Surface Methodology (RSM) is a set of mathematical and statistical methods that model and analyze the effects of independent variables on the observed response [6]. Once the lawfulness or relationship of independent variables is established through a mathematical form i.e. response function, such phenomenon description form can serve for drawing concrete conclusions about the nature of the phenomenon and be a good basis for optimization by known optimization methods [8].

In this paper, the hydrogen input response and critical implant stress were observed, and the independent influencing variables were heat input and temperature. This type of experiment design is most commonly used in the technical sciences. The basic idea of the response surface methodology is to obtain the relationship of influential (independent) factors to the dependent variable (response) through the response function. In this case, the RSM prerequisite is also satisfied because there are two independent variables ( $x_1$  and  $x_2$ ) and response ( $y$ ). In this paper are analyzed two responses that are based on two independent variables ( $y_1$ ;  $y_2$ ). The process result is formulated according to the following calculation:

$$y = f(x_1, x_2) + \varepsilon \quad (1)$$

where  $\varepsilon$  is the error or noise that occurs in the response  $y$ .

For this case, the set equation is:

$$H_D, R_{ik} = f(E, T_p) - \varepsilon \quad (2)$$

Where is:  $H_D$  – amount of diffuse hydrogen, ppm;  $R_{ik}$  – critical implant stress, MPa;  $E$  – heat input, kJ/cm;  $T_p$  – preheating temperature.

Considering the initial settings, a centrally composite experimental plan was selected, which also belongs to the class of experimental plans that most often appear in the response surface methodology.

The observed values were determined at three levels, at three different heat inputs, and at three different preheating temperatures, the concept of a centrally composite experimental plan sets a total of five preheating temperature levels and five heat input levels, as shown in Fig. 2.

Fig. 2 shows the experiment states of the centrally composite experimental plan, with the largest number of

repetitions in the centre. A total of 6 repetitions were performed in the centre. This test plan was used for both welding wires, rutile and basic, and for testing the hydrogen input with a glycerol method, and for testing the X80 steel's susceptibility to cold cracks by the Implant test. All points, except the centre, were performed with only one measurement.

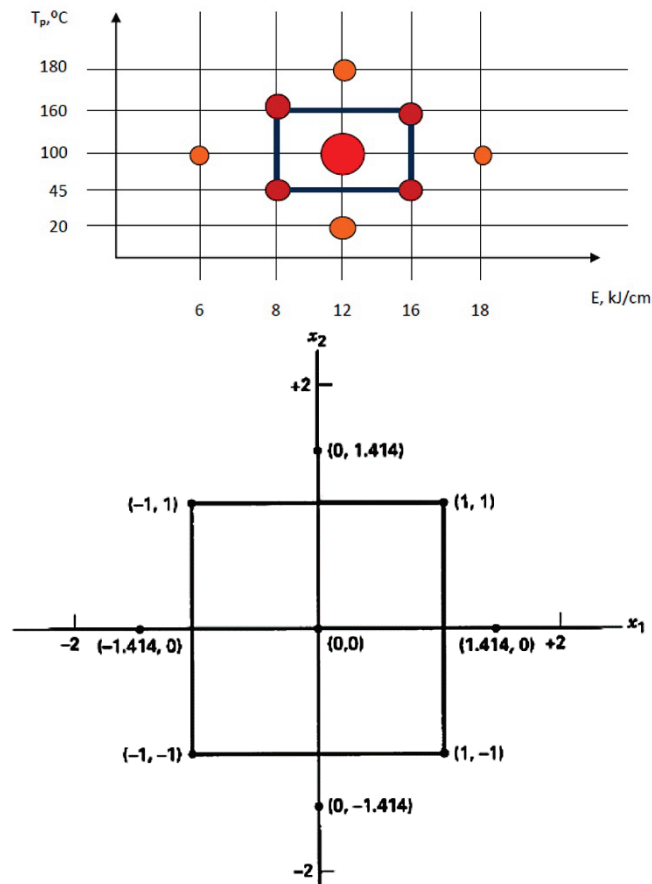


Figure 2 Display of welding parameters in accordance with the experimental conditions and CCD experimental plan for 2 factors [7]

Table 1 Display of experiment state and corresponding welding parameters by experiment stages for basic and rutile wire

Experiment state		Heat Input, kJ/cm	Preheat temperature, °C
Rutile wire	Basic wire		
RUT1	BAS1	12	20
RUT 2	BAS 2	8	45
RUT 3	BAS 3	12	100
RUT 4	BAS 4	12	100
RUT 5	BAS 5	12	100
RUT 6	BAS 6	12	100
RUT 7	BAS 7	12	100
RUT 8	BAS 8	12	100
RUT 9	BAS 9	16	45
RUT 10	BAS 10	6	100
RUT 11	BAS 11	18	100
RUT 12	BAS 12	8	160
RUT 13	BAS 13	16	160
RUT 14	BAS 14	12	180

The central point provides information on the nonlinearity in the response, while the axial points provide

the possibility of efficient estimation of the second-order parameters.

Fig. 2 shows the independent variables,  $E$  and  $T_p$ , heat input, and preheating temperature.

A total of 14 experiment states were performed for both wires used, and for the glycerine measurement method, and the Implant test. Tab. 1 shows the centrally composite experimental plan to determine the experiment state according to which the experimental paper was carried out. The electrode tip was 15 mm, and the welding was conducted with a neutral electrode angle 90°.

Welding parameters such as current type and current polarity, current amount, wire speed, voltage, wire diameter, shielding gas flow, welding speed, electrode inclination, and heat input were determined. Welding parameters are shown in Tab. 2. The wire diameter was 1.2 mm, welding current and polarity was DC+, gas flow was 18 l/min, and the weldment was conducted with a neutral electrode angle 90°.

Heat input is calculated according to the calculation [9]:

$$E = \frac{U \cdot I}{v_z} \cdot \eta \quad (3)$$

Where is:  $U$  – welding voltage, V;  $I$  – welding current, A;  $v_z$  – welding speed, mm/s;  $\eta$  – degree of utilization of the welding process.

Table 2 Display of welding parameters

	Welding current, A	Voltage, U	Welding speed, cm/s	Heat input, kJ/cm
BASIC WIRE				
1	162	24	30	6.22
2	164	24	25	7.56
3	200	26	20	12.48
4	240	27.5	19	16.67
5	268	28.5	20	18.33
RUTILE WIRE				
1	180	23.5	27	6.68
2	180	23.5	23	8.83
3	220	24	20	12.67
4	250	25.5	19	16.11
5	270	27	20	17.50

After the experimental part of the research, the obtained data need to be subjected to statistical processing and analysis. For this purpose, a program called Design Expert, version 7.1.4 was used which confirmed that the selected experimental plan is satisfying. As mentioned earlier, the experiment was developed in 14 experiment states, of which were 6 repetitions in the center. The scope of the experiment is large because four tubes for one experiment state were used to measure the amount of diffused hydrogen, and a minimum of five tubes was used to determine the critical Implant stress. Such an approach ensures the reduction of the possibility of error or noise that could occur due to human factors, or some other irregularities caused by the environment. Each test was performed under controlled laboratory conditions with monitoring of ambient temperature and humidity so that excessive deviations would not affect the results.

After entering the measured values according to the selected concept of the experimental plan, analysis of the results in the Design Expert program 7.1.4. is performed in several steps for each response surface. This is followed by an analysis of variance (ANOVA), post-ANOVA analysis of individual coefficients, and statistical data processing of residues and points that are not within the limits. It is necessary to validate the model using various diagnostic tools. If the model is appropriate, graphical analysis is performed.

In this particular case, transformations of experimental data were carried out in order to obtain an overview of the operation of the model, but they were not applied because the inverse observation of the data can give a distorted image.

### 3 STATISTICAL ANALYSIS AND DEVELOPMENT OF A MATHEMATICAL MODEL

By establishing a centrally composite experiment plan with a total of 14 states, of which are 6 repetitions in the centre, the results used in the development of the mathematical model according to the response values of diffuse hydrogen,  $H_D$ , and critical implant stress  $R_{ik}$  were recorded.

#### 3.1 Mathematical Models for Rutile Wire

##### 3.1.1 $H_D$ Diffuse Hydrogen Content for Rutile Wire

The ANOVA analysis gave an equation with the following significant members:  $A$ ,  $A^2$  and  $B^2$ . The value of  $F$  is 23.53, which implies that the model is significant and that there is only 0.01% of the possibility for the insignificance of the model due to error or noise. The value " $Prob>F$ " that is less than 0.05 implies that significant factors are  $A$  (0.0242),  $A^2$  (0.0292), and  $B^2$  (<0.0001). The value " $Adeq Precision$ " defines the relationship between noise and signal and it is satisfactory if it is more than 4. In this case, it is 12,576, which indicates that the signal is appropriate. The value of the predicted  $R^2$  is 0.5970, while the value of the adjusted  $R^2$  is 0.8739. The difference is 0.27. The reference amount that would indicate a good match between the data and the model is 0.2, and the value of 0.27 is negligible in this case, so it can be assessed that the match between the data and the model is good. The model diagnostics determined that all data are within the critical test values.

The final calculation for  $H_D$  for rutile-type flux cored arc welding

$$H_D = 6.18458 + 5.09862 \times 10^{-3} \cdot T_p - 0.61113 \cdot E - 3.46125 \times 10^{-5} \cdot T_p^2 - 0.024621 \cdot E^2 \quad (4)$$

Where is:  $H_D$  – amount of diffuse hydrogen, ml  $H_2$ /100 g weld;  $T_p$  – preheating temperature, °C;  $E$  – heat input, kJ/cm.

Fig. 3 shows the graphical display of the response surface and a contour display of the isoquants for the diffuse hydrogen content according to the performed experiment states.

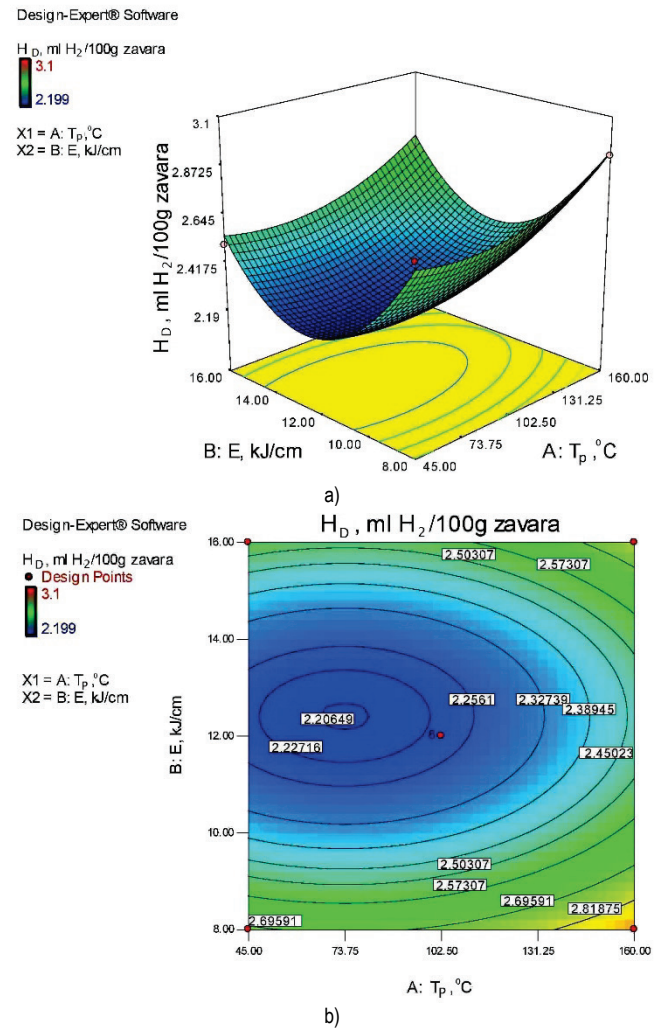


Figure 3 (a)  $H_D$  response surface display for rutile wire; (b) contour display of the isoquants for the diffuse hydrogen content

According to Fig. 3, it is visible that the largest amount of diffused hydrogen was determined in boundary conditions, i.e. the process indicates stability in the center where the smallest values of the amount of diffused hydrogen were measured. Namely, a cold crack was noticed on metallographic samples tested by implant testing, on a sample welded at  $T_p = 45$  °C and  $E = 16$  kJ/cm, and on a sample welded at preheating temperature  $T_p = 20$  °C and  $E = 12$  kJ/cm. The cold crack arise through the HAZ to the WM, which can be seen in Fig. 4. Fig. 4 is therefore directly related to the response surface shown in Fig. 3 where it can be seen that the largest amount of diffused hydrogen was found at the lowest preheating temperatures. The literature [11] indicates the possibility of cold cracks if the preheating temperature is lower than 50 °C. Fig. 4b also shows an inclusion in the weld that can attract enough hydrogen and act as hydrogen trap with a potential to develop a hydrogen crack. These inclusions are usually not considered as welding defects, but they can produce cold cracking if critical conditions occur. This particular inclusion shown on Fig. 4b has an uneven surface of approximative 1120  $\mu m^2$  and is made of O, Mg and Si. Because of his uneven surface this inclusion can act as a

hydrogen trap. Ref. [12] proves how micro vacancy can play an impact role on the crack initiation, especially if there are conditions for stress corrosion cracking.

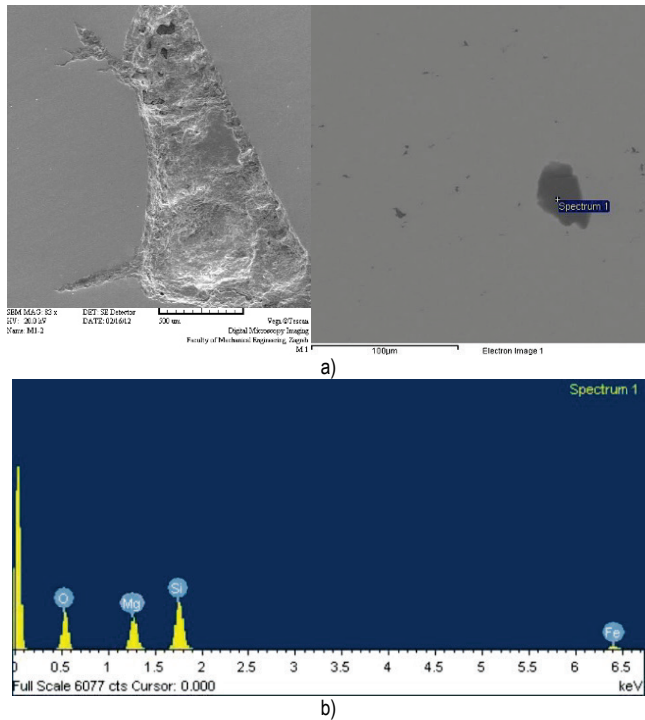


Figure 4 (a) Display of a crack located in the area of weld metal and coarse-grained HAZ; (b) display of a spectrum with inclusion susceptible to hydrogen accumulation and cracking in the weld metal.

### 3.1.2 $R_{ik}$ Critical Implant Stress for Rutile Wire

The reduction of the model was performed. It was determined that member  $B$  (0.0239) is significant, however, the interaction of  $AB$  (0.0530) can also be assessed as significant.

The simplified quadratic model's ANOVA value is 4.11, meaning that there is a 3.85% possibility that the model's significance is the result of error or noise.

Significant model components are indicated by the value " $Prob>F$ " being less than 0.0500.

The value " $Adeq\ Precision$ " determinates the signal-to-noise ratio and the result is 7.622 which is more than 4 and proves that there is a corresponding signal. Model diagnostics do not indicate excessive deviation of results beyond critical values.

The final term for  $R_{ik}$  for rutile-type flux cored arc welding is:

$$R_{ik} = 630.93664 - 1.77887 \cdot T_p - 8.50624 \cdot E - 0.15985 \cdot T_p \cdot E \quad (5)$$

Where is:  $R_{ik}$  – critical implant strain, MPa;  $T_p$  – preheating temperature, °C;  $E$  – heat input, kJ/cm.

Fig. 5 shows the results of the response surface analysis, isoquant display, and optimization  $H_D$  and  $R_{ik}$ .

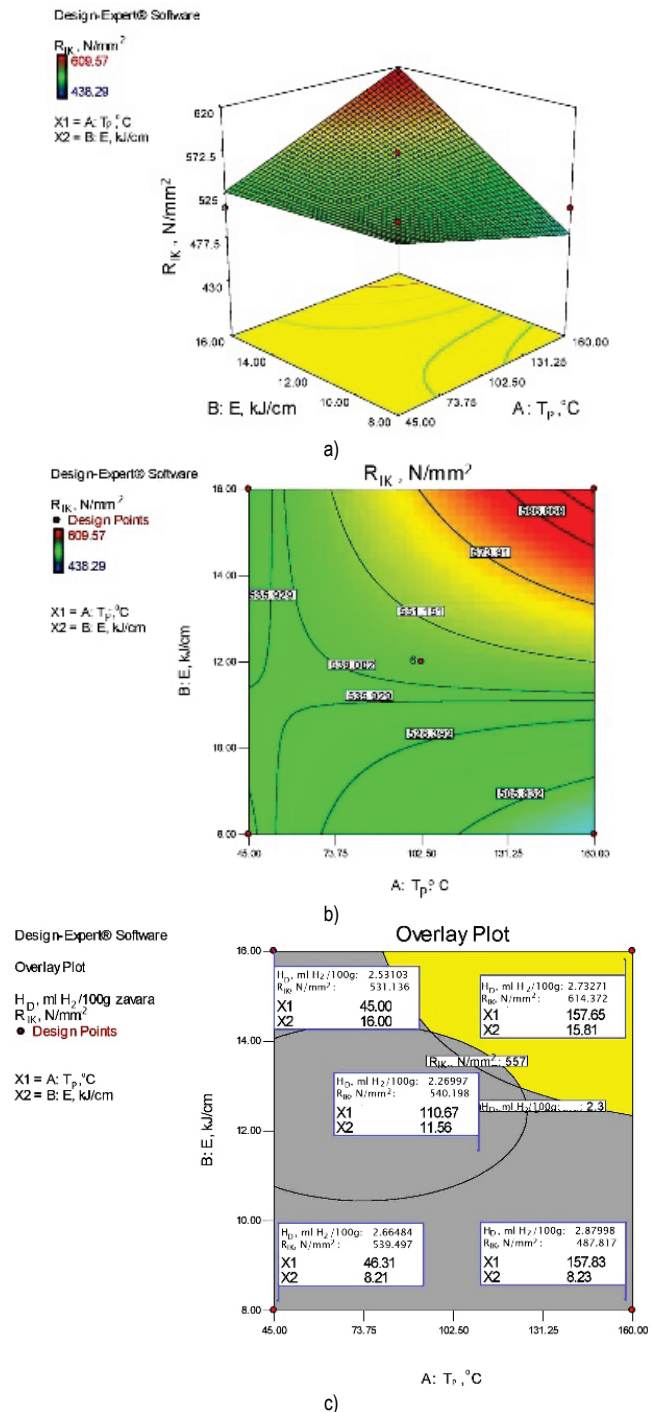


Figure 5 (a)  $R_{ik}$  response surface for rutile wire; (b) display of  $R_{ik}$  isoquants for rutile wire; (c) optimization of  $H_D$  for  $H_D = 2.3 - 2.9$  ml H₂/100 g weld and  $R_{ik} = 557$  MPa.

Fig. 5 shows that the maximum  $R_{ik}$  is the highest at the maximum  $E$  and  $T_p$ , so the optimization of  $H_D$  and  $R_{ik}$  is performed according to the criteria of minimum  $H_D$  and maximum  $R_{ik}$ . Here, also, the phenomenon of more diffuse hydrogen being measured at lower preheating temperatures is visible, and the observed appearance of cold cracks indicates a direct interaction between the amount of hydrogen and the state of the Implant stress.

### 3.2 Mathematical Models for the Basic Wire

#### 3.2.1 $H_D$ Diffuse Hydrogen Content for Base Wire

By analysis of variance was obtained a model with active members  $A, AB, A^2, B^2, AB^2$ . This model was accepted due to the decrease in the value of  $R^2$ .

The proposed quadratic model's ANOVA results in a  $F$  value of 134.87, indicating that it is significant and that there is only a 0.01% chance that it was produced accidentally or by noise.

Value " $Prob>F$ " which is less than 0.0500 indicates that  $A$  - preheating temperature ( $<0.0001$ ) is a significant member, while  $B$  - heat input is less significant and that its action is seen in combination with member  $A$  (preheating temperature). However, due to the retention of the hierarchy of the form of the equation, the action of member  $B$  (heat input) whose " $Prob>F$ " value is 0.5156 is accepted since based on the literature this member cannot be completely excluded.

Value " $Adeq Precision$ " determinates the relationship between noise and corresponding signal and if the mentioned value is greater than 4 then such a state is considered desirable. In this case, the value of " $Adeq Precision$ " is 32.457, which indicates the appropriate signal. This model can be used to determine the spatial design.

The predicted  $R^2$  value of 0.8672 is consistent with the adjusted value of  $R^2$  that is 0.9841. Since this value in the amount of 0.1169 is less than 0.2, this indicates a good match between the model and the data.

The final model for  $H_D$  for flux cored arc welding when the electrode is a wire with a basic flux:

$$H_D = 3.98784 - 0.036367 \cdot T_p - 0.55250 \cdot E + 4.6383 \times 10^{-3} \cdot T_p \cdot E + 3.59294 \times 10^{-5} \cdot T_p^2 + 0.021108 \cdot E^2 - 1.74195 \times 10^{-4} \cdot T_p \cdot E \quad (6)$$

Figs. 6a and 6b show the response surfaces and isoquants for the diffuse hydrogen content.

The Fig. 6 shows that the highest concentrations of diffuse hydrogen are expected at the lowest heat input and the lowest preheating temperature. However, the center is a more relevant landmark because the stability of the process is visible, indicating a rather low content of hydrogen intake. No cold cracks were observed on the samples welded with wire filled with basic character. Although, in any case, after the implementation of the optimization, it would be recommended to carry out preheating at temperatures around 100 °C and at  $E = 8$  to 16 kJ/cm. All measured values of diffuse hydrogen are within the permitted limits, below 5 ml  $H_2/100$  g weld. However, the literature states that 1 ml of  $H_2/100$  g of weld is sufficient for the appearance of cold cracks on API 5L X80 grade steels [13, 14].

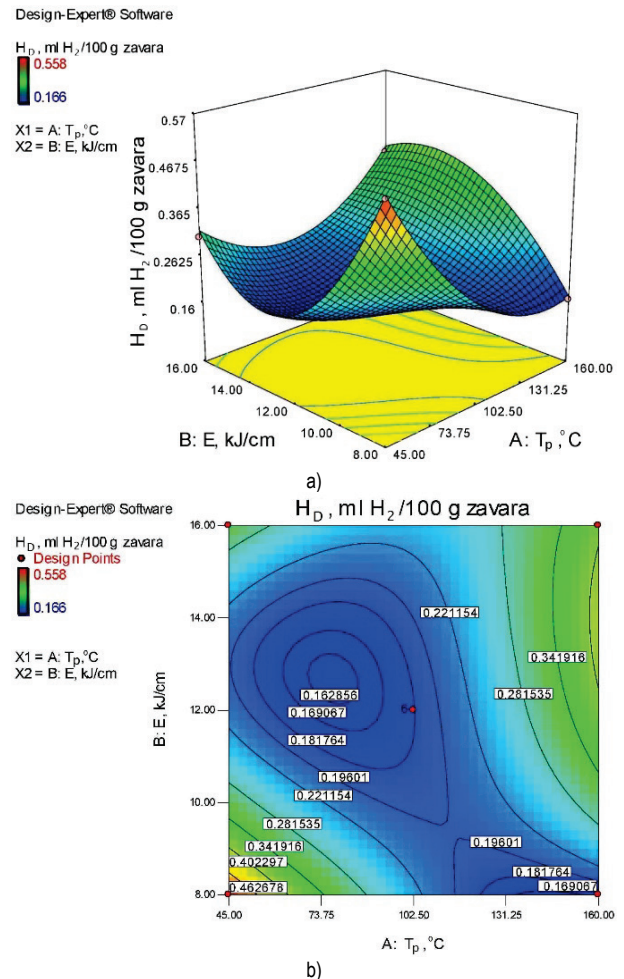


Figure 6 (a) Display of the response surface for  $H_D$  when welding with wire filled with basic flux; (b) showing the isoquants of diffuse hydrogen content for a wire filled with a basic flux.

#### 3.2.2 $R_{ik}$ Critical Implant Stress for Base Wire

The chemical composition of the base wire is accountable for the dehydrogenization of the weld metal as indicated by the low values of the measured amount of diffused hydrogen, especially in the centre of the central composite test plan in which the measured values are 0.2 ml  $H_2/100$  g weld. Phenomena related to the occurrence of cold cracks at such a low hydrogen content have not been described in the literature. The base wire guarantees better mechanical properties and is mainly used to make more demanding steel structures.

No mathematical model was established for this experiment state because the deviations between the measured values were very small and possible deviations could be determined with more sophisticated testing equipment. However, the results presented in this way indicate a good resistance of the material to the occurrence of cold cracks and the possibility of applying the base and additional material in edge and harsher conditions with a satisfactory outcome in members of satisfactory weldability.

## 4 CONCLUSIONS

It has been determined by the methods of scientific research that the results of measuring the amount of diffused hydrogen by the glycerol method according to JIS Z 3118: 1992 and the performed analysis and developed mathematical models indicate lawfulness. With two distinct experiment variables, the developed centrally composite experimental design (RSM method) generated 14 experiment states with 6 repetitions in the middle.

The presented results show that the centre almost always had the same value, which indicates the existence of physical law and repeatability. The ideal center for working conditions is one with six repetitions, a heat input of 12 kJ/cm, and a preheating temperature of 100 °C. No cold cracks were observed in this area, and this area is described as an area of stable conditions. Mathematical models indicate that heat input has a stronger influence on the hydrogen diffusion behaviour model while the preheating temperature is viewed as a secondary influence quantity. The chemical composition of the additional material, i.e. the chemical composition of the flux in the filled wires, is responsible for the diversity of mathematical models. Namely, elements from the different chemical compositions of the flux form compounds of the size of 1 to 3 µm, which indicate the heterogeneity of the structure and thus the different possible paths of hydrogen diffusion through the material.

The obtained mathematical models correspond to a wider range of welding parameters for the tested steel and additional material. Also, in the case of rutile wire, boundary conditions were determined at which there is an increased possibility of the appearance of cold cracks in the area where the preheating temperature is less than 50 °C, and conditions were determined in which the stability of the process is indicated. With the help of a detailed methodology of scientific research, this research established the dependence of the amount of diffused hydrogen on the welding parameters, heat input, and preheating temperature.

## 5 REFERENCES

- [1] Zelenika, R. (2016). Tehnologija znanstvenog i razvojnog istraživanja, IQ PLUS d.o.o., Kastav. (in Croatian)
- [2] Montgomery, D. C. (2001). Design and analysis of experiments, 5th Edition.
- [3] Sun, Y. & Frank Cheng, Y. (2021). Hydrogen permeation and distribution at high strength X80 steel weld under stressing conditions and the implication on pipeline failure. *International Journal of Hydrogen Energy*, 46(44), 23100-23112. <https://doi.org/10.1016/j.ijhydene.2021.04.115>
- [4] Wang, R. (2009). Effects of hydrogen on the fracture toughness of a X70 pipeline steel. *Corrosion Science*, 51(12), 2803-2810. <https://doi.org/10.1016/j.corsci.2009.07.013>
- [5] Pitrun, M. (2004). The effect of welding parameters on level of diffusible hydrogen in weld metal deposited using gas shielded flux cored wires. *Doctoral Thesis*, University of Wollongong.
- [6] Cottis, R. A. (2010). Hydrogen Embrittlement. *Shreir's Corrosion*, 2, 902-922. <http://doi.org/10.1016/B978-0-444-52787-5.00200-6>

- [7] Tomić Kovačević, T. (2012). Utjecaj sadržaja vodika na zavarljivost čelika API 5L X80. *Doktorski rad*, Fakultet strojarstva i brodogradnje, Sveučilište u Zagrebu. (in Croatian)
- [8] Cajner, H. (2011). Višekriterijsko adaptivno oblikovanje planova pokusa. *Doktorski rad*, Fakultet strojarstva i brodogradnje, Sveučilište u Zagrebu. (in Croatian)
- [9] Cooper, R., Silva, J. H. F., & Trevisan, R. E. (2010). Influence of preheating on API 5L-X80 pipeline joint welding with self-shielded flux cored wire. *Welding International*, 19(11), 882-887. <https://doi.org/10.1533/wint.2005.3494>
- [10] Anderson, M. J. (2004). FAQ - Interpretating Lack of Fit, News from Stat-Teaser, Inc. May 2004.
- [11] Kannengiesser, T. & Lausch, T. (2012). Diffusible Hydrogen Content depending on welding and cooling parameters. *Weld World*, 56, 26-33. <https://doi.org/10.1007/BF03321392>
- [12] Liang, P., Xiaogang, L., Cuiwei, D., & Chen, X. (2009). Stress corrosion cracking of X80 pipeline steel in simulated alkaline soil solution. *Materials and Design* 30(5), 1712-1717. <https://doi.org/10.1016/j.matdes.2008.07.012>
- [13] Bericht 5154/2010. (2010). Untersuchung zur Vermeidung der Wasserstoffversprödung beim Lichtbogenbolzen-schweißen an Stahlwerkstoffen, GSI SLV München. (in German)
- [14] Tomić, T., Kralj, S., & Kožuh, Z. (2014). Mathematical model of critical implant stress testing in the weld metal of API 5L X80 steel (Mathematisches Modell für den Implant-Versuch an der Schweißnaht am API 5L X80 Stahl). *Material Science & Engineering Technology (Materialwissenschaft und Werkstofftechnik)*, 45(11), 970-981. <https://doi.org/10.1002/mawe.201400344>

### Authors' contacts:

#### Tanja Tomić

(Corresponding author)  
University North,  
104. brigade 3, 42000 Varazdin, Croatia  
ttomic@unin.hr

#### Lidija Tepeš Golubić

Zagreb University of Applied Sciences,  
Vrbik 8, 10000 Zagreb, Croatia  
University North,  
104. brigade 3, 42000 Varazdin, Croatia

#### Jana Žiljak Gršić

Zagreb University of Applied Sciences,  
Vrbik 8, 10000 Zagreb, Croatia  
University North,  
104. brigade 3, 42000 Varazdin, Croatia

#### Matija Bušić

University North,  
104. brigade 3, 42000 Varazdin, Croatia

# Touchard Series for Solving Volterra Integral Equations Form of the Lane-Emden Equations

Mustapha Dilmi

**Abstract:** This study is concerned by the Collocation method for solving Volterra integral equations form of the Lane-Emden type numerically through the so-called Touchard polynomials, which are essentially binomial polynomials. Where the system of miniature linear equations is solved numerically using the MATALEB program. Then some examples are presented to verify the reliability and effectiveness of the method in addition to the speed of its convergence.

**Keywords:** Collocation Method; Lane-Emden equation; Touchard polynomials; Volterra integral equations

## 1 INTRODUCTION

Let the Lane-Emden equation be in the following form [20]

$$y'' + \frac{\mu}{x} y' + \beta f(x)g(y) = 0, \mu \geq 0, 0 < x \leq 1, \beta \geq 0. \quad (1)$$

With the following initial conditions

$$y(0) = a, y'(0) = 0.$$

Where  $f$  and  $g$  are given functions of  $x$  and  $y$  respectively. In physics and astronomy, the above equation can represent many problems, depending on the change of  $\beta$ .

$$y'' + \frac{\mu}{x} y' + f(x)g(y(x)) = h(x), \mu \geq 0, x > 0.$$

Where  $y(x)$  represents temperature. In the steady state and when  $\mu = 2$ , we call this type the generalized Emden-Fowler equation. As we know, the Volterra integral equation has been raised in many scientific applications, and many numerical solutions to the integral equations and Volterra has been studied by [1, 6, 8, 10, 13, 15]. For methods using the square rule, collocation and interpolation, degenerate kernels, Chebyshev, and Euler series see [9, 11, 13, 15]. The variational iteration method, which is an efficient method, and the variational iteration method for solving Volterra integral form for lane-Emden and Emden Fowler problems in terms of initial and boundary value [20]. Where is the Lane-Emden equation converted to the equivalent Volterra integral form. In this work, we will study the solution to the integral Volterra equation, whose solution is also a solution to the Lane-Emden equation.

## 2 VOLTERRA INTEGRAL AND INTEGRO-DIFFERENTIAL FORM OF THE SINGULAR EMDEN-FOWLER TYPE DIFFERENTIAL EQUATION

Let Emden-Fowler equations be defined in Eq. (1).

$$y'' + \frac{\mu}{x} y' + \beta f(x)g(y) = 0, \quad (2)$$

$$\mu > 1, \beta > 0, y(0) = a, y'(0) = 0.$$

Eq. (2) can be converted to the following form

$$y(x) = a - \frac{\beta}{\mu-1} \int_0^x t \left( 1 - \frac{t^{\mu-1}}{x^{\mu-1}} \right) h(t)g(y(t))dt. \quad (3)$$

By differentiating Eq. (3) twice in a row, and depending on Leibniz's principle, we arrive in the form of the integro-differential equation of Emden-Fowler's equation

$$y'(x) = -\beta \int_0^x \left( \frac{t^\mu}{x^\mu} \right) h(t)g(y(t))dt, \quad (4)$$

$$y''(x) = \beta h(x)g(y(x)) - \beta \int_0^x k \left( \frac{t^\mu}{x^{\mu+1}} \right) f(t)g(y(t))dt.$$

Therefore, for  $\mu = 1$ , the integral form becomes

$$y(x) = a - \beta \int_0^x t \ln \left( \frac{t}{x} \right) h(t)g(y(t))dt.$$

Where we can get it, assuming that  $\mu$  belongs to the  $(\mu \rightarrow 1)$  in Eq. (3). Based on the last results, we set the Volterra integral form of Emden-Fowler equations to the following mathematical form

$$y(x) = \begin{cases} a - \beta \int_0^x t \ln \left( \frac{t}{x} \right) h(t)g(y(t))dt, & \mu=1 \\ a - \frac{\beta}{\mu-1} \int_0^x t \left( 1 - \frac{t^{\mu-1}}{x^{\mu-1}} \right) h(t)g(y(t))dt, & \mu > 1 \end{cases}$$

For the solution of the Eq. (3) In the complete function spaces, usually take it  $C(\Omega)$ , we choose a sequence finite dimensional subspace  $X_n, n \geq 1$  having  $n$  basis functions  $\{T_1, T_2, \dots, T_n\}$  with dimension of  $X_n = n$ . Seeking the approximate function  $y_n \in X$  of the function  $y$  given by

$$y_n = \sum_{k=1}^n \alpha_k T_k(x) \quad (5)$$

Where the expression Eq. (5) describes the truncated Touchard series of the solution of the Eq. (3), with the functions  $\{T_k\}_{0 \leq k \leq n}$  represent the Touchard polynomials and

$\{\alpha_k\}_{0 \leq k \leq n}$  the coefficients to be determined. In other words, we can write Eq. (3)

$$y(x) = a - \frac{\beta}{\mu-1} \int_0^x t \left( 1 - \frac{t^{\mu-1}}{x^{\mu-1}} \right) h(t) g(y(t)) dt, \quad (6)$$

$$r_n(x) = y_n(x) + \frac{\beta}{\mu-1} \int_0^x t \left( 1 - \frac{t^{\mu-1}}{x^{\mu-1}} \right) h(t) g(y(t)) dt - a.$$

Change the variable  $t \rightarrow \varepsilon x$  where the previous Volterra integral can be converted to the Fredholm integral form

$$y(x) = a - \frac{x^2}{\mu-1} \int_0^1 \varepsilon (1 - \varepsilon^{\mu-1}) h(\varepsilon x) g(y(\varepsilon x)) d\varepsilon. \quad (7)$$

### 3 COLLOCATION METHOD WITH TOUCHARD POLYNOMIALS

Choose a selection of distinct points  $x_1, x_2, x_3, \dots, x_n \in \Omega$ , where  $0 < x_1 < \dots < x_n \leq 1$ .

And require:

$$r_n(x_j) = 0, j = 1, 2, \dots, n \quad (8)$$

Then we can replace  $y$  with  $y_n = \sum_{k=1}^n \alpha_k T_k(x)$  so Eq. (7)

becomes. The condition Eq. (8) leads us to determine the coefficients  $\{\alpha_1, \alpha_2, \dots, \alpha_n\}$  solution of the linear system:

$$\begin{aligned} \sum_{k=1}^n \alpha_k T_k(x) &= \\ &= a - \frac{x^2}{\mu-1} \int_0^1 \varepsilon (1 - \varepsilon^{\mu-1}) h(\varepsilon x) g\left(\sum_{k=1}^n \alpha_k T_k(\varepsilon x)\right) d\varepsilon, \quad (9) \\ x &\in [0, 1] \end{aligned}$$

Placing  $x$  with the evaluation points of  $x_1, x_2, x_3, \dots, x_n$  in Eq. (9), we will arrive at the system of equations in the application description

$$\begin{aligned} \sum_{k=1}^n \alpha_k T_k(x_j) &+ \\ &+ \frac{(x_j)^2}{\mu-1} \int_0^1 \varepsilon (1 - \varepsilon^{\mu-1}) h(\varepsilon x_j) g\left(\sum_{k=1}^n \alpha_k T_k(\varepsilon x_j)\right) d\varepsilon = a, \quad (10) \\ x &\in [0, 1]. \end{aligned}$$

Using the quadrature formula with the coefficients  $(\tau_i)$  and weights  $(w_i) = 1$  in the interval  $[0, 1]$  for numerically solving the integration in Eq. (10) Yields

$$\begin{aligned} \sum_{k=1}^n \alpha_k T_k(x_j) &+ \\ &+ \frac{(x_j)^2}{\mu-1} \sum_{k=1}^n \tau_i (1 - \tau_i^{\mu-1}) h(\varepsilon x_j) g\left(\sum_{k=1}^n \alpha_k T_k(\tau_i x_j)\right) w_i d\varepsilon = a, \\ x &\in [0, 1]. \end{aligned}$$

Then the values of  $y(x)$  at any point of  $x \in [0, 1]$  can be approximated by the equation

$$y_n = \sum_{k=1}^n \alpha_k T_k(x_j).$$

We transform Eq. (7) into the following form

$$(\lambda - A)y = f. \quad (11)$$

Where

$$Ay = \int_{\Omega} k(x, \varepsilon) g(y(\varepsilon x))$$

Therefore, Eq. (9) can be written in the following form

$$(\lambda - A)y_n = f. \quad (12)$$

Assume that  $A$  is a compact operator.

**Lemma** if Eq. (11) is uniquely solvable and  $\|y - y_n\| \rightarrow 0$  then Eq. (12) is uniquely solvable.

**Proof.** See [12].

### 3.1 Properties of Touchard polynomials

The  $n^{\text{th}}$  Touchard polynomials  $T_n(x)$  is defined by  $T_0(x) = 1$  and the following recursion

$$T_n(n) = \sum_{k=0}^n \binom{n}{k} (x)^n$$

Noting that, the Touchard polynomial  $T_n(x)$  is polynomials with rational coefficients.

**Table 1** Rational coefficients of the Touchard polynomials.

$n$	$T_n$
0	1
1	$1 + x$
2	$1 + 2x + x^2$
3	$1 + 3x + 3x^2 + x^3$
4	$1 + 4x + 6x^2 + 4x^3 + x^4$
5	$1 + 5x + 10x^2 + 10x^3 + 5x^4 + x^5$
6	$1 + 6x + 15x^2 + 20x^3 + 15x^4 + 6x^5 + x^6$
7	$1 + 7x + 21x^2 + 35x^3 + 35x^4 + 21x^5 + 7x^6 + x^7$
8	$1 + 8x + 28x^2 + 56x^3 + 70x^4 + 56x^5 + 28x^6 + 8x^7 + x^8$
9	$1 + 9x + 36x^2 + 84x^3 + 126x^4 + 126x^5 + 84x^6 + 36x^7 + 9x^8 + x^9$
10	$1 + 10x + 45x^2 + 120x^3 + 210x^4 + 252x^5 + 210x^6 + 120x^7 + 45x^8 + 10x^9 + x^{10}$

### 4 ERROR ANALYSIS

To illustrate the underlying ideas, validity, effectiveness, accuracy and performance of the proposed technique, we analyze several linear Lane-Emden or Emden-Fowler equations. Throughout the calculations, the absolute error between the exacted and approximated solution (error norm) is defined by  $e_r = |y(x_i) - y_n(x_i)|$ .

### 5 ILLUSTRATING EXAMPLES

**Example 1.** Consider the following linear homogeneous Lane-Emden equation

$$y'' + \frac{2}{x}y' - (4x^2 + 6)y = 0, 0 < x \leq 1$$

Subject to initial conditions

$$y(0) = 1, y'(0) = 0$$

The exact solution for this problem is

$$y(x) = e^{-x^2}.$$

This equation is equivalent to the following integral equation

$$y(x) = 1 + \int_0^x \left( \frac{xt - t^2}{x} \right) (4t^2 + 6)y(t) dt, 0 < x \leq 1$$

**Table 2** Approximate and exact solutions for Example 1

$x$	Exact solution $y$	Approx solution $y_n$	Error for $n = 10$
0.0	1.0000E+00	1.0000E+00	3.1086E-15
0.1	1.0101E+00	1.0101E+00	2.2542E-10
0.2	1.0408E+00	1.0408E+00	2.7722E-10
0.3	1.0942E+00	1.0942E+00	2.8983E-10
0.4	1.1735E+00	1.1735E+00	3.1393E-10
0.5	1.2840E+00	1.2840E+00	3.4539E-10
0.6	1.4333E+00	1.4333E+00	3.8359E-10
0.7	1.6323E+00	1.6323E+00	4.4465E-10
0.8	1.8965E+00	1.8965E+00	4.9153E-10
0.9	2.2479E+00	2.2479E+00	7.1219E-10
1	2.7183E+00	2.7183E+00	3.3111E-10

**Example 2.** Consider the Emden-Fowler equation

$$y'' + \frac{2}{x}y' - 2(2x^2 + 3)y = 0, 0 < x \leq 1$$

Subject to initial conditions

$$y(0) = 1, y'(0) = 0$$

This problem has the exact solution

$$y(x) = e^{-x^2}.$$

This equation is equivalent to the following integral equation

$$y(x) = 1 + 2 \int_0^x \left( \frac{xt - t^2}{x} \right) (2t^2 + 3)y(t) dt, 0 < x \leq 1$$

**Table 3** Approximate and exact solutions for Example 2

$x$	Exact solution $y$	Approx solution $y_n$	Error for $n = 10$
0.0	1.0000E+00	1.0000E+00	3.1086E-15
0.1	1.0101E+00	1.0101E+00	2.2542E-10
0.2	1.0408E+00	1.0408E+00	2.7722E-10
0.3	1.0942E+00	1.0942E+00	2.8983E-10
0.4	1.1735E+00	1.1735E+00	3.1393E-10
0.5	1.2840E+00	1.2840E+00	3.4539E-10
0.6	1.4333E+00	1.4333E+00	3.8359E-10
0.7	1.6323E+00	1.6323E+00	4.4465E-10
0.8	1.8965E+00	1.8965E+00	4.9153E-10
0.9	2.2479E+00	2.2479E+00	7.1219E-10
1	2.7183E+00	2.7183E+00	3.3111E-10

**Example 3.** Consider the following Lane-Emden equation

$$y'' + \frac{2}{x}y' + y^\varepsilon = 0, 0 < x \leq 1$$

Subject to initial conditions

$$y(0) = 1, y'(0) = 0$$

For  $\varepsilon = 1$  we have

$$y(x) = 1 - \int_0^x t \left( 1 - \frac{t}{x} \right) y(t) dt, 0 < x \leq 1$$

This problem has the exact solution

$$y(x) = \frac{\sin(x)}{x}$$

**Table 4** Approximate and exact solutions for Example 3

$x$	Exact solution $y$	Approx solution $y_n$	Error for $n = 10$
0.0	1.0000E+00	1.0000E+00	4.4409E-16
0.1	9.9833E-01	9.9833E-01	1.5210E-14
0.2	9.9335E-01	9.9335E-01	1.8097E-14
0.3	9.8507E-01	9.8507E-01	1.7986E-14
0.4	9.7355E-01	9.7355E-01	2.0983E-14
0.5	9.5885E-01	9.5885E-01	5.7065E-14
0.6	9.4107E-01	9.4107E-01	3.6671E-13
0.7	9.2031E-01	9.2031E-01	2.2352E-12
0.8	8.9670E-01	8.9670E-01	1.1019E-11
0.9	8.7036E-01	8.7036E-01	4.5200E-11
1	8.4147E-01	8.4147E-01	1.5982E-10

**Example 4.** Consider the linear Lane-Emden equation

$$y'' + \frac{1}{x}y' - 4(x^2 + 1)y = 0, 0 < x \leq 1$$

Subject to initial conditions

$$y(0) = 1, y'(0) = 0$$

The exact solution for this problem is

$$y(x) = e^{-x^2}.$$

This equation is equivalent to the following integral equation

$$y(x) = 1 + 4 \int_0^x t \ln \left( \frac{t}{x} \right) (t^2 + 1)y(t) dt, k = 1, 0 < x \leq 1$$

**Table 5** Approximate and exact solutions for Example 4

$x$	Exact solution $y$	Approx solution $y_n$	Error for $n = 10$
0.0	1.0000E+00	1.0000E+00	1.2790E-13
0.1	1.0101E+00	1.0101E+00	2.3704E-10
0.2	1.0408E+00	1.0408E+00	3.9754E-10
0.3	1.0942E+00	1.0942E+00	4.8524E-10
0.4	1.1735E+00	1.1735E+00	5.7053E-10
0.5	1.2840E+00	1.2840E+00	6.5991E-10
0.6	1.4333E+00	1.4333E+00	7.6140E-10
0.7	1.6323E+00	1.6323E+00	8.9231E-10
0.8	1.8965E+00	1.8965E+00	1.0330E-09
0.9	2.2479E+00	2.2479E+00	1.3366E-09
1	2.7183E+00	2.7183E+00	6.6797E-10

## 6 CONCLUSION

In this paper, the Touchard series with the Collocation method was introduced in order to solve the Volterra integral equations obtained from the Lane-Emden equations, where we found that the approximate solutions are very close to the exact solutions, that is, the higher the degree  $n$  of the polynomial.

The four examples studied in this paper confirmed the effectiveness of the method and the speed of its convergence. The error obtained through the difference between exact solutions and approximate solutions confirms what was mentioned above.

On the other hand, the obtained solutions of the Volterra integral equations are also solutions of the Lane-Emden equations.

## 7 REFERENCES

- [1] Abbasbandy, S. & Shivanian, E. (2011). A new analytical technique to solve Fredholm's integral equations. *Numer. Algor.*, 56, 27-43. <https://doi.org/10.1007/s11075-010-9372-2>
- [2] Al-Hayani, W., Alzubaidy, L., & Ahmed, E. (2017). Solutions of Singular IVP's of Lane-Emden type by Homotopy analysis method with Genetic Algorithm. *Appl. Math. Inf. Sci.*, 11(2), 407-416. <https://doi.org/10.18576/amis/110208>
- [3] Asadpour, S., Hosseinzadeh, H., & Yazdani, A. (2019). Numerical Solution of the Lane-Emden Equations with Moving Least Squares Method. *Applications and Applied Mathematics*, 14(2), 762 - 776.
- [4] Babolian, E. & Davari, A. (2005). Numerical implementation of Adomian decomposition method for linear Volterra integral equations of the second kind. *Appl. Math. Comput.*, 165, 223-227. <https://doi.org/10.1016/j.amc.2004.04.065>
- [5] Bencheikh, A., Chiter, L., & Abbassi, H. (2017). Bernstein polynomials method for numerical solutions of integro-differential form of the singular Emden-Fowler initial value problems. *J. Math. Computer Sci.*, 17, 66-75. <https://doi.org/10.22436/jmcs.017.01.06>
- [6] Chakrabarti, A. & Martha, S. C. (2009). Approximate solutions of Fredholm integral equations of the second kind. *Applied Mathematics and Computation*, 211, 459-466. <https://doi.org/10.1016/j.amc.2009.01.088>
- [7] Karimi, S. & Aminataei, A. (2010). On the numerical solution of differential equations of Lane-Emden type. *Computers and Mathematics with Applications* 59, 2815-2820. <https://doi.org/10.1016/j.camwa.2010.01.052>
- [8] Kress, R. (1989). *Linear Integral Equations*. Springer-Verlag, Berlin, Heidelberg. <https://doi.org/10.1007/978-3-642-97146-4>
- [9] Maleknejad, K. & Aghazadeh, N. (2005). Numerical solution of Volterra integral equations of the second kind with convolution kernel by using Taylor-series expansion method. *Appl. Math. Comput.*, 161, 915-922. <https://doi.org/10.1016/j.amc.2003.12.075>
- [10] Mamadu, J. & Njoseh, I. (2016). Numerical Solutions of Volterra Equations Using Galerkin Method with Certain Orthogonal Polynomials. *Journal of Applied Mathematics and Physics*, 4, 376-382. <https://doi.org/10.4236/jamp.2016.42044>
- [11] Mirzaee, F. (2012). Numerical Solution for Volterra Integral Equations of the First Kind via Quadrature Rule. *Applied Mathematical Sciences*, 6(20), 969-974.
- [12] Mirzaei, D. & Dehghan, M. (2010). A meshless based method for solution of integral equations. *Appl. Numer. Math.*, 60, 245-262. <https://doi.org/10.1016/j.apnum.2009.12.003>
- [13] Mustafa, G. & Yalçın, Ö. (2010). Chebyshev polynomial approximation for solving the second kind linear Fredholm integral equation. *Journal of the Institute of Science and Technologie*, 26(3), 203-216.
- [14] Nadir, M. (2014). Solving Fredholm integral equations with application of the four Chebyshev polynomials. *Journal of Approximation Theory and Applied Mathematics*, 4, 37-44.
- [15] Nadir, M. & Mustapha, D. (2017). Euler Series solutions for linear Integral equations. *AJMAA*, 14(2), Art. 11, 1-7.
- [16] Rach, R., Wazwaz, A. M., & Duan, J. (2015). The Volterra integral form of the Lane-Emden equation new derivations and solution by the Adomian decomposition method. *J. Appl. Math. Comput.*, 47, 365-379. <https://doi.org/10.1007/s12190-014-0780-7>
- [17] Smarda, Z. & Khan, Y. (2015). An efficient computational approach to solving singular initial value problems for Lane-Emden type equations. *J. Comput. Appl. Math.*, 290, 65-73. <https://doi.org/10.1016/j.cam.2015.04.045>
- [18] Tivonchuk, V. I. (1981). Solution of linear Volterra integral equations by the method of averaging functional corrections in conjunction with splines. *Dnepropetrovsk State University. Translated from Ukrainskii Matematicheskii Zhurnal*, 32(3), 423-431. <https://doi.org/10.1007/BF01089772>
- [19] Wazwaz, A. W. (2002). A new method for solving singular initial value problems in the second-order ordinary differential equations. *Appl. Math. Comput.*, 128, 45-57. [https://doi.org/10.1016/S0096-3003\(01\)00021-2](https://doi.org/10.1016/S0096-3003(01)00021-2)
- [20] Wazwaz, A. W. & Khuri, S. A. (2015). The variational iteration method for solving the Volterra integro-differential forms of the lane-Emden and the Emden-Fowler problems with initial and boundary value conditions. *De Gruyter Open Eng.*, 5, 31-41. <https://doi.org/10.1515/eng-2015-0006>

### Author's contacts:

**Mustapha Dilmi**  
 Department of Mathematics,  
 College of Mathematics and Computer Science,  
 University of M'sila,  
 PO Box 166 Ichebilila, 28000 M'sila, Algeria  
[moustafa.dilmi@univ-msila.dz](mailto:moustafa.dilmi@univ-msila.dz)

# A Novel Method for Solving Multi-objective Shortest Path Problem in Respect of Probability Theory

Maosheng Zheng\*, Jie Yu

**Abstract:** Transportation process or activity can be considered as a multi-objective problem reasonably. However, it is difficult to obtain an absolute shortest path with optimizing the multiple objectives at the same time by means of Pareto approach. In this paper, a novel method for solving multi-objective shortest path problem in respect of probability theory is developed, which aims to get the rational solution of multi-objective shortest path problem. Analogically, each objective of the shortest path problem is taken as an individual event, thus the concurrent optimization of many objectives equals to the joint event of simultaneous occurrence of the multiple events, and therefore the simultaneous optimization of multiple objectives can be solved on basis of probability theory rationally. The partial favorable probability of each objective of every scheme (routine) is evaluated according to the actual preference degree of the utility indicator of the objective. Moreover, the product of all partial favorable probabilities of the utility of objective of each scheme (routine) casts the total favorable probability of the corresponding scheme (routine), which results in the decisively unique indicator of the scheme (routine) in the multi-objective shortest path problem in the point of view of system theory. Thus, the optimum solution of the multi-objective shortest path problem is the scheme (routine) with highest total favorable probability. Finally, an application example is given to illuminate the approach.

**Keywords:** concurrent optimization; favorable probability; multi-objective; probability theory; shortest path

## 1 INTRODUCTION

The shortest path was a classic problem in network optimization. A shortest path problem with single objective has been well solved by Dijkstra's algorithm in 1950s and Floyd's algorithm in 1960s [1]. However in 1990s, some new problems have raised owing to the new development of intelligent technology, communication technology, and information science. These new problems concrete the new aspect of the shortest path problem with multiple objectives, which makes the study of the shortest path problem active again [2-7].

Usually, the minimization of one objective, such as cost, or transportation time, etc., is considered as the general problem of shortest path. However, since the route selection of the transportation network often needs to consider multiple objectives at the same time, such as cost, time, risk, safety, etc., different objectives need to be compromised in the solution processing simultaneously.

The classification and generalization of multi-objective shortest path problem were stated by Current et al. [8]. The main methods for solving multi-objective shortest path problem can be classified into three types:

- 1) Utility function method
- 2) Interactive method
- 3) Production method.

The utility function method requires prior preference information of the decision maker to determine the corresponding utility function and the interactive method uses preference information in the entire problem solving process. The production method could only directly give the set of Pareto optimization or set of approximate optimization solution, it mainly includes dynamic programming method, Pareto labeling method and Pareto ranking method, etc. [9].

For the multi-objective shortest path algorithm, the usual processing method is to linearly weight different objectives, or convert some objectives into constraints. As to the linear weighting method, the determination of its weight is very

problematic. For the constrained shortest path problem, it has been proved to be NP-hard. In fact, above methods not only deviate from the original intention of multi-objective actually, but also consume large time and space, or even unsolved when the scale of the problem is large [10, 11].

The dual-objective shortest path problem is a common situation in the multi-objective shortest path issues. In order to solve the dual-objective shortest path problem, J. Current, C. Revelle, J. Cohon [12] and J. Coutinho-Rodrigues, J. Climaco, J. Current [13] studied the general dual-objective shortest path algorithm and proposed an interactive dual-objective algorithm. In the shortest path problem with dual objectives, it is often necessary to obtain an effective path and then select it. Hansen [14], Climaco and Martins [15] got certain achievement on the acquisition of effective paths for dual objectives.

In this paper, a novel method for solving multi-objective shortest path problem is developed in respect of probability theory. It takes the each objective of the shortest path problem as an individual event analogically, the concurrent optimization of many objectives thus equals to the joint event of simultaneous occurrence of the multiple events. The partial favorable probability of each objective (event) of every scheme (routine) and the total favorable probability of each scheme (routine) are evaluated as the uniquely decisive indexes of the scheme (routine) in the multi-objective shortest path problem, which is in the viewpoint of system theory. Examples are given to illuminate the approach in detail.

## 2 A NOVEL PROBABILITY THEORY - BASED METHOD

### 2.1 Assessment of Favorable Probability of the Probability-Based Method

The recently proposed probability-based multi-objective optimization (PMOO) is in the viewpoint of system theory [16, 17], each objective can be analogically taken as an individual event, and the concurrent optimization of many

objectives thus equals to the joint event of simultaneous occurrence of multiple events in the respect of probability theory. Therefore, the problem of concurrent optimization of many objectives is thus converted into a joint probabilistic problem of simultaneous occurrence of multiple events analogically. Furthermore, the preference degree of utility of each objective (event) of a scheme is transferred into its partial favorable probability. The concurrent optimization of multiple objectives is described by the integral (overall) event, its total (overall) favorable probability is thus rationally the product of all the partial favorable probabilities of all individual events of the scheme, which is in the respect of probability theory. In the evaluation, the utility of the objective is preliminarily classified as unbeneficial or beneficial type in accordance with the characteristic of the preference or role in the assessment. The methodology of PMOO is shown in Fig. 1.

The meanings of the variables and factors in Fig. 1 are as following:

$P_{ij}$  expresses the partial favorable probability of the  $j^{\text{th}}$  performance utility indicator of the  $i^{\text{th}}$  candidate scheme,  $X_{ij}$ ;  $n$  reflects the total number of the candidate scheme;  $m$  shows the total number of the performance (objective);  $X_j$  indicates the arithmetic value of the  $j^{\text{th}}$  performance utility indicator;  $X_{j\max}$  and  $X_{j\min}$  express the maximum and minimum values of the  $j^{\text{th}}$  performance utility indicator, respectively;  $\alpha_j$  and  $\beta_j$  represent the normalized factors of the  $j^{\text{th}}$  performance utility indicator  $X_{ij}$  in beneficial status and unbeneficial status, individually; the beneficial status or unbeneficial status of the  $j^{\text{th}}$  performance utility indicator  $X_{ij}$  is specified according to its particular preference or role in the problem;  $P_i$  is the total (overall) favorable probability of the  $i^{\text{th}}$  candidate scheme [16, 17].

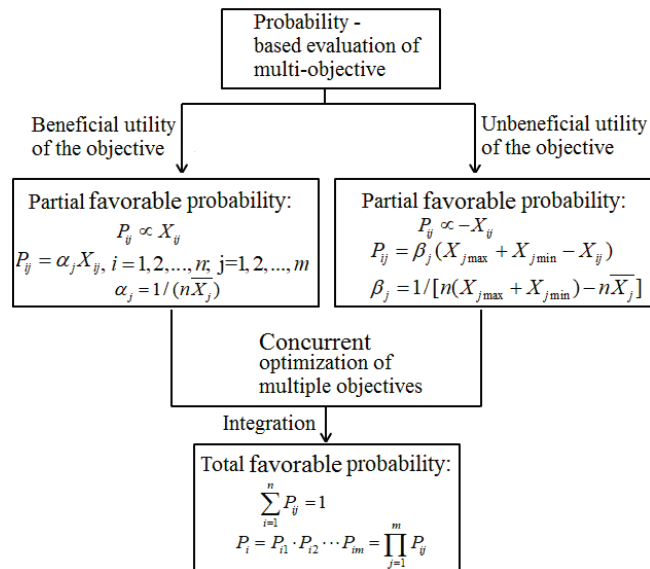


Figure 1 Evaluation of the PMOO methodology

The probability-based multi-objective optimization is a brand new methodology, which has the potential applications in many fields concerning multi - objectives, such as material

selection, mechanical design, programming problem, operation research, engineering design, etc.

## 2.2 Assessment Procedure of Concurrent Optimization of Shortest Path Problem with Many Objectives in Respect of Probability Theory

### 1) Assessment of objective and event

As to the multi-objective shortest path problem, the cost, time, risk, safety, etc., are different objectives, of which each objective can be analogically taken as individual event. Thus, the multi-objective shortest path problem is transferred into the joint probabilistic problem of simultaneous occurrence of multiple events equivalently. The accumulated cost, time, risk, safety, etc., in each scheme (route) are accounted according to the actual interval of each scheme (route) individually.

### 2) Assessment of favorable probability

The partial favorable probabilities of cost, time, risk, safety, etc., are assessed according to their specific function or characteristic of the preference for every scheme analogically. Finally, the overall (total) favorable probability of the integral event is the product of all the partial favorable probabilities of all events of each scheme (route) in the respect of probability theory, it thus completes the concurrent optimization of multi-objective, and provides the decisively unique indicator of each scheme (routine) in the shortest path problem with many objectives.

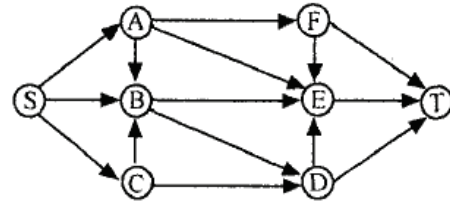


Figure 2 Transportation Network

### 3) Solution of the multi-objective shortest path problem

At last, the optimal solution of the multi-objective shortest path problem is the specific scheme (routine), which is with highest total favorable probability.

## 3 APPLICATION IN IMPORTANT GOODS TRANSPORTATION SHORTEST PATH PROBLEM

The important goods transportation path problem is a significant thing; the distance, the cost, and accident rate are taken as the evaluating objectives [18].

The transportation network is shown in Fig. 2. Tab. 1 shows the basic values of each interval path [18]. The current problem is to find the multi-objective shortest path of this transportation for important goods.

As can be seen from Fig. 2, the transportation process is from the start point S to destination T. After every round of the  $k$  shortest path searching, the algorithm produces a multi-objective shortest path or alternative path by the intersection

[18], which is shown in Tab. 2 for the 13 routes and accounted from the data in Tab. 1 and Fig. 2.

**Table 1** Basic values of each interval path

Interval path	Objective		
	Distance (km)	Cost (¥RMB)	Accident rate (%)
SA	52	120	0.20
SB	48	100	0.38
SC	45	84	0.15
AB	42	30	0.40
CB	29	70	0.60
AF	40	60	0.50
AE	35	50	0.45
BE	38	90	0.10
BD	23	30	0.80
CD	42	30	0.20
FE	60	75	0.70
DE	31	50	0.35
FT	48	30	0.45
ET	40	80	0.50
DT	50	200	0.40

**Table 2** Selected alternative paths and their target values

No.	Route	Distance, $d$ (km)	Cost, $c$ (¥RMB)	Accident rate, $a$ (%)
1	S-B-D-T	121	330	1.58
2	S-B-E-T	126	270	0.98
3	S-A-E-T	127	250	1.15
4	S-C-D-T	137	314	0.75
5	S-A-F-T	140	210	1.15
6	S-B-D-E-T	142	260	2.03
7	S-C-B-D-T	147	384	1.95
8	S-C-B-E-T	152	324	0.9
9	S-C-D-E-T	158	244	1.20
10	S-C-B-D-E-T	168	314	2.40
11	S-A-B-E-T	172	320	1.20
12	S-A-B-D-E-T	188	310	2.25
13	S-A-F-E-T	192	335	1.90

### 1) Without considering weight factor

Here in this section, let's study the transportation path problem under condition of each objective with equal importance, i.e., without comparable weight factor.

In this transportation problem, the objectives (events), i.e., the distance, the cost, and accident rate are all unbeneficial type indexes for each scheme in the assessment. The evaluations of partial favorable probabilities and the total favorable probabilities  $P_i$  for each of the five possible transport options can be conducted according to Fig. 1.

**Table 3** Assessments of partial favorable probabilities and the total favorable probabilities for each scheme from S to T

No.	$P_d$	$P_a$	$P_c$	$P_i \times 10^4$	Rank
1	0.0915	0.0684	0.0730	4.5699	7
2	0.0891	0.0840	0.1009	7.5499	2
3	0.0886	0.0892	0.0930	7.3485	3
4	0.0838	0.0726	0.1116	6.7917	4
5	0.0824	0.0996	0.0930	7.6297	1
6	0.0815	0.0866	0.0521	3.6733	9
7	0.0791	0.0544	0.0558	2.4022	10
8	0.0767	0.0700	0.1046	5.6166	6
9	0.0738	0.0907	0.0907	6.0748	5
10	0.0691	0.0726	0.0349	1.7486	13
11	0.0672	0.0710	0.0907	4.3262	8
12	0.0596	0.0736	0.0418	1.8347	12
13	0.0576	0.0672	0.0581	2.2495	11

Tab. 3 presents the partial favorable probabilities and the total favorable probabilities  $P_i$  enlarged by  $10^4$  for each of the five possible transport options from S to T. Tab. 3 shows that scheme No. 5 S-A-F-T exhibits the highest total favorable probability, which might be taken as our optimum route.

### 2) Considering weight factor

If there is weight factor to reflect the comparable importance of the objective, the weight factor can be taken as the exponent of partial favorable probability in the product of individual partial favorable probability for the total favorable probability assessment [16], i.e.,  $P_i = P_{i1}^{w_1} \cdot P_{i2}^{w_2} \cdot \dots \cdot P_{im}^{w_m}$ , in which  $w_j$  expresses the weight factor of the  $j^{\text{th}}$  objective.

Here, for this problem, let us assume the weight factors for the distance, the cost, and accident rate are 0.1, 0.4 and 0.5, respectively, thus the evaluation can be conducted accordingly. Tab. 4 gives the partial favorable probabilities and the total favorable probabilities enlarged by  $10^2$  for each of the five possible transport options from S to T with the weight factors of 0.1, 0.4 and 0.5, individually. Tab. 4 shows that scheme No. 5 (S-A-F-T) displays the highest total favorable probability  $P_i$  luckily, which might be selected as our optimum route.

**Table 4** Assessments of partial favorable probabilities and the total favorable probabilities of each scheme from S to T with weight factors (weighted 0.1, 0.4, 0.5)

No.	$P_d$	$P_c$	$P_a$	$P_i \times 10^2$	Rank
1	0.0915	0.0684	0.0730	7.2761	8
2	0.0891	0.0840	0.1009	9.2600	2
3	0.0886	0.0892	0.0930	9.1006	4
4	0.0838	0.0726	0.1116	9.1306	3
5	0.0824	0.0996	0.0930	9.4413	1
6	0.0815	0.0866	0.0521	6.6740	9
7	0.0791	0.0544	0.0558	5.7209	11
8	0.0767	0.0700	0.1046	8.6357	6
9	0.0738	0.0907	0.0907	8.8850	5
10	0.0691	0.0726	0.0349	5.0062	13
11	0.0672	0.0710	0.0907	7.9803	7
12	0.0596	0.0736	0.0418	5.4340	12
13	0.0576	0.0672	0.0581	6.1522	10

## 4 CONCLUSION

From above analysis and discussion, a probability-based shortest path approach is proposed. In the evaluation, each objective is taken as an individual event analogically; the favorable probability of each objective is evaluated according to its preference degree of the corresponding objective (event) individually; the concurrent optimization of many objectives equals to the simultaneous occurrence of the multiple events with their favorable probabilities, which thus completes the concurrent optimization of multiple objectives shortest path rationally; under condition of weight factor existence, the weight factor can be taken as the exponent of partial favorable probability in the product of individual partial favorable probability for the total favorable probability assessment.

### Conflict Statement

There is no conflict of interest.

## 5 REFERENCES

- [1] Dijkstra, E. W. (1959). A note on two problems in connection with graphs. *Num. Math.*, 1, 269-271. <https://doi.org/10.1007/BF01386390>
- [2] Erciyes, K. (2021). *Algebraic Graph Algorithms*. Springer Nature Switzerland AG, Cham, Switzerland. <https://doi.org/10.1007/978-3-030-87886-3>
- [3] Korte, B. & Vygen, J. (2018). *Combinatorial Optimization Theory and Algorithms 6<sup>th</sup> Ed.* Springer-Verlag GmbH, Berlin, Germany. <https://doi.org/10.1007/978-3-662-56039-6>
- [4] Sepehrifar, M. K., Fanian, A., & Sepehrifar, M. B. (2020). Shortest Path Computation in a Network with Multiple Destinations. *Arabian Journal for Science and Engineering*, 45, 3223-3231. <https://doi.org/10.1007/s13369-020-04340-w>
- [5] Wakuta, K. (2001). A multi-objective shortest path problem. *Math. Meth. Oper. Res.*, 54, 445-454. <https://doi.org/10.1007/s001860100169>
- [6] Ren, Y., Ay, A., & Kahveci, T. (2018). Shortest path counting in probabilistic biological networks. *BMC Bioinformatics*, 19, No. 465. <https://doi.org/10.1186/s12859-018-2480-z>
- [7] AliAbdi, A., Mohades, A., & Davoodi, M. (2021). Constrained shortest path problems in bi-colored graphs: a label-setting approach. *GeoInformatica*, 25, 513-531. <https://doi.org/10.1007/s10707-019-00385-8>
- [8] Current, J. & Marsh, M. (1993). Multi-objective transportation network design and routing problems: taxonomy and annotation. *European Journal of Operational Research*, 65, 1-15. [https://doi.org/10.1016/0377-2217\(93\)90140-l](https://doi.org/10.1016/0377-2217(93)90140-l)
- [9] Hao, G., Zhang, D., & Feng, D. (2007). Model and algorithm for shortest path of multiple objectives. *Journal of Southwest Jiaotong University*, 42(5), 641-646.
- [10] Wei, H., Pu, Y., & Li, J. (2005). An approach to bi-objective shortest path. *Systems Engineering*, 23(7), 113-117.
- [11] Hao, G., Zhang, D., & Wang, D. (2007). A fast algorithm for bi-objective shortest path. *Journal of Highway and Transportation Research and Development*, 24(11), 96-104.
- [12] Current, J., Reville, C., & Cohon, J. (1990). An interactive approach to identify the best compromise solution for two objective shortest path problems. *Computer & Ops. Res.*, 17(2), 187-198. [https://doi.org/10.1016/0305-0548\(90\)90042-6](https://doi.org/10.1016/0305-0548(90)90042-6)
- [13] Coutinho-Rodrigues, J., Climaco, J., & Current, J. (1999). An interactive bi-objective shortest path approach: search for unsupported non-dominated solutions. *Computer & Ops. Res.*, 26, 789-798. [https://doi.org/10.1016/S0305-0548\(98\)00094-X](https://doi.org/10.1016/S0305-0548(98)00094-X)
- [14] Hansen, P. (1979). Bicriterion path problems. In Fandel, G., Gal, T. Ed., *Multiple criteria decision making theory and application*. 109-127, Springer Berlin, Heidelberg. [https://doi.org/10.1007/978-3-642-48782-8\\_9](https://doi.org/10.1007/978-3-642-48782-8_9)
- [15] Climaco, J. C. N. & Martins, E. Q. V. (1982). A criterion shortest path algorithm. *European Journal of Operational Research*, 11, 399-404. [https://doi.org/10.1016/0377-2217\(82\)90205-3](https://doi.org/10.1016/0377-2217(82)90205-3)
- [16] Zheng, M., Yu, J., Teng, H., Cui, Y., & Wang, Y. (2024). *Probability-Based Multi-objective Optimization for Material Selection*. 2nd ed., Springer Science and Business Media LLC, Singapore. <https://doi.org/10.1007/978-981-99-3939-8>
- [17] Zheng, M., Wang, Y., & Teng, H. (2021). A new "intersection" method for multi-objective optimization in material selection. *Technicki Glasnik*, 15(4), 562-568. <https://doi.org/10.31803/tg-20210901142449>
- [18] Kang, T., Zhang, X., Wang, Z., & He, S. (2011). Algorithm for shortest path of multi-objectives based on *k* short path algorithm. *Journal of Changzhou Institute of Technology*, 34(3, 4), 26-27, 33.

## Authors' contacts:

**Maosheng Zheng**  
(Corresponding author)  
School of Chemical Engineering,  
Northwest University,  
No. 229 Taibai North Road,  
Xi'an, 710069, China  
E-mail: mszhengok@aliyun.com

**Jie Yu**  
School of Life Science & Technology,  
Northwest University,  
No. 229 Taibai North Road,  
Xi'an, 710069, China

# Parametric Study for Optimising Building Form and Height: An Approach toward Net Zero Energy & Carbon in Buildings

Abdelhakim Walid Makhoulfi\*, Samira Louafi

**Abstract:** Due to the excessive use of natural resources and fossil fuels, our planet has started to show its weak points. Several ecological and economic crises have occurred in the last decades. The building sector is held primarily responsible for one-third of global energy consumption and greenhouse gas emissions, and the advent of COVID-19 has not improved this with its containment. For this reason, improving the energy efficiency of buildings and reaching the net zero concept have become the primary objectives of all policies. Several measures are to be undertaken to achieve this concept, ranging from passive and active strategies to the use of renewable energy. This work aims to analyse and study the morphology of the building with geometric plan and height variables to know their influences on the energy consumption of residential buildings in three different types of Algerian climates, semi-arid, arid, and Mediterranean. Using SketchUp and the cloud-based simulation tool Sefaira, the results showed that the triangular-shape based plan has the best energy consumption, allowing a reduction of 18% from the worst-case scenario, and that the difference in height can save up to 17.5%, which is worth 51 kWh/m<sup>2</sup>/year.

**Keywords:** building morphology; energy use intensity; greenhouse gases; net zero energy; residential buildings

## 1 INTRODUCTION

Strong economic growth and rapid urbanisation have resulted in standardisation and flatness in building environmental design, increasing both energy demands and greenhouse gas emissions in the building sector [1]. As a result, this sector has also become responsible for about one-third of global energy and carbon emissions and more than half of the world's electricity consumption [2].

Most of this energy is derived from air conditioning in hot climates and space heating in cold climates. At this rate, the global energy consumption and carbon emissions of buildings is expected to increase at an average annual rate of 1.5% from 2012 to 2040 [1]. Global warming resulting from this increase has become the most pressing issue facing the planet today [3]. Continuing with this trend, a global warming of 2 degrees would affect people and nature. One third of the world's population would be regularly exposed to high heat, which would lead to health problems [4].

Demand for the building sector may increase further in the future due to economic and demographic growth in southern hemisphere regions such as Africa [5]. Because of this demand and the lack of housing, Algeria has experienced a standardisation of housing types in the different regions of the country [6], resulting in the same conceptual and architectural characteristics for different needs, aiming more at the quantity than the quality, generating typical buildings that does not meet the environmental needs or the needs of users.

The residential building sector is one of the largest consumers of energy in Algeria, responsible for over 30% of CO<sub>2</sub> emissions and 36.6% of energy consumption, with an annual increase that continues to grow (2.6% compared to 2018, 17% compared to 2017) [7]. With this in mind, Algeria has tried to develop some programs, such as the programme of the national agency for the promotion and rationalisation of energy use (APRUE), the Algerian national programme of energy efficiency for the building sector 2016 and the

renewable energy program, which aims to improve energy efficiency and reduce both the growth of energy demand and dependence on fossil fuels by using more renewable energy [8].

At the Conference of the Parties 26 (COP26), adhering countries were asked to present ambitious energy and emission reduction targets for 2030, which are in line with the main objective of this COP, namely to ensure global net zero by mid-century [4]. As the sector consuming most of the world's energy, we can conclude that the building sector is also a element of this energy transition, which is becoming necessary [9]. An energy transition in the building sector means ensuring minimum energy consumption in order to achieve optimal living comfort and use of the building [10].

In this context, the topic of Net Zero Energy Buildings (NZEB) has received increasing attention in recent years. The European Energy Performance of Buildings Directive (EPBD) defines it as a building with a very high energy performance, while the remainder must be supplied by renewable energy sources located on site or nearby. In other words, a NZEB combines the design of buildings with high energy efficiency systems and the use of on-site renewable energy [2]. Torcellini et al. also define NZEB as a building whose energy consumption is reduced to balance energy demand with energy supply from renewable energy technologies [11].

The transition to NZEB can be done by following a path based on passive bioclimatic design and then using energy-saving systems to finally balance the rest with renewable energy. The integration of passive design measures into buildings has been the subject of much research, with one of its measures being the optimization of building morphology. According to Pacheco, the design phase of a building is the best time to study and integrate passive strategies. When these strategies are implemented at the very beginning of the construction phase, it allows for a reduction in the implementation costs compared to the case where they would be installed during the later stages of the construction. One

of these strategies is the study of the building morphology that influences the heating and cooling requirements, which can be done by studying the following indices: compactness, form factor, and climate [12]. The studies of Menezo et al. on a single morphological group (parallelepiped), which was chosen for its representativeness of the majority of the structures already built, have shown that the more compact the building, the lower the energy consumption. And that climatic variation (temperatures, solar irradiation) is one of the most important parameters in the study of building morphology [13]. Catalina et al.'s various works confirm that building morphology is an important design parameter in the process of finding an energy-efficient project, with a significant impact on daylighting [14]. Straube says that the ratio of envelope area to floor area is important in all building types and that simple, more compact forms are better in terms of energy efficiency, but also less expensive to build and maintain. He points out that the German energy code goes so far as to prescribe higher thermal resistance values for less compact buildings than for others [15]. Hemsath & Alagheband Bandhosseini were able to determine with a sensitivity analysis on the morphology of the building by studying different ratios of geometric dimensioning and different variables of stacking in height, that these two aspects have, in some cases, depending on the location and climate, a greater impact on the energy performance of a building than the materials used in the envelope or other energy-efficiency variables [16].

That is why our article aims to fill the various gaps in knowledge about the impact of building morphology on energy consumption in the three Algerian climates studied. The research will take place on a basic parallelepiped building with a residential function, whose characteristics, configuration, and structure represent a typical and standard reference case of the Algerian building stock, so that subsequently several other variables of shape and height are introduced.

The first part of this research uses a simulation tool, which is the Sefaira plugin integrated into the modelling software SketchUp, to collect information on the impact of the morphology of the building on the energy consumption and emissions of the different variables. The second part aims to calculate the cost that can be saved by changing variables, to finally have optimal variables for each climate.

## 2 METHODS

The purpose of this article is to compare the different performances of eight types of form: rectangular, square, triangular, trapezoidal, circular, H, O and C; and eight variables of height, which are: 2, 3, 4, 5, 13, 26, 39, and 52 floors, under three different climates Algerian climates, semi-arid with the climate of Constantine, arid with the climate of Ghardaïa and Mediterranean with the climate of Algiers. The goal is to generate a comparative analysis of the various variables to see how they differ in terms of energy performance, CO<sub>2</sub> emissions, and economic aspects, and to try to provide an optimal shape and height for each climate (Based on our comprehensive observations, studies of the

Algerian building stock and the state of the art, the aforementioned variables were considered to be the most representative of the basic forms and heights).

In order to have a fair comparison with comparable results, all the shapes and heights used are made with the same construction materials established according to the DTR3.2/4 and summarized in Tab. 1 [17] and with the same fenestration ratio (22%).

**Table 1** Components of the basic model

		Thickness (m)	$\lambda$ (Wm <sup>-1</sup> K <sup>-1</sup> )	R (m <sup>2</sup> KW <sup>-1</sup> )	U-Value (Wm <sup>-2</sup> K <sup>-1</sup> )
External wall	Plaster	0.02	0.35	0.06	0.95
	Brick	0.10	0.48	0.21	
	Air gap	0.05	0.11	0.45	
	Brick	0.15	0.48	0.31	
	Cement	0.02	1.15	0.02	
Internal wall	Plaster	0.02	0.35	0.06	3.10
	Brick	0.10	0.48	0.21	
	Plaster	0.02	0.35	0.06	
Floor	Tile	0.01	2.1	0.00	5.63
	Mortar	0.02	1.15	0.02	
	Slab	0.20	1.45	0.14	
	Mortar	0.02	1.15	0.02	
Roof	Bitumen	0.02	0.23	0.09	4.13
	Slab	0.20	1.45	0.14	
	Mortar	0.02	1.15	0.02	

The study of the different shapes and heights has been relativised by using the formula of compactness and relative compactness to facilitate the comparison.

The geometry and morphology of the building can be defined using the building form factor ( $L_b$ ) (also called building characteristic length), which is defined as the ratio of the heated volume of the building (Volume) to the sum of all heat loss surfaces that are in contact with the exterior, the ground or adjacent unheated spaces (Exterior surfaces) (see Eq. (1) [14].

$$L_b = \frac{\text{Volume}}{\text{Exterior surfaces}}. \quad (1)$$

Another indicator that can be used is the relative compactness of the building ( $R_c$ ). The  $R_c$  of a shape is derived from the comparison of its volume to area ratio to the most compact shape with the same volume (see Eq. (2)) [14].

$$R_c = \frac{\left(\frac{V}{S}\right)_{\text{Building}}}{\left(\frac{V}{S}\right)_{\text{Ref Form}}} = \frac{(\text{Surface Area})_{\text{Ref Form}}}{(\text{Surface Area})_{\text{Building}}}. \quad (2)$$

The methodology and path used can be summarised in Fig. 1.

## 3 RESULTS AND DISCUSSION

Using the data for occupancy, HVAC, building materials, footprint, height, and volume, it was found that the results generated by the simulation differ from climate to

climate, with the highest total consumption for the Constantine climate, followed by the Ghardaïa climate, and finally by the Algiers climate.

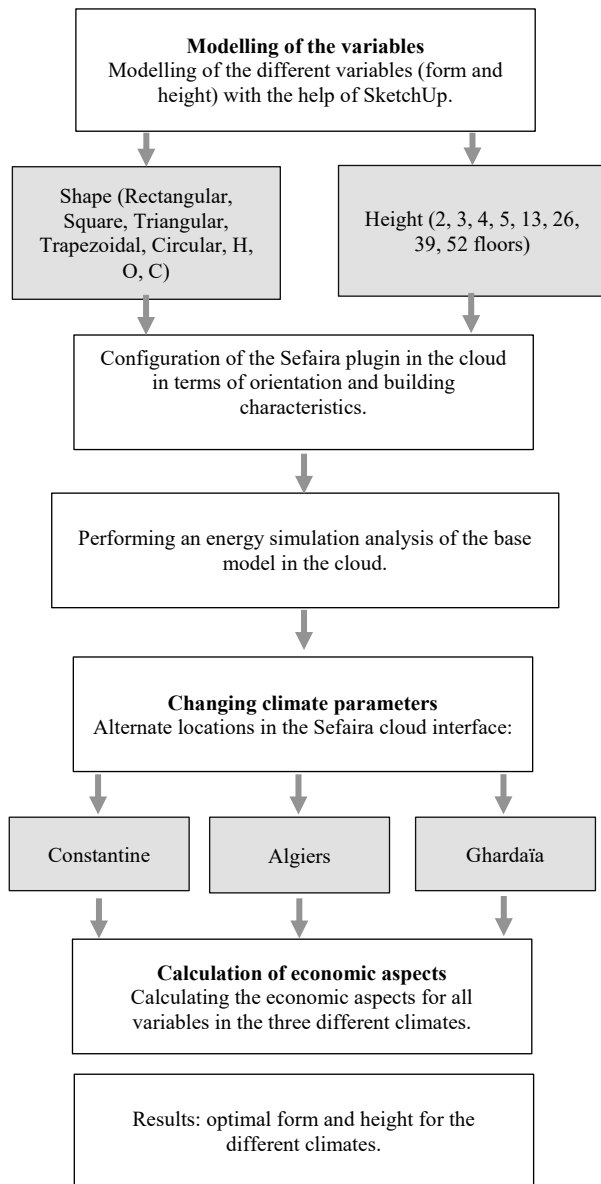


Figure 1 Overview of the flow and arrangement of research methods

For the semi-arid climate of Constantine, the most energy-efficient shape, is the triangular, with a savings of 12.9 kWh/m<sup>2</sup>/year with the basic parallelepiped shape, and a total of 55.3 kWh/m<sup>2</sup>/year from the worst case.

For the Mediterranean climate of Algiers, the change in shape does not allow for a big difference in energy consumption, with the cubic shape being the most economical, allowing to save 2.1 kWh/m<sup>2</sup>/year on the basic shape, with a maximum saving of 13.8 kWh/m<sup>2</sup>/year compared to the most unfavourable shape.

For the arid climate of Ghardaïa the results are almost the same as for Constantine, but with a clear decrease in energy consumption. For this climate, the difference between the most optimum form (Triangle) and the basic form

(Rectangle) is 7.1 kWh/m<sup>2</sup>/year, and 31.7 kWh/m<sup>2</sup>/year with the most unfavourable form (C), as seen in Fig. 2.

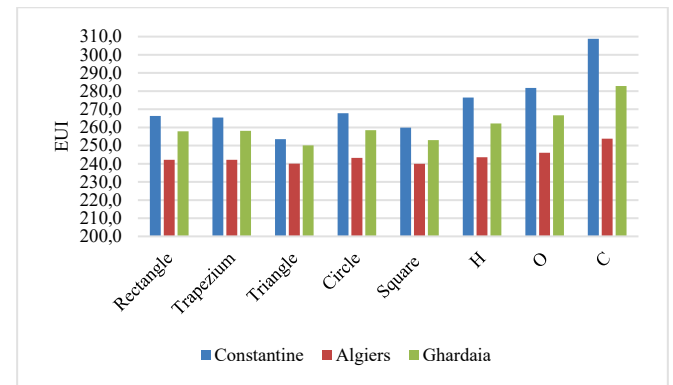


Figure 2 Energy consumption of different forms in the three climates

Table 2 The different simulated forms and their initial data

Type	Foot print m <sup>2</sup>	Height m	Perimeter m	Volume m <sup>3</sup>	Exterior Surface m <sup>2</sup>	$L_b$	$R_c$
	200	15.30	60.00	3060	1318	2.32	0.89
	200	15.30	62.36	3060	1354	2.26	0.86
	200	15.30	64.72	3060	1390	2.2	0.84
	200	15.30	50.15	3060	1167	2.62	1
	200	15.30	56.57	3060	1266	2.42	0.92
	200	15.30	90.00	3060	1777	1.72	0.66
	200	15.30	107.20	3060	2040	1.5	0.57
	200	15.30	88.48	3060	1754	1.74	0.67

After calculating the different indicators, such as the building shape factor ( $L_b$ ) and the relative compactness factor ( $R_c$ ) represented in Tab. 2 we deduced that the most compact shape is the cylindrical shape, which was used as a reference shape for the calculation of the relative compactness, followed by the cube, the parallelepiped, the trapezoidal shape, the triangular shape, the C-shape, the H-shape, and finally the O-shape. It seems that the compactness of the shapes is not a decisive element and that it does not have a great effect on the energy consumption, based on the results we gathered. The number of three-dimensional junctions (corners) seems to be the most decisive element in increasing energy consumption, as it can be seen for the different climates with the triangular base form as the optimal shape and the H, O, or C shapes as the most unfavourable shapes.

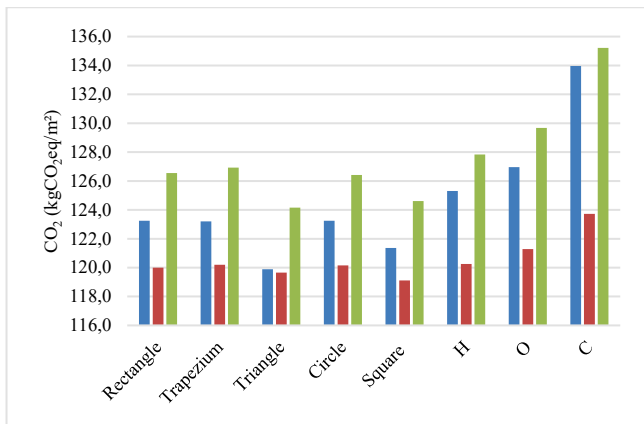


Figure 3 CO<sub>2</sub> emissions of different forms in three different climates.

For the CO<sub>2</sub> emissions obtained from the simulation software, we could note that the emissions in the climate of Ghardaïa are the greatest, followed by Constantine and then by Algiers. However, the order of the various forms is nearly identical to the order of energy consumption, allowing a maximum reduction between the optimal and the most unfavourable forms of 14.1 kgCO<sub>2</sub>eq/m<sup>2</sup>, 11 kgCO<sub>2</sub>eq/m<sup>2</sup>, 4.6 kgCO<sub>2</sub>eq/m<sup>2</sup> for the climates of Constantine, Ghardaïa and Algiers. It can be noted that the CO<sub>2</sub> emissions are related to the consumption of heating and air conditioning than to the total consumption of the building, as seen in Fig. 3.

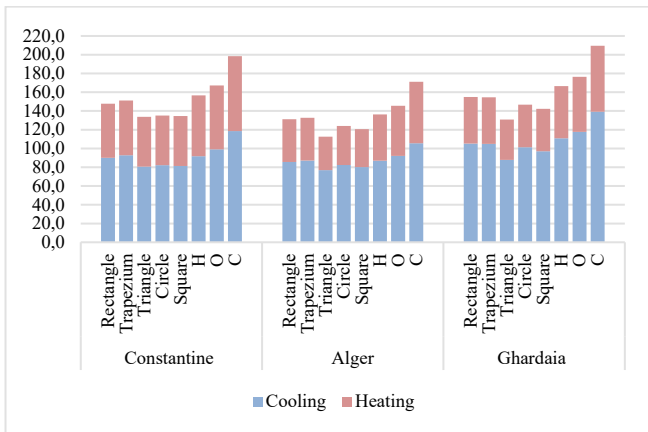


Figure 4 Heating and cooling consumption of different heights in three different climates

For air conditioning, there is a similarity across all climates with the triangular shape as the most optimal shape, followed by the square and circular shape. For heating, the regions of Algiers and Ghardaïa share the same optimal shape as they do air conditioning, but with a change for the city of Constantine, which is now the circular shape as seen in Fig. 4.

Thanks to the different changes in shape, a budgetary saving in energy costs can be made compared to the basic shape (rectangular), with a maximum of -54 DA/m<sup>2</sup>/year for the city of Constantine, -9.1 DA/m<sup>2</sup>/year for the city of Algiers, and -33 DA/m<sup>2</sup>/year for Ghardaïa. Conversely, by choosing the most unfavourable form (O), one can arrive at a rate of loss equal in maximum to 177 DA/m<sup>2</sup>/year for the city

of Constantine, 48.6 DA/m<sup>2</sup>/year for the city of Algiers, and 104 DA/m<sup>2</sup>/year for the city of Ghardaïa. Due to changes in shape. All the results are summarised in Fig. 5.

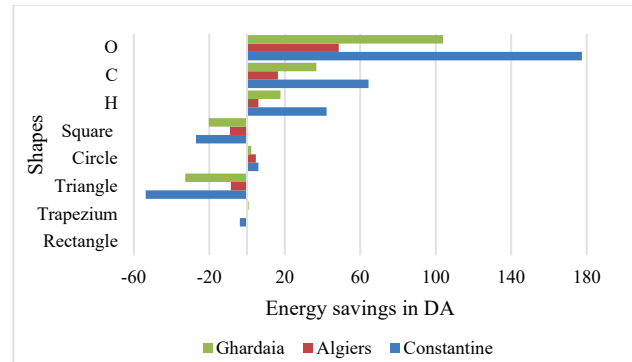


Figure 5 Economic potential of different forms in three different climates

The results concerning the change in shape can be summarised in Tab. 3, ranking the various shapes from the most optimal form, identified as number 1, to the least favourable, denoted as number 8:

Table 3 Simulation results summary of different forms

	1	2	3	4	5	6	7	8
EUI								
Constantine	T	S	Tz	R	C	H	O	C
Alger	S	T	R	Tz	C	H	O	C
Ghardaïa	T	S	R	Tz	C	H	O	C
CO <sub>2</sub>								
Constantine	T	S	Tz	R	C	H	O	C
Alger	S	T	R	Tz	C	H	O	C
Ghardaïa	T	S	C	R	Tz	H	O	C
Air conditioning								
Constantine	T	S	C	R	Tz	H	O	C
Algiers	T	S	C	R	H	Tz	O	C
Ghardaïa	T	S	C	Tz	R	H	O	C
Heating								
Constantine	C	T	S	R	Tz	H	O	C
Algiers	T	S	C	R	Tz	H	O	C
Ghardaïa	T	S	C	Tz	R	H	O	C
Economy								
Constantine	T	S	Tz	R	C	H	O	C
Algiers	S	T	R	Tz	C	H	O	C
Ghardaïa	T	S	R	Tz	C	H	O	C
Optimal								
Constantine	T	S	Tz	R	C	H	O	C
Algiers	S	T	R	Tz	C	H	O	C
Ghardaïa	T	S	C	Tz	R	H	O	C

With: T = Triangle; Tz = Trapezium; R = Rectangle; S = Square; C = Circle

Using the same data in terms of occupancy, HVAC, building materials, and the footprint of the basic module, which is a rectangular shape and changes with the number of floors, it could be seen that there was a change in energy consumption, and this also varied for each climate.

The Constantine climate has the highest energy consumption compared to the other climates, with a maximum of 303.8 kWh/m<sup>2</sup>/year for the 2-story building. The 26-storey building has the most optimal consumption and saves up to 52.7 kWh/m<sup>2</sup>/year. It should be noted that the results for the Algiers climate are similar and that there is

only a slight difference between the optimal number of floors (4 floors) and the most energy-consuming number of floors (52 floors) of about 3.8 kWh/m<sup>2</sup>/year. The climate of Ghardaïa also does not have a big difference between the optimal number of floors (13 floors) and the most energy-consuming number of floors (2 floors), with about 7.3 kWh/m<sup>2</sup>/year. It can be seen that the variation in energy consumption does not have a specific relationship with the number of floors, but that there is a trend in all climates of decreasing EUI until an optimal height is reached, and then increasing again as the number of floors increases.

**Table 4** The different simulated heights and their initial data

N° Levels	Surface m <sup>2</sup>	Footprint m <sup>2</sup>	Height m	Perimeter m	Volume m <sup>3</sup>	Surface, Ext m <sup>2</sup>	$L_b$	$R_c$
2	400	200	6.12	60	1224	767	1.6	1.00
3	600	200	9.18	60	1836	951	1.93	0.81
4	800	200	12.24	60	2448	1134	2.16	0.68
5	1000	200	15.30	60	3060	1318	2.32	0.58
13	2600	200	39.78	60	7956	2787	2.85	0.28
26	5200	200	79.56	60	15912	5174	3.08	0.15
39	7800	200	119.34	60	23868	7560	3.16	0.10
52	10400	200	159.12	60	31824	9947	3.2	0.08

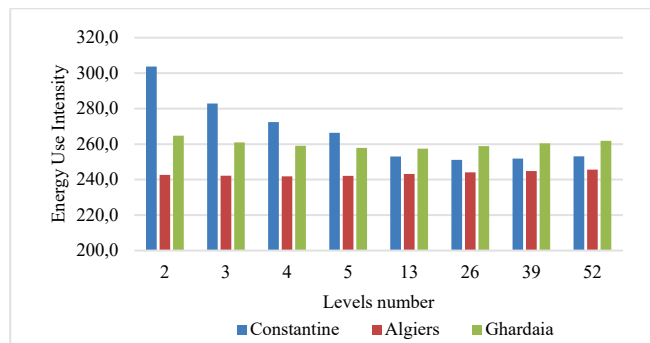


**Figure 6** Energy consumption of different building heights in three different climates

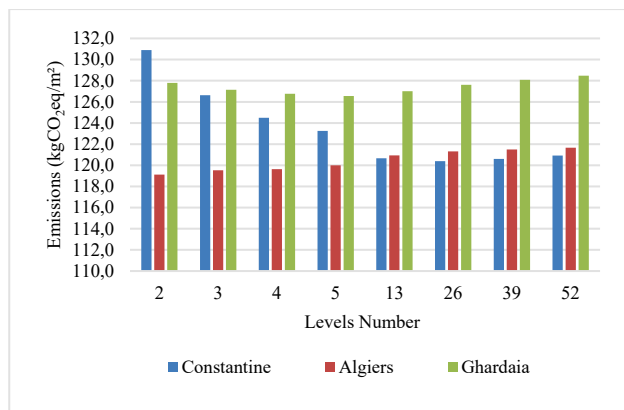


**Figure 7** CO<sub>2</sub> emissions of different forms in three different climates

CO<sub>2</sub> emissions are stable at different heights for the two climates of Ghardaïa and Algiers, ranging between 126 and 128 kgCO<sub>2</sub>eq/m<sup>2</sup> for Ghardaïa and 119 and 121 kgCO<sub>2</sub>eq/m<sup>2</sup> for Algiers. On the other hand, the climate of Constantine has

a large difference between the most optimal case of 26 floors and the most unfavourable case of 2 floors, with a total of 10.5 kgCO<sub>2</sub>eq/m<sup>2</sup> of CO<sub>2</sub> as can be seen in Fig. 7.

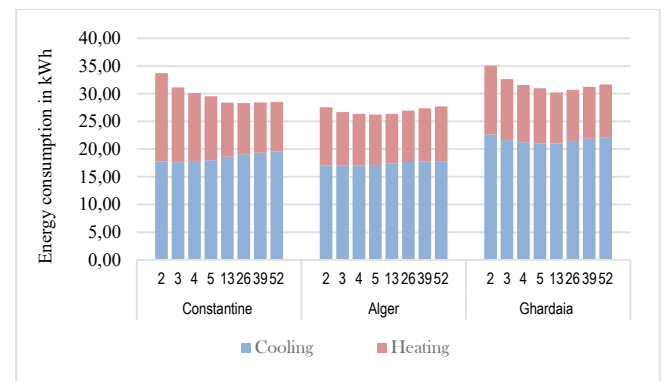


**Figure 8** Heating and cooling consumption of different heights in three different climates

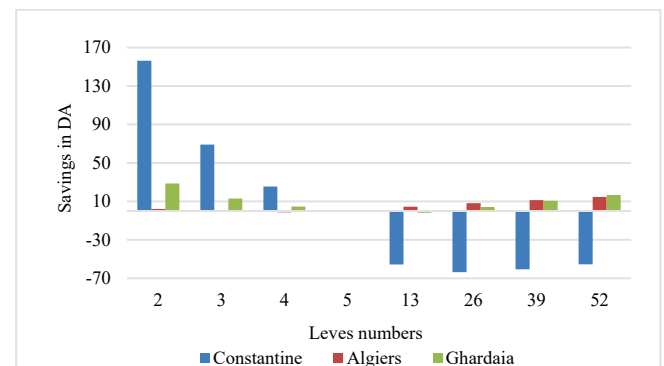


**Figure 9** Potential economies of different heights in the three studied climates

**Table 5** Simulation results summary of different heights

	1	2	3	4	5	6	7	8
EUI								
Constantine	26	39	13	52	5	4	3	2
Algiers	4	5	3	2	13	26	39	52
Ghardaïa	13	5	26	4	39	3	52	2
CO <sub>2</sub>								
Constantine	26	39	13	52	5	4	3	2
Algiers	2	3	4	5	13	26	39	52
Ghardaïa	5	4	13	3	26	2	39	52
Air conditioning								
Constantine	3	2	4	5	13	26	39	52
Algiers	2	3	4	5	13	26	39	52
Ghardaïa	13	5	4	26	3	39	52	2
Heating								
Constantine	52	29	26	13	5	4	3	2
Algiers	13	5	26	4	39	3	52	2
Ghardaïa	13	26	39	52	5	4	3	2
Economy								
Constantine	26	39	13	52	5	4	3	2
Algiers	4	5	3	2	13	26	39	52
Ghardaïa	13	5	26	4	39	3	52	2
Optimal								
Constantine	26	39	13	52	5	4	3	2
Algiers	4	5	3	2	13	26	39	52
Ghardaïa	13	5	26	4	39	3	52	2

The air conditioning results show a stable energy consumption for the majority of the heights in all three climates, reaching a maximum of 1.79 kW difference in the

city of Constantine. On the other hand, a greater difference can be seen for heating, with a maximum of 6.97 kW for that climate.

For the economic aspect, a saving of up to -64 DA/m<sup>2</sup> (26 floors) and a loss for the most favourable case of 156 DA/m<sup>2</sup> (2 floors) compared to the basic height (5 floors) can be achieved for the city of Constantine, while for the other two climates, only a saving of 2 DA/m<sup>2</sup>/year and -1.3 DA/m<sup>2</sup>/year can be achieved for Ghardaïa and Algiers, respectively, Fig. 9.

The results concerning the change in height can be summarised in Tab. 5 which ranks the various heights from the most optimal, identified as number 1, to the least favourable, denoted as number 8.

## 4 CONCLUSION

Nowadays, the design of a sustainable built environment poses some challenges, usually related to energy consumption, carbon emissions, human wellbeing, the depletion and scarcity of natural resources, and fossil fuels, but it plays a key role in the society's sustainable development as a whole. The objective of the study was to generate a comparative analysis for the different variables to see their differences in terms of energy performance, CO<sub>2</sub> emissions and financial energy savings, the following conclusions were reached:

- It seems that the compactness of the shapes is not a decisive element for the choice of the optimal shape and that it does not have a big effect on the energy consumption as stated in the art review; instead, the number of three-dimensional junctions (corners) seems to be the most decisive element in increasing energy consumption, as can be seen in the different climates with the triangular based shape as the optimal shape and the H, O, or C shape as the most unfavourable shapes.
- It is very difficult to generalise and give an optimal shape for energy consumption for a whole country. The optimal shape differs according to the climate, but also according to the initial characteristics of the building.
- There is a trend in all climates of decreasing EUI until an optimal height is reached, and then increasing again as the number of floors increases.
- The change of shape allows a financial saving of up to 54 DA/m<sup>2</sup>/year for the most favourable case.
- The change in height can allow the semi-arid climate of Constantine, unlike the other two climates, to have perceptible savings in terms of EUI, CO<sub>2</sub>, and economic aspects.
- It was noted that CO<sub>2</sub> emissions are related to heating and air conditioning consumption plus the total consumption of the building.

## 5 REFERENCES

- [1] Valladares-Rendón, L. G., Schmid, G., & Lo, S. L. (2017). Review on energy savings by solar control techniques and optimal building orientation for the strategic placement of façade shading systems. *Energy Build.*, 140(71), 458-479. <https://doi.org/10.1016/j.enbuild.2016.12.073>
- [2] Marino, C., Nucara, A., & Pietrafesa, M. (2017). Does window-to-wall ratio have a significant effect on the energy consumption of buildings? A parametric analysis in Italian climate conditions. *J. Build. Eng.*, 13, 169-183. <https://doi.org/10.1016/j.job.2017.08.001>
- [3] IEA. (2021). World Energy Outlook. <https://www.iea.org/reports/world-energy-outlook-2021>
- [4] COP26. (2021). COP26 Explained. *UN Clim. Chang. Conf. UK*, Available: <https://ukcop26.org/>
- [5] Vera, S. et al. (2017). Influence of vegetation, substrate, and thermal insulation of an extensive vegetated roof on the thermal performance of retail stores in semiarid and marine climates. *Energy Build.*, 146, 312-321. <https://doi.org/10.1016/j.enbuild.2017.04.037>
- [6] Ministère de l'Habitat. (1997). Réglementation thermique des bâtiments d'habitation: règles de calcul des déperditions calorifiques DTR C 3-2. *Doc. Tech. Réglementaire*, Ministère l'Habitat, Algérie, p. 72. (In France)
- [7] Ministère de l'Energie. (2020). Bilan Energétique National 2019, p. 44. Available: [www.energy.gov.dz](http://www.energy.gov.dz) (In France)
- [8] Ministère de l'Energie et des mines. (2021). Energies Nouvelles, Renouvelables et Maitrise de l'Energie. <https://www.energy.gov.dz/?rubrique=energies-nouvelles-renouvelables-et-maitrise-de-lrenergie> (Accessed Nov. 01, 2021). (In France)
- [9] Abanda, F. H. & Byers, L. (2016). An investigation of the impact of building orientation on energy consumption in a domestic building using emerging BIM (Building Information Modelling). *Energy*, 97, 517-527. <https://doi.org/10.1016/j.energy.2015.12.135>
- [10] Kadraoui, H., Mohammed, S., Amine, E., & Chikhaoui, A. (2019). Analysis of energy consumption for Algerian building in extreme North-African. *Int. J. Sustain. Energy Plan. Manag.*, 19, 45-58.
- [11] Torcellini, P., Pless, S., Deru, M., & Crawley, D. (2006). Zero Energy Buildings: A Critical Look at the Definition. *ACEEE Summer Study Pacific Grove*, p. 15. Available: <http://www.nrel.gov/docs/fy06osti/39833.pdf>
- [12] Pacheco, R., Ordóñez, J., & Martínez, G. (2012). Energy efficient design of building: A review. *Renew. Sustain. Energy Rev.*, 16(6), 3559-3573. <https://doi.org/10.1016/j.rser.2012.03.045>
- [13] Menezo, C., Lepers, S., Depecker, P., & Virgone, J. (2001). Design of buildings shape and energetic consumption. *Build. Environ.*, 36(5), 627-635. [https://doi.org/10.1016/S0360-1323\(00\)00044-5](https://doi.org/10.1016/S0360-1323(00)00044-5)
- [14] Catalina, T., Virgone, J., & Iordache, V. (2011). Study on the impact of the building form on the energy consumption. Proceedings of Building Simulation 2011. *The 12<sup>th</sup> Conference of International Building Performance Simulation Association*.
- [15] Straube, J. (2012). The Function of Form: Building Shape and Energy. Building Science Corporation, BSD-61, 1-4. <https://buildingscience.com/documents/insights/bsi-061-function-form-building-shape-and-energy>
- [16] Hemsath, T. L. & Alagheband Bandhosseini, K. (2015). Sensitivity analysis evaluating basic building geometry's effect on energy use. *Renew. Energy*, 76, 526-538. <https://doi.org/10.1016/j.renene.2014.11.044>
- [17] Makhloufi, A. W. & Louafi, S. (2022). The Impact of Glazing Types and Window-to-Wall Ratios on Energy Consumption in Semi-arid, Mediterranean and Arid Climates. *Prostor*, 30(2(64)), 140-153. [https://doi.org/10.31522/p.30.2\(64\).1](https://doi.org/10.31522/p.30.2(64).1)

**Authors' contacts:**

**Abdelhakim Walid Makhloufi, PhD**

(Corresponding author)

Department of Architecture and Urbanism, University Constantine,  
3 - Salah Boubnider, Laboratory of Bioclimatic Architecture and Environment  
(ABE), Constantine, Algeria

+213 657 72 72 55

walid.makhloufi@univ-constantine3.dz

<https://orcid.org/0000-0001-5215-8158>

**Samira Louafi, PhD Senior Lecturer**

Department of Architecture and Urbanism, University Constantine,  
3 - Salah Boubnider, Laboratory of Bioclimatic Architecture and Environment  
(ABE), Constantine, Algeria

samira.louafi@univ-constantine3.dz

# Designing a Desirable House with consideration of Strengthening the Sense of Peace of the Residents: A Case of District 6 of Tehran

Maryam Sabaroo, Abazar Mehrali\*

**Abstract:** Humans in modern society are faced with different environmental changes; creation of residential spaces is one of these changes in environmental structure of people in society. The sense of place means people's mental perception of the environment and their more or less conscious feelings about their environment, which places one in an internal relationship with the environment so that one's understanding and feeling are linked and integrated with the semantic context of the environment. This feeling is a factor that transforms a space into a place with special sensory and behavioral characteristics for certain people. This study investigates the sense of peace in residential buildings and its constituent factors. Now the question is, how to increase the sense of peace in people with proper design in residential environments? For this purpose, this study tends to examine the effect of a desirable house on strengthening the sense of peace of the residents by using a quantitative-qualitative method and using documents, observation, and questionnaires to find out how a suitable design induces a sense of peace in people. Based on findings obtained from field studies and data extracted from the questionnaire, it was found that residential complex indicators and residents' sense of peace have a significant effect on the satisfaction of the residents of the residential complex ( $p < 0.05$ ). Therefore, it can be claimed with 95% confidence that residential complex indicators and residents' sense of peace had a significant effect on the satisfaction of the residents of the studied residential complex in Tehran. The results also show that using more simple lines and fewer broken lines in the design of building form and considering areas and separating them from each other, as well as color, light, perception, and psychology of the environment are factors that cause a sense of satisfaction and a sense of peace in residents.

**Keywords:** environmental psychology; residential spaces; sense of belonging; sense of peace

## 1 INTRODUCTION

The importance that is now given to the relationship between architecture and human activities is one of the most important reasons for this study. This study discusses the recognition of human collective activities concerning the architecture of the Iranian courtyard from the perspective of cinema [1]. In the contemporary era, with the increase of individualism, the physical environment as a carrier of neighboring people has been highlighted to bring them closer to each other and to compensate for a part of the lost social interactions in the buildings and architectural and urban arrangements of the past [2]. Contemporary man faces many dangers; due to the increase in the population of the world, the shrinking of residences, and the increase in working hours outside residences, the human spirit and psyche have been irritated. This has manifested itself in industrialized societies, and depression has increased among youth and caused a loss of motivation to continue living more. Natural elements in indoor spaces increase the presence of people in the indoor environment and people feel a sense of belonging to the environment. This improvement in the quality of interior spaces stimulates the motivation and desire for life in the subconscious of people [3]. House, as a space for living, has always been one of the first spaces that humans have dealt with since the beginning of history; characteristics of this building, especially its interior, have been of great importance due to its direct connection with humans during the long hours of the day. Peace is one of the mental needs of every person. Nowadays, we humans usually spend most of our time at home and hence we seek to find peace at home and rest our body and soul in this place [4]. For a long time, housing satisfaction has been one of the favorite subjects of environmental psychologists; this is an attitude that reflects the satisfaction of residents living in a particular place that can meet their needs, expectations, and goals [5]. One's goal

in building a house is to have a peaceful residence. Peace in the Moin dictionary means leisure, comfort, stillness, security, peace, and reconciliation [6]. Among the spaces around the house, it is the immediate space related to a person. It is the first space in which one experiences a sense of spatial belonging [7]. Under these conditions, the design of the home environment should have a favorable effect on the human psyche. Due to the direct connection of the living space with the human psyche, proper and desirable design can have positive effects and inappropriate design can have destructive effects, and even indifference and lack of standards in design can cause people to become discouraged [8]. One of the related items in design is color, which is one of the most important effective factors in people's lives and plays an essential role in establishing a relationship between humans and the surrounding environment. Humans and colors are a subset of the whole world system that are constantly interacting and balancing each other, and ultimately humans are affected by colors [9]. Color is one of the most important and prominent features in the peacefulness of residential environments, which can stimulate emotions in people and can even affect human vision [10]. On the other hand, the phenomenon of light in general and daylight, in particular, is one of the most basic physical and psychological needs of humans. Studies show that intensity, type of source, color, direction, and distribution of light in different environments of human activity may affect behavior, mood, productivity, and efficiency largely [11]. In architectural spaces, the lighting environment is an important factor in physiological and psychological effects. As for life, recent studies show that many people spend most of their time at home, and environmental studies have focused on the production of high-performance lighting and color rendering to achieve visual satisfaction in residential environments [12]. Light has a long history in Iranian architecture, so that the light of the

experience of Iranian houses has been the voice of architectural text and is still considered in Iranian architecture. Studies show that visual perception of each color and light is different and it is important to consider this item in design of residential spaces in order to provide peace and reduce anxiety and mental disorders [13].

The present study tends to achieve a desirable residential environment, which can meet the needs of modern people due to their busyness and mental anxieties, and to design an environment where people can achieve a relaxing atmosphere considering psychological characteristics of the environment. Because a major part of one's life is spent at home, particularly during childhood, when every image around the environment is engraved on human mind and soul, or in adulthood when sensitive hours and moments of life such as hours of solitude and loneliness, or happiness and unhappiness usually happen at home. Undoubtedly, architecture of residential houses affects psyche of the people living in that house. Because the fact is that residential houses should be designed in a way that they are a place of peace for body and mind of the people living in those houses. This topic is important because if residential houses are designed desirably, they will have a positive and significant effect on the mood and psyche of the residents. As a result, lifestyles are better, intimacy is more, reducing crime, violence, divorce, etc. at home.

## 2 LITERATURE REVIEW

In addition to reviewing the views of scholars and theorists of architecture and environmental psychology, Eslami Mahmoodabadi et al. [14] tend to extract the factors that create peace from the perspective of Islam and adapt it to current spatial-behavioral patterns of the residents. Accordingly, this study addresses exhibition of peace in two common models of contemporary houses, including apartment houses and independent houses with courtyards. This study finally asserted that super meaning of peace and its different levels (physical comfort, mental peace and spiritual peace) is more evident in independent houses with courtyards than in apartments, which is also influenced by variety of spatial features and environmental capabilities existing in this model of houses compared to apartments.

Karmi and Hosseinpour [15] analyzed essentials of the Iranian house in traditional architecture; among physical features of the Iranian house, peace, which is one of the most important elements due to its importance for peace of users, was recognized in the past architecture, finding these elements effective in physical space of the contemporary house. The results show that the recognition and implementation of elements of the physical design of traditional Iranian house architecture played an important and influential role in the peace of its users, and modern architecture has not managed to preserve it. Modernism, i.e. forgetting one's own origins and adopting a Western way of thinking [26, 30], has shown its control over Iranian house architecture in a forced and commanding process.

In their study, Taghipour et al. [16] stated that economic status of people in current societies plays an important role in their tendency to live in apartments and turn it into a common pattern in urban housing. Meanwhile, living in these

spaces is associated with many problems such as increased vitamin D deficiency, overweight and decreased physical health, various social harms, decreased personal spaces and decreased mental health, which are threats to health of residents. According to World Health Organization, however, health means simultaneous provision of three physical, mental and social dimensions of people. Therefore, it seems that economic status of people has a direct and immediate effect on their quality of life and health. For this purpose, the current study tends to examine three dimensions of health in preferences of people with different economic status, when choosing apartment housing, and priority of influential components in their choice in these three areas. In other words, the current study tends to clarify which aspect of health is the priority in people preferences in choosing housing and whether economic status of people is effective on their preferences. The results of this study show that economic level of people is effective on their preferences in choosing housing from the health aspect. In this way, attention to mental health indicators is at the highest level in selection of housing for all economic groups; with increase in economic power of the household, attention to social health indicators surpasses physical health indicators. Farahani et al. [17] investigated the perceived sense of peace in traditional houses of Iran through a case study on the House of Tabatabais in Kashan and found a relationship between architecture of these houses and the perceived sense of peace. Finally, they compiled the factors of sense of peace in spaces of the houses; given the lack of peace in current houses, they recommended the principles and basics of their design.

Haghju et al. [18] reviewed design methods used to create peace in houses through a case study on a design by creating peace in houses of Tabriz city; they investigated housing as a space for living, and peace as one of spiritual and psychological needs of every person. Finally, they concluded that interior architecture could help considerably in creating peace by inducing a sense of peace in the home.

Sheikh Al-eslami et al. [19] examined the effect of natural light on user comfort, survival and physical, mental and moral health in residential spaces through a case study on bedrooms. They concluded that light is the most non-material tangible element of nature and one of the effective factors on spatial value. Salehipour and Gholampour [20] investigated the environmental psychology in design of residential complexes and considered human behavior in physical environments and indicators of environments that cause social interactions. As a result, they identified human needs, which orient behaviors in collective spaces; by examining these needs, they increased mental peace in these spaces. Safari and Qaraguzlu [21] examined the effect of natural light on human peace in residential complexes, through a case study on Kausar residential complex in Sohank neighborhood in northeast Tehran. The results indicate that natural light has psychological effects on people. That is, psychologically, the ego dimension of human beings, the need to belong, self-esteem and self-actualization have the greatest effect on people. Radwan [10] investigated whether color is just an aesthetic value or a real human need. In this study, color is considered as an integral element. They concluded that the environment is made not only in living

organisms from the natural environment but also in humans. Different environments with their different colors play an important role in human evolution. Kellett and Moore [22] concluded that a hotel room leads to different behaviors and meanings attributed by the occupants. The meaning of home for some is more related to social dimensions, while for others it is more related to comfort and physical features. Therefore, housing design can be improved when the relationships between physical environment and various meanings of the home are better understood.

Lewinson [23] found that long-term hotel dwellers positively emphasize options that make room use more home-like. For example, a small kitchen in the room increases dignity. Overtoom et al. [24] investigated the design of a better house for people in temporary accommodation (investigating the relationships between the meanings of house, activities and indoor quality). Professionals involved in the design process, whether for new or renovated buildings, rarely consult with the people who live in short-term rental (temporary) apartments. Knowing what temporary residents need to feel at home and how their meanings of home are related to home features, activities, and the quality of indoor space can lead to better design for these typically small homes. To investigate views of temporary residents on their home environment, a survey was designed and administered to Dutch youth likely to be familiar with temporary accommodation (141 university students, 58 refugees who received a residence permit). Multiple regression analysis and analysis of variance showed that the meaning of house is related to some characteristics of household and presence of light and cleanliness. This study showed that significant house measurement might help to understand not only how houses are used, but also how to improve the design of small temporary houses.

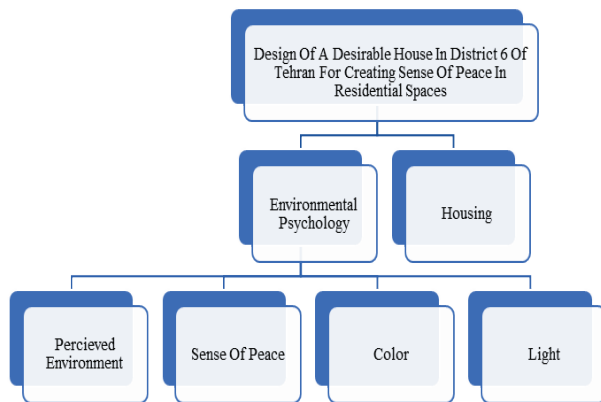


Figure 1 The conceptual model

This study is a step towards proper design of a residential complex, considering simple lines and use of less broken lines in design of the building form, as well as areas and separating them from each other, considering right colors for each space according to its type of function, considering suitable lighting for spaces to create a sense of vitality and considering natural resources. Fig. 1 shows the conceptual model of the study.

Research Questions are as follows: 1) Can peace be increased in residential environments by considering appropriate forms and psychological features? 2) Can peace

be created in residential environments by considering light and color features?

### 3 RESEARCH METHODOLOGY

The research method is analytical and descriptive; data collection method is library and observation using written and internet references and documents [25]. In this applied research, a mixed quantitative and qualitative method was used, the quantitative part of which was done with a descriptive survey and the qualitative part of which included case study. For literature review, data was collected and criticized from articles, treatises, and textbooks, and theoretical framework was developed to extract variables and develop the objective table; then, the questionnaire was developed and surveyed in the area [27-38].

The instrument used for collecting the required data was a questionnaire made by the author, which was designed based on two components, residential complex and sense of peace, and its effect on satisfaction of residents in District 6 of Tehran. A questionnaire with 10 questions was made after consultation with experts. In order to measure reliability of the questionnaire, 50 questionnaires were distributed among the statistical population. According to the calculated value, the alpha value was higher than 0.7 (Tab. 1), indicating that the questionnaire had the necessary reliability or validity to collect data and information.

#### 3.1 Population

Statistical population of the study was residents of a residential complex in district 6 of Tehran. Among them, 50 people were selected for statistical sample by cluster sampling method and the questionnaire was distributed among them. Then the completed and returned questionnaires were analyzed.

Table 1 Reliability of the reference questionnaire

Variable	N	Cronbach's alpha
Residential complex	4 items	0.890
Resident sense of peace	6 items	0.855

#### 3.2 Data Gathering

This study was done with the focus on two components, residential complex and sense of peace and its effect on satisfaction of residents in district 6 of Tehran. Residential complex indicators mean considering simple lines and less use of broken lines in design of the building form and considering the areas and separating them from each other, which are used in design of the residential complex and make the residents feel peace, followed by satisfaction of residents. Color, light, perception and environmental psychology are factors of satisfaction and sense of peace of residents.

#### 3.3 Data Analysis Method

The research method in this study is descriptive analytical method. The method of data analysis is deductive reasoning. SPSS software was used to analyze the

questionnaire and obtain the weighted average of each question for comparison and evaluation [35].

## 4 RESULTS

Characteristics of the statistical samples are listed in the table below in terms of gender (30% male and 70% female), education level (32% diploma, 46% bachelor's degree, and 46% master's degree and above) and age (7% younger than 20 years, 38% between 21 and 35 years and 55% between 36 and 45 years).

Description of the variables for both indicators, residential complex and resident sense of peace, is described in Tab. 2.

**Table 2** Description of residential complex and resident sense of peace

	N	Min.	Max.	Mean	Std.	Variance
Residential complex	50	1.50	5.00	3.2100	0.79597	0.634
Resident sense of peace	50	2.00	5.00	3.3200	0.70537	0.498

In order to measure the significant effect of each variable, hypothesis testing was conducted and the results are described in Tabs. 3 to 4.

Hypothesis 1: By considering appropriate forms and psychological features, peace can be increased in residential environments.

$H_0: R = 0$  there is no correlation.

$H_1: R \neq 0$  there is a correlation.

**Table 3** Results of Hypothesis 1

	Residential complex	Resident sense of peace
Appropriate form and psychological feature	1	0.614**
Pearson correlation (residential environment)	0.614**	1

\*\*  $p < 0.01$

According to the results obtained from Tab. 3, the relationship between these two variables is significant ( $p < 0.01$ ). On the other hand, the value of this relationship is equal to 0.614, which is positively significant.

Hypothesis 2: By considering light and color features, peace can be created in residential environments.

$H_0: R = 0$  there is no correlation.

$H_1: R \neq 0$  there is correlation.

**Table 4** Results of Hypothesis 2

	Traditional architecture	Sense of place in architecture
Color and light	1	0.623**
Pearson correlation (peace in residential environment)	0.623**	1

\*\*  $p < 0.01$

According to the results obtained from Tab. 4, the relationship between these two variables is significant ( $p < 0.01$ ). On the other hand, the value of this relationship is equal to 0.623, which is positively significant.

## 4.1 District Six of Tehran

District six of Tehran municipality with a population of 231024 people and an area of 2144 hectares is connected to the Hemet highway from north, to the Enghelab-Azadi Street from south, by Modarres highway on the eastern border, and to the Shahid Chamran highway from west.



**Figure 2** District 6 of Tehran on the map of Tehran; Source: Detailed plan of District 6 of Tehran

On the one hand, District 6 is located approximately in the geographical center of Tehran city, and on the other hand, it is in the spatial-activity center due to its proximity to the old center of gravity of the city and gradual transfer and movement of Tehran center to the north. In the meantime, with construction of elements such as the Ministry of Agriculture in the current Keshavarz Blvd., administrative buildings in the Taleghani and Iranshahr streets, and new urban centers in a more limited functional scale along the streets or intersection of main streets of the city, such as Enghelab and Valiasr squares, which were located in District 6, the district has taken a double central position (Detailed plan of District 6 of Tehran).

The population of District 6 in 2006 was counted as 232,583 people, while population peak was 258,838 people in 2007, after which, the population began to gradually decrease. In terms of social quality, population of the district includes social groups, which are higher than average; in terms of education, some blocks, and neighborhoods of the district are among the best ones in the city. The stabilization period of population has been associated with an increase in its activity so the number of employees in the district has increased from 239,945 people in 1994 to 283,148 people in 2002. The district covers 3% of area, 3.1% of population and 17.6% of employees of Tehran. Gross population density is 108 and gross density of employees is 132 people per hectare (Detailed plan of District 6 of Tehran).

## 4.2 Building Structure

The building structure is an eco-friendly metal structure. Then, a series of resins were used for the structure so that no moisture penetrates it and it does not corrode by growth of plants and in fact, it is insulated. Then wood plastic composite was used on the structures. The plants on the structure were forest plants and tended to grow on the facade. The facade of the windows was in the form of curtain wall

and glass, and cement board or dry concrete was used in the walls, and behind them, gypsum panel insulation, mineral wool, and kenaf were used, respectively. All the materials of this residential complex are light. Western light was solved with expanded metal or stretch metal technology due to sunlight problem. Expanded metal is an aluminum mesh which is able to absorb 50% of natural light and allows growing plants on this material. The site is located in the 6<sup>th</sup> district of Tehran, Iranshahr neighborhood, one of the neighborhoods of Tehran. This site with 12841 m<sup>2</sup> area is located on Mousavi Street and a dead end (Fig. 3).



Figure 3 Site location, source: author

Reasons for Choosing the Site are as follows: Artist House located in Iranshahr Park (Artists) is one of the historical-artistic monuments in Iranshahr neighborhood. It has relatively healthy weather. Easy access to this district by public transportation (taxi, bus and subway) and by personal vehicles is one of advantages of this area. On the other hand, beautiful and old trees, green boxwoods, and ditches have given a beautiful effect to Iranshahr neighbourhood. The selected site is located in a place that, in addition to being cozy and having good air, is on a wide street and alley where you can experience silence and peace (Fig. 4).



Figure 4 Usage and various features around the site; source: author

The site is adjacent to residential and administrative buildings, galleries, restaurants and cafes, green spaces and artists park (Fig. 5). The suggested physical plan is shown in Tab. 5. View from outside to the site and View from the site to outside are shown in Figs. 6 and 7 respectively.



Figure 5 Site adjacencies

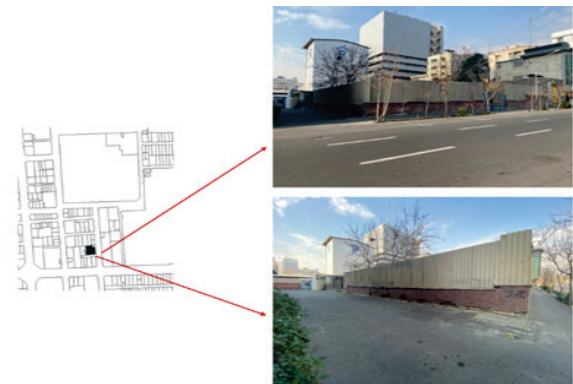


Figure 6 View from outside to the site



Figure 7 View from the site to outside

## 5 CONCLUSION

The increasing population and the following transformation of apartment living into the dominant form of urban housing, have created new outcomes and challenges in the field of mental health of humans. One of the most important missions of the house is to provide peace for its residents. This is so important that God Almighty has directly emphasized the comforting role of the house in the Qur'an. On the other hand, man is a creature with different egos, and the concept of peace is expressed in a special way for each ego. In this way, peace in connection with the plant and animal ego of man is manifested in the form of physical comfort; the rational ego needs to provide mental peace, and the spiritual ego of man seeks the concept of peace in spiritual peace. Considering that the house is the residence of all

human egos, it is essential to provide different levels of peace according to the four human egos.

**Table 5** Physical plan

Name of spaces	Area of space	N	Total area
Lobby	20	3	60
Parking	7	83	581
Warehouse	3	57	171
Facilities	28	2	56
Stairs	9	4	36
Elevator	3	4	12
Maintenance	60	1	60
			Total: 976 m <sup>2</sup>
One-bedroom unit			
Restroom	2	1	2
Bathroom	3	1	3
Kitchen	8	1	8
Living room	20	1	20
Bedroom	12	1	12
Total in number of units: 45 m <sup>2</sup>		Number of units: 1	Total: 45 m <sup>2</sup>
Two bedroom unit			
Restroom	2	1	2
Bathroom	4	1	4
Kitchen	12	1	12
Living room	30	1	30
Master room	16	1	16
Bedroom	9	1	9
Total number of units: 1168 m <sup>2</sup>		Number of units: 16	Total: 73 m <sup>2</sup>
Three bedroom unit			
Restroom	3	1	3
Bathroom	4	2	8
Kitchen	16	1	16
Living room	80	1	80
Master room	20	1	20
Bedroom	12	2	24
Total number of units: 4077 m <sup>2</sup>		Number of units: 27	Total: 151 m <sup>2</sup>
Four bedroom unit			
Restroom	3	1	3
Bathroom	6	3	18
Kitchen	20	1	20
Living room	100	1	100
Master room	30	1	30
Bedroom	16	3	48
Total in number of units: 438 m <sup>2</sup>		Number of units: 2	Total: 219 m <sup>2</sup>
		Total units: 46	Total area: 1464 m <sup>2</sup>
			Total building area: 11296 m <sup>2</sup>
			Total site area: 12841 m <sup>2</sup>

It seems that knowledge of physical and mental characteristics and understanding of the different needs of the elderly and an attempt to respond to these needs and respect for their preferences in designing and improving their special spaces can be effective in the good life of the elderly and improve their quality of life and life expectancy. This study tends to evaluate architectural spaces for the elderly to improve their quality of life. In this study, it was found that the factors and elements that lead to a sense of peace and comfort, and satisfaction of residents of the residential complex are known as indicators of the residential complex

and residents' sense of peace. Based on the findings of the field studies and extracted data from the questionnaire, it was determined that indicators of the residential complex and residents' sense of peace have a significant effect on the satisfaction of the residents of the residential complex ( $P < 0.01$ ). Hence, indicators of the residential complex and residents' sense of peace have a significant effect on the satisfaction of the residents of the residential complex in district 6 of Tehran with 95% confidence. Considering simple lines and less use of broken lines in the design of the building form and considering the areas and separating them from each other as well as color, light, perception, and psychology of the environment are factors that lead to a sense of peace and satisfaction of residents of the complex.

## 6 REFERENCES

- [1] Noghrekar, A., Hamzenejad, M., & Baqeri, H., (2013). Sociability in the Iranian courtyard (recognizing the reinforcing features of presence in the courtyard, through the analysis of movie scenes). *Journal of Iranian Architecture & Urbanism*, 12(1), 45-56.
- [2] Askarizad, R. & Safari, H. (2020). Investigating the role of semi-open spaces on the sociability of public libraries using space syntax (Case Studies: Sunrise Mountain and Desert Broom Libraries, Arizona, USA). *Ain Shams Engineering Journal*, 11(1), 253-264. <https://doi.org/10.1016/j.asej.2019.09.007>
- [3] Emami, B. D., Song, Y., & Khani, A. (2022). Prioritizing Bus Routes for Electrification: GIS-Based Multi-Criteria Analysis Considering Operational, Environmental, and Social Benefits and Costs. *Transportation Research Record*, 2676(8), 10-23. <https://doi.org/10.1177/03611981221082565>
- [4] Varolgünes, F. K. (2019). Evaluation of vernacular and new housing indoor comfort conditions in cold climate—a field survey in eastern Turkey. *International Journal of Housing Markets and Analysis*, 13(2), 207-226. <https://doi.org/10.1108/IJHMA-02-2019-0019>
- [5] Chen, N., Hall, C. M., Yu, K., & Qian, C. (2019). Environmental satisfaction, residential satisfaction, and place attachment: The cases of long-term residents in rural and urban areas in China. *Sustainability*, 11(22), 6439. <https://doi.org/10.3390/su11226439>
- [6] Pourmehdi Ghaem Maghami, H., & Khaki Ghasr, A. (2022). The Inside-Outside Relationship of Traditional Houses: A Case Study from Yazd, Iran. *Iran University of Science & Technology*, 32(4), 1-22. <https://doi.org/10.22068/ijaup.727>
- [7] Abbas Mofrad, H., Khalatbari, J., Malihi Zakerini, S., Mohammadi Shirmahalleh, F., & Shafati, V. (2021). Analysis of Structural Equations in the Relationship of Marital Conflicts and Affective Security with Perceived Stress and Pregnancy Worries and Biological Indexes with the Mediation of Psychological Wellbeing in Pregnant Women. *Women Studies*, 12(35), 97-127.
- [8] Seitz, C. M., Reese, R. F., Strack, R. W., Frantz, S., & West, B. (2014). Identifying and improving green spaces on a college campus: A photovoice study. *Ecopsychology*, 6(2), 98-108. <https://doi.org/10.1089/eco.2013.0103>
- [9] Torres, A., Serra, J., Llopis, J., & Delcampo, A. (2020). Color preference cool versus warm in nursing homes depends on the expected activity for interior spaces. *Frontiers of Architectural Research*, 9(4), 739-750. <https://doi.org/10.1016/j.foar.2020.06.002>

- [10] Radwan, A. H. (2015). Color in architecture is it just an aesthetic value or a true human need. *International Journal of Engineering Research & Technology (IJERT)*, 4, 523-533.
- [11] Murdoch, L. C., DeWolf, S., Germanovich, L. N., Moysey, S., Hanna, A., Roudini, S., & Moak, R. (2023). Using the Shallow Strain Tensor to Characterize Deep Geologic Reservoirs. *Water Resources Research*, 59(2), e2022WR032920. <https://doi.org/10.1029/2022WR032920>
- [12] Kim, I. T., Choi, A. S., & Sung, M. K. (2017). Development of a Colour Quality Assessment Tool for indoor luminous environments affecting the circadian rhythm of occupants. *Building and Environment*, 126, 252-265. <https://doi.org/10.1016/j.buildenv.2017.10.009>
- [13] Fattahi Marnani, P. & Cuocci, S. (2022). Foreign Language Anxiety: A Review on Theories, Causes, Consequences and Implications for Educators. *Journal of English Learner Education*, 14(2), p. 2. <https://stars.library.ucf.edu/jele/vol14/iss2/4>
- [14] Eslami Mahmoodabadi, M., Peyvastegar, O., & Heydari, A., (2021). Peace at home, a search for peace at home from the perspective of Islam in two models of apartment and independent housing with courtyard in Kerman city. *Baghe Nazar*, 18(99), pp. 5-24.
- [15] Karami, R. & Hosseinpour, E. (2020). Home, a medium to reach peace. *Research in Civil Engineering*, 60, 182-207.
- [16] Taghipour, M., Heidari, A., & Haghayegh, M. (2020). Evaluating the effects of health components on choosing the optimal rental housing among citizens of Shiraz. *Motaleate Shahri*, 9(36), 55-68. <https://doi.org/10.34785/J011.2021.299>
- [17] Farahani, F., Zekavat, M., & Momenian, A., (2017). Investigating the perception of the sense of peace in traditional Iranian houses; a case study: The Tabatabai house in Kashan. *International conference on modern studies in civil engineering and urban planning with the approach of Islamic Iran*, Tehran, Iran.
- [18] Haghju, A., Tarahomju, A., & Mosafari, S., (2017). Design methods to create peace in houses; a case study: design by creating peace in houses of Tabriz. *International congress of civil engineering, architecture and contemporary urban planning of the world*, Tehran, Iran.
- [19] Sheykh Al-eslami, A., Niazi, S., & Qavami, A., (2017). The effect of light on user comfort in residential spaces' a case study: bedroom. *Annual conference on urban planning architecture and urban management research*, Tehran, Iran.
- [20] Salehipour, A. & Gholampour, M., (2016). Environmental psychology in design of residential complexes. *The first national technology conference in applied engineering club of young and elite researchers*, Tehran, Iran.
- [21] Safari, H. & Qaraguzlu, S., 2016. The effect of natural light on the peace of people in residential complexes, a case study of Kausar residential complex in Sohank neighborhood in the northeast of Tehran. *The second annual conference on urban planning architecture and urban management research*, Teran, Iran.
- [22] Kellett, P. & Moore, J. (2003). Routes to home: homelessness and home-making in contrasting societies. *Habitat International*, 27(1), 123-141. [https://doi.org/10.1016/s0197-3975\(02\)00039-5](https://doi.org/10.1016/s0197-3975(02)00039-5)
- [23] Lewinson, T. (2010). Capturing environmental affordances: Low-income families identify positive characteristics of a hotel housing solution. *Journal of Community & Applied Social Psychology*. <https://doi.org/10.1002/casp.1060>
- [24] Overtoom, M. E., Elsinga, M. G., & Bluyssen, P. M. (2022). Towards better home design for people in temporary accommodation: exploring relationships between meanings of home, activities, and indoor environmental quality. *Journal of Housing and the Built Environment*, 1-27. <https://doi.org/10.1007/s10901-022-09947-z>
- [25] Abbas Mofrad, H., Khalatbari, J., Malih Al-zakerini, S., Mohammadi Shir Mahalla, F., & Shafti, V. (2022). Modeling Structural Equations in the Relationship between Marital Conflicts and Emotional Security with Perceived Stress and Prenatal Concerns with Psychological Well-Being in Pregnant Women. *Middle Eastern Journal of Disability Studies*, 12(140), 1-8. <https://jdisabilstud.org/article-1-2259-en.html>
- [26] Abedi, M., Tan, X., Klausner, J., & Benard, A. (2022). Solar Desalination Chimneys. Bulletin of the American Physical Society. *The 75<sup>th</sup> Annual Meeting of the Division of Fluid Dynamics*. November 20-22, 2022; Indiana Convention Center, Indianapolis, Indiana. <https://meetings.aps.org/Meeting/DFD22/Session/S01.13>
- [27] Cuocci, S., & Fattahi Marnani, P. (2022). Technology in the Classroom: The Features Language Teachers Should Consider. *Journal of English Learner Education*, 14(2), 4. <https://stars.library.ucf.edu/jele/vol14/iss2/4>
- [28] Khorsandi, H., Khorsandi, R., Khorsandi, M.A. (2022). Effects of multimedia (motion graphics) versus traditional teaching method on student learning, *International Journal of Early Childhood Special Education*, 14(2), 9115-9124. <https://doi.org/10.9756/INTJECSE/V14I2.995>
- [29] Murdoch, L. C., Germanovich, L. N., Roudini, S., DeWolf, S. J., Hua, L., & Moak, R. W. (2021). A Type-Curve Approach for Evaluating Aquifer Properties by Interpreting Shallow Strain Measured During Well Tests. *Water Resources Research*, 57(9), e2021WR029613. <https://doi.org/10.1029/2021WR029613>
- [30] Khorsandi, H. & Khorsandi, R. (2022). Ranking the effective factors in creative marketing in Iran Novin insurance. *Journal of Positive School Psychology*, 6(5), 10009-10020.
- [31] Esmailzadeh, Y. (2023). Potential Risks of ChatGPT: Implications for Counterterrorism and International Security. *International Journal of Multicultural and Multireligious Understanding*, 10(4), 535-543.
- [32] Heydari, P., Asgharpour, A. R., Nazoktabar, M., & Zahedinejad, M. (2014). Fabrication and Optical Characterization of Silicon Nanostructure Arrays by Laser Interference Lithography and Metal-Assisted Chemical Etching. *Journal of Nanostructures*, 4(4), 419-424. <https://doi.org/10.1016/j.renene.2022.11.069>
- [33] Shakouri Mahmoudabadi, N. (2021). The Use of Viscous Dampers for Retrofitting of Reinforced Concrete Frames. *Turkish Journal of Computer and Mathematics Education*, 12(13), 7739-7744
- [34] Soltanmohammadi, R., Iraj, S., de Almeida, T. R., Munoz, E. R., & Vidal, A. C. (2022). Upscaling Challenges of Heterogeneous Carbonate Rocks: A Case Study of Brazilian Pre-Salt Analogous. In *Third EAGE Conference on Pre Salt Reservoirs*, EAGE Publications BV, 2022(1), 1-6.
- [35] Heidari, S., Zarei, M., Daneshfar, A., & Dokhanian, S. (2023). Increasing Sales through Social Media Marketing: The Role of Customer Brand Attachment, Brand Trust, and Brand Equity. *Marketing and Management of Innovations*, 14(1), 224-234. <https://doi.org/10.21272/mmi.2023.1-19>
- [36] Azizi, S., Dadarkhah, A., & Masouleh, A. A. (2020). Multi-Objective Optimization Method for Posture Prediction of Symmetric Static Lifting Using a Three-Dimensional Human Model. *Ann Mil Health Sci Res.*, 18(2), e104283. <https://doi.org/10.5812/amh.104283>
- [37] Vahid, R., Farnood Ahmadi, F., & Mohammadi, N. (2021). Earthquake damage modeling using cellular automata and

fuzzy rule-based models. *Arabian Journal of Geosciences*, 14, 1-14. <https://doi.org/10.1007/s12517-021-07595-1>

- [38] Abedi, M., Tan, X., Klausner, J. F., & Bénard, A. (2023). Solar desalination chimneys: Investigation on the feasibility of integrating solar chimneys with humidification–dehumidification systems. *Renewable Energy*, 202, 88-102. <https://doi.org/10.1016/j.renene.2022.11.069>

**Authors' contacts:**

**Maryam Sabaroo**, MSc student  
Art and Architecture Department,  
Yazd Branch, Islamic Azad University,  
Yazd, Iran

**Abazar Mehrli**, Assistant professor  
(Corresponding author)  
Faculty of Architecture, Art and Architecture Department,  
Yazd Branch, Islamic Azad University,  
Yazd, Iran  
[abazarmehrli@chmail.ir](mailto:abazarmehrli@chmail.ir)

# The Role of SCM practices in Competitive Advantage and Firm Performance: A Mediating Role of Supply Chain Innovation and TQM

Erfan Mehregan\*, Somayeh Sanaei, Mohsen Manna, Hamed Bozorgkhoh, Shahin Heidari

**Abstract:** The present study aimed to propose a theoretical framework that elucidates the impact of supply chain management (SCM) practices on the competitive advantage and performance of firms while considering the mediating effects of supply chain innovation and total quality management (TQM). This research article employed a descriptive correlational methodology based on a questionnaire, complemented by structural equation modelling. The study involved the participation of 279 individuals, including managers, assistants, and supply chain experts from small and medium-sized enterprises. The study findings suggest that SCM practices significantly influence TQM, supply chain innovation, competitive advantage, and firm performance. Additionally, TQM has a significant effect on supply chain innovation, competitive advantage, and firm performance. Similarly, supply chain innovation has a positive and significant impact on competitive advantage and firm performance. Furthermore, the positive and significant mediating role of supply chain innovation and TQM in the effect of SCM practices on competitive advantage and firm performance was observed. Therefore, it can be concluded that SCM practices enhance firm performance and competitive advantage through the improvement of supply chain innovation and TQM.

**Keywords:** competitive advantage; firm performance; SCM; supply chain innovation; TQM

## 1 INTRODUCTION

Firm performance is a broad concept that includes what the firm produces as well as the areas it interacts with. In other words, firm performance refers to the way of performing organizational missions and activities and their outcomes [1]. In most firms, managers and leaders are always looking to promote and improve their performance, because firms need to continuously improve their performance to maintain their survival and progress in a current competitive world. After all, improving performance is the key to success in competition. Therefore, the survival and success of companies in a current competitive environment, which is characterized by change and transformation, complexity, and uncertainty require the adoption and implementation of effective strategies and continuous performance improvement [2]. Performance management has become more important due to factors like rapid change, budget deficits, downsizing, and restructuring, as well as societal pressures to make organizations responsible for their performance. As a result of this, Organizations are constantly seeking methods to enhance their overall performance and this is one of the underlying themes of organizational analysis. Therefore, this research article investigates the mediating influence of supply chain innovation and total quality management (TQM) on the link between practices of supply chain management (SCM) and the performance of a firm as well as a competitive advantage.

A supply chain is a structured combination of all business processes whose purpose is to satisfy the customer with the required goods and services. The supply chain process commences with the procurement of raw materials based on the specific requirements of the customer and culminates with the transportation and delivery of the finished product to the customer [3]. In a well-managed supply chain, all members of the developed organization work together to bring to market a common product or service that the customers are willing to pay for. Supply chain

management is the joint effort of companies to improve strategic positions and improve group performance. This integrated value-creating process must be managed from procurement of materials to delivery of goods/services to the final customer [4]. High quality and low cost for the final consumer, one of the key points in SCM is that the supply chain should be considered as a coherent whole. Therefore, when managers tend to make an individual decision in a component of the supply chain, i.e. supply, production, or distribution, this should be made clear to them the chosen solution optimizes the entire supply chain [5]. Practices in SCM consist of a series of tasks that an organization undertakes to enhance the efficiency of its supply chain. A team of researchers examined four supply chain management practices in this article: customer relationship management, supplier relationship management, information sharing between companies in the supply chain, and quality of information that gets passed between companies in the supply chain.

Firms and their suppliers establish strategic collaborative relationships called supplier relationships that use their capabilities and competencies to obtain mutually beneficial rewards [6]. Relations with customers are defined as the process of handling complaints from customers and developing long-term relationships with them. Good customer relationships enable the firm to fulfill its customers' needs [7]. In order to drive business growth, the importance of information is widely acknowledged. Several studies have examined the quality and quantity of information shared as a key practice of SCM. A firm's information-sharing policy refers to how much information it shares with its business partners. A successful supply chain relies on the flow of information throughout the organization. As a result of accurate, timely, adequate, and reliable information being exchanged throughout a supply chain, it is of high quality. Providing information without errors or delays is of great importance for the effectiveness of the supply chain [7].

Today, competition between companies has become a topic of discussion among managers, politicians, academics, and researchers. As a result of its competitive advantage, a company is positioned better than its competitors in a given industry [8]. When a company consistently earns more profit than other companies that compete in the same industry, it is known as an organization that has a competitive advantage over its competitors in this market. The competitive advantage of a company depends on its ability to design, produce and deliver valuable products and services based on the needs of the customer. Without achieving a competitive advantage, the firm will have little economic justification for its continued survival and will decline financially. Under these circumstances, only companies can survive and improve their position by focusing on quality, price, speed, responsiveness, and all other aspects of competition to customers, and innovation, to achieve sustainable competitive advantage and outperform their competitors. Studies have also shown that competitive advantage leads to improved firm performance [9].

Today's business environment is extremely competitive and everything changes, but the phenomenon of change remains constant. There is increasing importance of innovation in organizations due to rapid technological changes in multiple industries and the consequent shortening of product life cycles and intensified competition [10]. Innovation will enable more organizations to respond to changing environments more effectively by creating and developing new capabilities. This is why nowadays innovation is noted as the most important factor of sustainable competition in the organization. An organization's innovation capability refers to its willingness to support experimentation, new ideas, and creative processes when developing new products/services or technological developments [6, 11]. An organization's ability to innovate enables it to exceed customers' expectations. As a result, innovation not only allows companies to increase their performance, but also to create mechanisms that are rare, valuable, diverse, distinctive, and difficult to duplicate. The goal of supply chain innovation is to provide new, effective, and innovative solutions for end users by dealing with uncertainties and disruptions in an internal and external environment. Innovative supply chains are essential in competing in the industry and are increasingly recognized by organizations, and their business strategies are accordingly adjusted [12]. Additionally, research has demonstrated that innovation can have a beneficial and noteworthy effect on both competitive advantage and performance [13].

TQM means directing and controlling activities based on the leadership of top management and extending them to all employees and units. These control and management measures focus on quality assurance achieved through the quality created in services provided to customers [14].

There is a management philosophy known as quality management that recognizes the needs and common goals of a company as inseparable. This philosophy is utilized in business, industry, and services to ensure maximum efficiency and effectiveness. Its application results in business leadership through the governance of processes and systems. Additionally, it promotes stability, increases efficiency, and helps prevent errors in the decision-making

process of managers. Furthermore, this philosophy ensures that organizations meet the needs of their customers by aligning all their goals in that direction [1, 6]. If a quality management system is provided according to the conditions and requirements of the company, it can be effective in improving management and increasing effectiveness and modifying the decision-making processes and performance of the organization. Findings of the conducted studies have also shown that the effectiveness of TQM is positively correlated with innovation and firm performance [15].

As noted, the role of SCM practices, supply chain innovation, and TQM has been emphasized in competitive advantage and firm performance throughout the academic literature. However, empirical research shows that few studies have developed a model for SCM practices on firm performance and competitive advantage with the mediating role of supply chain innovation and TQM in small and medium-sized enterprises (SMEs). Therefore, the purpose of the present research is to formulate a model for SCM practices concerning firm performance and competitive advantage, taking into account the mediating roles of supply chain innovation and TQM.

## 2 CONCEPTUAL MODEL

A conceptual model is illustrated in Fig. 1 as a result of the literature and theoretical framework outlined in the background. In this model, SCM practices are considered independent variables; supply chain innovation, TQM, and competitive advantage as mediating variables, and firm performance is the dependent variable.

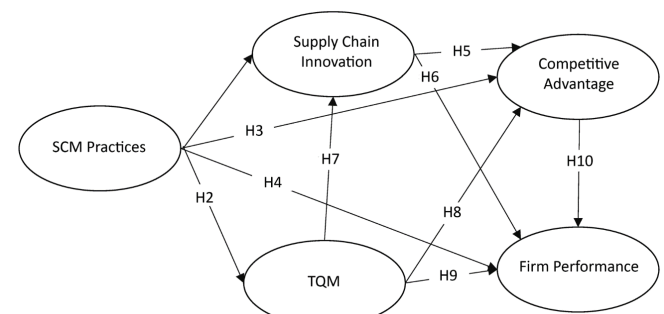


Figure 1 Conceptual model

Therefore, the following are the hypotheses:

- H1: SCM practices influence supply chain innovation.
- H2: SCM practices influence TQM.
- H3: SCM practices influence competitive advantage.
- H4: SCM practices influence firm performance.
- H5: Supply chain innovation influences competitive advantage.
- H6: Supply chain innovation influences firm performance.
- H7: TQM influences supply chain innovation.
- H8: TQM influences competitive advantage.
- H9: TQM influences firm performance.
- H10: Competitive advantage influences firm performance.
- H11: Supply chain innovation plays a mediating role in the effect of SCM practices on competitive advantage.

H12: Supply chain innovation plays a mediating role in the effect of SCM practices on firm performance.

H13: TQM plays a mediating role in the effect of SCM practices on competitive advantage.

H14: TQM plays a mediating role in the effect of SCM practices on firm performance.

H15: Competitive advantage plays a mediating role in the effect of supply chain innovation on firm performance.

H16: Competitive advantage plays a mediating role in the effect of TQM on firm performance.

### 3 RESEARCH METHODOLOGY

In the present study, a descriptive correlation with SEM was used because structural equations were used to examine the relationships between variables.

#### 3.1 Population and Sampling

The population was managers, assistants, and supply chain experts of SMEs in Iran, among whom 340 questionnaires were distributed. Once incomplete questionnaires were removed, 279 questionnaires were analyzed.

#### 3.2 Data Collection Instruments

SCM practices: In this study, the SCM practices were evaluated using a questionnaire developed by Amedofu et al. [15]. The questionnaire included 21 items that assessed various features of SCM practices, including the relationship of customer (5 items), the relationship of supplier (5 items), information sharing of supply chain (6 items), and supply chain information quality (5 items). Likert scales were used to measure the responses, ranging from strongly disagree (1) to strongly agree (5).

TQM: The TQM practices were evaluated using the questionnaire developed by Modgil and Sharma [16]. The questionnaire comprises 16 items, which are categorized into four dimensions. These dimensions include quality information and reporting, product innovation, research and development management, and management of technology. Each dimension consists of four items.

Supply chain innovation: The measurement was conducted using the questionnaire created by Afraz et al. [12], which comprises five items.

Competitive advantage: The measurement of competitive advantage was conducted using a questionnaire developed by Chang [17], which comprises six items.

Firm performance: The measurement of firm performance was conducted using a questionnaire developed by Wijethilake et al. [18], which comprises of five items.

## 4 RESULTS

### 4.1 Reliability and Validity

As part of the testing of measurement models, the reliability of constructs and instruments (internal consistency) and the validity of the instruments (discriminant

validity) are evaluated. The reliability of a construct can be determined by three criteria, which are as follows: 1) the reliability, 2) the composite reliability, and 3) the average variance extracted. According to confirmatory factor analysis, loading  $\geq 0.6$  for each item indicates that the item is reliable within that construct. Additionally, item factor loads should be significant at least at the 0.01 level [11].

**Table 1** Factor loadings, CR, and AVE

Variable	Item	Factor	Alpha	CR	AVE
Supplier relationship	1	0.786	0.68	0.91	0.88
	2	0.816			
	3	0.861			
	4	0.893			
		0.769			
Customer relationship	1	0.772	0.54	0.86	0.79
	2	0.737			
	3	0.704			
	4	0.735			
	5	0.744			
Supply chain information sharing	1	0.713	0.57	0.89	0.85
	2	0.708			
	3	0.808			
	4	0.803			
	5	0.770			
	6	0.724			
Supply chain information quality	1	0.755	0.56	0.86	0.81
	2	0.749			
	3	0.690			
	4	0.807			
	5	0.748			
Supply chain innovation	1	0.820	0.71	0.92	0.90
	2	0.837			
	3	0.912			
	4	0.863			
	5	0.788			
Quality information and reporting	1	0.713	0.62	0.87	0.80
	2	0.786			
	3	0.832			
	4	0.823			
Product innovation	1	0.753	0.74	0.92	0.88
	2	0.905			
	3	0.856			
	4	0.912			
R&D management	1	0.919	0.74	0.92	0.88
	2	0.881			
	3	0.749			
	4	0.885			
Technology management	1	0.868	0.81	0.90	0.86
	2	0.846			
	3	0.892			
	4	0.751			
Competitive advantage	1	0.827	0.60	0.90	0.87
	2	0.746			
	3	0.838			
	4	0.714			
	5	0.739			
	6	0.770			
Firm performance	1	0.814	0.60	0.88	0.83
	2	0.824			
	3	0.776			
	4	0.710			
	5	0.737			

In order to assess the importance of factor loadings, a bootstrap test was conducted using 500 subsamples. The reliability of each construct was measured using the Dillon-

Goldstein coefficient ( $\rho_c$ ). A value of  $\rho_c$  greater than 0.7 is considered ideal for reliability. Lastly, the average variance is a criterion of reliability [11]. It is suggested that constructs should have an AVE value of at least 0.50, indicating that the construct explains at least 50% of the variance in its markers [11]. In Tab. 1, factor loadings, composite reliability, and AVEs are reported. It can be seen from the values displayed in these tables that the constructs are adequate and appropriate in terms of their reliability.

In order to determine the validity of a construct or its discriminant validity, two criteria are applied. Items of a construct must have the greatest factor load on their respective constructs and a low cross-sectional load on other constructs. Considering Gefen and Straub's [19] suggestion that factor loads should be at least 0.1 higher for each item on its related construct. Tab. 2 shows that cross-sectional loads are reported for the items on the constructs.

**Table 2** Cross-sectional factor loads for checking the validity of questionnaires

Variable Item	Supply chain management	Supply chain innovation	Competitive advantage	Firm performance	TQM
AS1	0.582	0.548	0.506	<b>0.814</b>	0.381
AS2	0.511	0.518	0.454	<b>0.824</b>	0.431
AS3	0.564	0.471	0.438	<b>0.776</b>	0.366
AS4	0.486	0.502	0.484	<b>0.71</b>	0.38
AS5	0.529	0.506	0.395	<b>0.737</b>	0.39
CA1	0.574	0.57	<b>0.827</b>	0.522	0.405
CA2	0.547	0.58	<b>0.746</b>	0.585	0.396
CA3	0.513	0.494	<b>0.838</b>	0.545	0.35
CA4	0.443	0.379	<b>0.714</b>	0.409	0.328
CA5	0.416	0.425	<b>0.739</b>	0.457	0.38
CA6	0.494	0.535	<b>0.77</b>	0.515	0.367
SCI1	0.516	<b>0.82</b>	0.42	0.499	0.403
SCI2	0.512	<b>0.837</b>	0.406	0.541	0.392
SCI3	0.585	<b>0.912</b>	0.506	0.5	0.434
SCI4	0.587	<b>0.863</b>	0.558	0.587	0.393
SCI5	0.5	<b>0.788</b>	0.479	0.504	0.346
SCM1	<b>0.786</b>	0.483	0.555	0.545	0.287
SCM2	<b>0.816</b>	0.509	0.574	0.533	0.361
SCM3	<b>0.861</b>	0.426	0.425	0.465	0.26
SCM4	<b>0.893</b>	0.481	0.471	0.504	0.228
SCM5	<b>0.769</b>	0.415	0.433	0.448	0.239
SCM6	<b>0.737</b>	0.374	0.435	0.451	0.285
SCM7	<b>0.704</b>	0.332	0.388	0.44	0.204
SCM8	<b>0.735</b>	0.263	0.38	0.357	0.228
SCM9	<b>0.744</b>	0.618	0.611	0.581	0.417
SCM10	<b>0.772</b>	0.484	0.461	0.537	0.328
SCM11	<b>0.713</b>	0.438	0.455	0.496	0.322
SCM12	<b>0.708</b>	0.362	0.474	0.501	0.279
SCM13	<b>0.808</b>	0.464	0.468	0.52	0.333
SCM14	<b>0.803</b>	0.369	0.377	0.453	0.252
SCM15	<b>0.77</b>	0.474	0.391	0.532	0.347
SCM16	<b>0.724</b>	0.485	0.393	0.532	0.358
SCM17	<b>0.755</b>	0.369	0.34	0.445	0.265
SCM18	<b>0.749</b>	0.371	0.429	0.389	0.131
SCM19	<b>0.69</b>	0.326	0.316	0.33	0.087
SCM20	<b>0.807</b>	0.47	0.314	0.477	0.246
SCM21	<b>0.748</b>	0.487	0.313	0.474	0.224
TQM1	0.353	0.295	0.332	0.386	<b>0.713</b>
TQM2	0.413	0.379	0.424	0.423	<b>0.786</b>
TQM3	0.255	0.389	0.352	0.368	<b>0.832</b>
TQM4	0.328	0.403	0.407	0.411	<b>0.823</b>
TQM5	0.359	0.323	0.325	0.419	<b>0.753</b>
TQM6	0.44	0.539	0.469	0.532	<b>0.905</b>
TQM7	0.375	0.561	0.497	0.505	<b>0.856</b>
TQM8	0.432	0.543	0.553	0.57	<b>0.912</b>
TQM9	0.403	0.527	0.564	0.526	<b>0.885</b>
TQM10	0.374	0.481	0.46	0.563	<b>0.919</b>
TQM11	0.416	0.506	0.444	0.547	<b>0.881</b>
TQM12	0.544	0.438	0.448	0.547	<b>0.749</b>
TQM13	0.555	0.417	0.487	0.591	<b>0.868</b>
TQM14	0.462	0.538	0.545	0.546	<b>0.846</b>
TQM15	0.593	0.435	0.568	0.581	<b>0.892</b>
TQM16	0.564	0.498	0.539	0.426	<b>0.751</b>

A minimum distance between factor loadings associated with the dimensions and their constructs is more than 0.1, suggesting good validity for the constructs based on Tab. 2. Based on correlation analysis and the square root of AVE, Tab. 3 shows the results related to validity. We have been

able to meet the second criterion for the discriminant validity of variables in our study. Furthermore, the correlation matrix's values below the diagonal have been reported to confirm that the variables are interrelated. All variables show a positive and significant correlation.

**Table 3** Correlation matrix

Variable	SCM	TQM	Supply chain innovation	Competitive advantage	Firm performance
SCM practices	<b>0.85</b>				
TQM	0.61**	<b>0.86</b>			
Supply chain innovation	0.63**	0.66**	<b>0.84</b>		
Competitive advantage	0.59**	0.61**	0.58**	<b>0.77</b>	
Firm performance	0.57**	0.53**	0.64**	0.61**	<b>0.77</b>

Note: The square root of AVE is represented by the values on the diagonal of the correlation matrix.

## 4.2 Tests of a Structural Model

To anticipate the performance of a firm, the conceptual model was assessed through SEM; in accordance with the hypotheses, a PLS analysis was used to estimate the model. Furthermore, *t*-values were calculated using the bootstrap method. Fig. 2 illustrates the proposed model for examining the relationship between variables.

As shown in Tab. 4, the estimated path coefficients are reported, as well as an explanation of the variance of the variables. A significant and positive mediating effect of TQM can be seen in Tab. 4 with regard to the effect of SCM practices on supply chain innovation, competitive advantage, and firm performance. There is a significant and positive mediating role played by supply chain innovation in relation

to competitive advantage, firm performance, TQM, competitive advantage, and firm performance. The mediating effect of competitive advantage on firm performance is positive and significant in the context of SCM practices, TQM practices, and supply chain innovation. The model variables can explain 78% of the variance in firm performance, 61% of the variance in competitive advantage, 58% of the variance in supply chain innovation, and 38% of the variance in TQM.

PLS uses the GOF index to measure the fit of the overall model. GOF was measured at 0.65 for the tested model in the current study, which indicates that the model is well-fitted. It is considered that the quality of the model is good and acceptable when the value is greater than 0.36.

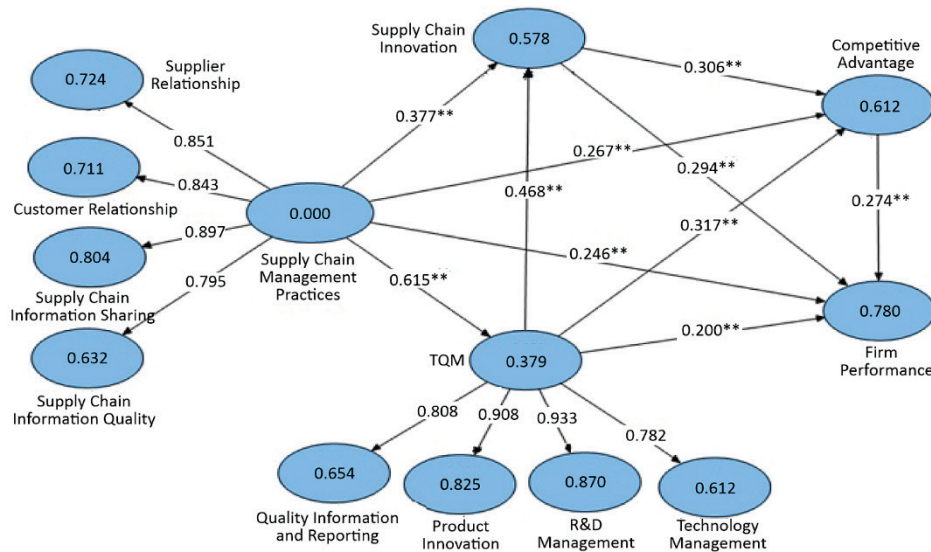


**Figure 2** The tested model

## 5 DISCUSSION

Upon analysis, it was discovered that SCM practices had a positive and significant correlation with TQM, supply chain innovation, competitive advantage, and overall firm performance. According to Nazari-Shirkouhi et al. [7], Agyabeng-Mensah et al. [20], and Cousins et al. [21], Tavana et al. [27], the results are consistent with this finding. The present study suggests that firms can improve their TQM,

supply chain innovation, and competitive advantage by considering quality in supplier selection. Additionally, regular joint problem-solving with suppliers, enhancing the quality of products/services, and having ongoing development/growth plans with suppliers can lead to improved firm performance. Involving key suppliers in the process of planning and setting goals, frequently measuring and evaluating customer satisfaction, setting future customer expectations through frequent interaction, informing

business partners of changes in needs that affect their business, sharing proprietary information with business partners, and exchanging information that might impact the partnership are also important factors for improving firm performance. These findings highlight the importance of a collaborative approach to supplier management and suggest

that firms should take into account quality and engage in ongoing communication with their business partners to achieve better outcomes. It is essential that this exchange of information be timely, accurate, complete, sufficient, and reliable to ensure that informed decisions are made by all parties.

**Table 4** Path coefficients and explained variance

Variable	$\beta$	t-value	Variance explained
On firm performance via: Competitive advantage Supply chain innovation TQM SCM practices	0.27** 0.29** 0.20** 0.25**	5.853 5.592 3.825 5.618	0.78
On competitive advantage via: Supply chain innovation TQM SCM practices	0.30** 0.32** 0.27**	5.315 5.208 4.960	0.61
On supply chain innovation via: TQM SCM practices	0.47** 0.38**	8.825 7.192	0.58
On TQM via: SCM practices	0.61**	12.688	0.38
The mediating role of TQM in the effect of: SCM practices on supply chain innovation SCM practices on competitive advantage SCM practices on firm performance	0.29** 0.19** 0.12**	7.245 4.818 3.662	-
The mediating role of supply chain innovation in the effect of: SCM practices on competitive advantage SCM practices on firm performance TQM on competitive advantage TQM on firm performance	0.11** 0.11* 0.14** 0.14**	4.274 4.414 4.553 4.723	-
The mediating role of competitive advantage in the effect of: SCM practices on firm performance TQM on firm performance Supply chain innovation on firm performance	0.07** 0.09** 0.08**	3.784 3.891 3.935	-

\* $p < 0.05$ ; \*\* $p < 0.01$

According to the model, TQM influences supply chain innovation, competitive advantage, and firm performance. The results of this study are in agreement with the findings reported in previous research studies including Masoudi [22], Ezenyilimba et al. [15], and Ali et al. [23]. For clarity, the current research aims to demonstrate how supply chain innovation, competitive advantages, and firm performance can be achieved through the availability of quality information. Such quality information should be timely, accurate, and reliable as well as used to improve management practices. To achieve these goals, firms should make use of the latest technological innovations in the development of new products which should be done significantly fast. Additionally, having products that have been introduced to the market for the first time is a crucial aspect of this process. Crucially, the research and development (R&D) department must have satisfactory communication processes with other departments in the firm and should follow innovative and progressive research. High-risk projects with opportunities for high returns should be the main characteristics of a sound R&D strategy. Moreover, R&D department should always be an integral part of the business strategy, emphasizing the importance of staying ahead in new technologies related to the industry, anticipating the full potential of new practices and technologies, pursuing long-term plans to achieve

technological capabilities and constantly considering the next generation of technology.

The study reveals that supply chain innovation influences significantly both competitive advantage and firm performance. The present study's findings are consistent with previous research conducted by Banmairuoy et al. [24], Afraz et al. [12], and Fatoki [25]. The study aims to explain this finding by highlighting the importance of a supplier-buyer relationship that is strengthened through various factors. These factors include delivering products/services to customers using the latest technologies, ensuring that all supply chain partners provide the highest quality to customers, developing new products before competitors, actively adapting to customer needs, relying on suppliers as a source of innovation in products/services, and allocating more funds to the R&D department. By focusing on these factors, firms can improve their supplier-buyer relationships and ultimately enhance their overall performance in the market. Currently, innovation is considered one of the most valuable and stable sources of creating a comparative advantage for different companies, and it is considered one of the main necessary tools for developing new organizational practices for business management. Therefore, considering the dynamic and complex conditions that organizations face in a highly competitive environment, the continuous need to develop organizational innovation has

become more tangible for various organizations and companies. It seems that this phenomenon is likely to play a pivotal role in developing and strengthening consulting services and increasing income and stabilizing their activities.

The effect of competitive advantage influences firm performance. Therefore, competitive advantage leads to improvement in firm performance. The discovery is in agreement with the studies conducted by Wijayanto et al. [26]. To provide a better understanding of this phenomenon, it is important to note that a firm's performance can be significantly enhanced if it possesses superior product or service quality compared to its competitors. Additionally, a company's proficiency in R&D, management capabilities, financial profitability, corporate image, and difficult-to-replicate competitive advantages all contribute to better performance. Therefore, it is crucial for firms to focus on these factors to gain a competitive edge over their competitors. Note that the success of a company is based on a sustainable competitive advantage and maintaining it. In fact, understanding which resources or behaviors lead to competitive advantage is the main issue in marketing strategy.

According to the findings, TQM significantly contributes to the innovation of supply chain, competitive advantage, and firm performance when it comes to SCM practices. SCM practices and TQM both influence competitive advantage and firm performance positively and significantly through supply chain innovation. Firm performance is positively affected by SCM practices, TQM, and supply chain innovation through competitive advantage. In conclusion, through supply chain innovation and TQM, SCM practices can boost performance and competitive advantage.

## 6 CONCLUSION

This research article investigated the influence of SCM practices on firm performance and competitive advantage, with a focus on the mediating role of supply chain innovation and TQM. The results elucidated that the data fit the proposed model, explaining 78% of the variance in firm performance, 61% of the variance in competitive advantage, 58% of the variance in supply chain innovation, and 38% of the variance in TQM. However, it should be noted that these findings are limited to a sample of managers, assistants, and supply chain specialists in SMEs in Iran. Additionally, self-report data were used for analysis. Therefore, mixing qualitative and quantitative methods is recommended to further investigate the implications of SCM practices and TQM.

## 7 REFERENCES

- [1] Noruzi, A., Dalfard, V. M., Azhdari, B., Nazari-Shirkouhi, S., & Rezazadeh, A. (2013). Relations between transformational leadership, organizational learning, knowledge management, organizational innovation, and organizational performance: an empirical investigation of manufacturing firms. *The International Journal of Advanced Manufacturing Technology*, 64(5), 1073-1085. <https://doi.org/10.1007/s00170-012-4038-y>
- [2] Nazari-Shirkouhi, S., Keramati, A., & Rezaie, K. (2013). Improvement of customers' satisfaction with new product design using an adaptive neuro-fuzzy inference systems approach. *Neural Computing and Applications*, 23(1), 333-343. <https://doi.org/10.1007/s00521-013-1431-x>
- [3] Nazari-Shirkouhi, S., Shakouri, H., Javadi, B., & Keramati, A. (2013). Supplier selection and order allocation problem using a two-phase fuzzy multi-objective linear programming. *Applied Mathematical Modelling*, 37(22), 9308-9323. <https://doi.org/10.1016/j.apm.2013.04.045>
- [4] Zekhnini, K., Cherrafi, A., Bouhaddou, I., Benghabrit, Y., & Garza-Reyes, J. A. (2020). Supply chain management 4.0: a literature review and research framework. *Benchmarking: An International Journal*, 28(2), 465-501. <https://doi.org/10.1108/BIJ-04-2020-0156>
- [5] Hugos, M. H. (2018). *Essentials of supply chain management*. John Wiley & Sons. <https://doi.org/10.1002/9781119464495>
- [6] Nazari-Shirkouhi, S., Keramati, A., & Rezaie, K. (2015). Investigating the effects of customer relationship management and supplier relationship management on new product development. *Tehnički vjesnik*, 22(1), 191-200. <https://doi.org/10.17559/TV-20140623130536>
- [7] Nazari-Shirkouhi, S., Tavakoli, M., Govindan, K., & Mousakhani, S. (2023). A hybrid approach using Z-number DEA model and Artificial Neural Network for Resilient Supplier Selection. *Expert Systems with Applications*, 119746. <https://doi.org/10.1016/j.eswa.2023.119746>
- [8] Tavana, M., Nazari-Shirkouhi, S., & Farzaneh Kholghabad, H. (2021). An integrated quality and resilience engineering framework in healthcare with Z-number data envelopment analysis. *Health care management science*, 24, 768-785. <https://doi.org/10.1007/s10729-021-09550-8>
- [9] Nazari-Shirkouhi, S., Mousakhani, S., Tavakoli, M., Dalvand, M. R., Šaparauskas, J., & Antuchevičienė, J. (2020). Importance-performance analysis based balanced scorecard for performance evaluation in higher education institutions: an integrated fuzzy approach. *Journal of Business Economics and Management*, 21(3), 647-678. <https://doi.org/10.3846/jbem.2020.11940>
- [10] Kahn, K. B. (2018). Understanding innovation. *Business Horizons*, 61(3), 453-460. <https://doi.org/10.1016/j.bushor.2018.01.011>
- [11] Alipour, N., Nazari-Shirkouhi, S., Sangari, M. S., & Vandchali, H. R. (2022). Lean, Agile, Resilient, And Green Human Resource Management: The Impact On Organizational Innovation and Organizational Performance. *Environ Sci Pollut Res.*, 29(55), 82812-82826. <https://doi.org/10.1007/s11356-022-21576-1>
- [12] Afraz, M. F., Bhatti, S. H., Ferraris, A., & Couturier, J. (2021). The impact of supply chain innovation on competitive advantage in the construction industry: Evidence from a moderated multi-mediation model. *Technological Forecasting and Social Change*, 162, 120370. <https://doi.org/10.1016/j.techfore.2020.120370>
- [13] Le, T. T., & Ikram, M. (2022). Do sustainability innovation and firm competitiveness help improve firm performance? Evidence from the SME sector in vietnam. *Sustainable Production and Consumption*, 29, 588-599. <https://doi.org/10.1016/j.spc.2021.11.008>
- [14] Sotiřelis, P., & Grigoroudis, E. (2021). Total quality management and innovation: Linkages and evidence from the agro-food industry. *Journal of the Knowledge Economy*, 12(4), 1553-1573. <https://doi.org/10.1007/s13132-020-00683-9>
- [15] Ezenyilimba, E., Ezejiofor, R. A., & Afodigbueokwu, H. E. (2019). Effect of total quality management on organizational

- performance of deposit money banks in Nigeria. *International Journal of Business & Law Research*, 7(3), 15-28.
- [16] Modgil, S. & Sharma, S. (2016). Total productive maintenance, total quality management and operational performance: An empirical study of Indian pharmaceutical industry. *Journal of Quality in Maintenance Engineering*, 22(4), 353-377. <https://doi.org/10.1108/JQME-10-2015-0048>
- [17] Chang, C. H. (2011). The influence of corporate environmental ethics on competitive advantage: The mediation role of green innovation. *Journal of Business Ethics*, 104(3), 361-370. <https://doi.org/10.1007/s10551-011-0914-x>
- [18] Wijethilake, C., Munir, R., & Appuhami, R. (2018). Environmental innovation strategy and organizational performance: Enabling and controlling uses of management control systems. *Journal of Business Ethics*, 151(4), 1139-1160. <https://doi.org/10.1007/s10551-016-3259-7>
- [19] Gefen, D., & Straub, D. (2005). A practical guide to factorial validity using PLS-Graph: Tutorial and annotated example. *Communications of the Association for Information Systems*, 16(1), 91-109. <https://doi.org/10.17705/1CAIS.01605>
- [20] Agyabeng-Mensah, Y., Afum, E., Agnikpe, C., Cai, J., Ahenkorah, E., & Dacosta, E. (2020). Exploring the mediating influences of total quality management and just in time between green supply chain practices and performance. *Journal of Manufacturing Technology Management*, 32(1), 156-175. <https://doi.org/10.1108/JMTM-03-2020-0086>
- [21] Cousins, P. D., Lawson, B., Petersen, K. J., & Fugate, B. (2019). Investigating green supply chain management practices and performance: The moderating roles of supply chain ecocentricity and traceability. *International Journal of Operations & Production Management*, 39(5), 767-786. <https://doi.org/10.1108/IJOPM-11-2018-0676>
- [22] Masoudi, E. (2021). Impact of total quality management on innovation in small and medium enterprises with the mediating role of organizational learning. *Quarterly journal of Industrial Technology Development*, 19(43), 77-92.
- [23] Ali, G. A., Hilman, H., & Gorondutse, A. H. (2020). Effect of entrepreneurial orientation, market orientation and total quality management on performance: Evidence from Saudi SMEs. *Benchmarking: An International Journal*, 27(4), 1503-1531. <https://doi.org/10.1108/BIJ-08-2019-0391>
- [24] Banmairuoy, W., Kritjaroen, T., & Homsombat, W. (2022). The effect of knowledge-oriented leadership and human resource development on sustainable competitive advantage through organizational innovation's component factors: Evidence from Thailand's new S-curve industries. *Asia Pacific Management Review*, 27(3), 200-209. <https://doi.org/10.1016/j.apmr.2021.09.001>
- [25] Fatoki, O. (2021). Dynamic Capabilities and Performance Of Hospitality Firms In South Africa: The Mediating Effect Of Innovation. *Geo Journal of Tourism and Geosites*, 36, 616-623. <https://doi.org/10.30892/gtg.362spl08-690>
- [26] Wijayanto, A., Dzulkriom, M., & Nuzula, N. F. (2019). The effect of competitive advantage on financial performance and firm value: evidence from Indonesian manufacturing companies. *Russian Journal of Agricultural and Socio-Economic Sciences*, 85(1), 35-44. <https://doi.org/10.18551/rjoas.2019-01.04>
- [27] Tavana, M., Nazari-Shirkouhi, S., Mashayekhi, A., & Mousakhani, S. (2022, March). An Integrated Data Mining Framework for Organizational Resilience Assessment and Quality Management Optimization in Trauma Centers. *Operations Research Forum*, 3(1), p. 17. <https://doi.org/10.1007/s43069-022-00132-0>

#### Authors' contacts:

##### Erfan Mehregan

(Corresponding author)  
Department of Management, Sharif University of Technology,  
Khayaban Azadi, Khayaban Habib Elahi, Exhumation of Timurid Square,  
Tehran, Iran  
E-mail: erfan.mehregan@alum.sharif.edu

##### Somayeh Sanaei

Management & Economics School, Science & Research branch,  
Islamic Azad University, Tehran, Iran

##### Mohsen Manna

Department of Mechanical Engineering, University of Hormozgan,  
KM 9 of Minab Road, Bandar Abbas, Iran

##### Hamed Bozorgkhoh

Department of Business Administration, University of Tehran,  
16th Azar St., Enghelab Sq., Tehran, Iran

##### Shahin Heidari

Pompea College of Business, University of New Haven,  
300 Boston Post Rd, West Haven, CT 06516, USA

# Properties of Magnesia Composites According to Replacement Ratio of Perlite

Jeon-Ho Lee, Woo-Jun Hwang, Chang-Woo Lee, Sang-Soo Lee\*

**Abstract:** Recently, passive and zero-energy construction has increased in Korea due to the government's continuous application of budget-conscious policies for establishments. Accordingly, construction materials are being advanced, and the required performance standards for insulation materials are increasing. However, problems such as fire vulnerability and degradation of physical properties for organic and inorganic insulation materials are shown, so it is necessary to solve this problem. The objective of this research is to examine the properties of the composites by analyzing the flexural breaking load, impact resistance, density, VOCs concentration reduction rate, and fine dust concentration reduction rate of the composites manufactured based on the perlite substitution rate of the magnesia composites. The flexural breaking load test of the composites was assessed according to 'KS F 3504', a gypsum board standard and the impact resistance was assessed according to 'KS F 4715'. The performance evaluation of adsorption performance of air pollutants of the VOCs and fine dust in the context of the small chamber technique suggested by Hanbat University. The results of this study are as follows: The flexural breaking load according to the perlite replacement rate tended to decrease as the perlite replacement rate increased. It is determined that the flexural breaking load is reduced by generating a large amount of pores inside due to the perlite porous structure characteristics. In the case of impact resistance, the impact resistance tended to increase as the perlite displacement rate increased. It is determined that the volume of the binder in the board is reduced, and pores inside the board are generated due to perlite, which is a porous material, thereby reducing the overall bonding force of the board. In the case of VOCs and fine dust concentrations, the VOCs and fine dust concentration reduction rates tended to increase as the perlite replacement rate increased. In the case of the perlite displace rate of 30%, the VOCs concentration decreased by 82.6%, and the fine dust concentration decreased by 87.9%. It has been established that the porous properties of perlite used to create a huge number of pores in the hardened body cause the concentration to be lowered physically through adsorption. This study's findings are thought to be fundamental information for securing the engineering properties and air pollution absorption of magnesia composites blended with perlite.

**Keywords:** eco-friendly; finishing materials; indoor air quality; magnesia composites; perlite

## 1 INTRODUCTION

In 2020, the Korea Energy Corporation, the Ministry of Land, Infrastructure, Transport, and the Ministry of Trade and Industry will emphasize the significance of cutting carbon emissions, saving energy, and improving efficiency due to the arrival of the fourth industrial revolution. Due to the government's continuing application of energy reduction programs, the performance requirements for building materials have increased, and passive and zero-energy construction has expanded. Accordingly, construction materials are being advanced, and the required performance standards for insulation materials are increasing. Demand for organic insulation is high due to high insulation and economy, but the problem of fire safety of organic insulation materials continues to be raised. In 2015, a fire broke out in an apartment in Uijeongbu-si, and the cause of the spread of the fire was pointed out as a problem with dryvit construction. The fire begin on the ground floor extensively expand along the outer wall, casualties occurred because of the smoke and toxic gases [1]. Most of the finishes currently used for internal finishes are organic materials such as cork and wooden boards, but organic sound-absorbing finishes have a high risk of fire. As a result, fire safety is emphasized, and there is growing need for inorganic insulation [2]. ALC panels and blocks are often produced as an inorganic insulation material, and the majority of them are used extensively as lightweight or insulating materials. However, inorganic insulating materials are susceptible to moisture, which can lead to mold growth owing to condensation and the deterioration of physical qualities [3]. In order to balance the fire risk of organic insulation with the economics and moisture sensitivity of inorganic insulation, this study will

analyze the properties of the composites based on the perlite replacement rate.

Table 1 Experimental factors and levels		
Experimental factors	Experimental levels	
Binder	Magnesia, Potassium phosphate	2
Magnesia: Potassium phosphate	1 : 0.8 (%)	1
Replacement rate of perlite	30, 35, 40, 45, 50 (%)	5
Additional rate of retardant	5 (%)	1
Additional rate of water reducing agent	0.1 (%)	1
W/B	45 (%)	1
Curing condition	Temp. 20±2°C, Hum. 60±5%	1
Experimental item	Flexural breaking load, Impact resistance, Density, VOCs reduction, Fine dust reduction	5

## 2 EXPERIMENTAL PLAN

Perlite was swapped out for a level made of MPC in order to create an insulating composite based on non-cement in this experiment to test the production of an environmentally friendly inorganic finishing material. In the MPC, light burned magnesia and monopotassium phosphate was combined at a ratio of 1.0:0.8 as a binder, and borax was added as a delay material because it did not have a sufficient time for punching due to the initial heat generation. In addition, when perlite was mixed into MPC, the absorption rate of perlite was high, and a reducing agent was added 0.1% compared to the binder due to the reduction in the number of constraints required for the hydration reaction. The perlite replacement rate range was divided into five levels from 30 to 50 (%), and on the 28<sup>th</sup>, post-curing flexural breaking load, impact resistance, density, VOCs reduction, and fine dust reduction tests were conducted. Accordingly, the

experimental factors and levels are as follows in Tab. 1 [4].

## 2.1 Materials

### 2.1.1 Perlite

Perlite refers to an extremely lightweight aggregate obtained by grinding and firing perlite or graphite. When the perlite gemstone is pulverized below 8 to 12 mesh and high heat of 1000 °C or higher is rapidly applied, the contained volatile components gasify and expand inside the softened particles, forming internal pores. In addition, it has excellent moisturizing power and is lightweight with 0.15 g/cm<sup>3</sup>, so it is easy to work, and it has excellent insulation, fire resistance, air permeability, and sound absorption. Since Ph is neutral, it is harmless to the human body and is used as an insulation material, spray material, and sound absorbing material [5].

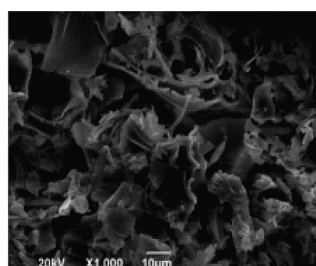


Figure 1 Perlite



Figure 2 SEM of perlite

Table 2 Physical properties of perlite

Density (g/cm <sup>3</sup> )	Porosity (%)	Thermal conductance (kcal/mh°C)	Available temperature (°C)	pH	Fineness modulus
0.15	Around 90	0.03-0.05	-250-1,000	6.5-7.5	2.94

### 2.1.2 Light Burned Magnesia

In this experiment, light burned magnesia, which is used as an alternative material for cement, is fired at a low temperature of 600-1000 °C from the magnesia mined at the bottom of the mine or magnesia separated from seawater. Accordingly, the density of light burned magnesia used in this study is 3.46 g/cm<sup>3</sup> and the fineness is 2,591 cm<sup>3</sup>/g [6].

Table 3 Physical properties of light burned magnesia

Fineness (cm <sup>3</sup> /g)	Porosity (%)	Density (g/cm <sup>3</sup> )	Grain size (%)	Volumetric specific gravity (%)
2,591	0.50	3.46	-200 mesh ≥ 97	1.25

Table 4 Chemical properties of light burned magnesia

Composition ratio (%)						
MgO	CaO	SiO <sub>2</sub>	Fe <sub>2</sub> O <sub>3</sub>	SO <sub>3</sub>	Al <sub>2</sub> O <sub>3</sub>	Cl
93.30	2.06	3.14	0.60	0.11	0.52	0.06

### 2.1.3 Monopotassium Phosphate

Monopotassium phosphate is a colorless crystalline or white granular crystalline powder. When monopotassium phosphate is heated, it is dehydrated at 400 °C and produces potassium metaphosphate. It dissolves in water and its aqueous solution is weakly acidic and does not dissolve in

ethyl alcohol. The physical composition of monopotassium phosphate used are shown in the following table.

Table 5 Physical properties of monopotassium phosphate

Molecular Weight (g)	Melting point (°C)	Boiling Point (°C)	Density (g/mL)	pH	Solubility (g/100 mL)
136.09	253	450	2.338	5.7~7.5	1.05

### 2.1.4 Borax

Borax used as a condensation retardant of the magnesia composites is an inorganic mineral extracted from a mine or salt lake, and the chemical structural formula is expressed as Na<sub>2</sub>B<sub>4</sub>O<sub>7</sub>×10H<sub>2</sub>O. The specific gravity is 1.7, and when the crystal contains 10 molecules of water and is heated to 350-400°C, the crystal water is lost and expanded to become anhydride. The properties of borax are shown in the Tab. 6 [7].

Table 6 Physical properties of borax

Molecular weight (g)	Melting point (°C)	Boiling point (°C)	Specific gravity (g/mL)	Solubility (g/100 mL)
381.36	75	320	2.338	6.025

## 2.2 Experimental Methods

### 2.2.1 Density and Flexural Breaking Load

Density test method is carried out according to 'KS F 3503', and the flexural breaking load test method is carried out in accordance with 'KS F 3504'. The test piece is dried in a dryer adjusted to a temperature of 40±2 °C until it is shaped and tested immediately. The span shall be 350 mm and the concentrated load shall be applied to the full width of the center of the span. The average load speed shall be 250 N/min ± 20%.

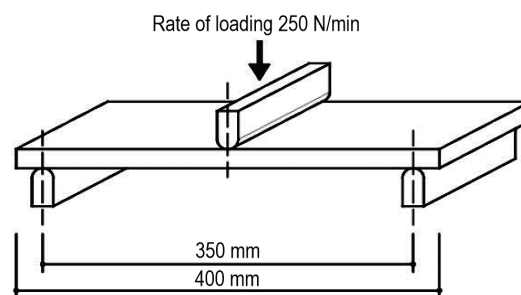


Figure 3 Test method for flexural breaking load

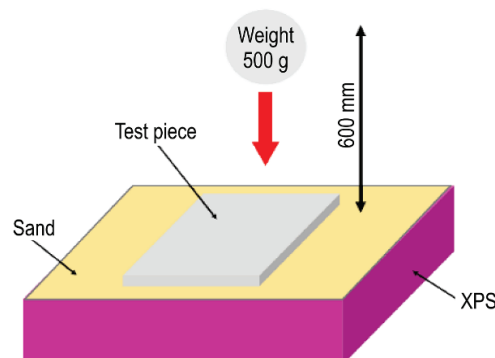


Figure 4 Test method for impact resistance

## 2.2.2 Impact Resistance

Impact resistance test method is carried out in according to 'KS F 4715'. Measure a weight of 500 g away from the top of the test specimen at a height of 60 cm, and conduct the test at three locations that are more than 5 cm apart, and visually check for cracks, swelling, deformation, and peeling.

## 2.2.3 Reduction of Pollutants

Evaluation of the reduction performance of the sound-absorbing finishing material mixed with perlite measures the amount of VOCs and fine dust reduction on its own. VOCs and fine dust reduction measurements are carried out in the manner proposed by Hanbat University because there are no standards. For the first time, a substance that generates pollutants is put inside an empty chamber that is sealed and the reference concentration is adjusted inside the chamber. After adjusting the reference concentration, remove the contaminant-producing substance, put the test specimen in, measure it for a certain period of time, analyze and calculate how much it has decreased in the reference concentration, and evaluate the pollutant purification performance [8-12].

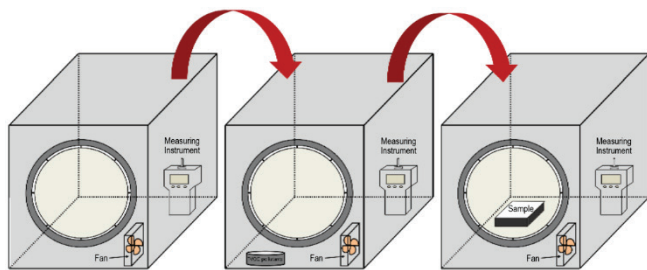


Figure 5 Test method for VOCs and fine dust reduction

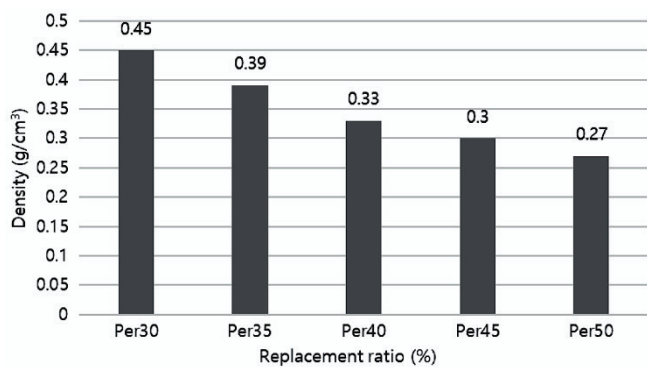


Figure 6 Density

## 3 EXPERIMENTAL RESULT AND ANALYSIS

### 3.1 Density

The graph showing the density based on the perlite replacement rate is shown in Fig. 6. The density have a tendency to lessen as the perlite replacement rate augmented. When comparing a unit weight, the density of the magnesia composites is smaller than that of the magnesia cured body, and the density of the perlite is much lower than that of the light burned magnesia and the monopotassium phosphate, so that the density is decreased as the perlite replacement rate

increased [13].

## 3.2 Flexural Breaking Load

The graph showing the flexural breaking load according to the perlite replacement rate is presented in Fig. 7. As the perlite displacement rate increased, the flexural breaking load tended to decrease. Because of the properties of the porous structure of perlite, it is believed that developing a large number of pores inside reduces the flexural breaking load.

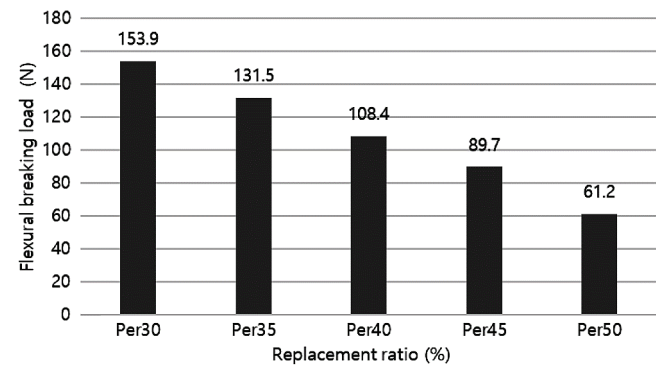


Figure 7 Flexural breaking load

Table 7 Impact resistance

Replacement rate of perlite (%)	Diameter of the concave portion (mm)	Picture
30	14.3	
35	21.2	
40	26.8	
45	Crack occurred	
50	Crack occurred	

### 3.3 Impact Resistance

The graph showing impact resistance according to the perlite replacement rate is presented in Tab. 7. As the perlite replacement rate increased, the impact resistance have a tendency to increase. It is determined that the volume of the binder in the board is reduced, and pores inside the board are generated due to perlite, which is a porous material, thereby reducing the overall bonding force of the board [14, 15].

### 3.4 VOCs Concentration Reduction Rate

The graph showing the VOCs concentration reduction rate according to the perlite replacement rate is shown in Fig. 8. The VOCs concentration reduction rate have a tendency to increase as the perlite replacement rate increased. When it approaches the surface, mutual attraction by the dipole acts, drawing the contaminant to the surface when it approaches, and accumulating it inside the perlite pores by electrostatic attraction. Accordingly, it is determined that the VOCs concentration reduction rate rises as the perlite replacement rate increases.

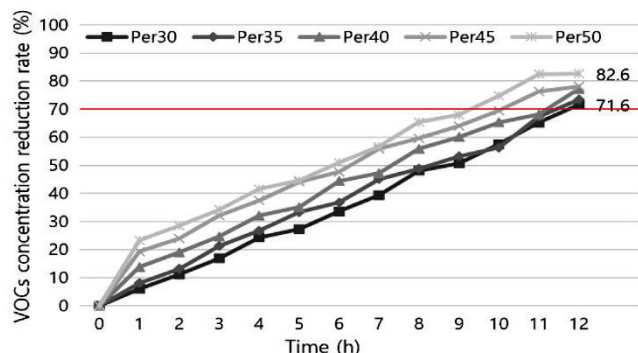


Figure 8 VOCs concentration reduction rate

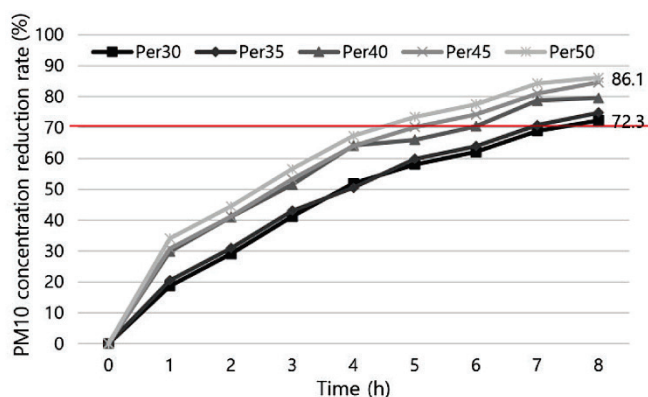


Figure 9 PM2.5 concentration reduction rate

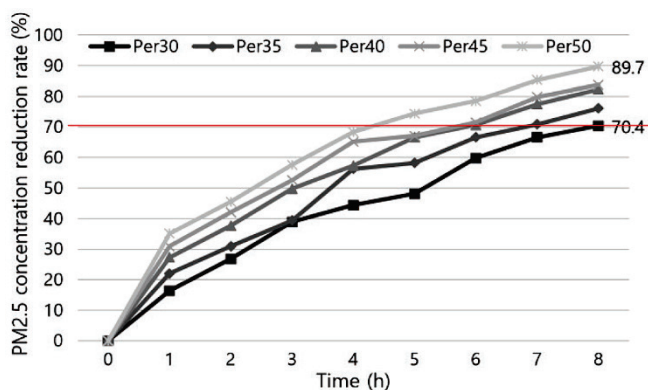


Figure 10 PM10 concentration reduction rate

### 3.5 Fine Dust Concentration Reduction Rate (PM2.5, PM10)

The graph showing the rate of reduction of fine dust (PM2.5, PM10) concentration based on a perlite replacement

rate is presented in Fig. 9 and Fig. 10. As the perlite replacement rate increased, the fine dust concentration reduction rate have a tendency to increase. The physical adsorption produced by creating a significant number of pores in the hardened body due to the perlite's porous structure properties is believed to lower the concentration of fine particles.

## 4 CONCLUSION

This research is to analyze the density, flexural breaking load, impact resistance, VOCs concentration, and fine dust concentration of magnesia composites manufactured according to the perlite replacement rate and examine the characteristics of magnesia composites as follows. Findings shows that, as the perlite replacement rate increased, the flexural breaking load decreased. Because of the properties of the porous structure of perlite, it is believed that developing a large number of pores inside reduces the flexural breaking load. For flexural breaking loads, it is deemed appropriate to have a perlite displacement rate of 35% according to 'KS F 3504'. In the case of impact resistance, the result showed that the diameter of the concave part defined in 'KS F 4715' was within 25 mm up to a perlite replacement rate of 35%. In addition, when the perlite replacement rate was 45,50%, cracks occurred, which is determined to reduce the overall bonding force of the board as voids inside the board occur due to the perlite, which is a porous material. In the case of VOCs and fine dust concentrations, the VOCs and fine dust concentration reduction rates tended to increase as the perlite replacement rate increased. In the case of the perlite replacement rate of 30%, the VOCs concentration decreased by 82.6%, and the fine dust concentration decreased by 87.9%. It is discovered that the concentration is decreased by physical adsorption accumulated in the pores of the perlite by electrostatic attraction when the pollutant approaches the surface and is attracted to the surface when it is close by a dipole. Therefore, the appropriate perlite replacement rate for the magnesia composites is considered to be the most appropriate 30%, it can be used as a fundamental data to secure the engineering characteristics and the air pollutant adsorption of the magnesia composites mixed with perlite. In addition, further studies such as fire stability evaluation and sound absorption coefficient are needed to evaluate the usability of magnesia complexes mixed with perlite in the future.

## Acknowledgments

This work was supported by the Technology Development Program (202104340001) and financed by the Ministry of SMEs and Startups (MSS, Korea).

## 5 REFERENCES

- [1] Kim, S. S. (2015). Fire at apartment blocks kills 4, leaves 124 injured. *Korea Joongang Daily*, 2015, January. [https://www.koreatimes.co.kr/www/nation/2018/11/113\\_171493.html](https://www.koreatimes.co.kr/www/nation/2018/11/113_171493.html)

- [2] Choi, B. C. (2021). Properties of Cement Matrix for Thermal Insulation using Cork. *International Journal of Mechanical Engineering*, 6(3), 826-831. [https://kalaharijournals.com/resources/IJME2021Dec81-100/DEC\\_88.pdf](https://kalaharijournals.com/resources/IJME2021Dec81-100/DEC_88.pdf)
- [3] Lee, C. W. (2021). Properties of CLC using Silica to Suppress Cracking due to Drying Shrinkage. *Journal of the Korea Institute of Building Construction*, 22(2), 125-126. <http://www.riss.kr/link?id=A107913808>
- [4] Song, H. Y., Lim, J. J., Khil, B. S., & Lee, S. S. (2019). Properties of Inorganic Adhesives according to Phosphate Type and Borax Ratio. *Journal of the Korea Institute of Building Construction*, 19(4), 289-297. <http://www.riss.kr/link?id=A106330281>
- [5] Shin, J. H., Kim, D. Y., Lee, D. H., & Lee, S. S. (2018). Thermal insulation property according to perlite addition ratio of non cement matrix using paper ash and polysilicon sludge. *Journal of the Korea Institute of Building Construction*, 18(2), 165-166. <http://www.riss.kr/link?id=A105955870>
- [6] Pyeon, S. J., Lim, H. U., & Lee, S. S. (2018). Evaluation of Decreasing Concentration of Radon Gas for Indoor Air Quality with Magnesium Oxide Board using Anthracite. *Journal of the Korea Institute of Building Construction*, 18(1), 9-15. <http://www.riss.kr/link?id=A105108565>
- [7] Kim, D. Y., Pyeon, S. J., Lim, J. J., & Lee, S. S. (2018). Strength properties of inorganic adhesives using dead burned magnesia and phosphate according to addition ratio of borax. *Journal of the Korea Institute of Building Construction*, 18(2), 48-49. <http://www.riss.kr/link?id=A105955953>
- [8] Gwon, O. H., Lim, H. U., & Lee, S. S. (2017). Properties of Radon Gas Absorption of Matrix According to Types of Absorbent. *Journal of the Korea Institute of Building Construction*, 17(1), 15-21. <https://doi.org/10.5345/JKIBC.2017.17.1.015>
- [9] Lee, H. E. & Lee, S. S. (2021). Properties of Binder Board Mixed with Chitosan. *Journal of the Architectural Institute of Korea*, 37(12), 329-338. <http://www.riss.kr/link?id=A107969948>
- [10] Kim, Y. H. (2021). Evaluation of Applicability of Cementless Matrix Board Using ZrO<sub>2</sub>. *Master's Thesis*, Hanbat University: 2021, 31-38. <http://www.riss.kr/link?id=T15748047>
- [11] Choi, B. C. (2022). Properties of Granular Activated Clay Added Water-Based Paint for Improving Indoor Air Quality. *Master's Thesis*, Hanbat University: 2022, 26. <http://www.riss.kr/link?id=T16045744>
- [12] Lee, J. H. (2022). Properties of Adsorption Matrix Using Sodium Bicarbonate and Citric acid. *Master's Thesis*, Hanbat University: 2022, 26-27. <http://www.riss.kr/link?id=T16045776>
- [13] Jung, B. Y., Kim, H. T., Song, C. H., Lee, S. S., & Song, H. Y. (2014). Density and Compressive Strength Properties of Magnesium Oxide Matrix According to Addition Ratios of Perlite. *Korea : Korea Concrete Institute*, 14(5), 427-428. <http://www.riss.kr/link?id=A103011926>
- [14] Shin, J.H. (2020). Properties of inorganic matrix using polysilicon sludge for finishing board. *Doctoral dissertation*, Hanbat University: 2020, 87-90. <http://www.riss.kr/link?id=T15642697>
- [15] Lim, H.U. (2020). Properties of magnesium oxide board for improving indoor air quality using vermiculite. *Doctoral dissertation*, Hanbat University: 2020, 99-100. <http://www.riss.kr/link?id=T15482853>

#### Authors' contacts:

**Jeon-Ho Lee**, Doctor's course  
Hanbat National University,  
125, Dongseo-daero, Yuseong-gu, Daejeon, Korea  
042-821-1635, ehdrkajh@naver.com

**Woo-Jun Hwang**, Master's course  
Hanbat National University,  
125, Dongseo-daero, Yuseong-gu, Daejeon, Korea  
042-821-1635, koo0012@naver.com

**Chang-Woo Lee**, Master's course  
Hanbat National University,  
125, Dongseo-daero, Yuseong-gu, Daejeon, Korea  
042-821-1635, lcw2509@naver.com

**Sang-Soo Lee**, Professor  
(Corresponding author)  
Hanbat National University,  
125, Dongseo-daero, Yuseong-gu, Daejeon, Korea  
042-821-1635, sslee111@hanbat.ac.kr

# A Study on Radiant Heat Application to the Curing Process for Improvement of Free-form Concrete Panel Productivity

Hyekwon Kim, Yejin Jeong, Sangwon Seo, Jongyoung Youn, Donghoon Lee\*

**Abstract:** As free-form panel production takes a long time, it extends the construction period and increases construction expenses. This study suggests a method to apply radiant heat to concrete for the purpose of shortening the curing and removal process in free-form panel production. The optimal temperature and time for removal are determined based on the results of constant temperature/humidity curing experiments and quartz tube heater curing experiments. Through an experiment in various time settings, the general time of FCP (Free-form Concrete Panel) production is measured to examine whether the productivity is enhanced. It is expected that findings of this study contribute to shortening the construction period and reducing construction expenses as well as future studies on the FCP manufacturing equipment.

**Keywords:** free-form concrete panel; productivity; radiant heat; shortening the curing period; surface of concrete

## 1 INTRODUCTION

### 1.1 Background and Purpose of Research

As design and construction technologies advance recently, it is possible now to embody new forms or free-form buildings different from existing ones. However, free-form buildings feature each unique outward configuration, and it is difficult to embody them in reality. To build up such free-form outward sections, free-curvature exterior parts of a complicated geometrical form are divided into workable shapes and sizes [1]. Free-form configurations are difficult to be produced or constructed because of the variance of curvatures and free curves. Therefore, it is necessary to reduce the panel production period by optimizing varied free-form configurations to the extent possible [2].

Many recent studies examine methods to realize such free-form construction in an economical and efficient manner, and the number is increasing. In contrast, there has been little research on the productivity of free-form panels. Free-form construction projects often involve problems due to lack of experience such as inaccurate estimation of construction costs, excessive change to the basic design, delayed completion, etc. [3]. In the case of Opera House in Sydney, the actual construction period was delayed for four years and cost USD 102 million, 15 times as much as estimated [4].

To overcome such limitations, studies have been conducted. Donghoon Lee [5] developed the equipment to automatically manufacture FCP (Free-form Concrete Panel) which were produced manually in general. This equipment consists of the lower-part multi-point press operation and the side configuration control operation. This equipment produces FCP in four steps: mold embodiment, extrusion, curing, and removal. The production period is shortened since the steps of mold embodiment and extrusion proceed automatically. In contrast, there has been little research on how to shorten the period of curing and removal.

This study applies radiant heat to concrete in the steps of curing and removal to shorten the FCP production period. If heat is applied to concrete in the curing step, the compressive

strength of concrete develops earlier. As a result, the productivity of FCP will be improved by securing fast hardening and as well as the proper mold removal strength as high as 5 MPa. This study applies radiant heat to the curing process for free-form panel production based the results of constant temperature/humidity curing and quartz tube heater curing experiments.

### 1.2 Scope and Method of Research

As to the scope of this study, the suggested radiant heater is applicable to the multi-point CNC equipment developed in the papers of Jeong and Yun [6, 7]. This study intends to improve the productivity and economical efficiency of FCP by shortening the curing time in FCP production. The curing time that is varied when radiant heat is applied to the surface of concrete is measured. In addition, experiments are conducted to examine defects that may harm the strength and durability of concrete. The top priority is to shorten the time that it takes for the strength to reach the mold removal strength after forming and to shorten the removal time compared to the existing method.

In this study, the temperature and timing of the highest efficiency to shorten the mold stripping time in the possible range of temperature for concrete curing is calculated based on the initial strength. First of all, the temperature and humidity are adjusted by using a thermohygrostat, and then concrete curing is initiated immediately after forming. The time when the compressive strength reaches the point of 5 MPa, which is the reference point for moldboard removal, is measured at each temperature. Based on the temperature and time measured in the above-stated experiment by means of a thermohygrostat, the specific range was reestablished in the next compressive strength experiment where the panel radiant heating method was applied by using a quartz tube heater. The long-term strength was then measured to examine the possibility of concrete durability problems.

## 2 THEORETICAL INVESTIGATION

### 2.1 Early Curing Technology of Concrete Panel by Calorific Control

This study applies the multi-point CNC equipment to the FCP production process. The multi-point CNC equipment consists of the lower-part multi-point press operation and the side configuration control operation. It is possible to adjust the panel shape and side angle. As shown in Fig. 1 regarding

the panel production process in use of this equipment, FCP is manufactured in the four steps of combination, extrusion, curing, and removal. First of all, the bottom and side molds are combined according to the shape of the panel to be produced. Concrete is then infused by using the concrete extrusion equipment for curing. Once concrete curing is completed, the mold is removed and the production process ends.

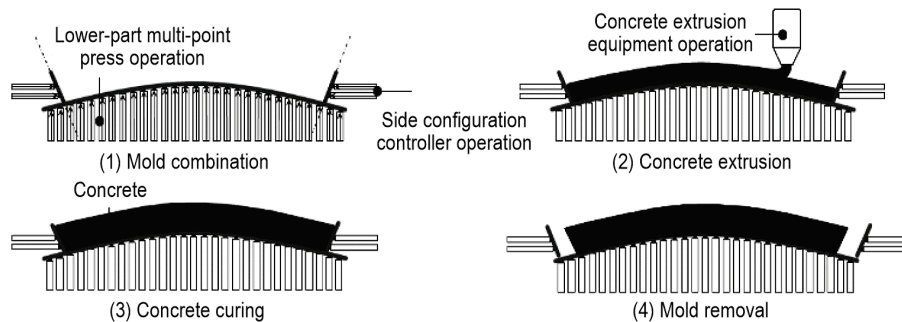


Figure 1 Panel fabrication process for multi-point CNC equipment

In contrast, there has been little research on how to shorten the period of curing and removal. In the process of selecting the way to adjust temperature for reduction of the curing time and mold stripping time, radiant heat is applied to the concrete surface in consideration of the fact that the free-form concrete panel is thinner and broader than other concrete panels in order to reduce the general mold stripping time.

To design the optimal method that suits the volume and condition of the multi-point CNC equipment, this study prioritizes the productivity and economical efficiency of free-form panel production. Accordingly, a quartz tube heater was used to apply radiant heat since it involved no significant financial burden regarding the volume and requirements of the multi-point CNC equipment and it involved a low risk as a heat source even it was used for a long time.

## 3 RADIANT HEAT CURING EXPERIMENT

### 3.1 Constant Temperature/Humidity Curing

#### 3.1.1 Experiment Planning

The constant temperature/humidity curing experiment was planned as summarized in Tab. 1. An experiment was conducted where the mortar mixing ratio common to the multi-point CNC equipment for free-form production was applied. Right after forming, curing was performed for 4 hours each time at each temperature setting (20 °C, 40 °C, 60 °C, and 80 °C) and then the compressive strength was measured. The compressive strength was then measured three times in consideration of the age, and then the measurements were used to calculate the average. The calculated strength was compared with the standard strength for mold removal to determine the method's suitability for the removal process.

Table 1 Experiment Procedures

Curing temperature (°C)	Curing hour (hr)					
20	4	8	12	16	20	24
40	4	8	12	16	20	24
60	4	8	12	16	20	24
80	4	8	12	16	20	24

Since this experiment aimed to examine the maximum value of time reduction depending on the temperature adjustment, the mortar was mixed at the most common ratio. Therefore, the effect would be better if an admixture was added. The materials used included cement, aggregate, water, and PVA. Tab. 2 shows the types and mixing ratios of materials used in this experiment.

Table 2 Materials used in the Experiment

W/C	Cement (g)	Aggregate (g)	Water (g)	PVA (g)
0.4	6,000	6,000	2,400	90

After sufficient dry mixing, mortar was mixed by using a concrete mixer. The mixed mortar was formed in a 4×4×16 cm mold. Prior to the experiment, the humidity of the thermohygrostat was all set to 60%, and then the temperature was adjusted to 20 °C, 40 °C, 60 °C, and 80 °C.

After forming, the mold itself was put into the thermohygrostat for curing with no preliminary curing. In the heated state at 20 °C, 40 °C, 60 °C, and 80 °C as set to the thermohygrostat, the high-temperature curing was performed. The mold was then taken out of the curing machine at intervals of 4 hours, followed by the removal step. Right after removal, the mortar was divided to test piece specimens of 4×4×8 cm in size, and these heated test piece specimens were compared in terms of the age and temperature setting by means of a concrete test piece compressive strength measuring device. The compressive strength was measured 3 times for each age value, and the average was used in the experiment.

### 3.1.2 Performance Experiment Results

**Table 3** Compressive strength at each temperature (20, 40 °C) (Unit: MPa)

day hr	20 °C			40 °C		
	0	7	28	0	7	28
4	-	27.5	35.6	-	22.0	31.2
8	-	28.9	35.8	8.3	28.1	30.7
12	2.1	30.0	37.8	16.3	34.1	34.9
16	7.2	28.9	36.4	21.2	31.8	34.9
20	11.5	28.2	31.7	25.2	32.5	38.8
24	15.4	28.7	33.2	26.4	33.5	37.4

**Table 4** Compressive strength at each temperature (60, 80 °C) (Unit: MPa)

day hr	60 °C			80 °C		
	0	7	28	0	7	28
4	3.8	25.4	26.5	6.1	21.1	24.3
8	16.3	26.0	30.9	16.6	23.8	28
12	20.5	22.9	31.5	16.1	22.3	25.9
16	21.7	26.1	32.0	17.1	20.4	27.1
20	21.3	28.7	31.0	17.6	21.7	25.6
24	20.5	27.4	28.4	18.3	22.7	26.6

Experiment results show that except certain samples in the existing condition (20 °C, less than 20 hours), most samples were found to meet the strength criteria for mold removal.

**Table 5** Compressive strength right after removal in the constant temperature/humidity curing experiment (Unit: MPa)

Initial	20 °C	40 °C	60 °C	80 °C
4 hr	-	-	8.8	6.1
8 hr	-	8.3	16.3	16.6
12 hr	2.1	16.3	20.5	16.1
16 hr	7.2	21.2	21.7	17.1
20 hr	11.5	25.2	21.3	17.6
24 hr	15.4	26.4	20.5	18.3

As in Tab. 5 that shows the strength right after removal in the experiment, when the temperature is 20 °C, removal is possible after at least 20 hours. At 40 °C, in contrast, the strength meets the criteria for removal 8 hours after forming. This is the same when the temperature is 60 °C and 80 °C. At 80 °C, however, the strength was inferior to that at 60 °C.

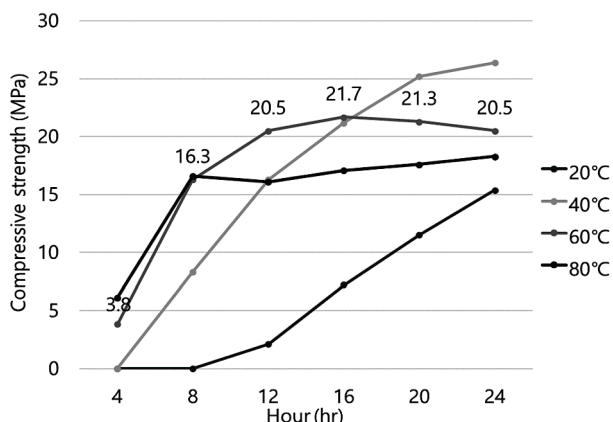


**Figure 2** Graph of compressive strength measurements in the constant temperature/humidity curing experiment

The strength right after forming was compared with the long-term strength at each temperature to determine the condition that involves less risk in a long run. The strength results in this experiment were compared with the compressive strength of concrete stated in concrete standard specifications in terms of the timing of moldboard removal.

As shown in Fig. 2, the condition where the proper mold removal strength was reached within the shortest time was 80 °C and 4 hours. However, the long-term strength at 80 °C was inferior to those at other temperature settings. Thus, this condition was excluded because of the instability in terms of long-term strength. With the top priority to time reduction, the curing condition of 60 °C and 8-hour heating showed the most appropriate result.

In view of the strength right after removal or the long-term strength, the condition of 40 °C and 8-12 hours heating also had potentials and thus was included in the quartz tube heater curing experiment. In comprehensive view of the strength right after removal and the long-term strength, the conditions of 40 °C and 60 °C were more specified to 40 °C, 50 °C, and 60 °C with the heated curing time in the range of 5 to 8 hours for the quartz tube heater curing experiment.

## 3.2 Quartz Tube Heater Curing

### 3.2.1 Experiment Planning

Based on the data acquired from the constant temperature/humidity curing experiment, the optimal curing temperature and curing time that met the strength criteria for mold removal and could shorten the stripping time were determined. The priority was given, not to the strength level, but to the condition of the shortest curing time among samples that reached the proper strength for removal. After samples of the highest efficiency were selected, it was verified whether the results would be the same if the concrete surface was heated by radiant heat. Samples selected from the quartz tube heater curing experiment were used to determine the condition of temperature and curing time where the constructability and economical efficiency would be the best when radiant heat was applied to the mortar surface after forming. Tab. 6 shows details of the experiment plan.

**Table 6** Experiment Procedures

Curing Temperature (°C)	Curing Hour (hr)			
40	5	6	7	8
50	5	6	7	8
60	5	6	7	8

Based on the results derived from the constant temperature/humidity curing experiment, the selected condition—the mold of 4×4×16 cm—was applied to forming. A quartz tube heater was selected as the heat source. The distance between the structure and concrete surface was adjusted according to the temperature setting. The experiment proceeded after it was confirmed that the set temperature maintained for 1 hour. In each temperature condition and at the time set, the removal step was conducted to measure the bending strength.

The concrete was divided to test piece specimens of 4×4×8 cm in size and then measured by using a concrete test piece compressive strength measuring device. The compressive strength was measured 3 times for each age value, and the average was used in the experiment. As shown in Tab. 7, it was determined that the time was appropriate for curing when it reached 5 MPa based on the criteria of mold removal. Tab. 7 below is based on standard specifications for construction work.

**Table 7** Timing of moldboard removal

Member materials		Compressive Strength of Concrete
Sides of spread footings, beam, pillars, etc.		At least 5 MPa
Slab and arches of the beam	Single-layered structure	At least 2/3 of the standard compressive strength, min. 14 MPa
	Multi-layered structure	At least the standard compressive strength (When the pillar supporting post structure is used, the construction period may be shortened based on the structure calculation data. Even in this case, however, the minimal strength should be at least 14 MPa)

### 3.2.2 Performance Experiment Results

In the temperature conditions of 40 °C, 50 °C, 60 °C selected in the constant temperature/humidity curing experiment as stated above, heating was performed for 5 to 8 hours and then right after concrete forming, radiant heat was applied onto the concrete surface by using a quartz tube heater as shown in Fig. 3.

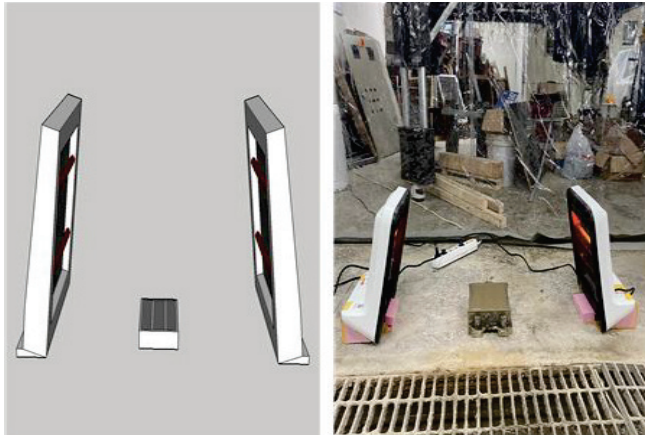


**Figure 3** The experiment plan (left) and the actual experiment image (right)

**Table 8** Compressive Strength Measurements in the Quartz Tube Heater Curing Experiment (Unit: MPa)

Initial	40 °C	50 °C	60 °C
5 hr	0.7	1.2	4.5
6 hr	1.1	5.4	8.7
7 hr	2.9	6.6	13.2
8 hr	7.3	9.5	18.5

After radiant heat curing for 5 to 8 hours at 40 °C, 50 °C, and 60 °C, the strength was measured as presented in Tab. 8 and Tab. 9. In the quartz tube heater curing experiment, both

the flexural strength and compressive strength were measured.

**Table 9** Bending Strength Measurements in the Quartz Tube Heater Curing Experiment (Unit: MPa)

Initial	40 °C	50 °C	60 °C
5 hr	0.2	0.3	1.2
6 hr	0.3	1.5	2.4
7 hr	1.3	1.8	2.5
8 hr	2.5	2.5	4.0

The results of the quartz tube heater curing experiment are shown in Fig. 4 and Fig. 5 at the bottom. The result shows that the strength suitable for mold removal was reached after 8 hours at 40 °C. At both 50 °C and 60 °C, the strength was reached after 6 hours, but the measurement at 60 °C was higher. This indicates that at 60 °C, the strength suitable for mold removal would be reached faster.

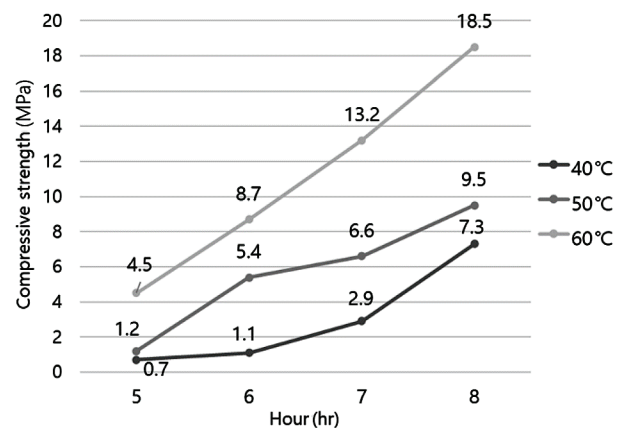


**Figure 4** Graph of compressive strength measurements in the quartz tube heater curing experiment

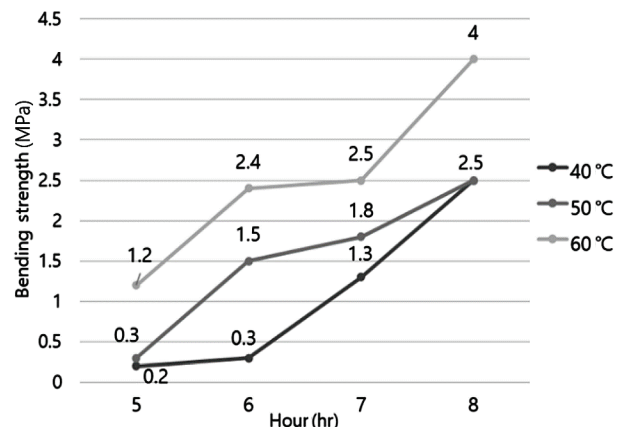


**Figure 5** Graph of Bending Strength Measurements in the Quartz Tube Heater Curing Experiment

In addition, the data obtained by using a thermohygrostat were compared with the data obtained after 8 hours by using a quartz tube heater, and the result shows that the strength when a quartz tube heater was used was higher and better in terms of effectiveness.

The result of the quartz tube heater curing experiment shows that the strength suitable for mold removal was reached after 8 hours at 40 °C. At both 50 °C and 60 °C, the

strength was reached after 6 hours, but the measurement at 60 °C was higher. This indicates that at 60 °C, the strength suitable for mold removal would be reached faster.

In addition, the data obtained by using a thermohygrostat were compared with the data obtained after 8 hours by using a quartz tube heater, and the result shows that the strength when a quartz tube heater was used was higher and better in terms of effectiveness.

#### 4 CONCLUSION

This study suggests a method to secure the productivity of free-form panels based on the results of concrete heating experiments, and this suggested method is applicable to the existing FCP production equipment. Specifically, the constant temperature/humidity curing experiment and the quartz tube heater curing experiment were conducted in this study, and the results may be summarized as below:

1) In the constant temperature/humidity curing experiment, curing was performed after mortar forming at different temperature settings on test piece specimens of a 4×4×16 cm mold with a thermohygrostat used. The condition of temperature and time where the compressive strength reached the strength criteria at the point of moldboard removal was determined in consideration of the age. The optimal condition was derived in application of different temperature settings, and the range was narrowed down based on the results to determine the specific condition for curing experiments where a quartz tube heater was used.

After experiments at 20 °C, 40 °C, 60 °C, and 80 °C respectively, it was confirmed that the condition of 8 hours heating at 40 and 60 °C was the most appropriate. To derive more specific values, the duration of radiant heat application was subdivided to 5, 6, 7, and 8 hours at 40 °C, 50 °C, and 60 °C.

2) In the range stated above, radiant heat was applied onto the surface of formed mortar by using a quartz tube heater in the experiment. Based on the results, it was confirmed that the compressive strength when a quartz tube heat was used was somewhat superior to that when a thermohygrostat was used for curing. In addition, after 6 hours at both 50 °C and 60 °C, the condition was proper for removal and there was no problem in terms of long-term strength either. Therefore, it was verified that the moldboard stripping time could be shortened by heating after mortar forming at 50 °C or 60 °C.

The findings of this study verify that the curing time can be shortened with the standard strength secured at the point of moldboard removal after 6 hours, which is expected to contribute to improving the productivity of free-form panels as well as the economical efficiency through cost saving and construction period reduction.

However, there is limitation in applying the suggested method to the existing equipment. In the quartz tube heater curing experiment, only the initial strength was measured within 5 to 8 hours, the time appropriate for removal. Besides, it was unable to adjust the humidity in the case of panel curing unlike the existing constant temperature/humidity curing method. Thus, there should be a solution to cracks that might occur inside or outside the panel. The future

study, therefore, needs to design a heater that is appropriate for the scale of the existing FCP production equipment and also can adjust the humidity.

If FCP is manufactured by applying the quartz tube heater to the FCP equipment for free-form concrete panel production based on the findings of this study, it is expected that the productivity of FCP, which requires a long production period, can be improved.

#### Acknowledgements

This work was supported by the National Research Foundation of Korea (NRF) grant funded by the Korea government (MSIT) (No. 2020R1C1C1012600).

#### 5 REFERENCES

- [1] Piegl, L. A. & Tiller, W. (2002). Biarc approximation of NURBS curves. *Computer-Aided Design*, 34(11), 807-814. [https://doi.org/10.1016/S0010-4485\(01\)00160-9](https://doi.org/10.1016/S0010-4485(01)00160-9)
- [2] Lim, J. S. & Ock, J. H. (2014). A Study on the Optimization of the Free-Form Buildings Facade Panels. *Transactions of the Society of CAD/CAM Engineers*, 19(2), 91-102. <https://doi.org/10.7315/cadcam.2014.091>
- [3] Lee, E. Y. & Kim, Y. S. (2014). An Analysis and Improvement of Free Form Building's Construction Productivity - Focused on Exposed Concrete Work. *Korean Journal of Construction Engineering and Management*, 15(3), 38-46. <https://doi.org/10.6106/KJCEM.2014.15.3.038>
- [4] Kim, Y. G. (2022). A Study on the Improvement of Ordering process for Non-linear Building Surface Panelizing using BIM-based Parameters. *Master's thesis*, Hanyang University. <https://repository.hanyang.ac.kr/handle/20.500.11754/168341>
- [5] Lee, D. H. (2015). A study of construction and management technology of free-form buildings. *Doctoral dissertation*, Kyung Hee University. [https://khis-primo.hosted.exlibrisgroup.com/permalink/f/mltik9/82KHU\\_ALMA21102907170004426](https://khis-primo.hosted.exlibrisgroup.com/permalink/f/mltik9/82KHU_ALMA21102907170004426)
- [6] Yun, J. Y. & Jeong, K. T. (2021). Development of Side Mold Control Equipment for Producing Free-Form Concrete Panels. *Buildings*, 11(4), 175-186. <https://doi.org/10.3390/buildings11040175>
- [7] Yun, J. Y. & Yoon, J. Y. (2021). Development of Double-Sided Multipoint Press CNC and Operational Technology for Producing Freeform Molds. *Buildings*, 11(10), 426-436. <https://doi.org/10.3390/buildings11100426>

#### Authors' contacts:

**Hyekwon Kim**, Bachelor's Degree  
Hanbat National University  
125, Dongseo-daero, Yuseong-gu, Daejeon, Korea  
042-821-1635, hyegwon12@naver.com

**Yejin Jeong**, Bachelor's Degree  
Hanbat National University  
125, Dongseo-daero, Yuseong-gu, Daejeon, Korea  
042-821-1635, wonder0560@naver.com

**Sangwon Seo**, Bachelor's Degree  
Hanbat National University  
125, Dongseo-daero, Yuseong-gu, Daejeon, Korea  
042-821-1635, mbul@naver.com

**Jongyoung Youn**, Master's course  
Hanbat National University  
125, Dongseo-daero, Yuseong-gu, Daejeon, Korea  
042-821-1635, 97colin@naver.com

**Donghoon Lee**, Assistant Professor  
(Corresponding author)  
Hanbat National University,  
125, Dongseo-daero, Yuseong-gu, Daejeon, Korea  
042-821-1635, donghoon@hanbat.ac.kr

# Properties of CLC According to Replacement Ratio of Cao-CSA Expansive Additive

Yong-Gu Kim, Chang-Woo Lee, Woo-Jun Hwang, Sang-Soo Lee\*

**Abstract:** According to the National Statistical Office's 2019 Population and Housing Survey in August 2020, the number of apartments, including apartments, was about 14 million last year, accounting for 77.2% of all houses, of which 11.287 million were 80.6% of apartments. Based on this change in housing trends, researchers have developed and studied cellular light-weight concrete (CLC) that can be cured at room temperature and normal pressure with advantages such as light weight, insulation, and construction. There have been several studies in Korea, including state-run projects, but they have not been commercialized, but the biggest reason is that stability has not been secured. Therefore, to improve the reliability of CLC that can be cured at normal temperature and pressure, this study attempts to analyze the properties of CLC by incorporating CaO-CSA expansive additive. Based on the drying density of 0.55-0.65 kg/m<sup>3</sup>, cement, blast furnace slag, animal foaming additive and fiber are utilized to analyze the properties of CLC with CaO-CSA expansive and the results are as follows. By using the CaO-CSA expansive additive, it is determined that the formation of calcium hydroxide and ettringite fills the CLC between the tobermorite layers and the internal structure becomes dense. Currently, based on KS F 2701, the compression strength based on 0.6 items is more than 4.9 MPa, and the strength is about twice as strong as that of the existing CLC, and durability of the CLC are improved by incorporating CaO-CSA expansive additive.

**Keywords:** CaO-CSA expansive additive; cellular light-weight concrete (CLC); drying shrinkage; settlement; tobermorite

## 1 INTRODUCTION

### 1.1 Background

According to the National Statistical Office's 2019 Population and Housing Survey in August 2020, the number of apartments, including apartments, was about 14 million last year, accounting for 77.2% of all houses, of which 11.287 million were 80.6% of apartments of these, the proportion of condominiums increased 4.3 percent year-on-year, and demand for condominiums is increasing every year. With the changing housing trends reflecting the needs of the domestic market, construction changes are being made to maximize the availability of housing by actively responding to various demand for space utilization by consumers for sustainable housing culture such as well as durability [1]. In addition, due to interlayer noise problems when living apartments, 99.9% of private apartments completed between 2007 and 2017 and 96.8% of public apartments (Ministry of Land, Infrastructure and Transport, structure of 500 or more apartments nationwide) are continuing to be converted. If the columnar structure is applied, water, electricity, and gas parts, which can be freely planarly arranged according to the arrangement of the non-tolerant wall and which, need maintenance are not embedded in the concrete wall matrix but can be easily replaced and repaired.

Since the 2050 carbon, neutrality declaration promised the international community that greenhouse gases would be reduced by 40% from 2018 by 2030, zero energy building certification will be mandatory for public buildings with a total area of more than 1,000 square meters from 2020. In addition, from 2024, the mandatory targets will be expanded to include private buildings with a total area of more than 1,000 square meters or apartment houses with a size of more than 30 households. However, according to the Korea Institute of Construction Industry's report on the "Diagnosis and Challenges of Zero Energy Building Policy in Korea," he criticized, "The certification system for zero energy buildings was implemented in 2017, but it is still sluggish. In addition,

the introduction of non-residential buildings such as shopping districts and office buildings will be delayed by 30 to 40 percent compared to existing construction costs and 4-8 percent higher than the standard construction cost limit for apartments. Currently, urethane foam, phenolic foam, PE foam, and Styrofoam, which are organic insulation materials used more than 80% compared to inorganic insulation materials, are utilized on the insulation side of the building. Although it has excellent insulation, easy construction and economic strength compared to weapons insulation, it is vulnerable to fire stability. Until recently, problems have been raised as the cause of fire incidents such as Incheon Logistics Warehouse Fire (2020) and Ulsan Column Fire (2020). In addition, the Ministry of Land, Infrastructure and Transport pointed out the cause of such large-scale fire accidents as the use of fire-resistant finishing materials, and is continuously strengthening regulations through the Ministry of Land, Infrastructure and Transport's Notice No. 2020-1053.

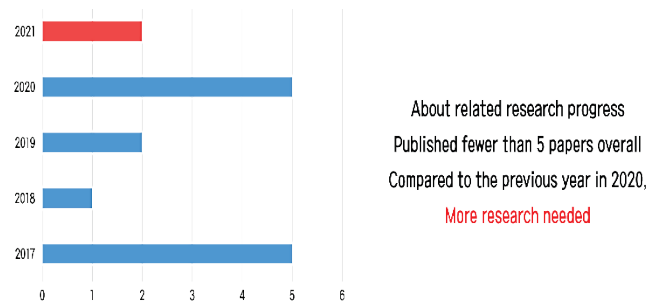
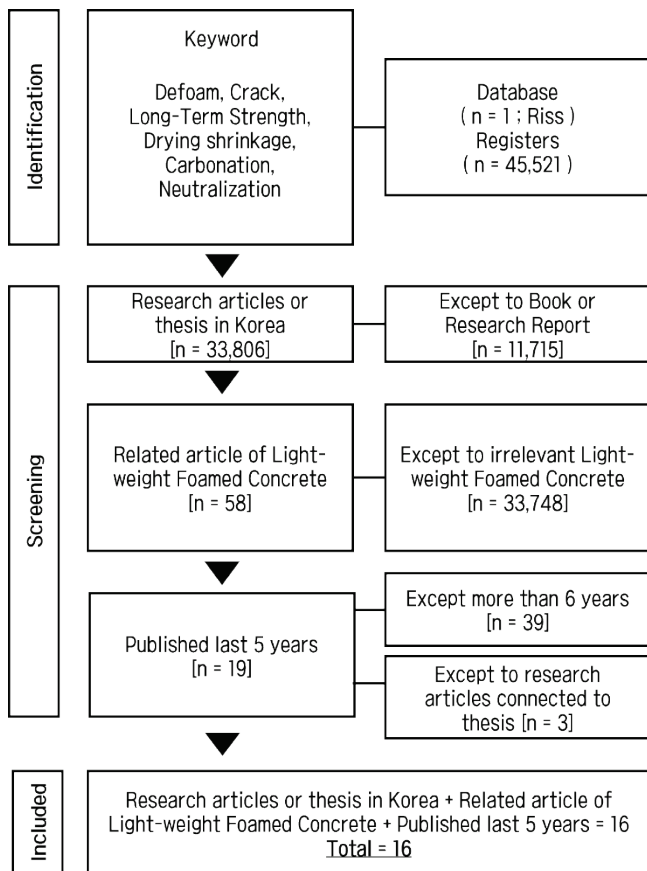
Thanks to this change in housing trends, lightweight, heat insulation and construction advantages (ALC) are widely used as indoor partitions, fire resistance, and insulation walls, and the annual usage is expected to expand to around 3 to 4 million m<sup>2</sup>. ALC is a common name for lightweight foamed concrete made by adding cement and a foaming additive to silica sand and curing porous mixture through autoclave curing at high temperature and high pressure (180° 10 atmospheric pressure). However, ALC has difficulty entering the market due to its high initial investment in production facilities and requires autoclave curing in the production method, so manufacturing costs are high and acts as a factor to increase overall construction costs [2]. To solve this problem, a lightweight concrete (Cellular Light-weight Concrete) that can be cured at room temperature and normal pressure is developed as an alternative to ALC, and research has been conducted on this. There have been several studies in Korea, including state-run projects, but they have not been commercialized, but the

biggest reason is that research progress and stability have not been secured enough to achieve Korean industrial standards such as ALC Block. Therefore, experiments are needed to ensure the stability of CLC.

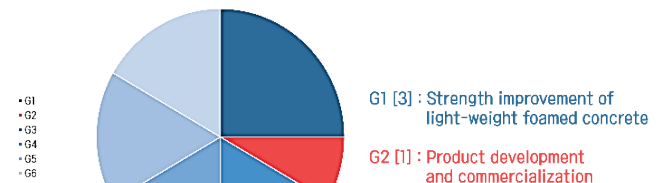
## 1.2 Case Study of the Research

### 1.2.1 In Korea

To identify domestic research trends, we categorized them by group for analysis of selected papers according to the inclusion and exclusion criteria in PRISMA Fig. 1. G1: Strength Improvement of Lightweight foamed Concrete, G2: Product Development and Practicalization, G3: Basic and Experimental Studies, G4: Carbonation, G5: Basic Physical Properties Analysis, and G6: Industrial By-product Utilization. Fig. 2 shows the proportion of papers by year, with 5 in 2017 and 2020, 1 in 2018, and 2 in 2019 and 2021, and Fig. 3 shows the number of papers by group. The research on product development and practicality in G1 3 (two academic papers, one Thesis), G2 1 (one academic paper), G3 2 (one academic paper, one Thesis), G4 2 (two academic papers), G5 2 (one academic paper, one degree paper), and G6 2 (two Thesis).



About related research progress  
Published fewer than 5 papers overall  
Compared to the previous year in 2020,  
More research needed



### 1.2.2 Foreign Cases

For comparative analysis based on the understanding of overseas cases due to the absence of CLC's domestic standards, foamed concrete blocks manufactured at room temperature in each country were analyzed.

In the case of Germany, we checked NeoPor's products. Maximum compressive strength that can be expressed for 0.4, 0.6 and 0.8 and 1.0 products is described as 1.0, 2.0, 3.0, and 4.0 MPa. For other products, the maximum compressive strength that can be expressed in 0.4 products is specified as 2.3 MPa even in the case of LithoPore.

In the case of India, ICS2185 is specified as the "Starting Foamed Concrete Block". Cement, a residue material, fly ash, a foaming agent and an admixture are presented as the materials to be used, and a manufacturing method and a sampling method are also presented.

As the standard physical properties to be satisfied, density, compression strength, thermal conductivity and absorption rate of the dry state are provided.

## 2 EXPERIMENTAL PLANS

Most domestic light-weight foamed concrete studies consist of studies on ALC manufacturing methods and their properties. However, the economics of equipment and manufacturing methods have become a problem. Therefore, to improve the reliability of CLC that can be cured at normal temperature and pressure, this study tries to analyze the properties of CLC by incorporating CaO-CSA expansive additive. Properties of CLC by mixing expansive additive and inhibition of crack by reducing drying shrinkage are analyzed by using cement, blast furnace slag, animal foaming additive and fiber based on drying density 0.55-0.65 kg/m<sup>3</sup>.

**Table 1** Experimental factors and levels

Experimental factors	Experiment levels	
Binder	High-early-strength Portland cement, Blast furnace slag	2
W/B	45%	1
Replacement ratio of Cao-CSA	0, 5, 10, 15, 20 (%)	5
Dilution concentration of foaming additive	3 (%)	1
Replacement ratio of water-reducing additive	0.8 (%)	1
Replacement ratio of foam stabilizer	1.5 (%)	1
Addition ratio of PVA fiber	1 (%)	1
Curing condition	Temp. 20±2 °C, Hum. 60±5%	1
Experimental items	Density, Absorption ratio, Compressive strength, Flow test, Drying shrinkage, Settlement	6

## 2.1 Materials

### 2.1.1 High-Early Strength Portland Cement

High-early strength Portland cement has a high content of alite effective for short-term strength and excellent expression of initial strength. Initial setting is within 235 minutes, and the strength (around 30 MPa) of the three-day ordinary Portland cement reference reoder can be expressed in one day. Furthermore, it has effects such as reduction of drying shrinkage, enhancement of strength, and acceleration.

**Table 2** Chemical component

Chemical component of high-early strength Portland cement (%)									
SiO <sub>2</sub>	Al <sub>2</sub> O <sub>3</sub>	CaO	Fe <sub>2</sub> O <sub>3</sub>	MgO	SO <sub>3</sub>	L.O.I	C <sub>3</sub> S	C <sub>2</sub> S	C <sub>3</sub> A
20.5	5.0	62.3	3.4	3.6	2.1	2.4	53.1	18.5	7.8

### 2.1.2 Blast Furnace Slag

Blast furnace slag fine powder refers to the addition of gypsum to the furnace slag in accordance with KS F 2563 (Ground granulated blast furnace slag for use in concrete) or the drying and grinding of the furnace slag. When used as an alternative material for cement, it has a characteristic of continuously increasing strength over a long period of time due to its latent hydraulic, and has effects such as increasing seawater resistance, improving watertightness, etc.

**Table 3** Chemical component

Chemical component of BFS (%)							
MgO	CaO	SiO <sub>2</sub>	Fe <sub>2</sub> O <sub>3</sub>	SO <sub>3</sub>	Al <sub>2</sub> O <sub>3</sub>	TiO <sub>2</sub>	Cl <sup>-</sup>
2.1	52.6	28.7	0.6	4.1	9.5	0.7	-

### 2.1.3 Animality Foaming Additive

In the case of an animal foaming additive, bone fine powder of livestock is mainly hydrolyzed with NaOH or the like, neutralized, and then filtered and preservative-treated to produce it. At the time of foaming, it exhibits a light tawny color and is formed of many independent fine foams of 0.2-0.8 mm inside the foam. An animal foam additive prepared by hydrolyzing an animal's sense of smell or the like to extract an animal protein and adding a foam stabilizer, a viscosity additive, a coagulation regulator, or the like is used [3, 4].

### 2.1.4 CaO-CSA Expansive Additive

Expansive additive used in this study is an ettringite-lime composite expansive additive that properly combines the reaction of Free CaO with Denka Power-CSA of domestic company C, which reduces drying shrinkage and affects watertightness.

**Table 4** Chemical Component

Chemical Component of CaO-CSA EA (%)					
SiO <sub>2</sub>	CaO	Fe <sub>2</sub> O <sub>3</sub>	SO <sub>3</sub>	Al <sub>2</sub> O <sub>3</sub>	F CaO
1.0	70.6	0.6	18.5	7.2	49.8

## 2.2 Experimental Methods

### 2.2.1 Mixing

Fig. 4 shows the method of blending for CLC production in this study is as follows. High-early strength cement, blast furnace slag, foam stabilizer, PVA fiber and level-specific silica sand or CaO-CSA expansive additive are mixed and charged into a mixer, and then a psoriasis beam is advanced for 35 rpm 1 minute. At the same time, 3% animal foam additive is mixed in water, and an appropriate amount of foam is put into a cup by using a foamed generator. After the psoriasis beam is finished, water and a water reducing additive are put into a mixer, foams are put into the primary beam for 30 seconds, and the secondary beam is placed at 45 rpm for 30 seconds for a total of 120 seconds.

### 2.2.2 Density and Absorption Ratio

To measure the density and absorption, a test specimen was prepared using 40 × 40 × 160 mm. To measure the water absorption, the cured specimen is demolded, dried in a dryer for 24 hours, and then the weight is measured.

### 2.2.3 Compressive Strength

To measure compressive strength, a matrix is prepared by placing paste on a cylindrical mold 100 mm in diameter and 200 mm in height and a cubic mold 100×100×100 in accordance with KS F 2459. The curing of the matrix strength was measured on the 7<sup>th</sup> and 28<sup>th</sup> of the second order. The compressive strength test was performed by increasing the load to 2,400±200 N/s.

### 2.2.4 Flow Test

Flow test of non-solidified paste was conducted in accordance with KS L 5111. After the flow mold is arranged on the fluid table plate, paste is filled into the flow mold in three installments, each layer is spirally hardened 20 times, and then the flow mold is vertically lifted to measure three places, and then the average is measure.

### 2.2.5 Thermal Conductivity

For CLCs manufactured according to the replacement ratio of silica sand or CaO-CSA expansive additive, the thermal conductivity after 28 days of reoder was measured

and the thermal conductivity test was conducted in accordance with ISO 22007. The thermal conductivity measuring instruments used Hot Disk M1 (Germany), which uses the TPS method.

### 2.2.6 Drying Shrinkage

In the drying shrinkage test, paste is placed on a 100×100×400 mold, cured for two days, and then demolded. After that, the surface of the CLC is subjected to surface treatment with sandpaper for smooth installation, and then the strain gauge connected to the data logger is fixed. After that, a test is advanced for seven days under temperature

conditions of −5 °C to 30 °C and a change period of two cycles per day using a constant temperature and humidity chamber.

### 2.2.7 Settlement

In the settlement test, paste is placed in a cylindrical mold with a diameter of 100 mm and a height of 2000 mm in accordance with KS F 2459. After that, 200 mm 4 is divided into the upper end part, the middle upper end part, the middle lower end part and the lower end part, and the sinking accuracy is measured through the respective weights.

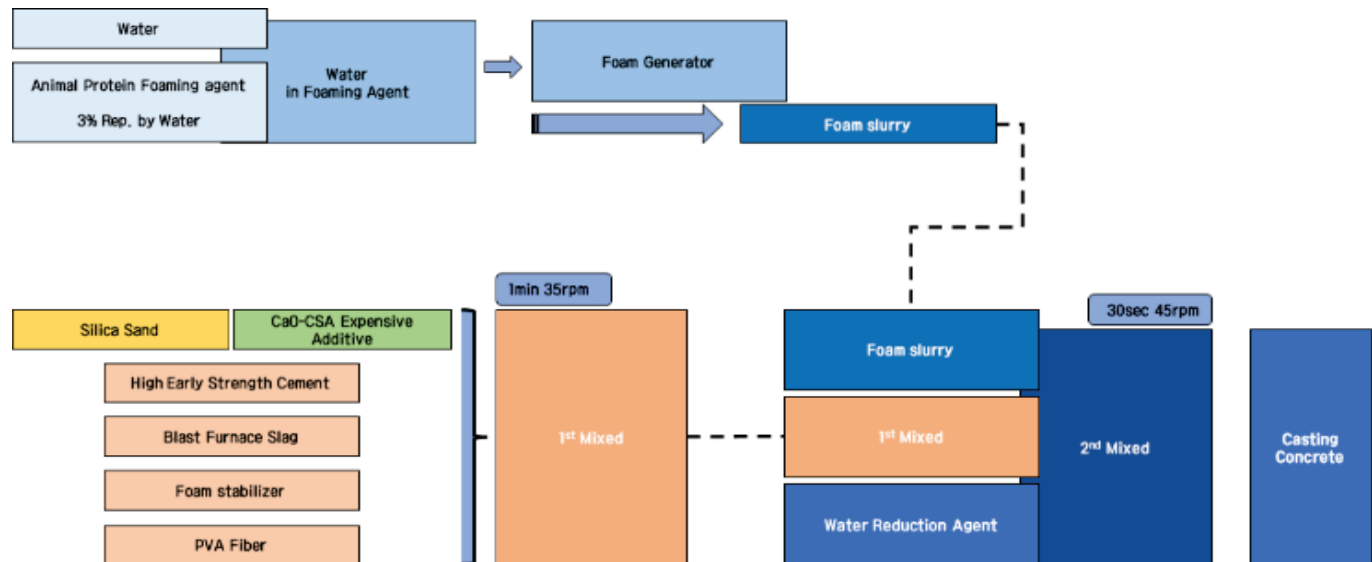


Figure 4 Mixing flow chart

Table 5 Chemical component of CLC by replacement ratio of CaO-CSA EA expansive material

Element	Replacement ratio of CaO-CSA EA (%)		
	0	60	80
	Weight (%)	Weight (%)	Weight (%)
C K	11.29	8.23	5.99
O K	54.18	53.14	51.17
Mg K	0.93	1.74	0.90
Al K	2.71	2.31	1.73
Si K	8.02	6.69	7.79
S K	1.31	1.76	2.54
K K	0.47	0.54	0.65
Ca K	20.23	24.24	28.31
Fe K	0.87	1.34	0.93
Totals	100.00	100.00	100.00

## 3 EXPERIMENTAL RESULT AND ANALYSIS

### 3.1 SEM and EDS Analysis

Tab. 5 and Tab. 6 are chemical components and photographs obtained by deriving CLCs of CaO-CSA expansion material replacement rates 0, 10, 20 (%) through SEM and EDS photography. As the replacement rate of the CaO-CSA expansion material increases, the total mass of S, Ca, and O in the chemical components tends to increase. This is determined to be the influence of calcium hydroxide (Ca(OH)) and ettringite ( $\text{Ca}_6\text{Al}_2(\text{SO}_4)_3(\text{OH})_{12} \times 26\text{H}_2\text{O}$ )

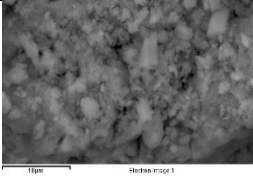
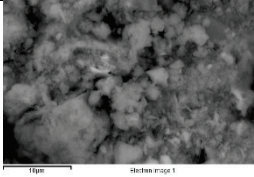
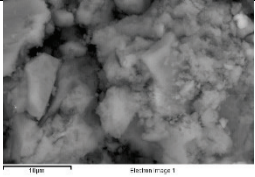
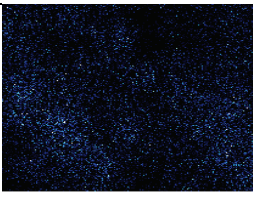
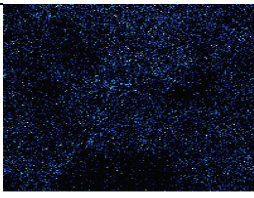
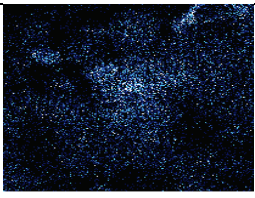
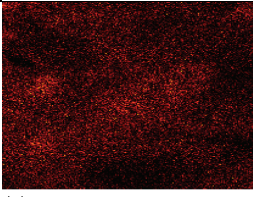
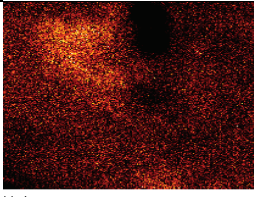
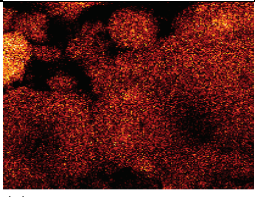
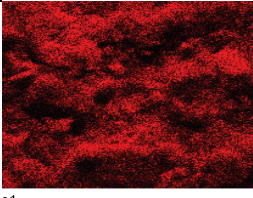
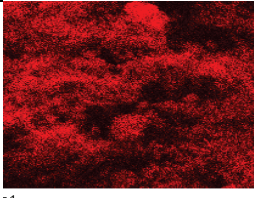
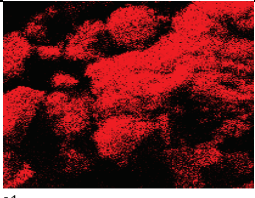
formed by reacting with internal surplus water by replacing CaO-CSA expansion material in CLC. If you look at the EDS, you can see that it is distributed evenly within the CLC.

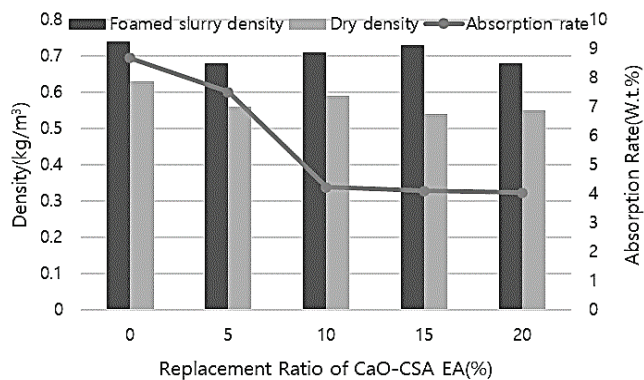
### 3.2 Density and Absorption Ratio

Fig. 5 is the result of measuring the density and absorption ratio of CLC due to CaO-CSA expansive additive incorporation by 0.6 item reference level. At CaO-CSA expansive additive replacement ratios 0, 5, 10, 15, 20 (%) the single weight of the foamed slurry is 0.74, 0.68, 0.71, 0.73, 0.68 ( $\text{kg/m}^3$ ), and the nodal dry density is 0.63, 0.56, 0. and 0.55 ( $\text{kg/m}^3$ ). As the specific gravity of the CaO-CSA expansive additive, which is lighter than the blast furnace slag, is increased, it is judged that the density decreased as the replacement ratio of the expansive additive increased. Furthermore, the density difference before and after curing is reduced to 1.20-1.29 times width. The absorption ratio due to CaO-CSA expansive additive incorporation by level tends to decrease to 8.68, 7.51, 4.23, 4.11, 4.04 (wt.%) when measured 24 hours, respectively. By mixing the CaO-CSA expansive additive, the inter-tobermorite layer is filled to form a stable structure of CLC, and it is determined that the absorption ratio decreases as the replacement ratio increases

[5, 6].

**Table 6** SEM and EDS photographs of CLC based on CaO-CSA expansive additive replacement rate ( $\times 5,000$ )

		Replacement ratio of CaO-CSA EA (%)		
		0	10	20
SEM				
	S K			
	Ca K			
EDS	O K			

**Figure 5** Density and Absorption ratio

### 3.3 Compressive Strength

Fig. 6 is the result of measurement of compressive strength of the circumferential specimen on the 28<sup>th</sup> day of the reorder when the CaO-CSA expansive additive is replaced by five levels of high loss lag ratio 0, 5, 10, 15, 20 (%) based on the blending of CLC 0.6 kg/m<sup>3</sup>. From 0 to 10%, the expansive additive tends to increase to 6.84, 7.13, and 7.88 (MPa) as the replacement ratio of the expansive additive increases, but from then on, the compressive strength decreases to 3.94 and 3.51 in 15 to 20%. Compression strength is increased as the tissue of CLC becomes dense by

the formation of calcium hydroxide and ettringite up to 10% CaO-CSA expansive additive replacement ratio, and compression strength is reduced due to excess product from 15% or more. It is judged that although the intensity of a fixed tendency is expressed as a whole, it is judged to be a result of reducing voids due to excess water evaporation and suppressing drying shrinkage by filling between the tobermorite layers.

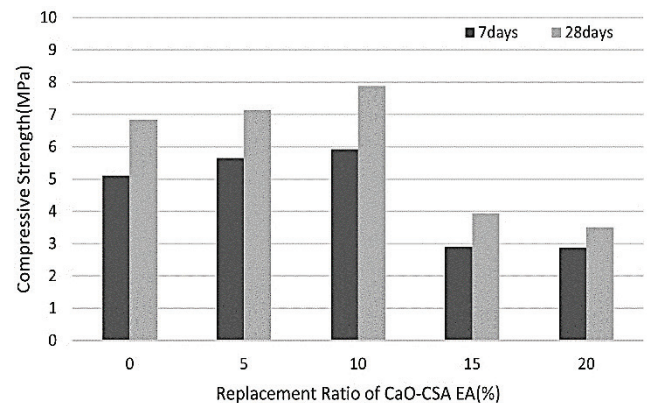
**Figure 6** Compressive strength (100×200)

Fig. 7 is the result of measurement of compressive strength of the cube specimen of CLC when the 0.6 item

reference CaO-CSA expansive additive is mixed in comparison with the blast furnace slag. The 28-day strength of CaO-CSA expansive additive replacement ratios 0, 5, 10, 15, 20 (%) is 8.25, 8.67, 9.51, 4.73, 4.21 (MPa), respectively, and the strength is about 1.2 times higher than that of a cylindrical specimen [7].

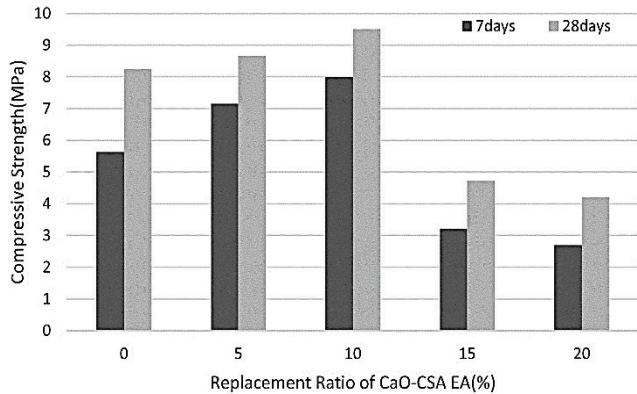


Figure 7 Compressive strength (50×50×50)

### 3.4 Flow Test

Fig. 8 shows the results of the flow test measurement of CLC due to the incorporation of CaO-CSA expansive additive by 0.6 item reference level. As the replacement ratio of the CaO-CSA expansive additive increases, the flow of the foamed slurry tends to decrease to 240, 220, 187, 156 and 139 (mm), respectively. As the CaO-CSA expansive additive replacement ratio increases, the decrease in excess water of the foamed slurry is large and the flow tends to decrease. A product, ettringite and calcium hydroxide is determined to have little effect on the enhancement of flow [8].

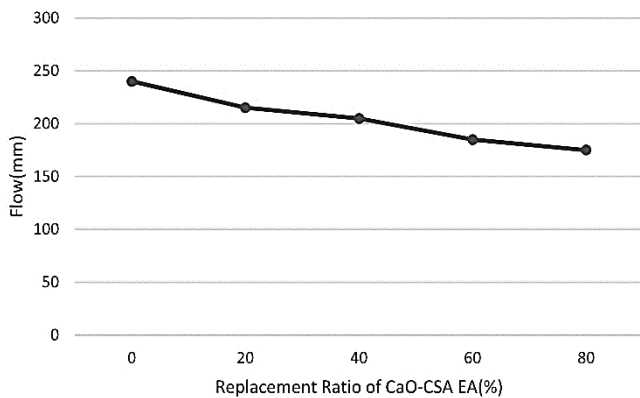


Figure 8 Flow

### 3.5 Thermal Conductivity

Fig. 9 shows the thermal conductivity measurement result of CLC by CaO-CSA expansive additive incorporation by 0.6 item reference level. Thermal conductivity tends to increase as CaO-CSA expansion material replacement rate increases. Thermal conductivity from 0-10% to 0.021 W/mK is judged to have increased sharply due to structural collapse

of CLC due to overproduction of calcium hydroxide and ettringite.

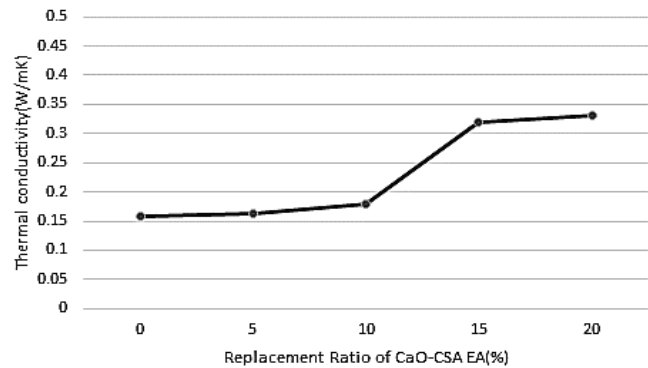


Figure 9 Thermal conductivity

### 3.6 Drying Shrinkage

Fig. 10 is the result of measuring the drying shrinkage ratio of CLC due to the mixing of CaO-CSA expansion material by level. As the replacement ratio of the CaO-CSA expansion material increases, the drying shrinkage ratio tends to be reduced and stabilized up to 15%. However, 20% shows the highest variation over time, which is judged to be the result of tissue relaxation due to excessive production [9, 10].

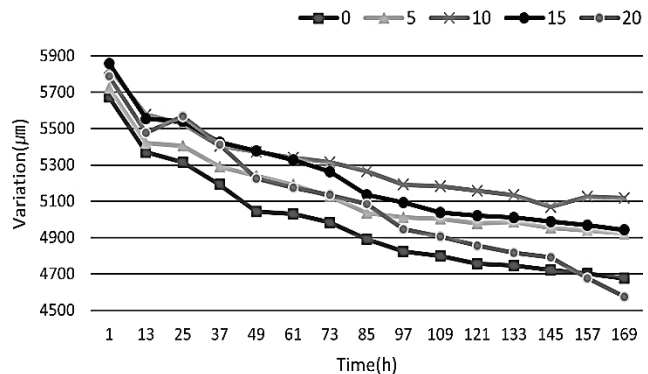


Figure 10 Drying shrinkage

### 3.7 Settlement

Fig. 11 is the result of measuring the degree of deposition of CLC by weight due to mixing of CaO-CSA expansive additive by level. A specimen demolded from a circular specimen of 1500 mm height is divided into upper, middle, middle, lower and lower stages by 200mm. Because of weight measurement, sedimentation occurred before CaO-CSA expansive additive was mixed, and the weight difference between the upper and lower stages was 353.9 g. After that, as the CaO-CSA expansive additive replacement ratio increases, there is no weight reduction, and it is determined that the upper and lower end error ratios are insufficient to reduce the settlement. By incorporating CaO-CSA expansive additive, drying shrinkage is suppressed by reacting with excess water inside the CLC, and the resulting calcium hydroxide and ettringites fill the void inside the CLC to increase durability, and it is judged that similar weight is

expressed without settling [11]. However, it is determined that at 20% CaO-CSA expansive additive replacement ratio, relaxation of CLC tissue occurs due to excessive product, and the weight difference between the upper end part and the lower end part is 80.2 g.

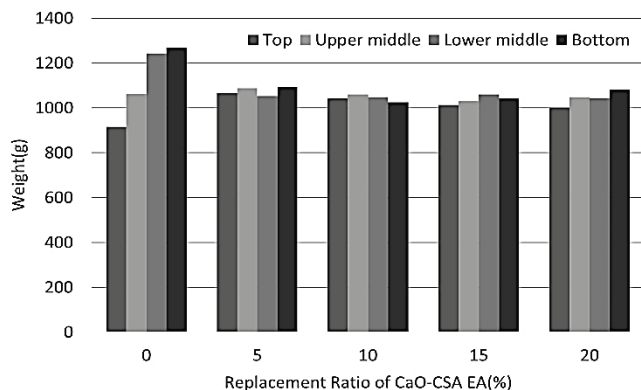


Figure 11 Settlement

#### 4 CONCLUSION

To improve the reliability of CLC, which can be cured at normal temperature and pressure, the properties of CLC by incorporating CaO-CSA expansive additive are analyzed by utilizing cement, blast furnace slag; animal foam additive and fiber based on a drying density of 0.55-0.65 kg/m<sup>3</sup> and the results are as follows:

- (1) The CaO-CSA expansive additive tends to increase in the range of 0-10 (%) as the replacement ratio of the CaO-CSA expansive additive increases. Compression strength is increased as CLC tissue becomes dense due to the formation of calcium hydroxide and ettringite, and it is judged that the compression strength is reduced due to excess production from over 15% of the replacement ratio.
- (2) As the replacement ratio of the CaO-CSA expansive additive increases, the density and absorption ratio tend to decrease. As the specific gravity of the CaO-CSA expansive additive lighter than the blast furnace slag is increased to the density, it is determined that the density decreases as the replacement ratio of the expansive additive increases, and that the absorption ratio decreases.
- (3) Liquidity tends to decrease as the replacement ratio of the CaO-CSA expansive additive increases. As a result, it is judged that the decrease in excess water of the foamed slurry is large and the fluidity is reduced, and the ettringite and calcium hydroxide as the producing substances have little influence on the fluidity enhancement.
- (4) As the replacement ratio of the CaO-CSA expansive additive increases, infiltration does not occur. In the 0-10% range, the resulting potassium hydroxide and ettringites filled the inside of the CLC, causing no precipitation and affecting strength enhancement, but after 15% it is judged that tissue relaxation occurred due to excessive production.

- (5) As the replacement ratio of the CaO-CSA expansive additive increases, the drying shrinkage ratio tends to be reduced and stabilized up to 15%. However, 20% shows the highest variation over time, which is judged to be the result of tissue relaxation due to excessive production.

By using the CaO-CSA expansive additive, it is determined that the formation of calcium hydroxide and ettringite fills the CLC between the tobermorite layers and the internal structure becomes dense. Currently, based on KS F 2701, the compression strength based on 0.6 items is more than 4.9 MPa, and the strength is about twice as strong as that of the existing CLC, and durability of the CLC are improved by incorporating CaO-CSA expansive additive.

#### 5 REFERENCES

- [1] Kim, J. G. (2010). A Study of Light Weight Wall in the Apartment with Column Type Structure. *The Korean Society for Noise and Vibration Engineering*, 10(1), 323-324. <https://doi.org/10.5050/KSNVE.2010.20.4.323>
- [2] Lee, C. W. (2021). Properties of CLC using Silica to Suppress Cracking due to Drying Shrinkage. *Journal of The Korea Institute of Building Construction*, 21(2), 125-126, <http://www.riss.kr/link?id=A107913808>
- [3] Lim, J. J. (2019). Properties of Lightweight Foamed Concrete According to Animality Protein Foaming Additive Type. *Journal of the Korea Institute of Building Construction*, 19(1), 34-35. <http://www.riss.kr/link?id=A106268352>
- [4] Lim, J. J. (2019). Properties of Foamed Concrete according to Dilution Concentrations of Animality Protein Foaming Additive. *Journal of the Korea Institute of Building Construction*, 19(2), 77-78. <http://www.riss.kr/link?id=A106521531>
- [5] Lee, H. W. (2014). Characterization of High Early Strength Type Shrinkage Reducing Cement Utilizing CSA Expansion Admixture of Low-Activity. *Journal of the Korean Recycled Construction Resources Institute*, 9(2), 38-45. <http://www.riss.kr/link?id=A101526174>
- [6] Lee, Y. O. (2010). Effects of Expansive Admixture on the Mechanical Properties of Strain-Hardening Cement Composite (SHCC). *Journal of the Korea Concrete Institute*, 22(5), 617-624. <https://doi.org/10.4334/JKCI.2010.22.5.617>
- [7] Park, C. J. (2015). Mechanical Properties and Autogenous Shrinkage of Ultra High Performance Concrete Using Expansive Admixture and Shrinkage Reducing Additive depending on Curing Conditions. *Journal of the Korea Concrete Institute*, 16(11), 7910-7916. <https://doi.org/10.5762/KAIS.2015.16.11.7910>
- [8] Yuan, T. F. (2016). Evaluating Shrinkage Characteristic of Ternary Grout for PSC Bridge Using Expansive Additive and Shrinkage Reducing Additive. *Journal of the Korea Concrete Institute*, 28(5), 519-525. <https://doi.org/10.4334/JKCI.2016.28.5.519>
- [9] Yuan, T. F. (2019). Effect of Expansive Additives and shrinkage Reducing Additive on the Shrinkage Reducing Properties of High-Performance Concrete. *Journal of the Korea Concrete Institute*, 31(1), 507-508. <http://www.riss.kr/link?id=A106207978>
- [10] Kim, J. Y. (2021). Characteristics of Shrinkage and Expansion before Curing of Grout According to Type of Expansion Material. *Journal of the Korea Concrete Institute*, 33(1), 447-448. <http://www.riss.kr/link?id=A107619457>

- [11] Lee, H. S. (2018). Influence of Rheological Properties of Lightweight Foamed Concrete on Preventing Foam Collapse. *Journal of the Korean Recycled Construction Resources Institute*, 6(4), 304-310.  
<http://www.riss.kr/link?id=A105981306>

**Authors' contacts:**

**Yong-Gu Kim**, PhD student  
Hanbat National University,  
125, Dongseo-daero, Yuseong-gu, Daejeon, Korea  
042-821-1635, kyg0824@hanmail.net

**Chang-Woo Lee**, Master's course  
Hanbat National University,  
125, Dongseo-daero, Yuseong-gu, Daejeon, Korea  
042-821-1635, lcw2509@naver.com

**Woo-Jun Hwang**, Master's course  
Hanbat National University,  
125, Dongseo-daero, Yuseong-gu, Daejeon, Korea  
042-821-1635, koo0012@naver.com

**Sang-Soo Lee**, Professor  
(Corresponding author)  
Hanbat National University,  
125, Dongseo-daero, Yuseong-gu, Daejeon, Korea  
042-821-1635, sslee111@hanbat.ac.kr

# Comprehensive Principles for Enhancing the Adhesive Bound Book Performances

Suzana Pasanec Preprotić\*, Gorana Petković, Mario Bracić, Ana Marošević Dolovski

**Abstract:** In addition to satisfying a book binding criterion, the paperback should provide content moments. Its binding style must be adjusted to book purpose. In publishing long-runs production, the perfect (adhesive) binding style with flexible hotmelt provides optimal binding durability with reasonable book price. Paperback should appeal to everyone through its visual-tactile senses. Taking the required actions in binding quality realization keeps track of comprehensive knowledge on various standardized paper substates (EN643:G3) that need to be wisely joined to realize perfect binding technique practices effectively. Moreover, designer technological awareness gained by experience provides potentials to understanding binding ability principles. The conducted research gives specific answers regarding paper cohesive capacity impact on consistency changes of adhesive bound book. It was concluded that higher paper drape capacity leads to increase of single sheet paper tension. Inappropriate bound book constructing was achieved although the flexible adhesive was used.

**Keywords:** adhesive bound book; binding performances; binding strength; paper cohesiveness

## 1 INTRODUCTION

An adhesive bound book (Paperback) is performed by hotmelt gluing without previous sewing book block with thread. As usual, the single paper sheets are stuck onto a cardboard cover that bound together create a distinctive shape of a book block spine (Fig. 1). This adhesive or unsewn binding style is the most preferable contemporary publishing binding technique in which the different standardized grammage rank of printing papers are used. Moreover, the book format sizes with their volumes are always adjusted to technological bindery features [1].

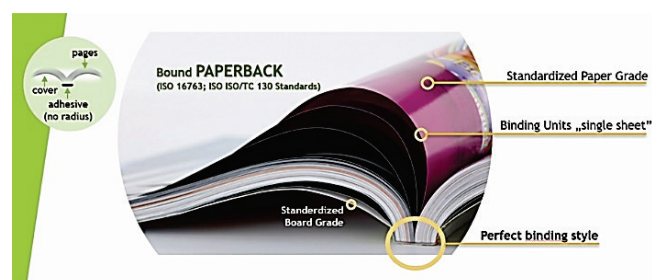


Figure 1 Perfect bound book construction

In addition, the perfect binding is specially dominated by hotmelt "one-shot" perfect binding technique in long-runs book manufacturing for various end-products (magazines, catalogues, brochures, class books, belles' letters, etc.). The reactive resin such as polyurethane is the most preferable hotmelt that is used with a standardized recycled and virgin paper stock. It is a flexible adhesive that provides initial bond strength by a chemical bonding paper substrate with resin. Therefore, the single paper sheets bond effectively with a paper cover. Bound together, they give desirable binding durability through a long period of time. This binding style is the most cost effective in a commercial book production.

Nowadays, the contemporary publishing perfect binding style provides productive manufacturing because of automated workflows with various hotmelts. The binding principles offer different variable procedures in which

various bound book semi-products are produced. Thus, a bound book is built by the specific number of single paper sheets that are known as "the binding units" (Fig. 1). In addition, the signature is created by various printed sheet folding procedures. It presents a binding unit in a book block construction as well.

The signature volume is determined by a book design concept that must always correlate with a book format size. In addition, it is important that a book format size follows the paper series (A-C), and the chosen paper size classes (1-6) according to ISO 216:2007. A book designing concept needs to be led according to the standardized offset printing technologies, while a printing paper sheet format (0-4) must be adjusted to standardized perfect binding processes with limited end-product sizes [2].

As previously mentioned, the book engineering concepts need to be guided by comprehensive knowledge and practice skills on how to manage binding technologies properly [3]. If a graphic arts designer does not make a great effort to design a book concept, the bindery efficiency will fail. Hence, a bindery knowledge must be the imperative in book concept creations.

A binding unit might consist of a certain number of pages, from minimum of 4 pages, 8 pages, 12 pages, 16 pages, 32 pages to maximum 64 pages. The volume of a binding unit needs to correlate to the chosen standardized printing press format and the chosen standardized paper grammage rank. If chosen paper rank does not follow the book binding rules in the beginning, the binding efficiency will be significantly reduced. The bookbinder is led to ensure correct folding procedures which relate to various book format sizes (tall, lying, square and narrow).

The main rule utilization of standardized paper classes (1-6) including their certain series and sizes in relation to the used binding technologies. Accordingly, the designers must respect the folding rules and to know the usages of various folding sequence (right-angle folds, combination folds, parallel folds). The defined designing approaches significantly contribute maximum utilization of technological capacities in bindery sector. The important rule

is to ensure the optimal number of binding units into a book block. So, the collected signatures with maximum constructed volume need to be put in order from the first to the last binding unit. Designer should achieve a bindery production with minimal semi-product loads.

In the perfect binding style, each signature into book block spine must be cut off before the gluing procedure [1, 4]. After cutting, the binding units "single paper sheets" construct a book block spine. Immediately after a book spine roughening procedure, the gluing block spine starts. The hotmelt is applied on the paper substrate. In most cases adhesion work is completed by resin bonding to the paper stock. The adhesion work intensity always depends on adhesive performance that appears at a moment of a book cover sticking onto the book block spine. By adhesive cooling, solidifying and moisture curing reactions more satisfying bond strength is reached. The bond line strength represents the binding strength capacity that is resistant to temperature and provides elastic resistance to pulling and flexing single pages out of a book block spine. Generally, reactive hotmelt resins provide excellent adhesion performances with various paper stocks and prevents block spine waving as well. Unfortunately, its high cost and particular properties make it unsuitable for widespread usages in bindery sector [5]. The standardized paper grades and adhesive usage (water emulsion, rigid hotmelt and flexible hotmelt) need to correlate with the book purpose, in which offered book designing concepts should reach the targets regarding economic, technological, and social aspects (Fig. 2).

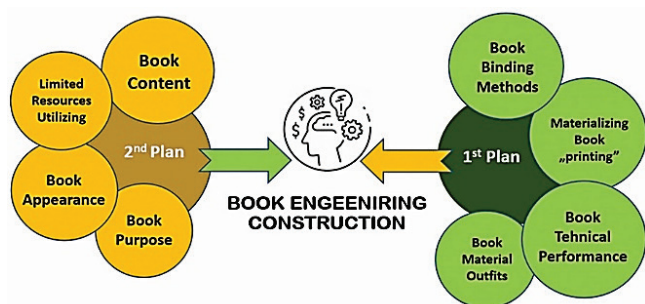


Figure 2 Book binding construction principles

It means to design procedures in prepress, printing and bindery departments effectively. By optimizing resource usage, the generated technological waste is reduced through a great number of binding procedures. Bindery efficiency copes with technological inappropriate book designing concepts (Fig. 2). Unfortunately, most designers haven't got technological knowledge and practice experience to predict the binding technology limitations. Correspondingly, the standardized paper grade choices (EN643:2001 Group 3) in book designing should be followed up through the standardized binding procedures (ISO 16763:2016 and Framework for ISO/TC 130 Standards-Graphic technology: 2019). Besides, paper binding capacities are sometimes not able to meet the technological expectations. Hence, the book designing constructions must lead to correct binding style solutions. In those situations, the designers should rely on

respectable technological practices that lead to bindery efficiency [6]. Moreover, the goal of this research evaluates the engineering comprehension of bindery strategies (Fig. 2). The designers should implement them in their book designing concepts. Dr. Ralf Speth said, *"If you think good design is expensive, you should look at the cost of bad design"*. [7]. These performed research methodologies provide understandable principles of engineering solutions and technological practices in a perfect "one-shot adhesive" binding style, in which various standardized paper grade with various grammage were used.

## 1.1 Comprehending Paper Bound Capacity in Perfect Adhesive Binding Technique

A paper substrate refers to graphic arts material that is made primarily from plant virgin fibers and/or recycled ones. A paper sheet is an inhomogeneous material that is arranged in fiber layer networks which contain various pore sizes. Paper features directly refers to flat sheet that is made primarily from plant origin fibers, inorganic furnish and specific coatings. Moreover, fiber sources mostly define paper mechanical strength. Thus, the increase of chemical fibers in the paper lead to higher density and lower thickness in the paper sheet. In addition, specific standardized paper printing properties are achieved in a papermaking process. The various paper grades (EN643:2001) with specific physical properties in different printing techniques are produced in controlled standardized conditions. The properties vary and depend on amount of added inorganic pigments and fillers, chemical compounds, and sizing agents in the paper sheet. These ingredients directly affect paper sheet printing and adhesive perfect binding performances. Thus, paper grammage rises with higher amount of coating and higher quantities of fiber network layers in a paper sheet. A paper grammage and its tensile and folding strength are the most important properties in performing an optimal adhesive "one-shot" perfect binding style. Above all, the engineered designing bound book concepts always support standardized printing paper grades such as wood-free, wood-contained (less 10%) and recycled ones [8]. In addition, the virgin and/or recycled fibers together create fibrous structure of standardized printing coated paper whose surface must be treated with reactive hotmelt. For that reason, in automatic workflow that includes bound book publishing production, it is obligatory to use a flexible reactive PUR hotmelt that is more expensive than non-reactive EVA hotmelts and environment-unfriendly as well.

Standardized coated paper grades have a complex-built structure. Because of that reactive hotmelt is an excellent choice to ensure the binding capacity for various standardized paper grammages. It is well-known that high grade coated printing papers consist a few layers of coating that have a significant effect on bound book appearance [9-13]. Therefore, the flexible PUR hotmelt is an excellent choice in improving a book durability. Moreover, these standardized coated layers on a paper sheet, must at the same time provide efficient multicolour printing and preferable book appearance.

In addition, by higher fillers loading into paper sheet, its mechanical strength (tensile and tear) and stiffness decrease. Moreover, a standardized coated paper mainly leads to the segregation of fillers from the top surface of paper sheet. Consequently, the separated inorganic particles directly create the dust on the paper surface. The accumulation of the dust is the largest immediately after cutting off the spine edges (roughening procedure) in perfect adhesive binding workflow production [8, 14].

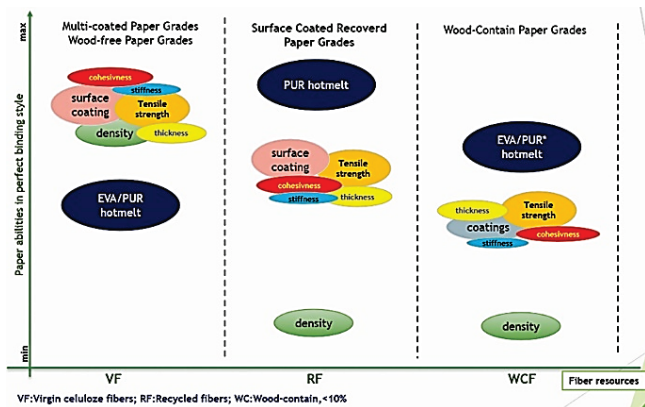


Figure 3 Various paper grades binding capacity by Perfect binding style

From previously mentioned, the standardized paper sheet stiffness relates to its compression or extension tensile strength, when a single paper sheet tends to resist an elastic deformation. In such circumstances, its stiffness increases with a higher fiber layers network which causes the higher bonding degree within the paper sheet.

In bookbinding the stiffness presents paper cohesive attributes. These attributes relate to paper toughness and its abilities to bend and drape well. The attribute "paper sheet draping well" is crucial in a bound book (Paperback) construction. Moreover, the paper binding capacity mainly correlates with standardized physical paper grades properties (Fig. 3). The critical point of view of each bookbinder is cohesive attributes of papers which need to provide controlled book opening and page scrolling at the same time. Perfect (adhesive) binding style efficiency directly depends on chosen and used standardized paper grade including their various grammage.

The efficient binding work quality is visible through reducing paper sheet tension that is located on the bond line of a book spine. Increasing paper cohesive attributes lead to its reduced bending, under which circumstances book pages haven't got ability to drape well under loads. It explains a higher possessed energy of each single paper sheet in book. Paper cohesive attributes may be revealed through their physical properties such as thickness and tensile strength. Both lead to tension increase on a book spine. Moreover, the increasing paper tensile strength always correlates with a higher quantity of virginal blanched beaten fibers. Paper sheet strength properties are increase with the higher number of fiber network layers [15]. Therefore, the virginal fiber network structures are a major contributor to providing paper cohesive attributes and they reduce paper stretching capacity as well [16].

In addition, the large share of recycled or wood contained fibers which are added to virginal ones [17] give the paper specific cohesive attributes. These paper grades show less tension on the bond line, but book page scrolling remain difficult. So, its cohesive attributes must be adjusted to adhesive perfect book binding style. It means that each individual paper sheet participates in creating a balanced shape of a book spine. Another reason to improving balanced shape is to take a correct paper sheet grain direction. Book designing construction must be led by paper sheet grain direction (MD) that always aligns parallel with book spine (Fig. 4-B). So, the accent is to reduce paper cohesive attributes, and this is possible to achieve by paper cross-grain direction (CD) in a book block. In that loaded circumstance (compression or extension), a paper sheet remains permanently deformed but it still tends to return into previous position (Fig. 4-A).

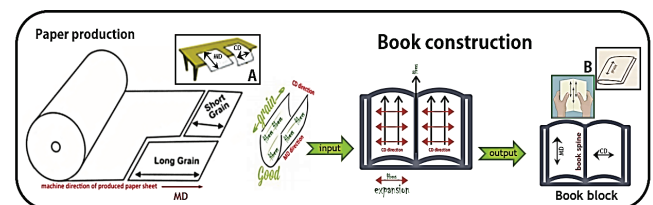


Figure 4 Book constructing and paper grain direction interrelation

## 1.2 Paper Drape Capacity

A bookbinder explains the term "paper draping" as a single paper sheet ability to fall easily in gutter margin. If a book page resists elastic deformation in a book spine it means that it doesn't drape well and its stiffness increases (Fig. 6). By higher paper drape capacity, the book pages tend to keep existing shape and resist falling naturally onto adjacent book pages. Determining the drape factor value and its higher result expresses higher paper rigidity because the book pages can't lay down easily. Therefore, book pages show tension that increase on the bond line and finally cause permanent book spine deformation. Moreover, a stiffer paper shows the resistance towards compression and extension. Hence, the loads are transferred directly into a book spine although book pages try to stretch. The constant balanced book spine shape is the most important factor in performing correct book construction. So, the obligation of each designer is to make judgement about paper drape capacity. It must be based on making book prototype by consulting a bookbinder long before starting bound book production. Another important factor for balancing book spine shape is paper sheet anisotropic behaviour. So, the arranged fiber network layers directly affect paper drape capacity. It means that its structural characteristics (fiber resource types, papermaking process types, intensity of fiber network connectivity, paper thickness, paper density, paper porosity, and paper consistency) significantly influence determined drape factor value. Moreover, other factors such as inorganic components and other chemical compounds [16] additionally contribute to paper cohesive attributes, which are responsible for preferable appearance of book construction.

The binding paper stiffness is a very important factor for a bookbinder [16]. If a designer takes inappropriate paper binding stiffness, problems occur that cause poor appearance and handling having difficulty in the bound book. Thus, understanding the term "paper drape capacity" leads to novel approaches on how to improve bound book functionality. In addition, the designers should perform comprehensive approaches to explain paper cohesive attributes. Nowadays, bookbinders confirm that many designers have no practical competence to offer functional and efficient bound book concepts. Unfortunately, the designers' policy is mainly focused on putting the correct paper grain direction of paper and book format size changes.

### 1.3 Evaluative Comprehension of Book Spine Control

Term drapability relates to the paper drape factor value. By reducing drape value, a paper sheet is capable falling naturally onto a gutter margin of an opened book as shown in Figure 4-A. Paper drapability is significantly lower through its cross-grain direction (CD). Therefore, the designers should choose the optimal paper cohesive attributes which will compensate stress on a bond line. This is the first step in making the best condition to bound book appearance during its handling (Fig. 4-B). Moreover, if designers understand the paper cohesive attributes well, a bound book construction should lead to its preferable impression (Fig. 4). It means that readers don't need a greater effort to open the book entirely and it won't ultimately lead to deformed book spine shape.

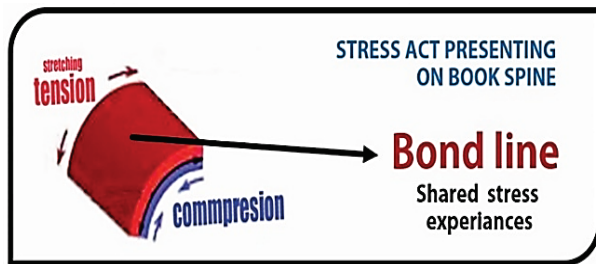


Figure 5 Existing stress shown on bond line

From previously mentioned, the term drapability refers to paper cohesive attributes that express potential paper energy. So different standardized paper grades with their various grammages give different potential energies which lead to various paper cohesive attributes. For that reason, the key practical element is the right choice of potential energy of paper which builds up the book pages. So, the spine shape book deformation is caused by an effect of increasing paper potential energy. Moreover, an adhesive flexible layer, which is formed on the bond line, needs to neutralise, and compensate stress that comes from single paper sheets inside of book block (Fig. 5). If the book pages the potential energy is too high, the pages are not able to move freely inside of block spine space. No doubt, inappropriately chosen paper cohesive attributes cause difficulty in book opening and scrolling. For that reason, comprehensive adhesive binding knowledge and practice skills together with standardized paper grades and their various grammages ensure a

functional designed book concept. This approach ensure satisfaction to readers because they are able to keep the book opened effortlessly without spine deformation, from book head to tail (Fig. 5 and Fig. 11).

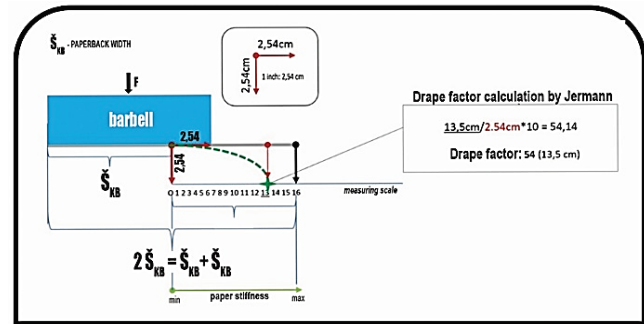


Figure 6 Drape factor measuring

In perfect (adhesive) binding, drape factor measuring (Fig. 6) is on a relative scale which is constructed by Pete Jermann [18]. A measured value relates to paper sheet stiffness, and it determines paper binder's possibilities. When drape number increases on a relative scale towards No.16, it means that it is stiff paper (Fig. 6). Moreover, whatever the drape number is potential paper energy always rises by reducing the book width ( $\delta_{KB}$ ) including different standardized paper grades and their various grammages. Potential paper energy falls with increasing of book formats as well.

Perfect (adhesive) binding technique, with reactive hotmelt, provides quite small radius of book opening. Hence, the apex arc is barely perceptible on a book spine. For that reason, paper cohesive attributes have a significant effect on the balanced book spine shape. So, the selected standardized paper grades and their specified grammage must drape well to avoid controlled opening of a book spine.

The designers must be aware that paper cohesive attributes generally lead to more tension on the bond line with hotmelt [19]. Moreover, its cohesiveness rises with inappropriate book format sizing. Hence, a compromising binding solution must involve favourable strength durability, practical usage, and desirable bound book appearance. As a rule, the designers should neglect present designing practices and start to engage in advanced solutions which rely on determined features of standardized paper grade properties. Primarily, a designer must be able to provide advanced designing concepts and to make great number of prototypes. The purpose of this approach certainly makes a preferable book construction that provides proper book spine stretching and returning to its initial shape.

### 1.4 Reflection on Paper Substrates Performance

Various standardized paper substrates must satisfy ink transfer conditions and perfect (adhesive) binding procedures as well. In multi-colour ink transferring, paper surface printable properties are improved with various finishing treatments like surface sizing or coating (Fig. 7). Various modified coated surfaces enhance internal paper resistance

towards fibrous release (fibers and fines) and other inorganic resources (fillers and pigments) that cause making dust within perfect (adhesive) binding manufacturing. Moreover, these inhomogeneous resources lead to insufficient paper cohesive strength which is a special feature of lightweight paper grades [20].

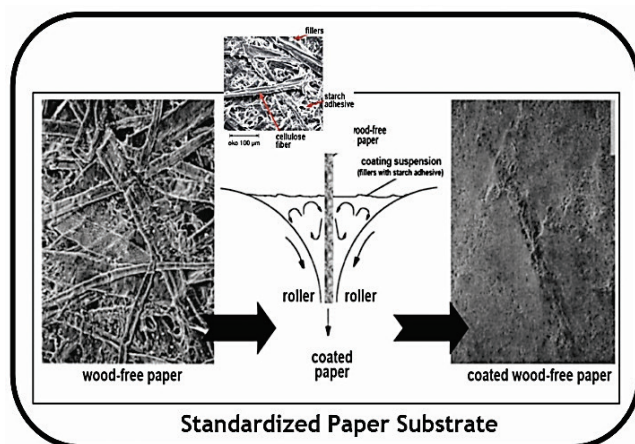


Figure 7 Paper substrates appearance

Standardized paper grades stability matches up with their structure (physical) properties that are achieved inside of papermaking procedures. Paper grades properties are tailored for end-use requirement, for printing sector exclusively. Standardized paper grades dimensions and their tensile strength are determined by fiber resources, inter-fibers bonding intensity and fiber arrangements during paper sheet formation. While the virgin cellulose fibers contribute to higher fiber networking, the lignin contained fibers and recycled one's cause lack of paper sheet formation. Such feature is characteristic for bulky and recycled standardized paper grades.

Flexible virgin that are mainly bleached are created in chemical pulp process. Tensile strength of standardized paper grades enhances because of inter-fibers connection. However, if the share of recycled fibers increases during fibers networking, it will finally lead to paper tensile strength reduction [21].

Standardized offset printing wood-free paper, with a significant low residual lignin content, is produced in various grammage. It is a high tensile strength paper that is made up of bleached fiber with the fine coated surface layers. In addition, book products (magazines, catalogues, books) preferring a variety of two-sided woodfree coated paper grades, while is the standardized art paper grades mostly suitable for illustrated books and brochures [22]. Moreover, high-quality magazines and catalogues for advertising, in long-runs adhesive perfect production, are always printed on standardized fine coated paper grades including double or triple surface coatings which is made up of a higher share of recycled fiber resources.

Nowadays, in papermaking production except virgin fibers are added recycled ones and the other components for achieving a preferable paper networking structure. Moreover, the various standardized paper grades contain

different quantities of inorganic and organic compounds such as fillers, adhesives, pigments, binders, etc. [23]. Thus, fillers improve a standardized paper sheet formation by filling the voids between the fiber-networking. Fillers directly enhance a printable performances of standardized paper grades. In addition, the inorganic pigments that are added in surface coatings generally are mixed with a starch. The starch is an adhesive that acts as binder to compose a complete paper structure [24]. While the starch as adhesive enhancing paper compressive strength [16], by fillers overloading lead to reducing its compressive strength. At the same time, the fillers cause weakening inter-fiber bonds and to enhance a paper dimensional stability because of fillers humid resistance [26]. So, the standardized paper strength capacity rises because of flexible fiber network that are mostly made of fibrillated virgin fibers and small fibrils. Moreover, a higher paper potential energy is a mutual relationship with a its strength capacity. For instance, some bookbinder experts have practical skills for estimating paper cohesive attributes.

They precisely observe the paper sheet structure to estimate its bending stiffness that always connected with other paper ingredients which are provided a denser layered paper structure. These standardized paper grades always generate the dimensional stable paper sheets regardless of its grammage. They have higher bending stiffness performing about others with lower share of added ingredients.

In bookbinding, the main target is to choose the standardized paper grades and grammages that have higher density of surface layers and lower density of middle layers [16]. This is one verifiable approach to determining preferable cohesive attributes of standardized paper grades and their grammages that should lead to a preferable bound book constructing.

## 1.5 Comprehensive Approach to Bound Book Designing Concept

As a rule, the book designing concepts are based on correct binding capacities of standardized paper grades and their grammages (EN643:G3.01-3.19.). Paper cohesive capacity (stretching and compression) affects book spine appearance because of bond line loading. Paper cohesive attributes are shown at the moment opening and scrolling of book pages, when a minor apex arch is created on a flexible and mobile book spine. So, the apex arch appearance on the bond line can help designers with constructing bound book prototypes, which will lead to connecting current experiences and a prior comprehensive binding knowledge.

Creative cognitive visualization helps everyone to understand problems. Moreover, designers should make a few book prototypes and finally ask themselves "Which chosen standardized paper grade and its grammage give a minor apex arch on a book spine?" By answering that question, awareness about book designing concepts create new approaches and strategies on how to advance perfect (adhesive) binding technical and technological aspects in accordance with bookbinder recommendations.

It is obvious that designers should learn more. They must be able to explain a designing concept in more details to a

bookbinder who produces an end-product in long-runs manufacturing and to use various technical-technological equipment inside machine processes. For that reason, designers must be superior in making decisions since they need to have background knowledge and technical practice in book making. Moreover, they should be aware of the significant differences between hand bookbinding (short-runs production) and edition bookbinding (middle-runs and long-runs production) features. In addition, designers must determine the importance of a book purpose long before it's end-producing. Therefore, they should come up with advanced approaches to interpret which binding forms and types are appropriate to the book content. Designers must move binding solutions forward with a reasonable meaningful manufacturing and economic efficiency as well. It is important to choose standardized paper grade and its grammage which will provide the book's visual-tactile sense and its durability at the same time. Furthermore, designers should enhance their book designing approaches to improve bindery efficiency. The implementation of comprehensive practices in bookbinding concepts will lead to the increase in the number of satisfied end-users.

## 2 EXPERIMENTAL

The Perfect bound books (Paperbacks) process was performed by gluing the single paper sheets on standardized cardboard cover (trade name: Symbol Card 240  $\text{gm}^{-2}$ ) and they together create the bound book spine. The adhesive (unsewn) binding style was performed in full automated Horizon-470 perfect binding machine including book block and cover feeding, book block spine milling (roughening) and gluing sections, smoke extractor of hotmelt and delivery conveyor as well. The minimum book block size is  $105 \times 145$  mm and the maximum book dimension that can be produced is  $320 \times 320$  mm including the maximum book block thickness of 65 mm. The reactive PUR flexible adhesive was used for various grammages and various formats of books (tall and square). The chosen standardized paper grammages ( $\text{gm}^{-2}$ ) refer to standardized paper basic weight that is determined by ISO Standard 536. The grammage term was used in representing the research results instead of the term basic weight. The evaluating procedures of book samples and standardized paper sheets were performed using standardized test methods and visual judgements.

### 2.1 Materials

#### 2.1.1 Paper

In Paperback edition (publishing) manufacturing, various paper grammages of the same grade were used as listed in Tab. 1. Paper substrates belong to standardized high quality wood-free 2-side fine coated printing paper (EN 643, Group 3). It has 100% chemically pulped fiber furnishers with fillers and binders (starch and pigments) which lead to the increase the paper's smoothness and strength [27].

**Table 1** List of used paper grade with its various grammages

Trade Name	Grammage ( $\text{gm}^{-2}$ )	Abbreviation
Garda Gloss	90	<b>90<sup>CP</sup></b>
Garda Gloss	115	<b>115<sup>CP</sup></b>
Garda Gloss	135	<b>135<sup>CP</sup></b>
Garda Gloss	150	<b>150<sup>CP</sup></b>
Garda Gloss	170	<b>170<sup>CP</sup></b>

### 2.1.2 Adhesive

The used reactive hotmelt adhesive (TECHNOMELT PUR 3317 BR known as PUMELT-QR 3317 BR) is reactive prepolymer polyurethan. According to material safety data sheet, it performs excellent adhesion (bond strength) to a various paper substrate. Final bond strength was achieved by physical curing process of the adhesive layer film on the paper substrate [28, 29].

## 3 MEASURING METHODS

### 3.1 Sample Preparation

A total of 250 Perfect-bound books were made (50 Paperbacks of each paper grammage) in order to determine the binding strength. Various grammages of identical unprinted paper grade were used in the perfect binding production samples.

Different Paperback formats (Tab. 2) included identical book spine width of 40 mm. The signatures as binding units in a book block were bound by using the perfect binding technique with standardized reactive polyurethan (PUR) hotmelt adhesive. Perfect bound book samples were manufactured under standardized conditions (ISO 16763; ISO 187; ISO/TC 130 Standards Framework).

**Table 2** List of used Paperback samples

Book spine width (mm)	Format sizing (mm)	Abbreviation
40 (75 KS*)	B5-tall (160×240)	<b>B590<sup>CP</sup></b>
40 (75 KS*)	A5-tall (148×210)	<b>A590<sup>CP</sup></b>
40 (75 KS*)	Square 310×310	<b>SQ90<sup>CP</sup></b>
40 (57 KS*)	B5-tall (160×240)	<b>B5115<sup>CP</sup></b>
40 (57 KS*)	A5-tall (148×210)	<b>A5115<sup>CP</sup></b>
40 (57 KS*)	Square 310×310	<b>SQ115<sup>CP</sup></b>
40 (50 KS*)	B5-tall (160×240)	<b>B5135<sup>CP</sup></b>
40 (50 KS*)	A5-tall (148×210)	<b>A5135<sup>CP</sup></b>
40 (50 KS*)	Square 310×310	<b>SQ135<sup>CP</sup></b>
40 (46 KS*)	B5-tall (160×240)	<b>B5150<sup>CP</sup></b>
40 (46 KS*)	A5-tall (148×210)	<b>A5150<sup>CP</sup></b>
40 (46 KS*)	Square 310×310	<b>SQ150<sup>CP</sup></b>
40 (40 KS*)	B5-tall (160×240)	<b>B5170<sup>CP</sup></b>
40 (40 KS*)	A5-tall (148×210)	<b>A5170<sup>CP</sup></b>
40 (40 KS*)	Square 310×310	<b>SQ170<sup>CP</sup></b>

The volume of a signature as a binding unit (KS\*) consist of 16 pages.

The chosen paper grade class is 1 and the chosen paper format series is B. "B1 paper sheet"

The tall book formats were made by right angle folds, for the square book formats were made combination folds.

### 3.2 Determination of the Binding Strength

The binding strength is evaluated according to ISO 19594. It is evaluated by pulling out a single sheet from the book block and measuring the maximum force which is result of the page-pull procedure. Page-pull test was performed in standardized conditions (ISO 187), on IDM Page Pull Tester,

Model P0011. The binding strength of the Perfect bound book samples is calculated according to ISO 19594:2017 and Eq. (1).

$$BS = \frac{F_{\max}}{l} \quad (1)$$

$F_{\max}$  - maximum force (N)

$l$  - distance from book's head to tail (cm)

**Table 3** Binding strength evaluation (ISO 19594)

Quality level of Binding Strength	Binding Strength (Ncm <sup>-1</sup> )
Very good durability	> 7.0
Good durability	≤ 7.0; > 6.1
Sufficient durability	≤ 6.1; > 5.1
Poor durability	≤ 5.1.

The quality levels for binding quality consistency are based on coefficient of variation (Tab. 4).

**Table 4** Binding quality expresses to the consistency level (ISO 19594)

Quality level of Consistency	Variation Coefficient
Very good durability	< 0.10
Good durability	> 0.10; ≤ 0.15
Sufficient durability	> 0.15; ≤ 0.20
Poor durability	> 0.20.

### 3.3 Drape Factor Determining

Paper drape factor was performed in standardized conditions (ISO 187), which influences Perfect bound book opening behaviour (Fig. 6). It presents how capable the unglued paper sheet is to exert at the bond line [18]. After the measurement of the paper extension length which drops one inch at the leading edge, drape factor was evaluated according to Eq. (2).

$$Drape\ Factor = \frac{1}{2.54} \times 10 \quad (2)$$

## 4 RESULTS AND DISCUSSION

Each measuring method was performed ten times. The obtained descriptive results of mean (M), standard deviation (σ) and coefficient of variation (CV) were used as an aid in estimating paper bindability (one high-quality paper grade with its five different grammages). The sample dispersion values were used in the evaluation of the bound books opening behaviour. Cohesive paper attributes were represented in relation to the binding performance of a single paper sheet in a bound book.

### 4.1 Determining Binding Strength Quality and Its Consistency

The paperback samples, with their spine thickness of 40 mm, were tested at seven test positions (5%, 20%, 35%, 50%, 65%, 80% and 95% of the total number of pages). For the page-pull testing, 10 samples of each paper grammages and book format size were measured in 7 different test positions

in accordance with the certain number of Paperback pages (1184 pages, 912 pages, 800 pages, 736 pages, 640 pages) as shown in Fig. 8. The obtained results of binding strength level quality and its consistency are presented in Fig. 9. The mean binding strength results refer to Perfect bound book durable permanence. Moreover, the variation coefficient (CV) results relate to stability of the bond line. The behaviour manner on how book pages hold together with adhesive is presented in this research.

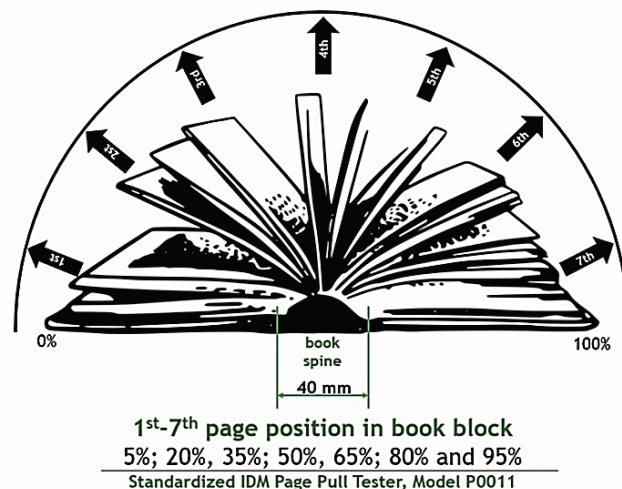


**Figure 8** Positioned pages in Perfect bound book

The binding strength measuring was conducted by pulling pages from a book spine. The obtained results by pulling out 7 single paper sheets from a book block in total of five groups of B5 book formats ( $B_590^{CP}$ ,  $B_5115^{CP}$ ,  $B_5135^{CP}$ ,  $B_5150^{CP}$  and  $B_5170^{CP}$ ) were classified as a very good book durability ( $> 7.0$  Ncm<sup>-1</sup>) as shown Fig. 9. Moreover, B5 format Perfect bound book is the most represented in edition binding production and therefore it is presented in this research.

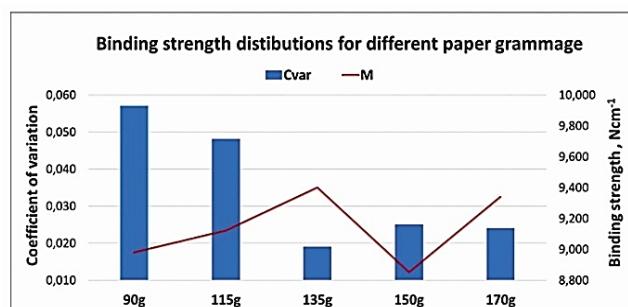


**Figure 9** Paper binding performances by using the Perfect binding style

The excellent binding strength mean results were achieved respectively sample  $B_5150^{CP}$  Paperback ( $> 8.51$  to  $> 9.18$  Ncm<sup>-1</sup>), followed by  $B_590^{CP}$  Paperback ( $> 8.10$  to  $> 9.68$  Ncm<sup>-1</sup>),  $B_5115^{CP}$  Paperback ( $> 8.19$  to  $> 9.50$  Ncm<sup>-1</sup>),  $B_5170^{CP}$  Paperback ( $> 9.05$  to  $> 9.69$  Ncm<sup>-1</sup>) and  $B_5135^{CP}$  Paperback ( $> 9.11$  to  $> 9.71$  Ncm<sup>-1</sup>). Considering the paper various grammages, the obtained order of results was expected because of PUR hotmelt elastic properties. Moreover, sample 90<sup>CP</sup> 2-side fine coated printing paper is not 1<sup>st</sup> on the

list although it showed very good drape performance ( $>11.42$  to  $>12.2$ ) as shown in Fig. 12. In addition, a very good durable performance was determined for all 7 test positions for five various grammages ( $90^{CP}$ ,  $115^{CP}$ ,  $135^{CP}$ ,  $150^{CP}$ ,  $170^{CP}$ ) of the same paper grade. The obtained coefficient of variation (CV) results were achieved respectively  $B_5 90^{CP}$  with 1184 book pages ( $0.057 \leq 0.10$ ) followed by  $B_5 115^{CP}$  with 912 book pages ( $0.048 \leq 0.10$ ),  $B_5 150^{CP}$  with 736 book pages ( $0.025 \leq 0.10$ ),  $B_5 170^{CP}$  with 640 book pages ( $0.024 \leq 0.10$ ) and  $B_5 135^{CP}$  with 800 book pages ( $0.019 \leq 0.10$ ). The weakest consistency was noticed for sample  $B_5 90^{CP}$  with the largest number of book pages. The obtained CV results decrease, and they do not follow book page reductions (1184 pages  $>$  912 pages  $>$  800 pages  $>$  736 pages  $>$  640 pages). The bound book sample  $B_5 135^{CP}$  with 800 pages showed the best performances and maximum stability on the bond line ( $9.40 \text{ Ncm}^{-1}$  and  $0.019$ ). The achieved performances are the result of the results derivate from a correct book construction and the efficient layered bound fiber network inside the paper sheet sample  $135^{CP}$ . Moreover, the paper sheet structure is denser on its surface and central part. Therefore, its structure shows affinity for adherence and the increased binding capacity with hotmelts. In addition, the CV results of other samples are significantly higher than sample  $B_5 135^{CP}$  ( $0.019 \leq 0.10$ ). The CV results were achieved respectively  $B_5 90^{CP}$  ( $0.057 \leq 0.10$ ) is 3 times higher than  $B_5 135^{CP}$ , followed by  $B_5 115^{CP}$  ( $0.048 \leq 0.10$ ) 2.5 times higher,  $B_5 150^{CP}$  ( $0.025 \leq 0.10$ ) 1.3 times higher and  $B_5 170^{CP}$  ( $0.024 \leq 0.10$ ) 1.26 times higher. It is noticed that by the decrease of CV results ( $90^{CP} < 115^{CP} < 150^{CP} < 170^{CP}$ ) the paper grammage decreases as well. In accordance with paper grammage reduction, the fiber network layers density decrease [16]. On the other hand, sample paper cohesive capacity rises under loading respectively ( $90^{CP} > 115^{CP} > 150^{CP} > 170^{CP}$ ) as shown in Fig. 9. From previously mentioned, paper sheet stability of sample  $135^{CP}$  is additionally insured by surface layered coating which boosts its cohesive attributes as well. The increased CV results are caused by inappropriate paper structure which is located in the middle and on the top of the paper cross section ( $90^{CP} \text{ CV: } 0.057 > 115^{CP} \text{ CV: } 0.048 > 150^{CP} \text{ CV: } 0.025 > 170^{CP} \text{ CV: } 0.024 > 135^{CP} \text{ CV: } 0.019$ ). In Figure 10, only the book sample  $B_5 135^{CP}$  showed stabile durability performances for all seven different book page positions.

The standardized paper-making machine is not able to entirely create a straight fiber layered networks inside the paper structure although they follow the machine direction [16]. Therefore, the aligned fibers of a paper sheet need to follow a book spine direction. It strictly means that the grain machine direction (MD) must be parallel with a book spine, from its head to tail (Fig. 11). Because of grain cross-machine direction (CD) a paper sheet has lower resistance to bending and it easily falls on a book cover. By reducing its bending stiffness, paper drape capacity increases. This is expressed by Jermann's a lower number of drape factor ( $DF < 16$ ) as shown in Fig. 6. In accordance with Jermann's observation criteria on a relative scale [18], preferable construction of book can be created only with an optimal paper cohesiveness by which additional loads on a book

spine are avoided (Fig. 5) in terms of using PUR flexible hotmelt which neutralizes loads on Paperback bound book spine, from head to tail as shown in Fig. 11.

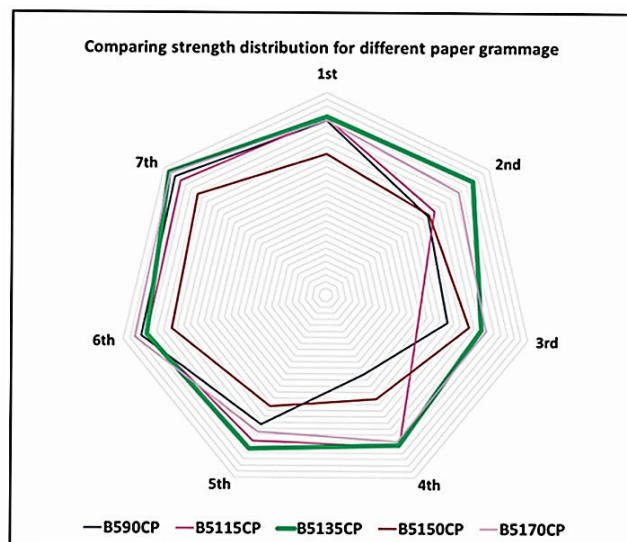


Figure 10 Permanence of Paperback sample  $B_5 135^{CP}$  on seven different page-pulling positions

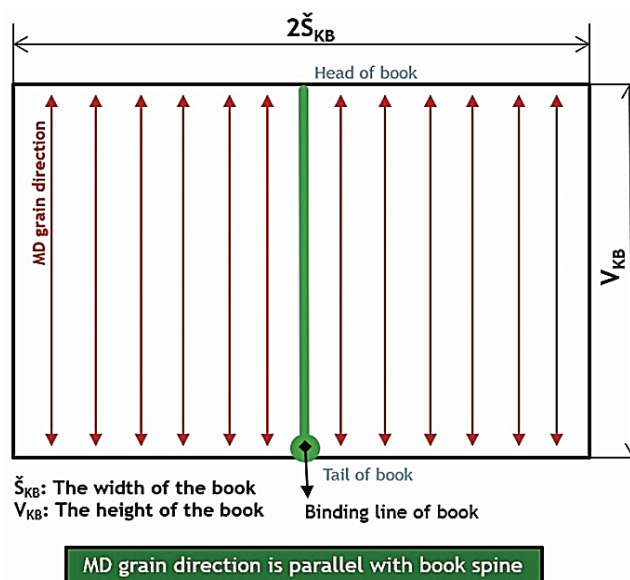


Figure 11 Perfect bound book construction rules

The obtained results of drape factor ( $DF$ ) for 5 various grammages of the same paper grade is presented in Fig. 12. The results were obtained by Jermann's unique relative scale [10] that presents binding paper stiffness, its capacity to fall into gutter margin of a book spine. The measurements were conducted on the paper sheet B5 format size samples ( $B_5 90^{CP}$ ,  $B_5 115^{CP}$ ,  $B_5 135^{CP}$ ,  $B_5 150^{CP}$  and  $B_5 170^{CP}$ ).

The obtained  $DF$  mean results were achieved respectively sample  $B_5 90^{CP}$  ( $>11.42$  to  $>12.20$ ), followed by  $B_5 115^{CP}$  ( $>13.39$  to  $>14.17$ ),  $B_5 135^{CP}$  ( $>14.57$  to  $>16.17$ ),  $B_5 150^{CP}$  ( $>17.32$  to  $>18.90$ ) and  $B_5 170^{CP}$  ( $>18.11$  to  $>20.87$ ). Considering the paper various grammages ( $90^{CP} < 115^{CP} < 135^{CP} < 150^{CP} < 170^{CP}$ ) the obtained order of  $DF$  results were

expected because the bending resistance increases together with the paper grammage increase. Moreover, the  $DF$  results increase approx. 2 points for each paper grammage in the sequence. The obtained CV results confirm the consistency of potential paper energy samples respectively  $B_5 170^{CP}$  ( $0.034 \leq 0.10$ ) followed by  $B_5 135^{CP}$  ( $0.029 \leq 0.10$ ),  $B_5 90^{CP}$  ( $0.029 \leq 0.10$ ),  $B_5 150^{CP}$  ( $0.026 \leq 0.10$ ) and  $B_5 115^{CP}$  ( $0.018 \leq 0.10$ ) because of tailored paper sheet structure with the higher virgin fiber networking.

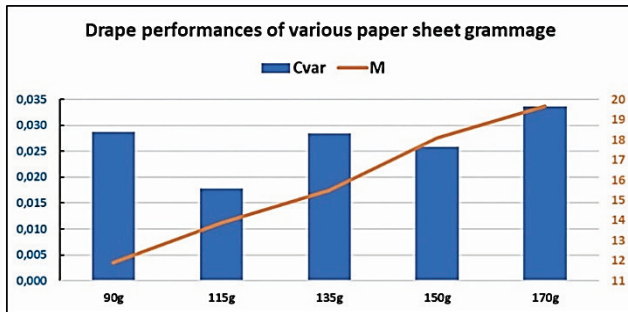


Figure 12 Drape performances of single paper sheet B5 size for different grammages

The higher drape variability was noticed in samples  $B_5 170^{CP}$ ,  $B_5 90^{CP}$ ,  $B_5 135^{CP}$  and  $B_5 150^{CP}$ , while higher drape stability was shown in the sample  $B_5 115^{CP}$  (Fig. 12). The higher drape stability matches up with paper structural properties. Paper cohesiveness relates to its denser layered structure. This various paper grammages, with their specific structural features, belong to the fine coated paper grade group, which is produced by additional treatment including finishing coatings [16].

## 4.2 Perfect Bound Book Opening Behaviour

This high-quality wood-free 2-side fine coated paper grade with its various grammages ( $90^{CP}$ ,  $115^{CP}$ ,  $135^{CP}$ ,  $150^{CP}$ ,  $170^{CP}$ ) gave very good book durability with PUR flexible hotmelt. Comprehensive understanding of book design concepts starts with creating optimal book spine mobility in which the appearance of apex arch on the bond line should be minimized. The spine mobility is estimated through visual and tactile experience of end-user (Fig. 12). The readers get the first expression of a book by opening and scrolling it. End-users can handle a book in different ways, which can lead to its worn out appearance. Therefore, it is not enough to choose a suitable paper grade with optimal binding capacity, but designers must choose appropriate paper "toughness" to withstand adverse conditions of book handling. Moreover, preferable paper cohesive features must contribute to creating an apex arch on a book spine. Cohesiveness features come from optimal paper drape capacity, which ensures a balanced shape of a book spine. The formed apex arch on a book spine must provide the ability of the pages to lie one on top of the other without loads.

The highest drape capacity showed sample  $A_5 170^{CP}$ , followed by  $A_5 150^{CP}$ ,  $B_5 150^{CP}$ ,  $A_5 135^{CP}$  and  $B_5 135^{CP}$ . Each of

them resists falling naturally onto adjacent pages in a bound book. Moreover, the additional force is necessary for a book to get fully open into the reading position without its self-closing. It is very important to emphasize that getting a full bound book opening is hard to achieve with perfect binding style, especially with A5 format size samples which include higher paper grammages respectively ( $170^{CP} > 150^{CP} > 135^{CP}$ ). In addition, by increasing potential paper energy the book spine mobility is reduced, which immediately leads to forming the higher apex arch. Unfortunately, in such conditions flexible PUR hotmelt cannot neutralize or compensate stress on a book spine.



Figure 13 Perfect bound book appearance depends on a book format size (A5 format, B5 format, square format)

The optimal book spine mobility is shown in the samples respectively  $A_5 115^{CP}$  followed by  $B_5 115^{CP}$ ,  $A_5 90^{CP}$  and  $B_5 90^{CP}$ . From previously mentioned, preferable opening behaviour of bound book is noticed in book format size samples A5 and B5. Moreover, paper grammage reduction leads to a good balanced book spine shape including a minimal apex arch ( $B_5 90^{CP} \geq A_5 90^{CP} > B_5 115^{CP} \geq A_5 115^{CP} > B_5 135^{CP}$ ). Because of flexible PUR hotmelt, book pages can fall naturally onto adjacent, while a lower potential paper energy contributes to its favourable visual and tactile performances.

On the other hand, the square format size samples ( $SQ 90^{CP}$ ,  $SQ 115^{CP}$ ,  $SQ 135^{CP}$ ,  $SQ 150^{CP}$ ,  $SQ 170^{CP}$ ) showed preferable opening behaviour, although paper cohesive features had no effect on the apex arch formation. The formed round book spine shape is the result of huge dimensions ( $310 \times 310$  mm) of Perfect bound book. For that reason, the balanced book shape of spine cannot be achieved.

## 5 CONCLUSIONS

An optimal adhesive bound book performance can be achieved by appropriate perfect binding manufacturing, in which a chosen book engineering concept contributes to its durability and binding efficiency at the same time. Moreover, its functional performances should satisfy end-users' expectations.

In this research, the novel approaches to book designing that contribute to maximum utilization of technological capacities were given. Moreover, they follow perfect (adhesive) binding standardized procedures ISO 16763 within Standards Framework of graphic arts industry ISO/TC 130. Comprehensive binding capacity of standardized paper grades (EN643:2001), including their specific drape features, should help designers in realization of bound book concepts with hotmelts. Moreover, they must be able to cope with technological bindery practices which ultimately lead to perfect (adhesive) binding style efficiency. The binding and drape capacity depends on cohesive attributes of standardized paper grades. Paper compression and extension abilities refer to its bending stiffness. These novel approaches ensure higher-level usability of a book by choosing appropriate drape features, including various grammages of the same paper grade. In addition, this advanced approach leads to satisfactory book spine appearance, in which book pages fall freely to the cover. Because the favourable paper drape features, the created apex arch on book spine ensures a balanced spine shape. Moreover, the flexible PUR hotmelt can compensate more stress on a book spine only if a designer finds out appropriate paper sheet cohesive attributes, which are the best ones in the same paper rank. Fiber resources and other paper ingredients affect its structure formation and cohesiveness. Therefore, the paper sheet cohesive attributes need to provide desirable binding strength quality level and at the same time show preferable performances to bending well, in accordance with standardized guidelines for perfect (adhesive) binding style.

The research proves enhancing performances of bound book with hotmelt in conditions when the layered fiber network structure is denser on the top surface and its central part of standardized paper sheet. Moreover, the cohesive attributes are additionally boosted by paper surface multi-layered coatings which stabilize drape performances and form a balanced book spine shape. In such conditions, the book is able to retain and return in previous position without damage. In addition, the research confirms that a square format gives a favourable book spine appearance regardless of the paper stiffness increase.

Considering the longer bookshelf-life, a designer should steer towards tailoring paper cohesive features in order to optimize the visual-tactile bound book appearance and not only its strength level quality or book durability. Therefore, designers should rely on previous practical knowledge which is connected to current experience and prior comprehensive binding knowledge. Moreover, constructing a great number of bound book prototypes help them to understand paper cohesive features and to cope with problems. The awareness of book designing concepts creates new advanced sustainable approaches and strategies on how to meet the bookbinders' expectations in accordance with technical and technological bindery aspects.

A future perspective in bindery sector should rely on designer superiority in making decisions which are based on background practical experiences (handmaking prototypes) in determining book purpose importance. Moreover, designers should be able to juggle easily with various

standardized paper grades and their grammages in accordance with the standardized bindery framework.

## 6 REFERENCES

- [1] Clark, T. (1994). *Bookbinding with adhesive*. London, UK: McGraw-Hill Book Company Europe.
- [2] Mesaroš, F. (1985). *Tipografski priručnik*. Zagreb, Grafički obrazovni centar: Viša Grafička škola. (In Croatian)
- [3] Pasanec Preprotić, S., Vukoje, M., Petković, G., & Rožić, M. (2022). Sustainable approach to book designing concepts in bindery sector: An overview. *Proceedings of the 11<sup>th</sup> International Symposium on Graphic Engineering and Design GRID 2022*, 629-645. <https://doi.org/10.24867/GRID-2022-p69>
- [4] Kipphan, H. (2001). *Handbook of Print Media*. Berlin, Germany: Springer-Verlag Berlin, 806-837. <https://doi.org/10.1007/978-3-540-29900-4>
- [5] Knysh, O., Rehei, I., Ternytskii, S., Kandiak, N., & Behen, P. (2021). Experimental researches of book blocks spine processing by cylindrical milling cutter during perfect binding. *Australian Journal of Mechanical Engineering*, 19(3), 347-355. <https://doi.org/10.1080/14484846.2019.1625102>
- [6] Dasović, E., Petković, G., & Pasanec Preprotić, S. (2015). Bookbinding Design and Its Future in the E-book World. *Technical Journal*, 9(4), 440-445. <https://hrcak.srce.hr/149763>
- [7] Speth, R. (2022). What is Product Design? International design foundation. Retrieved from <https://www.interaction-design.org/literature/topics/product-design>
- [8] Holik, H. (2013). *Handbook of Paper and Board*. Ravensburg, Germany: Wiley-VCH Verlag GmbH & Co. KGaA. <https://doi.org/10.1002/9783527652495>
- [9] Bracić, M. (2017). Utjecaj krutosti papira na kvalitetu bešavne forme s PUR ljepljivom. *Master thesis*, University of Zagreb, Faculty of Graphic Arts, 48-60. (In Croatian)
- [10] Pasanec Preprotić, S., Jurečić, D., Babić, D., & Lajić, B. (2010). Important factors of paperback books quality of adhesion strength in adhesive binding. *Proceedings of the 21<sup>st</sup> International DAAAM Symposium "Intelligent Manufacturing & Automation: Focus on Interdisciplinary Solutions"*, 0953-0954.
- [11] Pasanec Preprotić, S., Babić, D., & Tuzović, A. (2011). Vrednovanje kvalitete slijepljenog spoja obzirom na fizikalna svojstva papira. *Proceedings of the 2<sup>nd</sup> International GeTID Symposium Graphic technology and design*, 106-113.
- [12] Petrović, M., Pasanec Preprotić, S. & Majnarić, I. (2012). Paperback Block Spine Stiffness proposition. *Proceedings of the 16<sup>th</sup> International Conference on Print, Design and Graphic Communication Blaž Baromić 2012*, 262-272.
- [13] Pasanec Preprotić, S. & Jakovljević, M. (2013). Influence of high grades paper properties on adhesive binding strength in a humid condition. *Proceedings of the 11<sup>th</sup> Symposium on Graphic Arts, Conference Proceedings University of Pardubice, Department of Graphic Arts and Photophysics*, 144-150.
- [14] Pasanec Preprotić, S., Babić, D., & Tuzović, A. (2012). Research on adhesive joint strength dependency on loose leaf position in a text block. *Technical Gazette*, 19(1), 43-49. Retrieved from <https://hrcak.srce.hr/79156>
- [15] Pasanec Preprotić, S., Budimir, I., & Lajić, B. (2012). The Bulky Paper Properties Influence on the Adhesive Bond Strength. *Material Testing*, 54(4), 271-279. <https://doi.org/10.3139/120.110329>
- [16] Niskanen, K. (2008). *Paper Physics: Book 16*. Helsinki, FIN: Finnish Paper Engineers' Association/Paper ja Puu Oy.

- [17] Reference Manual (2022). IGGESUND Paperboard. Retrieved from <https://www.iggesund.com/globalassets/iggesund/services/knowledge/iam/reference-manual/rm-pdf----full-sections---en/reference-manual-baseboard-physical-properties.pdf>
- [18] Jermann, P. (2008). Reflection on Book Structure-Part 3 Spine Control, 1-17. Retrieved from [https://moam.info/reflections-on-book-structures-part-3-temper-productions\\_5a02e8691723dd94d76b1bd2.html](https://moam.info/reflections-on-book-structures-part-3-temper-productions_5a02e8691723dd94d76b1bd2.html)
- [19] Seo, Y. B. (2002). New Concept of Stiffness Improvement in Paper and Board. *Journal of Korea Technical Association of the Pulp and Paper Industry* 34(5), 63-69. Retrieved from file:///C:/Users/Suzana/Downloads/New\_Concept\_of\_Stiffness\_Improvement\_in\_Paper\_and\_.pdf
- [20] Roylance, D., McElroy, P., & McGarry, F. (1980). Viscoelastic properties of paper. *Fibre Science and Technology*, 13(6), 411-421. [https://doi.org/10.1016/0015-0568\(80\)90032-9](https://doi.org/10.1016/0015-0568(80)90032-9)
- [21] Roberts, J.C. (1996). *The chemistry of paper*. Cambridge, UK: Cambridge: Royal Society of Chemistry. <https://doi.org/10.1007/978-94-011-0605-4>
- [22] Sixta, H. (2006). *Handbook of Pulp*. Cambridge, Germany: Ravensburg: WILEY-VCH Verlag GmbH & Co. KGaA. <https://doi.org/10.1002/9783527619887>
- [23] Plazonić, I., Barbarić-Mikočević, Ž., & Džimbeg-Malčić, V. (2015). Optical stability of office papers treated with cocamidopropyl betaine. *Wood Research*, 60(2), 263-272. Retrieved from [https://www.researchgate.net/publication/282982912\\_Optical\\_stability\\_of\\_office\\_papers\\_treated\\_with\\_cocamidopropyl\\_betaine](https://www.researchgate.net/publication/282982912_Optical_stability_of_office_papers_treated_with_cocamidopropyl_betaine)
- [24] Maurer, H. W. & Kearney, R. L. (1998). Opportunities and Challenges for Starch in the Paper Industry. *Starch*, 50(9), 396-402. [https://doi.org/10.1002/\(SICI\)1521-379X\(199809\)50:9<396::AID-STAR396>3.0.CO;2-8](https://doi.org/10.1002/(SICI)1521-379X(199809)50:9<396::AID-STAR396>3.0.CO;2-8)
- [25] Lee, H.L., I., Shin, J. & Koh, C.H. (2002). Surface sizing with cationic starch: Its effect on paper quality and papermaking process. *Tappi Journal*, 1(3), 34-40. Retrieved from [https://www.researchgate.net/publication/280887077\\_Surface\\_sizing\\_with\\_cationic\\_starch\\_Its\\_effect\\_on\\_paper\\_quality\\_and\\_papermaking\\_process](https://www.researchgate.net/publication/280887077_Surface_sizing_with_cationic_starch_Its_effect_on_paper_quality_and_papermaking_process)
- [26] Hubbe, M. A. & Gill, R. A. (2016). Fillers for Papermaking: A Review of their Properties, Usage Practices, and their Mechanistic Role. *BioResources*, 11(1), 2886-2963. <https://doi.org/10.15376/biores.11.1.2886-2963>
- [27] GardaGloss Art (2022, September 25). Technical specifications Retrieved from [https://cmspro.lecta.com/coated\\_paper/LectaProductDocuments/GardaGloss%20Art\\_EN.pdf?rev=2022289](https://cmspro.lecta.com/coated_paper/LectaProductDocuments/GardaGloss%20Art_EN.pdf?rev=2022289)
- [28] Technomelt (2022, October 25). Technical Data Sheet TECHNOMELT PUR 3317 BR Known as Purmelt QR 3317 BR April-2013 Retrieved from [https://www.van-asperen.nl/userdata/file/TECHNOMELT\\_PUR\\_3317\\_BR\\_known\\_as\\_Purmelt\\_QR\\_3317\\_BR-EN.pdf](https://www.van-asperen.nl/userdata/file/TECHNOMELT_PUR_3317_BR_known_as_Purmelt_QR_3317_BR-EN.pdf)
- [29] Pasanec Preprotić, S., Vukoje, M., Petković, G., & Rožić, M. (2023). Novel Approaches to Enhancing Sustainable Adhesive System Solutions in Contemporary Book Binding: An Overview. *Heritage*, 6(1), 628-646. <https://doi.org/10.3390/heritage6010033>

**Authors' contacts:**

**Suzana Pasanec Preprotić**, PhD, Associate Professor  
(Corresponding author)  
Department of bookbinding and packaging,  
Faculty of Graphic Arts, University of Zagreb,  
Getaldićeva 2, 10000 Zagreb, Croatia  
Tel.: +385 (0)1 23 71 080  
[spasanec@grf.hr](mailto:spasanec@grf.hr)

**Gorana Petković**, PhD, Senior Research Assistant  
Department of bookbinding and packaging,  
Faculty of Graphic Arts, University of Zagreb,  
Getaldićeva 2, 10000 Zagreb, Croatia  
Tel.: +385 (0)1 23 71 080  
[gorana.petkovic@grf.unizg.hr](mailto:gorana.petkovic@grf.unizg.hr)

**Mario Bracić** mag. ing., Graduated Student  
Department of bookbinding and packaging,  
Faculty of Graphic Arts, University of Zagreb,  
Getaldićeva 2, 10000 Zagreb, Croatia  
[mario@fram.ba](mailto:mario@fram.ba)

**Ana Marošević Dolovski**, Scientific Researcher  
Department of bookbinding and packaging,  
Faculty of Graphic Arts, University of Zagreb,  
Getaldićeva 2, 10000 Zagreb, Croatia  
Tel.: +385 (0)1 23 71 080  
[amarosevicdolovski@grf.hr](mailto:amarosevicdolovski@grf.hr)

# Application of the Functional Flow Diagrams in a Design of the Level Crossing Hydraulic Barrier Drive

Mirko Karakašić\*, Ilija Svalina, Daniel Novoselović, Iva Samardžić, Hrvoje Glavaš, Radomir Đokić

**Abstract:** In a domain of a safety increasing of railway and road traffic, hydraulic barrier drives installed at level crossings have an important role. Frequent traffic accidents at level crossings, involving road vehicles and trains, are result of inappropriately equipped level crossings with signalling and safety equipment. Limited use of hydraulic barrier drives is the result of complicated adaptation in the process of implementing such systems to the existing infrastructure of some of the equipment manufacturers and railway operators. Hydraulic barrier drive PBH21, which uses a modular architecture, was developed and designed in this paper. Applying modular design principles and functional modeling methods, using functional flow diagrams, PBH21 has ability to adapt on the technologies and infrastructures of other major manufacturers of such equipment within EU countries and other countries in the world that have developed railway infrastructure. Due to the protection of certain design solutions from competition, certain details are not presented in this paper.

**Keywords:** functional modeling; hydraulic barrier drive; level crossing; modular design; technical systems; traffic safety

## 1 INTRODUCTION

Railway market can be divided into four segments: infrastructure, vehicles, maintenance and signal-safety equipment [1]. According to [1], hydraulic barrier drives in railway traffic belong to the category of signalling-safety equipment. Their importance and significance is reflected in safety increasing of the rail and road traffic participants.

According to the Law on Safety and Interoperability of the Railway System [2], the railway system of the Republic of Croatia is divided into structural subsystems and

functional subsystems. Structural subsystems consist of building subsystems, electric power subsystems, traffic-control and signal-safety subsystems on the railway, traffic-control and signal-safety subsystems on vehicles and vehicles. Railway equipment for safety, management and trains supervision was included on the traffic-control and signal-safety subsystems. Therefore, hydraulic barrier drives belong to the mentioned subsystem. Functional subsystems consist of traffic maintenance, development and management, as well as telematics applications for passenger and freight traffic.

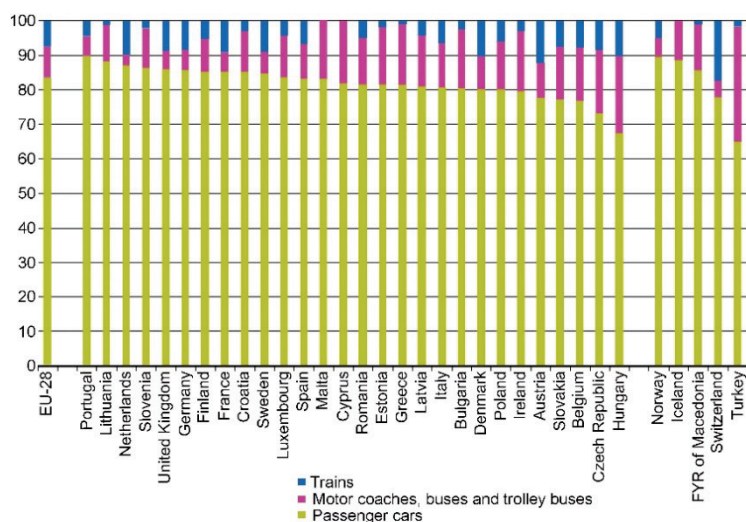


Figure 1 Share of rail traffic of EU-28 member states [3]

### 1.1 Rail Traffic Analysis in the EU and the Republic of Croatia

Rail transport takes an important role in the overall European transport sector. However, compared to the share of the private cars use, it lags behind significantly. According to [3], the share of passenger transport by train, between 2004 and 2016, was around 6,7% in the EU-28 member states. In Croatia, that number was smaller and was about 3% (Fig. 1).

For the same period, the share of passenger car use in EU-28 member states ranged from 83% to 83,7%. In Croatia, that number was around 85%. This data indicates that the share of train travel was lower in Croatia compared to EU-28 member states, that is, less importance is given to the importance of train travel.

An analysis of the railway transport of goods in the period from 1995 to 2014 shows its growth until 2007 [4, 5]. Then came the world economic crisis, which was reflected in

the drop in traffic until 2009. In the period from 2009 to 2014, there was a recovery and growth in rail transport of goods in the EU member states, which was over 400 billion tons per kilometer [4, 5]. This increase is continued until the 2018, and then there was a decrease, which in the second half of the 2020 was 400 billion tones per kilometer (Fig. 2). Then there is a recovery, i.e. an increase of transport of goods (Fig. 2).

In the passenger rail traffic there is a trend of constant growth with a smaller decline during the duration of the global economic crisis [4, 5]. During the outbreak of the pandemic caused by the corona virus, there is a sudden drop in passenger transport. Recovery is visible in the second half of the 2020 (Fig. 2).

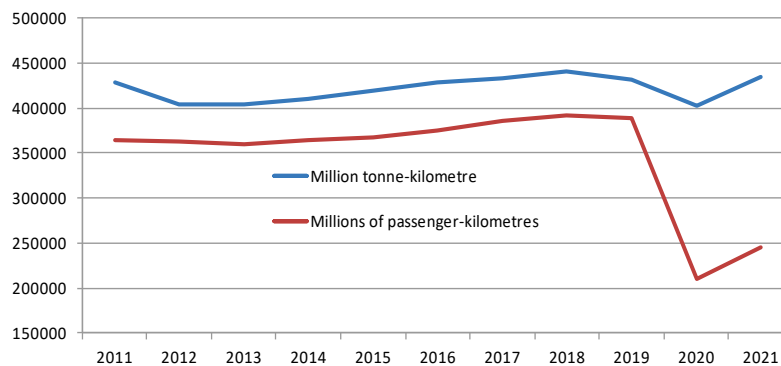


Figure 2 Movement of goods and passengers in EU countries for the period from 2011 to 2021 [6, 7]

Railway transport of goods in the Republic of Croatia had its own growth until 2007 [5, 8, 9]. Then it reached its maximum value, which was 16000000 tons [5, 8, 9]. As a result of the world economic crisis, it falls. The downward trend continued in the years to come, and in the second half of the 2013 the rail transport of goods amounted to 2000000 tons (Fig. 3). In the following years, there is an increase in

the transport of goods (Fig. 3). In the period from 1996 to 2008, passenger rail traffic in the Republic of Croatia grew [5, 8, 9]. The peak was reached in 2009, when it amounted to 7000000 passengers [5, 8, 9]. Then there was a continuous decline, and in the first half of the 2020, the number of passengers was 5000000 (Fig. 3). Then there is an increase in passenger transport in the second half of the 2020 (Fig. 3).

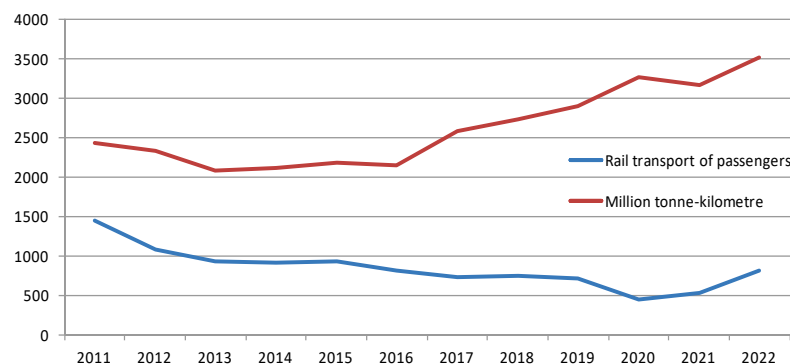


Figure 3 Movement of goods and passengers in the Republic of Croatia for the period from 2011 to 2021 [6, 7]

A well-developed and branched railway transport network is an important factor in the economic growth and integration of an individual country. The length of the transport network of the EU-28 countries is 217081 km [10]. Comparing the length of the railway network with countries such as the USA (203200 km), Japan (19200 km), China (121000 km), Russia (86000 km) and India (64600 km), the EU-28 countries have the longest railway network [10]. Despite the above, the length of the railway network of the EU-28 countries decreased by 20590 km from 1990 to 2016. The reasons should be sought in the dominance of road traffic in relation to rail traffic, which according to [10], dominates in the EU-28 countries with a ratio of 4,13.

Although a small country, Croatia has an important role in the European transport system, and is located on two

corridors of the basic EU transport network. Therefore, Croatia has an important role as part of the European strategy of creating a single transport market, that is, a single European market that the EU is aiming for. Railway network of the Republic of Croatia (Fig. 4), according to the data of the Croatian Bureau of Statistics, was 2604 km in 2015 [9]. According to [4], quality of the railway infrastructure in the Republic of Croatia is significantly lower than the EU average. Therefore, modernization of the railway infrastructure and increasing of the safety of railway transport is imperative for the Republic of Croatia.

Through the analysis of the current state of the market, conducted by Altpro d.o.o. [11], three problems of the European railway system were observed. The first problem relates to the dependence of railway operators on specific

technologies of dominant manufacturers. Multinational companies such as Alstom, Siemens, Thales, Ansaldo and Bombardier dominate in the development of the safety equipment in the segment of rail transport. Mentioned companies are not interested in the production of safety equipment that would be compatible with the equipment of the other manufacturers. Mentioned companies in the target markets want to completely replace the found existing equipment with their own equipment. Another problem relates to the fragmentation of the national railway systems. In this sense, there are 20 national signal-safety systems in the European countries. Each of these systems has its own specific requirements and norms. Because of this, cross-border rail traffic is disrupted. The third problem relates to

the level of security, which is insufficiently represented [3, 4]. One of the main reasons for the low level of safety stems from insufficient investment in railway infrastructure. Low-quality maintenance of the railway infrastructure is also one of the causes of the decrease in reliability and safety in railway traffic. Problem of reliability, quality and safety of the railway infrastructure is particularly pronounced in the countries of Eastern Europe [12]. Low level of safety is partly from the limited use of signal-safety devices in railway traffic. The Law on Safety and Interoperability of the Railway System [2] prescribes importance and significance of railway traffic safety in the Republic of Croatia. The law emphasizes the need to install and use signal-safety equipment along railroad tracks and level crossings.



Figure 4 Railway network in the Republic of Croatia

Importance and advantage of rail transport for the further economic development of EU countries is also indicated by the initiative undertaken by the European Commission to further encourage the development of a single European transport area. Significant progress has been made in the area of the 4th Railway Package, Blue Belt initiatives for maritime transport, proposed Single European Sky II, EU Aviation Strategy and NAIADES Program for inland waterways [12].

Railway transport has a significant number of advantages compared to other types of land transport (primarily road transport). First of all, speed of traffic, comfort for passengers, economy in medium and long distance cargo transport and significantly lower energy consumption than road transport [12].

If the impact of EU transport on greenhouse gas emissions is taken into account, then a quarter of greenhouse

gas emissions are derived from transport. In accordance with the need to reduce the impact of greenhouse gases, rail transport has a less harmful impact on the environment compared to other types of transport. Thus, over 70% of greenhouse gas emissions are produced by road traffic. Railway traffic emitted 0,6% of greenhouse gases (Fig. 5). Therefore gas emission from vehicles have significant influence on global warming and energy consumption [13,

14]. Analysing the share of total energy consumption, according to types of transport, railway traffic accounts for 1,6%. For the sake of comparison, road traffic accounts for 73,4% of the total energy consumption (Fig. 5). This is a very important indicator, which gives rail traffic, especially in the part of freight (goods) transportation, a comparative advantage compared to road freight transport and fits into the strategy of the European Green Plan [15].

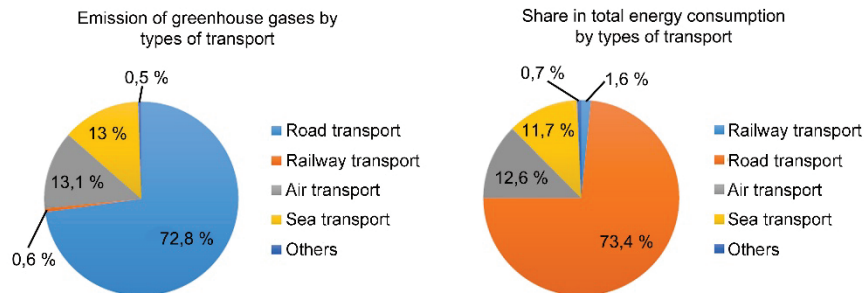


Figure 5 Influence of the type of transport within the EU on the emission of greenhouse gases and energy consumption, [5, 16]

In accordance with the conducted market analysis and the EU initiative for the greatest possible investment in the development of railway transport, the need for the development of safety equipment is indicated. Therefore, development and design of a new hydraulic barrier (semi-bumper) PBH21 was presented in this paper. Main purpose of this system is to secure level crossings. This is important from the aspect of the proper functioning of transport system, especially from the aspect to achieve the highest level of reliability at any stage of the transport process [17]. The system was designed with an emphasis on fulfilling the requirement to have a SIL4 (TYPE A) safety certificate according to the EN 17020 standard [18]. The PBH21 hydraulic barrier was developed to fulfil one of the main design requirements, which implies fulfilment most of the international standards and technical specifications of the individual countries for which the PBH21 is designed. Therefore, the principles of modular design were used in the development and design of this technical system. The system has a modular architecture that allows it to be adapted to the found existing infrastructure in the individual countries for which the system was designed. In this way, the reduced dependence of railway operators on the specific technologies of the dominant manufacturers was achieved. Using the method of the functional modelling of the technical systems, by using functional flow diagrams, modular functional structure of the hydraulic barrier PBH21 was developed. From the modular functional structure, in detail design phase, individual module of hydraulic barrier drive PBH21 was designed.

## 2 METHODS AND METHODOLOGY

Design process of a new product is a complex activity that uses methods and tools developed within the design theories [19-24] that aim to produce artifacts that fulfil the user's requirements by performing their functions. Artifacts according to [19] represent technical systems that are

connected to their environment through inputs and outputs, that is, they transform input sizes into output sizes. The sizes that are transformed can be grouped into three categories. These categories are energy, material and signal (information). Pahl and Beitz divided design process into the four phases: clarification and task definition, conceptual design, embodiment design and detail design [20]. Each phase transfers activities between them, which are connected with each other by information.

If the process analysis is observed within a specific functional structure of an individual technical system, then by monitoring of the energy, material and signal flow is possible to connect individual functions through the functional flow diagrams [25]. This approach is called functional modelling and is used in the design phase [26]. Solution of the conceptual design phase was shown through the functional structure. This solution does not depend on the final form of the design. Functional models represent basis for searching of working principles and working structures that are solutions of the partial and overall functions [27].

Design process in the development and design of new artefacts also uses modular design method. According to [28], a module represents an independent building block of a more complex technical system. Each module is connected with other elements of that complex technical system by loose connections. In embodiment and detail design, modules are physical structures that fully match with the functional structures [29]. According to [20], modular design enables connection of design elements into the structures from which different variants of technical systems can be designed. Stone [30] develops methods for extracting modules from a functional structure using module heuristics. With such methods, modules are identified from functional models.

In this paper, authors modeled functional models of the hydraulic barrier drive PBH21, which were described through the functional flow diagrams, and grouped them into the functional modules. Connections between functional modules are made through input and output flows of energy, material and signal. Thus, in the conceptual design phase, by realizing of the connection between the functional modules,

achieved connection between the working principles. Such working principles in the embodiment and detailed design represent modules of a certain more complex technical system. This approach through the design of the functional modules and their connection via flows enables a systematic approach in a design of the design modules from the functional structures.

After the previously described methods used in the development and design of the hydraulic barrier drive, research methodology and the structure of the paper are listed in the rest of this chapter. The necessary descriptive and technical data about the new hydraulic barrier drive PBH21 device, for the purposes of writing this paper, were collected by performing various activities during its development. This development period is divided into a two phases. First phase consists of industrial research for the development of the PBH21 prototype and a second phase consists of its experimental development. Research and analysis of the market trends was included in the first phase. In this phase, implementation of a barrier drive at railway-road crossings, was included. Also, as a final output, requirements were structured as an input to the design process of the new hydraulic barrier drive PBH21. Analysis of the market trends is described in the Introduction section. In the second phase, by applying of the functional decomposition method, was included selection of the design methods and the design of the functional structure. Also, in the second phase, tests of the prototype version of the hydraulic barrier drive device were carried out in laboratory and real working conditions. Obtained results of these tests are not presented in this paper. In the Requirement list and function decomposition section, general list of requirements and functional models of the four

modules of hydraulic barrier drive PBH21 are presented. Developed functional models served as a starting point for finding of the working principles of the module solutions and designing of the modular structure of the hydraulic barrier drive PBH21. Final design solution of the hydraulic barrier drive PBH21 is described in the section Design solution of the hydraulic barrier drive PBH21. Presented hydraulic barrier drive PBH21 was developed and designed by Altpro d.o.o. within the EU project "Center of Competences for Advanced Engineering Nova Gradiška CEKOM NI NG (KK.01.2.2.03.0011)".

### 3 REQUIREMENT LIST AND FUNCTIONAL DECOMPOSITION

#### 3.1 Requirements for Design of Hydraulic Barrier Drive PBH21

Development of the hydraulic barrier drive PBH21, which belongs to the category of signaling and safety equipment, complies with the prescribed norms in the domain of technical, operational and regulatory standards. During development process of the device, requirements in the field of communication security standards, standards for hardware, vibrations, temperature, electromagnetic compatibility and standards for infrastructure compatibility have been fulfilled. In the development of the device, requirements arising from the EU guidelines for the development of the trans-European transport network and directives of the European Commission on the technical specification for interoperability related to the traffic-control and signal-safety subsystems have been implemented.

**Table 1** General requirements list for hydraulic barrier drive PBH21

No.	Requirements	No.	Requirements
1	Safety requirements	4	Exploitative requirements
1.1	fulfilment of safety certificate SIL4 (TIP A)	4.1	Life cycle > 30 years
2	Design requirements	4.2	reliable operation
2.1	modular design	4.3	operation possibility at low / high temperatures (-30° to 70°)
2.2	operability by barrier arm up to 12 m long	4.4	operation in an atmosphere with a high moisture content
2.3	possibility of implementation on the existing operator infrastructure	4.5	supplying system with electricity
2.4	universal specification platform	5	Maintenance
2.5	generic design	5.1	simple installation of components
2.6	standardized components use	5.2	simple configuration according to customer requirements
2.7	drive unit - electric motor	5.3	simple operation with device
3	Technological requirements	5.4	simple assembly / disassembly
3.1	independent technological solution	5.5	reduce total number of maintenance intervals
3.2	compatible hardware interface	6	Costs
3.3	use materials of next - generation in production process	6.1	cheaper maintenance
3.4	simpler production	6.2	lower operating costs of device

Independent technological solution is an extremely important requirement that the hydraulic barrier drive PBH21 should fulfill. This requirement arises from a need for a long lifecycle of devices in the railway industry (over 30 years). Equipment that does not depend on the manufacturer and that can be used with equipment from other manufacturers should protect customer from the disappearance of a certain manufacturer from the market and in this way affects on the longer lifecycle of the device.

Application principles of generic design should allow replacement of existing technology with any technology that should developed in the future. Also through the generic

design, it should be possible more easily adapt system to the specific specifications of a particular market. Hardware interface of the barrier drive needs to be compatible with all types of peripheral units due to the requirement for interoperability and compatibility with products of other manufacturers.

A general overview of the basic design requirements that needs to fulfill a new hydraulic barrier drive PBH21 is collected in Tab. 1. These requirements are determined and defined at the beginning of the design process, and in accordance with them, development of the hydraulic barrier drive PBH21 began. Requirements are divided into six

categories: safety requirements, design requirements, technological requirements, exploitative requirements, maintenance requirements and cost requirements.

### 3.2 Functional Model of Hydraulic Barrier Drive PBH21

Barrier drive is a part of Level Crossing Protection System (LCPS) outdoor elements. This device, when train approaches, increases safety of all traffic participants (road vehicles and train). Device physically prevent passage over level crossing for all road vehicles when LC is switched-on. This is also the main purpose of hydraulic barrier drive PBH21.

After analysing requirement list and determining main purpose of the device, functional model of hydraulic barrier drive PBH21 was established. "Black box" is the starting

point for the functional structure of the overall function of hydraulic barrier drive. Overall function of the hydraulic barrier drive is to *"Make impossible to cross the level crossing by lowering of the barrier arm"*. A functional flow diagram is used to present a functional model of the barrier drive overall function. By monitoring of the energy, material and signal flow, a connection between partial functions within the functional model is realized. Functional structure, applying functional decomposition method, is divided into four functional levels. On the first level, there is the overall function of the hydraulic barrier drive PBH21. Second level consists of the overall functions of the modules, which are using modular design, implemented in the design structure of hydraulic barrier drive PBH21. Third and fourth level of the functional structure, represent partial functions that shape overall functions of an individual module.

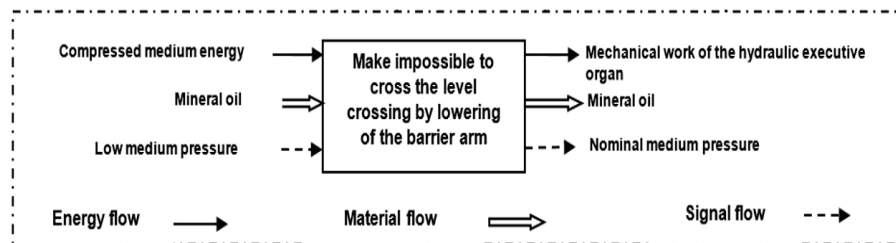


Figure 6 Functional model "black box" at the first level of the functional structure

Overall functional model of the hydraulic barrier drive at the first level of the functional structure is shown in Fig. 6. Energy flow at the input to the function is achieved through the energy of the compressed medium, that is, energy stored in the mineral oil under pressure. Through the transformation action of the overall function on the energy of the compressed medium, mechanical work of the hydraulic executive organ is achieved at the output of the function. Material flow is realized using mineral oil, as a medium used in the hydraulic system of the hydraulic barrier drive. At the first level of the functional structure, signal flow is realized by monitoring of the medium pressure at the input and output of the overall function.

Modular design principles were applied in the design of the hydraulic barrier drive. Therefore, second level of the functional structure consists of the overall functions of the modules, which are connected by energy, material and signal flows. Overall functions of the second level form main module group, which consists of four modules: Module 1, Module 2, Module 3 and Module 4 (Fig. 7).

Module 1 functional flow diagram consists of three levels of the functional structure. First level consists of the overall function *"Compress medium to the nominal pressure and supply system with the medium"*. Since the functional structure of the hydraulic barrier drive has four functional levels, functional structure of Module 1 starts from the second level of the functional structure of the hydraulic barrier drive. This means that the overall function of the Module 1 is on the second level of the functional structure of the hydraulic barrier drive. Other partial functions of the Module 1 are located on the third and fourth level of the functional structure of the hydraulic barrier drive (Fig. 8).

Functional structure of Module 1 uses six partial functions that solve overall function of the Module 1 by transforming energy, material and signal. When the hydraulic barrier drive is putted into operation, electrical energy supplied from the electrical network is transformed into the energy of the compressed medium. Mineral oil is used as a medium that needs to be stored in a tank, compressed to nominal pressure and used to manipulate with the barrier arm. By monitoring the signal flow, amount of the medium in the tank is controlled, as well as the pressure state of the mineral oil stored in the Module 1 system. Monitoring of these two conditions is achieved using sensors for detecting amount of the medium and a manometer for a pressure measuring. After generated functional structure of the Module 1, a Hydraulic aggregate group is working principle that represents solution of the functional structure of the Module 1 (Fig. 13 and Fig. 14).

Functional structure of Module 2, by process of functional decomposition, is divided into three levels. If the functional structure of Module 2 is viewed as a separate module, then on the first level the overall function is *"Store energy of the compressed medium"*. Since the functional structure of Module 2 is part of the functional structure of the hydraulic barrier drive, within this structure, the overall function of Module 2 is on the second level (Fig. 9). Therefore, partial functions of Module 2 are located on the third and fourth level of the functional structure of the hydraulic barrier drive. Overall function of Module 2 uses five partial functions that transform energy, materials and signal (Fig. 9).

With the start-up of the hydraulic barrier drive, electrical energy of the overall function of Module 1 is transformed

into the energy of the compressed medium. Due to the action of the overall function of Module 2, this energy remains unchanged. Mineral oil flow, due to the action of the overall function of Module 2, also remains unchanged. By monitoring of the signal flow, it can be seen that at the input to the overall function of Module 2, signal corresponds to the output signal of the overall function of Module 1 (Fig. 8, Fig. 9). Due to the action of the overall function of Module 2, two

signals are present at the output of the function: nominal medium pressure and medium flow (Fig. 9). Nominal pressure represents medium working pressure in the hydraulic system of the device. After generated functional structure of the Module 2, accumulator group is working principle that represents solution of the functional structure of the Module 2 (Fig. 13 and Fig. 14).

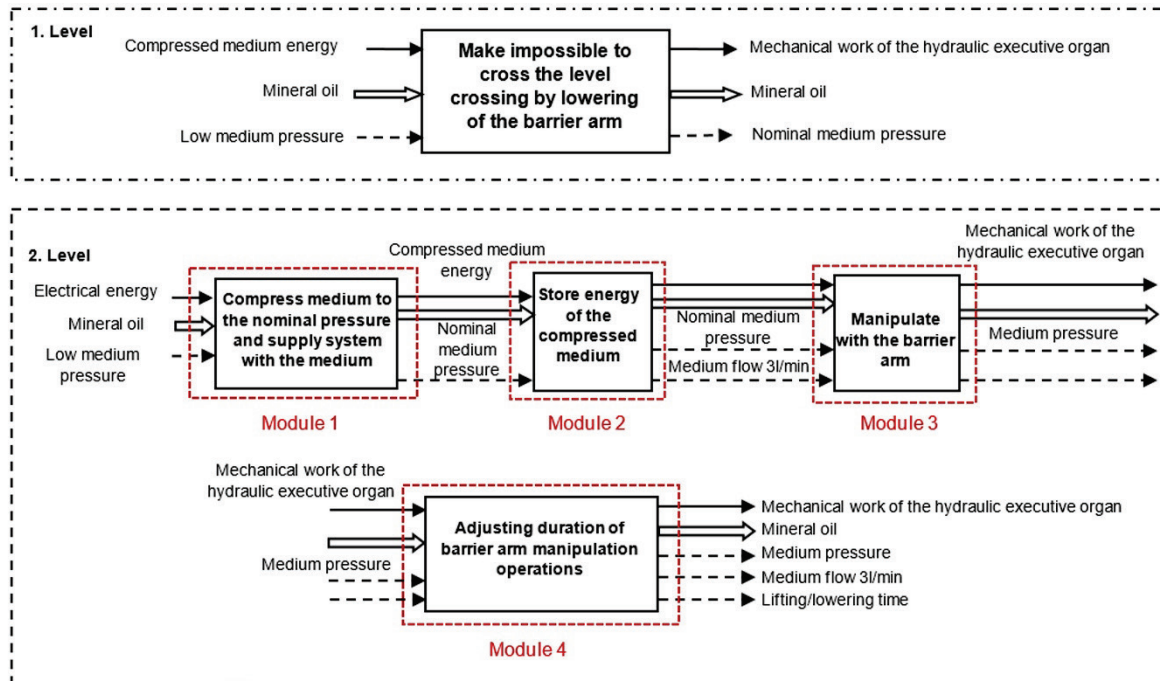


Figure 7 Functional flow diagram at the second level of the functional structure

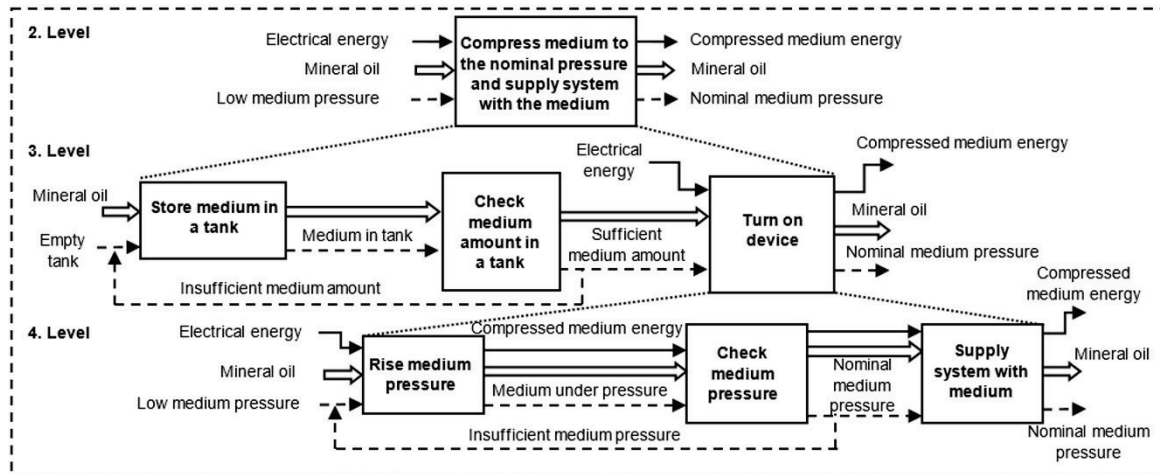


Figure 8 Module 1 functional flow diagram

Functional flow diagram of Module 3 describes functional structure on three levels. On the first level is overall function "Manipulate with the barrier arm". Other partial functions of Module 3 are located on the third and fourth level of the functional structure of the hydraulic barrier drive (Fig. 10). Functional structure of Module 3 uses seven partial functions that solve overall function of Module 3 by transforming energy, material and signal. Functions "Lower

barrier arm" and "Raise barrier arm" transform the energy of the compressed medium into the mechanical work of the hydraulic executive organ. In a case of the system electricity supply interruption or a failure occurrence, manipulation of the barrier arm lowering and of the barrier arm raising is possible to achieve by the action of the operator (human). Therefore, functions "Lower barrier arm" and "Raise barrier arm", by functional decomposition, generate partial

functions "Manually lower barrier arm" and "Manually raise barrier arm" (Fig. 10). These two functions, through the action of the operator, use the energy of human work, which they transform into mechanical work. This work performs

lowering and raising of the barrier arm. Module 3, as the working principle, represents solution of the functional structure. This module, after detail design process, represents valve block module (Fig. 13 and Fig. 14).

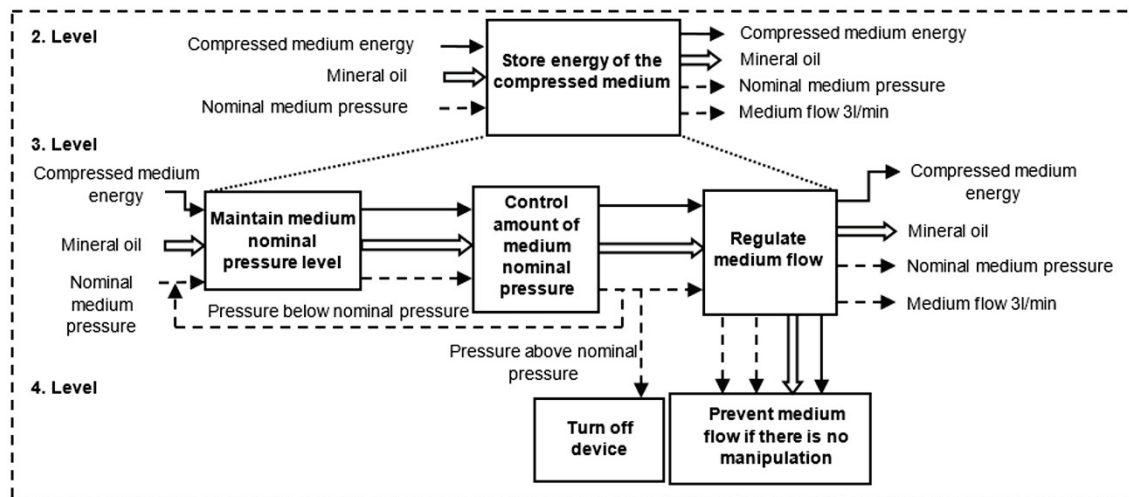


Figure 9 Module 2 functional flow diagram

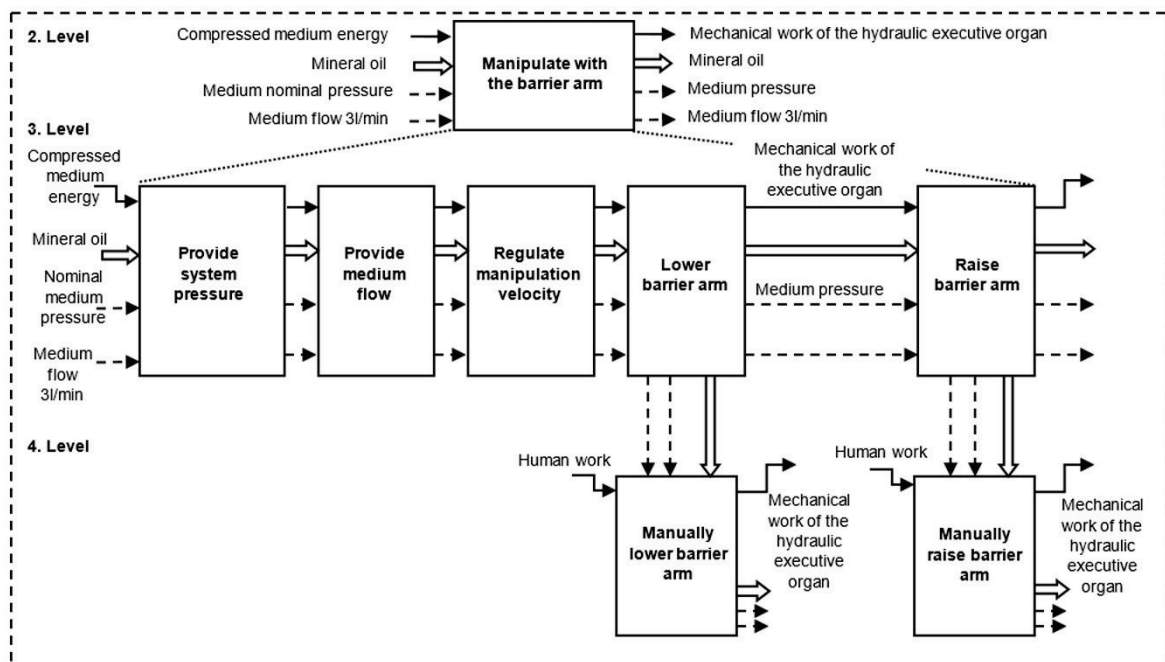


Figure 10 Module 3 functional flow diagram

Functional structure of Module 4 is described on two levels (Fig. 11). On the first level is overall function "Adjusting duration of barrier arm manipulation operations". Four partial functions that solve this overall function are located on the second level of the functional structure of the Module 4, i.e. on the third level of the functional structure of the hydraulic barrier drive. Input to the overall function contains two signals: medium pressure and medium flow 3 l/min (Fig. 11). By transforming of these signals, a third signal is generated at the output of the overall

function, i.e. raising / lowering time of the barrier arm (Fig. 11).

Partial function "Setting duration of the manipulation operation" at its input includes additional energy flow described through the human work. Through this function, operator has ability to adjust duration of the barrier arm raising and lowering operations, via the control panel of the device. After generated functional structure of the Module 4, slow motion valves is a working principle that represents solution of the functional structure of the Module 4 (Fig. 13 and Fig. 14).

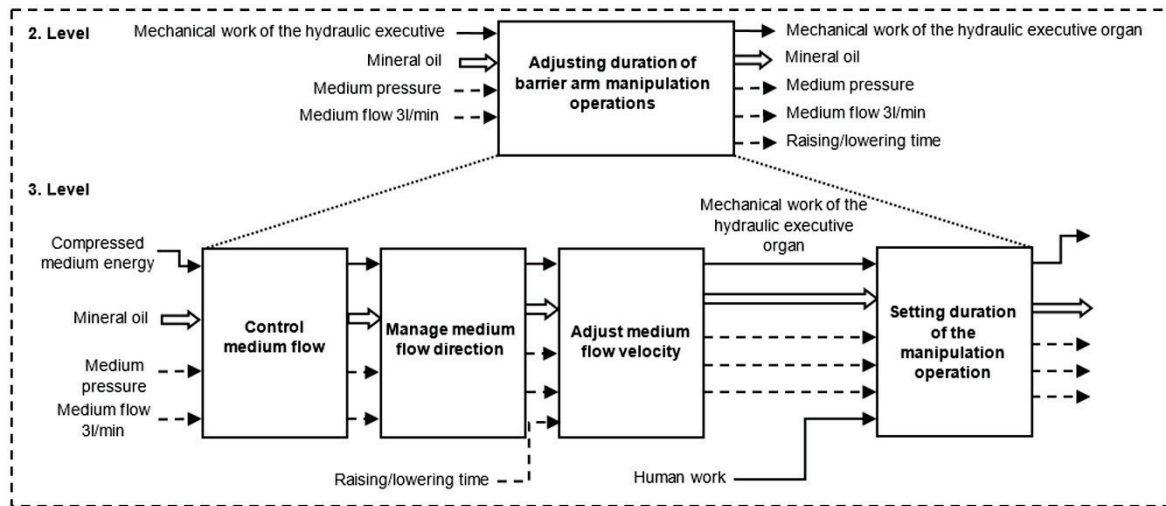


Figure 11 Module 4 functional flow diagram

#### 4 DESIGN SOLUTION OF THE HYDRAULIC BARRIER DRIVE PBH21

Barrier drive PBH21 (Fig. 12), developed by Altpro d.o.o., is made as hydraulic type. By the process of functional decomposition, through the monitoring of the energy, material and signal flow, mineral oil is selected as a drive medium of the hydraulic system (Fig. 6 and Fig. 7). For arm rising and lowering, it uses hydraulic drive with a two-way hydraulic cylinder as executive element. In a failure occurrence, it is possible manually to control device, using a main valve block system. For that matter, operator uses combination of manually activated / deactivated valves and moves barrier arm by hand (Fig. 10).

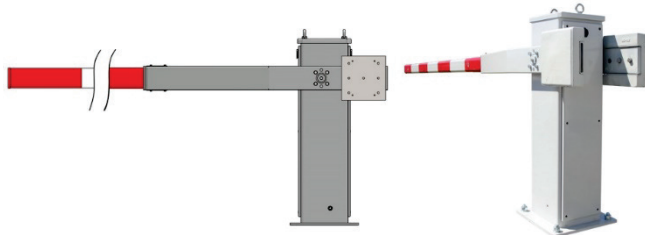


Figure 12 Barrier drive PBH21 [31]

Hydraulic barrier drive PBH21 is developed by modular design. Main system consists of sub-systems. These sub-systems in modular design represent modules. Modular architecture implemented in PBH21 product is suitable for adaptive design and easier maintenance process. Barrier drive is structured from six modules (Fig. 13). These modules is possible to divide in main module group and additional module group. Modules as accumulator group, hydraulic aggregate, slow motion valves and valve block represent main module group (Fig. 14). This group is an executive group, because it realizes by their functions, overall function of the technical system PBH21 (Fig. 6 and Fig. 7). Functional analysis, through the functional flow diagrams, preceded to

the development of the mentioned modules (Fig. 6 – Fig. 11). Electric parts module and positioning group micro switches module are part of the additional module group (Fig. 13). This group is control / management group, because it manages signals and information necessary to perform overall function of the technical system PBH21.

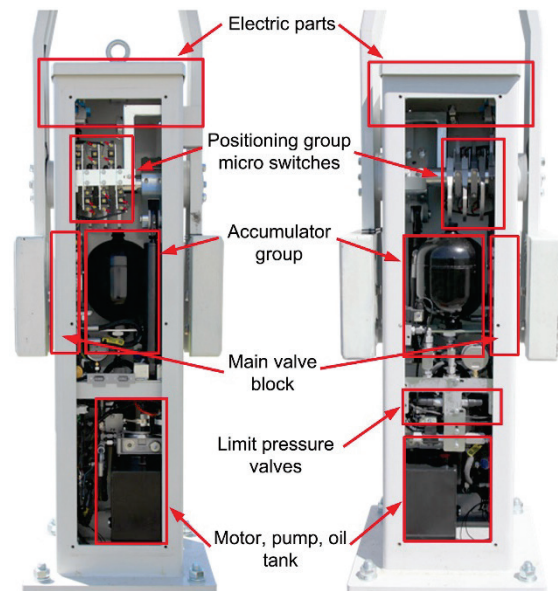


Figure 13 Barrier drive PBH21 modular architecture [31]

Principles of solution of the partial functions of Module 1, Module 2, Module 3 and Module 4 are part of the design structure of the hydraulic barrier drive. As such, they are actively involved in the energy, material and signal flow. Their fulfillment of partial functions is shown by the hydraulic scheme (Fig. 14). Scheme shows medium flow (mineral oil) through the elements that make main modules as well as manipulation operations in the executive part of the scheme.

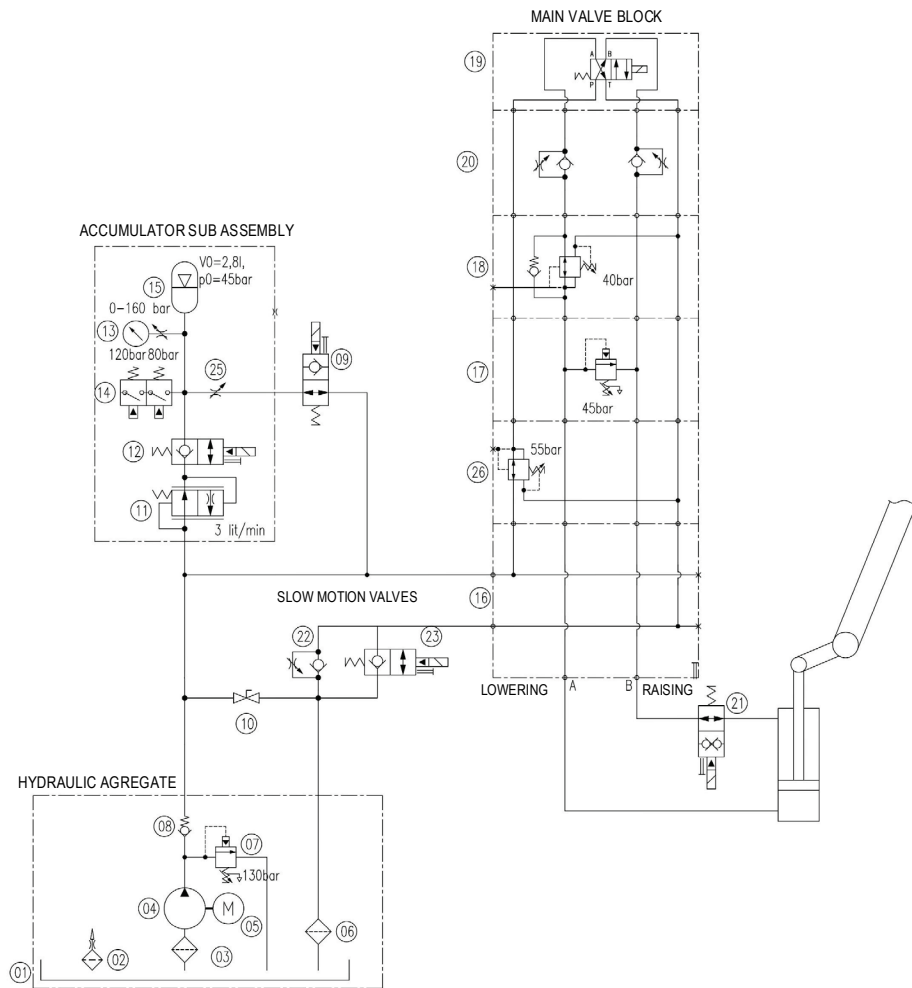


Figure 14 PBH21 hydraulic scheme with the four main module groups [31]

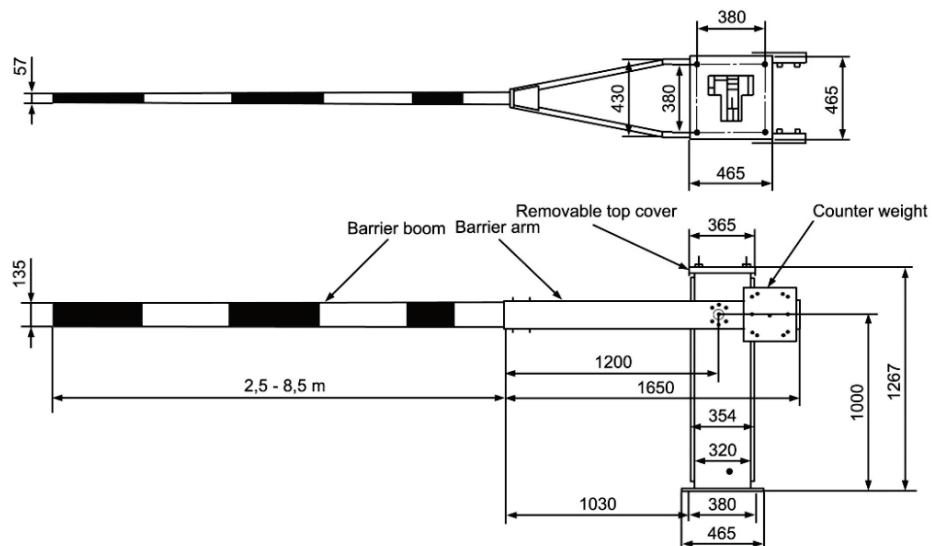


Figure 15 Top and side view of the PBH21 [31]

General measurements of the PBH21 are presented in Fig. 15. On the hydraulic barrier drive PBH21, according to customer requirement, is possible to install arm length from 2,5 m to 8,5 m. According to selected arm lengths is

necessary to calculate adequate counterweight. All calculations are made in correlation with the weight positioning from the center of the shaft to the weight gravity center (Fig. 15).

## 5 RECAPITULATION ANNOTATION

Importance of railway transport in the development of modern world economies is extremely great. EU countries recognized this and decided to invest significantly in the modernization of their railway infrastructure, i.e. rail traffic. Special advantage of rail transport, compared to other forms of transport, is reflected in the economy of freight transport, lower energy consumption and less impact on greenhouse gas emissions caused by transport.

Therefore, it is extremely important to invest in safety increasing of the rail transport. In order to reduce traffic accidents occurring at level crossings, the need for an increase in signaling and safety equipment was observed. Such equipment also includes hydraulic barrier drives. Due to the complicated adaptation on the existing infrastructure of manufacturers of such equipment, as well as the different needs of railway operators, these devices are not installed at all level crossings. In order to solve this deficiency, in this paper is presented development and design of a hydraulic barrier drive PBH21 that have possibility of implementation on existing infrastructure. PBH21 is compatible with the existing infrastructures and technologies of major manufacturers of this type of safety equipment in the world. This device uses a modular design to be able to adapt on the aforementioned requirements.

By applying functional modeling, functional structure of the PBH21 was generated. Through the monitoring and analyzing of the energy, material and signal flow, by functional flow diagrams, overall and partial functions of the four functional modules were designed. Using functional decomposition, for the mentioned modules, a four-level functional structure of the hydraulic barrier drive is modeled. From the functional structure of the hydraulic barrier drive PBH21, in a detailed design process, following modules were designed: accumulator group, hydraulic aggregate, slow motion valves and valve block.

Through this work, the sequence of the design process is presented by connecting four design phases, respectively clarification and task definition phase, conceptual design phase, embodiment design phase and detail design phase. Also, it is presented that by means of the functional decomposition method and functional modeling method, by using of functional flow diagrams, is possible to design functional structures of modules and connect them through the flow of energy, material and signal in one unique modular functional structure.

## Acknowledgments

Authors express their thanks to the partner and major coordinator of the EU project "Center of Competences for Advanced Engineering Nova Gradiška CEKOM NI NG (KK.01.2.2.03.0011)", who supported, enabled and participated in the implementation of the research presented in this paper. Within this project, a company Altpro d.o.o., which together with the Faculty of Mechanical Engineering of the University of Slavonski Brod, is one of the partners of the aforementioned project, has designed and developed a

hydraulic barrier drive PBH21 for level crossings, presented in this paper. Authors express their thanks to the Altpro d.o.o. for enabling and allowing presentation of the certain design solutions of the hydraulic barrier drive PBH21. Also, authors express their thanks to Mirela Brechelmacher, mag. ing. mech., who helped in the analysis of the railway traffic market trends.

## 6 REFERENCES

- [1] Mignot, A. Ed. (2016). *Railway Standardization Strategy Europe*. UIC-ETF, Paris. [https://uic.org/europe/IMG/pdf/rail\\_standardisation\\_strategy\\_europe\\_light.pdf](https://uic.org/europe/IMG/pdf/rail_standardisation_strategy_europe_light.pdf)
- [2] NN 63/2020. (2020). *Zakon o sigurnosti i interoperabilnosti željezničkog sustava*. Narodne novine, Zagreb. (in Croatian)
- [3] (2019). Eurostat 2019.27.06 Passenger transport statistics.
- [4] European Commission. (2016). *EU Transport in figures: Statistical Pocketbook 2016*. Luxemburg: Publications Office of the European Union.
- [5] Armanda, J. (2017). *Analiza utjecaja razvoja prometne infrastrukture EU na prometnu infrastrukturu RH*. Undergraduate thesis, University of Split, Faculty of economics Split, Croatia. (in Croatian)
- [6] Eurostat Statistics Explained. (2023). Railway freight transport statistics. [https://ec.europa.eu/eurostat/statistics-explained/index.php?title=Railway\\_freight\\_transport\\_statistics](https://ec.europa.eu/eurostat/statistics-explained/index.php?title=Railway_freight_transport_statistics)
- [7] Eurostat Statistics Explained. (2023). Railway passenger transport statistics – quarterly and annual data. [https://ec.europa.eu/eurostat/statistics-explained/index.php?title=Railway\\_passenger\\_transport\\_statistics\\_-\\_quarterly\\_and\\_annual\\_data](https://ec.europa.eu/eurostat/statistics-explained/index.php?title=Railway_passenger_transport_statistics_-_quarterly_and_annual_data)
- [8] Statistical Yearbook of the Republic of Croatia. Croatian Bureau of Statistics, 2010, Zagreb, Croatia, ISSN 1333-3305
- [9] Statistical Yearbook of the Republic of Croatia. Croatian Bureau of Statistics, 2016, Zagreb, Croatia, ISSN 1333-3305
- [10] Pupavac, D., Baković, I., & Knežević, J. (2019). Tržište željezničkog teretnog prijevoza Europske unije. *Željeznice 21*, 18(1), 7-13. <https://hrcak.srce.hr/256745> (in Croatian)
- [11] Altpro. (2023, May 28). <https://altpro.com/hr/>
- [12] European Commission. (2019). Transport in the European Union: Current Trends and Issues. European Commission, Directorate-General Mobility and Transport, Brussels.
- [13] Skrucany, T., Semanova, S., Milojević, S., & Ašonja, A. (2019). New Technologies Improving Aerodynamic Properties of Freight Vehicles. *Applied Engineering Letters*, 4(2), 48-54. <https://doi.org/10.18485/aeletters.2019.4.2.2>
- [14] Petrović, N., Bojović, N., Marinković, D., Jovanović, V., & Milanović, S. (2023). A Two-Phase Model for the Evaluation of Urbanization Impacts on Carbon Dioxide Emissions from Transport in the European Union. *Tehnčki vjesnik*, 30(2), 514-520. <https://doi.org/10.17559/TV-20221018103946>
- [15] European Commission. (2023). Delivering the European Green Deal. [https://commission.europa.eu/strategy-and-policy/priorities-2019-2024/european-green-deal/delivering-european-green-deal\\_en](https://commission.europa.eu/strategy-and-policy/priorities-2019-2024/european-green-deal/delivering-european-green-deal_en)
- [16] European Commission. (2023). Reducing Emissions from Transport: A European Strategy for Low – emission Mobility. [https://ec.europa.eu/clima/policies/transport\\_hr](https://ec.europa.eu/clima/policies/transport_hr)
- [17] Brkić, R., Adamović, Ž., & Bukvić, M. (2022). Modeling of Reliability and Availability of Data Transmission in Railway System. *Advanced Engineering Letters*, 1(4), 136-141. <https://doi.org/10.46793/adeletters.2022.1.4.3>
- [18] ISO/IEC 17020:2012. (2013). Inspection Standard Application Document. NATA, Australia.

- [19] Hubka, V. & Eder, W. E. (1988). *Theory of Technical Systems – A Total Concept Theory for Engineering Design*. Springer – Verlag Berlin Heidelberg, Germany.  
<https://doi.org/10.1007/978-3-642-52121-8>
- [20] Pahl, G., Beitz, W., Feldhusen, J., & Grote, K.-H. (2007). *Engineering Design: A Systematic Approach*. London: Springer. <https://doi.org/10.1007/978-1-84628-319-2>
- [21] Blessing, L. & Chakrabarty, A. (2009). *DRM, a Design Research Methodology*. Springer-Verlag London.  
<https://doi.org/10.1007/978-1-84882-587-1>
- [22] Suh, N. (2001). *Axiomatic Design: Advances and Applications*. Oxford University Press, New York.
- [23] Ulrich, K. T. & Eppinger, S. D. (2004). *Product design and development*. New York: 3rd Edition, McGraw-Hill.
- [24] Tomiyama, T., Gu, P., Y. Jin D., Lutters, D., Kind, Ch., & Kimura, F. (2009). Design methodologies: Industrial and educational applications. *CIRP Annals - Manufacturing Technology*, 58, 543-565.  
<https://doi.org/10.1016/j.cirp.2009.09.003>
- [25] Bojcetic, N., Valjak, F., Flegaric, S., & Storga, M. (2020). Application for Product Functional Model Creation. *Tehnički vjesnik*, 27(3), 883-890.  
<https://doi.org/10.17559/TV-20190923203841>
- [26] Patel, A., Kramer, W., Summers, J. D., & Shuffler-Porter, M. (2016). Function Modeling: A Study of Sequential Model Completion Based on Count and Chaining of Functions. *Proceedings of the 28<sup>th</sup> International Conference on Design Theory and Methodology*, 1-11.  
<https://doi.org/10.1115/DETC2016-59860>
- [27] Nagel, R. L., Stone, R. B., Hutcheson, R. S., McAdams, D. A., & Donndelinger J. A. (2009). Function Design Framework (FDF): Integrated Process and Function Modeling for Complex Systems. *International Design Engineering Technical Conferences and Computers and Information in Engineering Conference*, 273-286. <https://doi.org/10.1115/DETC2008-49369>
- [28] Hölttä-Otto, K. (2005). Modular product platform design. *Doctoral Dissertation*, Helsinki University of Technology, Department of Mechanical Engineering, Machine Design, TKK Dissertations 10, Espoo.
- [29] Ericsson, A. & Erixon, G. (1999). *Controlling Design Variants: Modular Product Platforms*. Society of Manufacturing Engineers, Dearborn, MI.
- [30] Stone, R. B., Wood, K. L., & Crawford, R. H. (2000). A heuristic method for identifying modules for product architectures. *Design Studies*, 21(1), 5-31.  
[https://doi.org/10.1016/S0142-694X\(99\)00003-4](https://doi.org/10.1016/S0142-694X(99)00003-4)
- [31] User manual PBH21. Altpro, 2021.

#### Authors' contacts:

**Mirko Karakašić**, Full professor, PhD  
(Corresponding author)  
University of Slavonski Brod, Mechanical Engineering Faculty in Slavonski Brod,  
Trg Ivane Brlić-Mažuranić 2, 35000 Slavonski Brod, Croatia  
E-mail: mirko.karakasic@unisb.hr

**Ilija Svalina**, Assistant professor, PhD  
University of Slavonski Brod, Mechanical Engineering Faculty in Slavonski Brod,  
Trg Ivane Brlić-Mažuranić 2, 35000 Slavonski Brod, Croatia  
E-mail: isvalina@unisb.hr

**Daniel Novoselović**, Associate professor, PhD  
University of Slavonski Brod, Mechanical Engineering Faculty in Slavonski Brod,  
Trg Ivane Brlić-Mažuranić 2, 35000 Slavonski Brod, Croatia  
E-mail: dnovoselovic@unisb.hr

**Iva Samardžić**, mag. ing. mech.  
University of Slavonski Brod, Mechanical Engineering Faculty in Slavonski Brod,  
Trg Ivane Brlić-Mažuranić 2, 35000 Slavonski Brod, Croatia  
E-mail: ivasamardzic@unisb.hr

**Hrvoje Glavaš**, Full professor, PhD  
Faculty of Electrical Engineering, Computer Science and Information Technology  
Osijek, University of Osijek,  
Kneza Trpimira 2B, 31000 Osijek, Croatia  
E-mail: hrvoje.glavas@ferit.hr

**Radomir Dokić**, Associate professor, PhD  
Faculty of Technical Sciences, University of Novi Sad,  
Trg Dositeja Obradović 6, 21102 Novi Sad, Serbia  
E-mail: djokic@uns.ac.rs

# Technologies for Web Animations and their Positive and Negative Sides Regarding Web Page Metrics

Nikolina Stanić Loknar\*, Tajana Koren Ivančević, Mateo Bekavac, Snježana Ivančić Valenko

**Abstract:** The development of web technologies has led to the availability of various multimedia content on the web. In addition to text, images, and videos, transitions, animations and interactivity are increasingly used. Transitions and animations present the content on the page in more interesting, attractive ways and can attract and retain users longer, improving the measurable parameters of page visits as well as the user experience. Animations on the web can be created in many ways. And if the animations are not executed well, they can slow down the page. The goal of this article is to compare the measurable parameters of animations created with different technologies. HTML, CSS, SVG, P5js, WebGL technologies and animations created with a 3D modeling tool were used. The article uses two different examples of animations created with different technologies and then tested on several devices.

**Keywords:** CSS; HTML; p5js; SVG; web animations; WebGL

## 1 INTRODUCTION

On today's web you can find very different web content and pages. From completely static pages to very dynamic and interactive pages. There are also pages that are fully responsive and pleasant to view and use, and those that are displayed the same on a mobile device and a desktop computer, for example. The importance of creating responsive web pages for user experience is highlighted and explained in articles [1-3]. The number of visitors, how long they stay, and whether they come back certainly depends on how the website was designed. Among other multimedia content available on the Web, there are various interactive elements, which nowadays often include transitions and animations. With them, the content stands out or is presented in a more interesting way. Animations can be triggered by themselves when the page loads, or they can be triggered by a mouse movement. They can be small and barely visible, or they can contain various graphical elements and define a large part of the content on the page. Every year there are changes and advances in the way animations are programmed and executed. From CSS animations of various HTML elements to completely new technologies that animate elements according to completely different principles. In addition to the functional animations themselves, they can also be artistic, interactive, where the visitor of the website creates a new and completely individual appearance of the website and changes the parameters of the animation. Web animations can be two-dimensional or three-dimensional. Some technologies support the third dimension of the object (HTML, CSS) and some do not (SVG). However, by combining technologies it is also possible to create a 3D SVG animation.

## 2 AN OVERVIEW OF THE HISTORICAL DEVELOPMENT OF WEB ANIMATION

Animation is the perception of motion and the illusion of change through sequences of images that differ only slightly from each other [4]. Today, there are several technologies for creating animations on web pages. Each of them has

advantages and disadvantages and the area in which it is used [5].

In the following, we describe the technologies that were used to perform the examples for the experimental part of this work.

HTML or HyperText Markup Language is a description language used to structure the web page and the content on the web page. The HTML elements are visible on the web page. An ordinary text editor (e.g., Notepad) and knowledge of the basic HTML elements are sufficient to write HTML [6]. HTML5 emphasizes simplifying the code needed to create a page that conforms to W3C standards and links CSS, JavaScript, and graphics files [7].

CSS (Cascading Style Sheet) consists of properties that define a value and is added to HTML elements. Thus, CSS is used to style the HTML elements that are displayed on the web page. CSS animations provide a lightweight solution for creating animations without the need for additional scripts. They can be controlled via CSS properties, making them relatively easy to implement. At the same time, complex and overused CSS animations that involve multiple elements or complex movements can increase page load times and rendering costs [8].

Scalable Vector Graphics (SVG) is a popular vector graphics format that provides good support for interactivity and animation [9]. With vector graphics, images are stored using mathematical formulas based on the coordinates of points and lines in a grid. This allows for significant resizing or scaling of SVG files without loss of resolution, making it ideal for creating icons and logos for websites. Scalable vector graphics are also used on websites for illustrations, 2-D and 3-D animations, interface parts, infographics and visual data representations [10]. The challenge with SVG animations is that SVG animations and interactions may not work equally well in all browsers, platforms, or versions. They may also require large resources and affect performance as they may consume a lot of CPU or GPU power. This can cause the website to lag, freeze, or crash if there are many elements [11].

WebGL or Web Graphics Library is a JavaScript API for displaying interactive 2D and 3D graphics in any compatible

web browser without using plugins [12]. The API allows users to experience interactive content on GPU-accelerated web pages without having to download or install plugins. WebGL was originally developed by Mozilla [13]. WebGL applications reside centrally on a web server and can be updated relatively easily for all users. The platform is independent of HTML and JavaScript. Some disadvantages are that the applications are slower than compiled programs whose code is translated directly into machine language and that there is no access to the full functionality of the specific platform [14].

In 2013, Lauren McCarthy developed p5.js, a native JavaScript alternative to Processing.js that is officially supported by the Processing Foundation. p5.js is a JavaScript library for creative programming, is free and open source [15]. The advantage of the JavaScript programming language is that it is available and supported everywhere. Every web browser has a built-in JavaScript interpreter, which means that p5.js programs will (usually) work in any web browser [16].

### 3 ANIMATION DESCRIPTION AND EXAMPLES

#### 3.1 Windmill

Fig. 1 shows three frames from the windmill animation. Uniform animation is achieved with a) HTML/CSS; b) SVG/CSS; c) SVG/HTML; and d) SVG technologies.

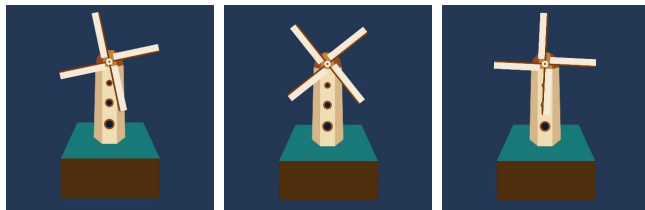


Figure 1 Three frames from 2D animations achieved by combining HTML, CSS, and SVG technologies

#### SVG/HTML, SVG

SVG Embed in HTML and SVG Standalone (.svg) are created with SVG animations. The command `<animateTransform>` was used and the transformation type is rotation. A group of 10 elements takes part in the rotation. For a group of elements that rotates, the rotation center, start angle and end angle are defined.

#### SVG/CSS

The SVG hierarchy is the same as in the previous example, but CSS was used for the animation. The `transform-origin` property defines the rotation centers for 10 animated elements. `Help @keyframes` are start and end angles defined at the beginning and end of the animation.

#### HTML/CSS

In this example, only HTML tags and CSS properties are used, and the entire model is rebuilt with div tags. As in the previous examples, only the group of 10 elements is animated, that is, the Rotor class, and the transformation parameters remain the same. An important difference in animating this example from the previous one is the need to

change the origin of the animation for the sails. The `transform-origin` property defines a new origin so that the sails rotate together around the same point.

#### 3.2 3D Animation Rotating Sphere HTML/CSS

The animation consists of 90 div elements placed in an inner and an outer container. The outer container contains perspective 1200px properties. The inner container contains animation with rotation along all three axes. At 0% animation, the rotation on all three axes is 0. At 20%, the sphere rotates 180 degrees along the *X* and *Y* axes and 10 degrees along the *Z* axis. At 50% animation, the sphere rotates 360 degrees along the *X* and *Y* axes and 45 degrees along the *Z* axis. At 100% animation, the sphere rotates 180 degrees along the *X* and *Y* axes and 0 degrees along the *Z* axis. All inner div elements (circles) are also transformed: 90 degrees along the *X* axis and for each subsequent circle 2 degrees more along the *Y* axis with a color change. The animation was created using HTML and CSS technologies only and contains 405 lines of code (internal CSS). The file weighs 9.48 KB. Fig. 2 shows 3 frames of the sphere animation.

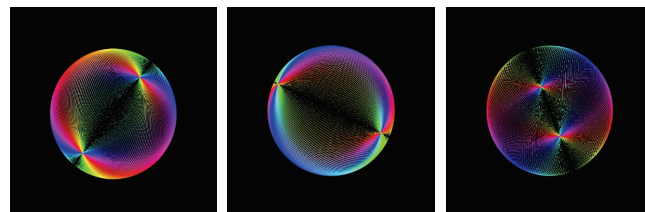


Figure 2 Three frames from a 3D sphere animation created using HTML and CSS technologies

#### 3.3 3D Animation of the Sphere using p5.js and WebGL Technologies

Animation using p5.js and WebGL technology is obviously much simpler. It uses a for loop and draws equal circles with rotation and color change. All the HTML and p5.js code consists of 34 lines of code in total. The files weigh 799 KB. Fig. 3 shows frames of a sphere animation created with HTML, p5.js and WebGL technologies.

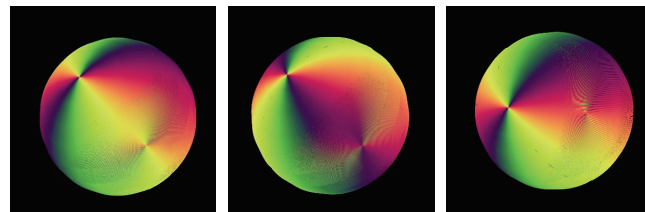


Figure 3 Three frames of a 3D sphere animation created with HTML, p5.js, and WebGL technologies

## 4 EXPERIMENTAL PART

In this research, Chrome DevTools were used to measure fps, CPU, GPU and animation load time until a stable maximum fps was reached. The devices used have the following specifications:

**DEVICE 1: Laptop Asus**

OS Name: Microsoft Windows 10 Pro  
 Version: 10.0.19045 BUILD 19045  
 System Manufacturer: Microsoft Corporation  
 System model: N76VZ  
 Processor: Intel® core (TN) i7-3630QM CPU  
 @2.40GHz, 2401 Mhz, 4 Core(s), 8 Logical Processor(s)

**DEVICE 2: Laptop Asus Zenbook**

OS Name: Microsoft Windows 11 Pro  
 Version: 10.0.22621 BUILD 22621  
 System Manufacturer: Microsoft Corporation  
 System model: Zenbook UX8402ZE\_UX8402ZE  
 Processor: 12th Gen Intel(R) core (TM) i9-12900H,  
 2500 MHz, 14 Core(s), 20 Logical Processor(s)

**DEVICE 3: Desktop HP**

OS Name: Microsoft Windows 7 Professional  
 Version: 6.1.7601 Service Pack 1 Build 7601  
 System Manufacturer: Microsoft Corporation  
 System model: HP Compaq Elite 8300 CMT  
 Processor: Intel(R) core (TM) i5-3470 CPU, 3.2 GHz,  
 3201 MHz, 4 Core(s), 4 Logical Processor(s)

**DEVICE 4: Laptop Lenovo**

OS Name: Microsoft Windows 11 Home  
 Version: 10.0.22000 Build 22000  
 System Manufacturer: Microsoft Corporation  
 System model: LAPTOP-OGQAONQO  
 Processor: AMD Ryzen 7 5700U with Radeon  
 Graphics, 1801 MHz, 8 Core(s), 16 Logical Processor  
 (s)

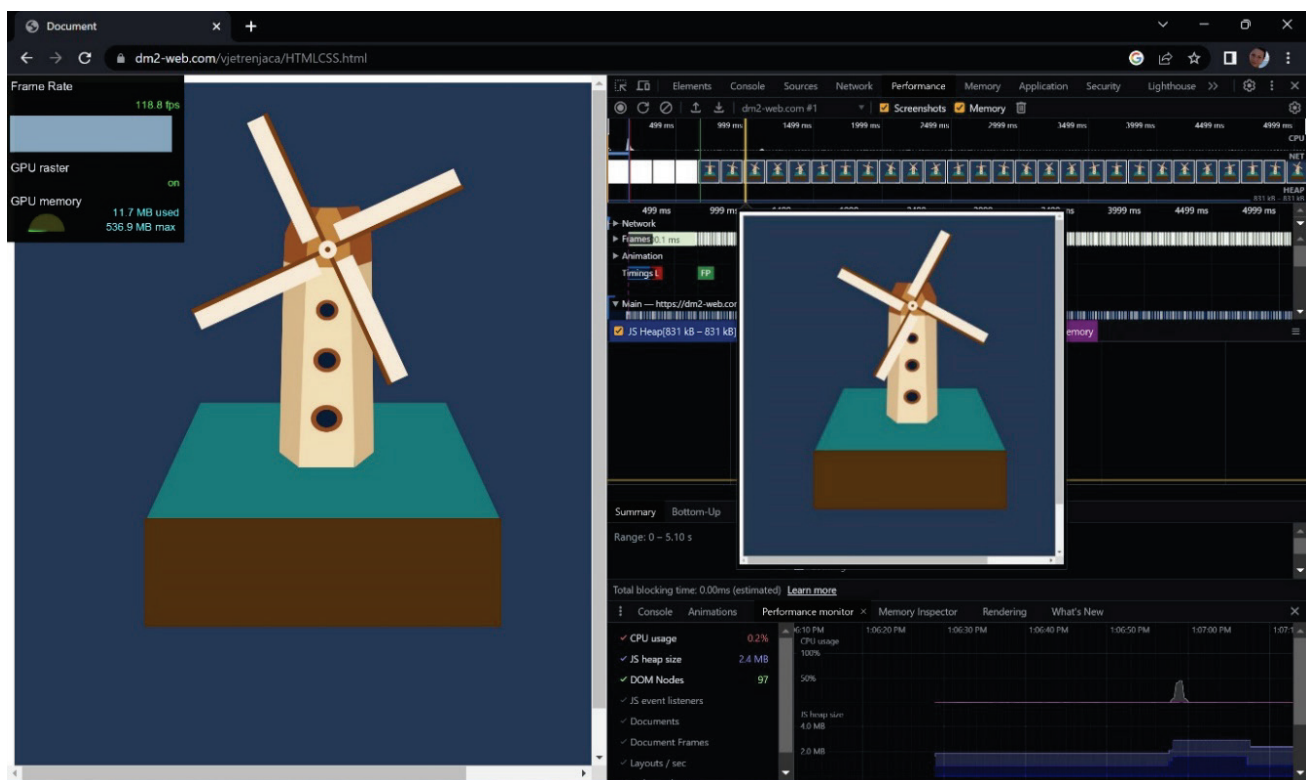


Figure 4 View of the Chrome DevTools interface from which the readings were taken

On each device, each animation was measured 10 times, and the average values were taken for the displayed results. All measurements were taken over the Eduroam network with a download speed of 155.16 Mbps and an upload speed of 154.96 Mbps. The speed was tested with the Ookla Speedtest.

#### 4.1 Measurements 2D Animation of a Windmill

HTML/CSS, SVG/CSS, SVG/HTML, and standalone SVG animations were measured on the four computers mentioned previously. Fig. 4 shows the appearance of the Chrome DevTools interface for an example of an animation created with HTML and CSS technologies.

The measurement results are presented in graphs. Fig. 5 shows the measured fps values of the individual animations on the individual devices.

The three devices performed the test of these four animations almost equally well, with a result very close to 60 fps. On device 2, the average readings are 118.8 fps for the first three animations. Only the standalone SVG animation has a slightly lower frame rate compared to the others, an average of 102.3 fps. Device 2 is the newest and most powerful computer, using an i9 processor.

The following measurement is for GPU memory usage (MB) for the four animations listed and four different devices. There are significant differences in the results of each device in this measurement. Fig. 6 shows the result of this measurement.

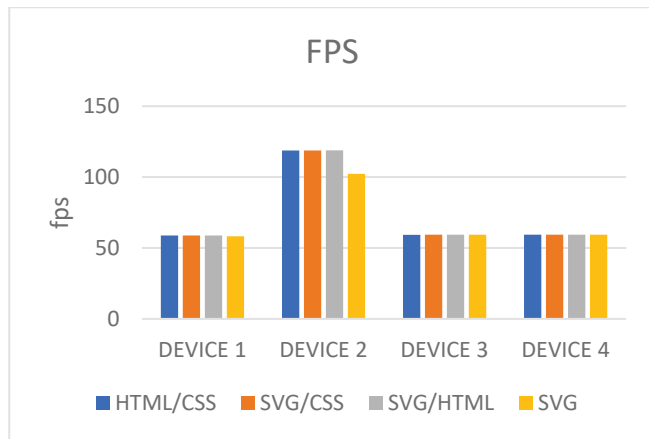


Figure 5 Measured values of frames per second of four animations on four different devices

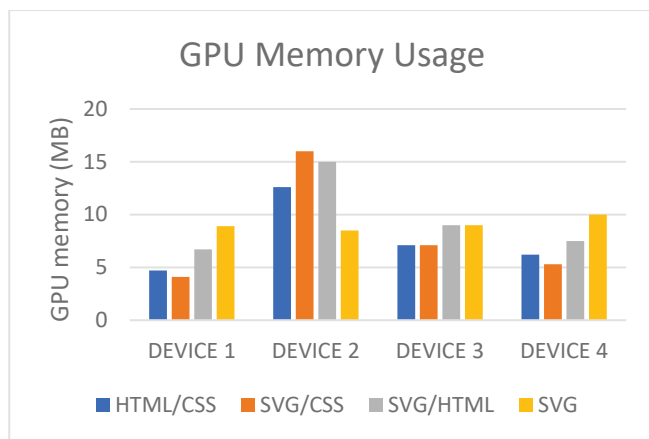


Figure 6 Shows the GPU memory usage in MB for four animations and four devices

On the three devices, GPU memory usage is lowest when performing SVG/CSS animations and highest when performing standalone SVG animations. On Device 2, the exact opposite values were measured. The highest GPU memory usage is recorded for standalone SVG animation, and the lowest for SVG/CSS animation.

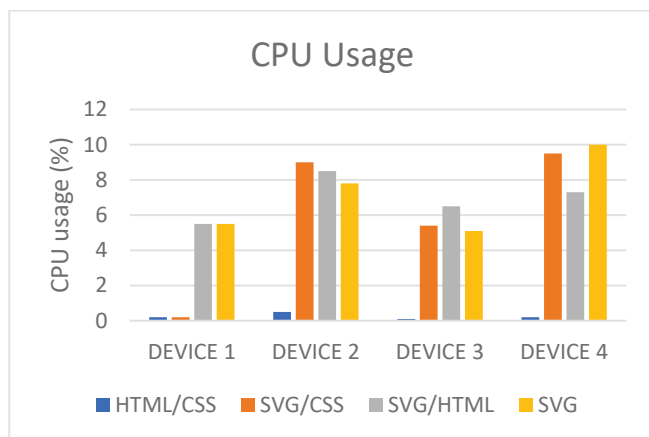


Figure 7 Measured values of CPU usage in % for four animations and four devices

The third measurement refers to the use of CPU (%). Fig. 7 shows the measured values. This graph shows that the use of CPU for HTML/CSS animations is by far the lowest on all four devices, at 0.1 and 0.5%. Other animations are measured quite colorfully on all four sites. SVG embedded in HTML and standalone SVG have the highest values.

The last measurement refers to the loading speed up to the moment when a stable maximum frame rate is reached. Fig. 8 shows the results of this measurement. The graph shows that the loading speed is highly dependent on the speed of the computer. For animations created with different technologies, different values were obtained on each computer. The HTML/CSS animation took the longest to load on two devices, the SVG/HTML animation on one, and the SVG/CSS animation on one.

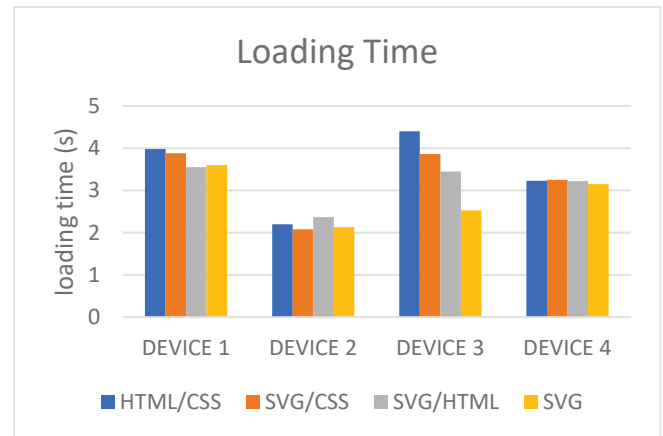


Figure 8 Animation loading speed in seconds to get a constant fps

#### 4.2 Measurements 3D Animation of the Sphere

As with the windmill animation, the same values were measured for these examples. Due to the complexity of performing animations, the differences are larger than in the previous measurements. Fig. 9 shows the appearance of the Chrome DevTools interface when measuring an example 3D animation of a sphere.

Fig. 10 shows the fps comparison of two 3D animations. One was created with HTML and CSS technologies and the other with HTML, p5.js and WebGL.

On the first and fourth devices, the animations responded the same, which is understandable since the characteristics of these two devices are quite similar. On the 2nd device, a big difference is visible in the number of fps. The HTML and CSS animation again reached almost 120 fps, while the HTML/p5.js/WebGL animation was measured just below 80 fps. Device 3 is an old desktop computer and on it these animations reached 12 and 8 fps respectively.

In the following measurement, the GPU usage values, expressed in MB, were measured for the same examples shown in Fig. 11.

When rendering HTML/CSS animations on all four devices, GPU usage is higher than when rendering HTML/p5.js/WebGL 3D sphere animation.

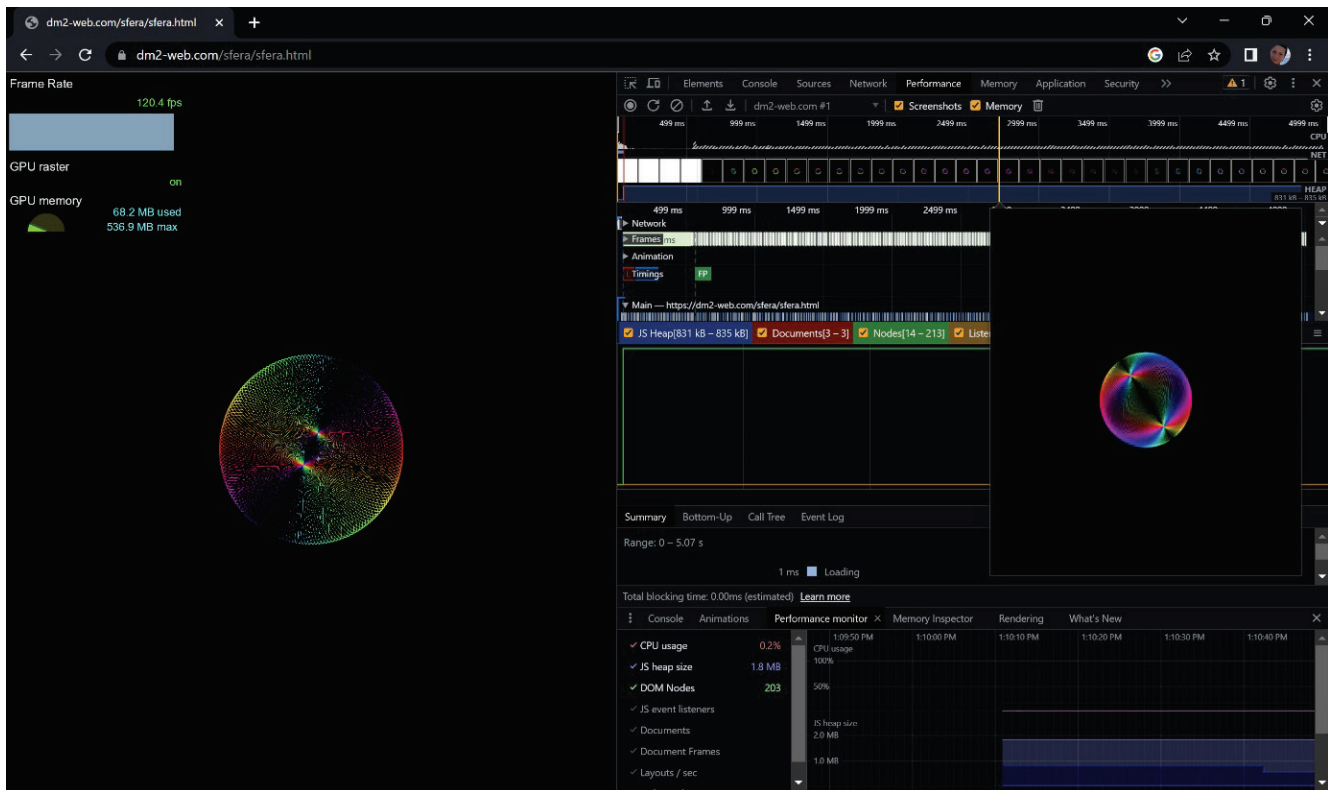


Figure 9 Chrome DevTools interface measuring a 3D sphere animation example

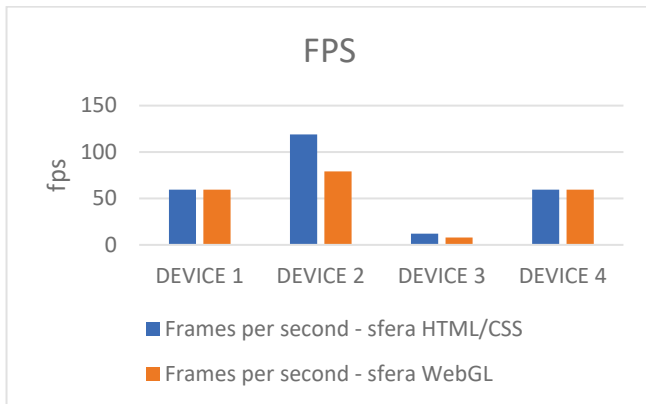


Figure 10 Comparison of measured fps of 3D animations created with HTML and CSS, and HTML, p5.js and WebGL technologies on 4 different devices

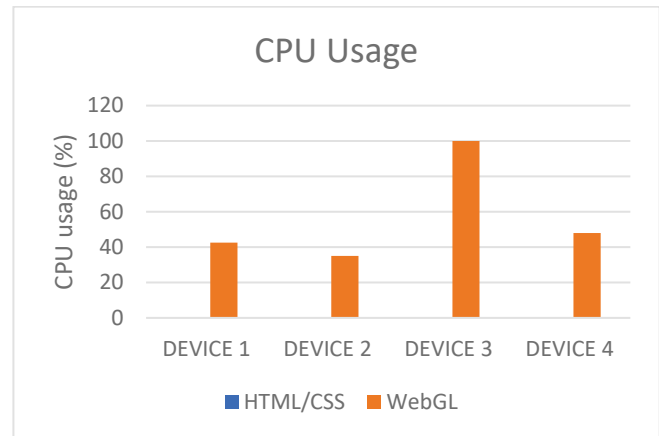


Figure 12 Comparison of measured values for CPU usage (%) for viewing 3D animations created with HTML and CSS and HTML, p5.js, and WebGL technologies on 4 different devices.

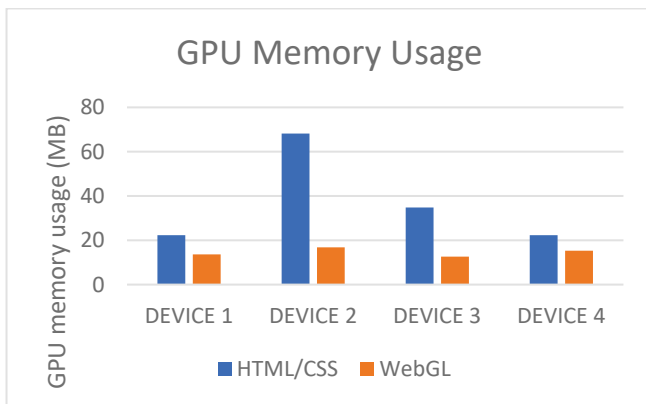
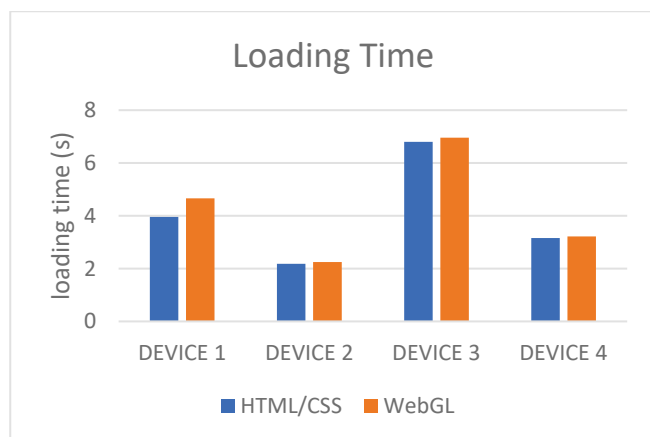


Figure 11 Comparison of measured values for GPU usage (MB) for displaying 3D animations created with HTML and CSS and HTML, p5.js and WebGL technologies on 4 different devices.

Fig. 12 shows the results of measuring the use of CPU for 3D animations. The values for the usage of HTML/CSS animations CPU range from 0 to 0.2 for all four devices. For animations created with HTML, p5.js and WebGL technologies, these values are quite high, especially for device 3 where they are 100%.

The last one, Fig. 13, shows the loading time of 3D animations until the frame rate has settled at its maximum.

Fig. 13 shows that the 3D HTML/CSS animation loaded faster on all four devices than the one created with HTML/p5.js/WebGL technologies.



**Figure 13** Comparison of measured values for the loading time of 3D animations created with HTML and CSS and HTML, p5.js and WebGL technologies on 4 different devices.

## 5 CONCLUSION

From the measurements and results, it can be concluded that the 'cleanest' animation is achieved with HTML/CSS technologies. The frame rate is very high, depending on the device. Also, there is a very big difference in the data obtained from different devices. Older devices will have a hard time playing the demanding animations and displaying them well. The animations (scenes) explored in this work were quite complicated. The 2D animation of the windmill is a scene built to simulate a 3D scene. The 3D animations of the sphere are real 3D animations. So the devices used in this work were really challenged to perform well. All the animations performed very well. The technologies used for their production really have their positive and negative sides. It is important to keep in mind that the animations should be moderate so that they do not affect the loading time of the landing page. Besides, not all users have new and very fast devices, and the network speed is also not equally fast and stable everywhere and for everyone. The performance of 3D spheres created with HTML/p5.js/WebGL technologies is somewhat disappointing. This is the area that should be explored further, as well as animation behaviour on mobile devices. The use of one technology should not exclude the other but can complement each other to achieve better results and new possibilities.

## 6 REFERENCES

- [1] Horbinski, T. & Cybulski, P. (2019). Functionality similarities of global web mapping services in the context of responsive map design. *Abstr. Int. Cartogr. Assoc.*, 1, 117. <https://doi.org/10.5194/ica-abs-1-117-2019>
- [2] Walsh, T. A., Kapfhammer, G. M., & McMin, P. (2020). Automatically identifying potential regressions in the layout of responsive web pages. *Journal of Software: Testing, Verification and Reliability*, 30(6), e1748. <https://doi.org/10.1002/stvr.1748>
- [3] Li, W., Zhou, Y., Luo, S., & Dong, Y. (2022). Design factors to improve the consistency and sustainable user experience of responsive interface design. *Sustainability*, 14(15), 9131. <https://doi.org/10.3390/su14159131>

- [4] Ferreira, M. (2017). The history of web animation. Medium. Available at: <https://medium.com/@milberferreira/the-history-of-web-animation-63b106c97fdf> (Accessed May 2023).
- [5] Crews T. B. May K. Skintik C. & South-Western Cengage Learning. (2017). Digital media: concepts and applications (Fourth). Cengage Learning. ISBN: 978-1-305-66172-1 <https://search.ebscohost.com/login.aspx?direct=true&scope=site&db=nlebk&db=nlabk&AN=2638755>. (Accessed June 2023)
- [6] W3Schools, 2021. HTML attribute reference. Available at: [https://www.w3schools.com/tags/ref\\_attributes.asp](https://www.w3schools.com/tags/ref_attributes.asp) (Accessed May 2023).
- [7] Frain, B. (2012). Responsive Web Design with HTML5 and CSS3, Packt Publishing; Illustrated edition.
- [8] Weyl, E. (2016). Transitions and animations in CSS: adding motion with CSS. Sebastopol, CA: O'Reilly Media, 6-55.
- [9] Wu, R., Su, W., Ma, K., & Liao, J. (2023). IconShop: Text-Based Vector Icon Synthesis with Autoregressive Transformers. arXiv preprint arXiv:2304.14400.
- [10] Drasner, S. (2017). SVG animations: from common UX implementations to complex responsive animation. Sebastopol, CA: O'Reilly Media, 17-19, 73-75.
- [11] Nolan D. A. & Lang D. T. (2014). Xml and web technologies for data sciences with r. Springer. <https://doi.org/10.1007/978-1-4614-7900-0>
- [12] Ivanušec, S. (2021) Ostvarivanje 3D grafike u Internet preglednicima pomoću biblioteke Three.js, University of Pula, *Master's thesis*, 2-7. (in Croatian)
- [13] WebGL, Available at: <https://www.techtarget.com/whatis/definition/WebGL> (Accessed May 2023).
- [14] <https://viscircle.de/webgl-basics-evaluation-and-examples/?lang=en> (Accessed June 2023)
- [15] 5P\*js. <https://p5js.org/> (Accessed May 2023)
- [16] <https://blog.logrocket.com/creating-animations-p5-js/> (Accessed June 2023)

### Authors' contacts:

**Nikolina Stanić Loknar**, PhD, Assist. Prof.  
(Corresponding author)  
University of Zagreb, Faculty of Graphic Arts  
Getaldićeva 2, 10 000 Zagreb, Croatia  
[nikolina.stanic.loknar@grf.unizg.hr](mailto:nikolina.stanic.loknar@grf.unizg.hr)

**Tajana Koren Ivančević**, PhD, Assist. Prof.  
University of Zagreb, Faculty of Graphic Arts  
Getaldićeva 2, 10 000 Zagreb, Croatia  
[tajana.koren.ivancevic@grf.unizg.hr](mailto:tajana.koren.ivancevic@grf.unizg.hr)

**Mateo Bekavac**, univ. bacc. ing. techn. graph.  
Otona Ivekovića 2a, 21000 Split, Croatia  
[mateobekav@gmail.com](mailto:mateobekav@gmail.com)

**Snježana Ivančić Valenko**, PhD  
University North,  
Jurja Križanića 31b, 42000 Varaždin, Croatia  
[snjezana.ivancic@unin.hr](mailto:snjezana.ivancic@unin.hr)

# Influence of Video Games on Cognitive Abilities and Intelligence

Dorja Hatlak, Andrija Bernik\*, Igor Tomičić

**Abstract:** This paper gives an overview of development in research concerning the influence of video games on cognitive development and intelligence. The first part of the paper mentions three categories used by different researchers in their research: generally speaking, the development of constructs and commercial games. StarCraft is mentioned in the paper, one of the most complex strategical games of all time, and its influence on professional players in eSport. Additionally, it presents a taxonomy of strategy games compared to real world situations, such as crisis management and control. The papers indexed in Scopus and Web of Science databases are chosen for this research since they are based on the cognitive relations between the games and players. One of the conclusions is that games can influence the enhancement of cognitive abilities in both directions.

**Keywords:** cognitive abilities; cognitive stimuli; computer games; intelligence; memory

## 1 INTRODUCTION

Entertainment Software Association reports in their 2020 research that 75% of American have at least one video game player in their household who plays (further on in the text - people who occasionally or often play video games). [1] Out of that percentage 65% of video gamers play with others (multi-player), while the average age range of video gamers is between 35 and 44 years old.

The same type of research in 2017 shows 67% of households has at least one video game player (that amounts to 16% more than in 2014), which indicates to further growth trend in the popularity of video games and their integration in daily lives.

To what extent is intelligence determined by genes, and to what extent is the development of intelligence susceptible to external conditions? There has been a lot of research on genetics up to date. Certain genes that play a role in intelligence and academic performance have even been identified. It is without a doubt that intelligence is primarily determined by genes. However, there are some significant factors that can influence cognition, especially at early age. A research team from King's College London shows nine general groups of hereditary traits (out of 83 possible ones) that are connected to GSCE (General Certificate of Secondary Education) or academic performance. Identical twins have a high probability of sharing these 9 traits. In research "Sources of Human Psychological Differences: The Minnesota Study of Twins Reared Apart" from 1990 Thomas J. Bouchard et al. [2] studies monozygotic twins reared apart after birth in order to explain environmental and genetic influences on traits. It concludes that twins reared apart can share 70% of genes. Differences in IQ results can be found in about 25% of the variance at adult age in twins with the same genetic predispositions.

Along with the change in trends, new discoveries in the field of psychology, cognition and increased quality, quantity and possibilities that games offer, a lot of new questions arise. One of the most controversial ones is perhaps "Do video games influence our intelligence?" Can cognitive

ability and general intelligence be extended beyond the genetic framework? If they can, could the games assume the role in these efforts of a means that serves to develop certain cognitive abilities?

## 2 LITERATURE OVERVIEW

### 2.1 Pioneer Studies

This research paper includes research that:

- a) Measures the correlation of success in playing video games and the results of standard intelligence tests using the Pearson correlation coefficient
- b) Research that confirms but also refutes the thesis
- c) Research that relies on medical instruments (MRI) or otherwise measures neuroplasticity of the brain and thus proves the effects (positive or negative) of playing video games on the human brain.

The first official effort to use video games in a cognitive processes study dates back to the 80s of the 20<sup>th</sup> century when Jones et al. [3] calculated correlation values between intelligence tests and cognitive measurement factors that varied between 0.18 and 0.50. The mentioned research examines the relationship between video games and determined dimensions of individual differences in cognitive and perceptual functioning performed on 63 male students with more than 2 hours of experience playing Atari video games, 5 games and 12 ETS (Educational Testing Service) intelligence paper-and-pencil tests; Hidden patterns (CF-2), copying (CF-3), Gestalt tasks of synthesizing an image elements into a whole picture (SC-1), addition and subtraction (N-4), searching for letter A (P-1), meaningless syllogisms (RL-1), card rotation (S-1), comparing cubes (S-2), map planning (SS-3), advanced vocabulary (V-5) and paper folding (VZ-2). From the mentioned tests, 3 were general intelligence tests and four spatial ability tests, since spatial perception is present in the chosen games. Games were not randomly chosen, but for specific reasons such as: quick reaction, fantasy elements, spatial and perceptual abilities. Almost all the tests have at least some positive

correlations, except for advanced vocabulary and meaningless syllogisms whose correlations has a minus sign. It should be taken into account that both tests refer to general intelligence. This means that 11 tests in total are in some type of relationship with the video games. The conclusion is brought that video games have a cognitive ability variability which is not included in classical intelligence tests, and that different intelligence test would most likely give different results. It is also suggested that video games could fill in for the disadvantages of classical intelligence tests.

As a continuation of the research, Rabbit et al. [4] obtain higher values (from 0.27 to 0.68) by applying a similar method and using AH4 intelligence test and Space Fortress game. This study takes a step further by using Space Fortress game made in association with cognitive psychologists as a tool for studying learning strategies. It requires more advanced motor and memory abilities, multi-tasking with visual components, many of which are directly copied from cognitive and psychology literature. The experiment included 56 participants 18 to 36 years old. The conclusion is that the game could be used as a tool that it can, with a precision similar to psychometric tests, determine individual differences in intelligence.

Haier et al. [5] report a correlation value of 0.39 and 0.41 using Tetris game and RAPM intelligence test and conclude that the performances of playing video games are not automated even after a higher number of repeated playing. This research methodology was innovative. There were 8 male volunteers, 19 to 32 years old, who were scanned using PET (CT) device before and after being given a complex task. The focus in this research is not really on video games and their influence on intelligence but on the changes in brain glucose metabolic rate (GMR) which occur after studying. In other words, the research aims to prove that learning and intelligence share the same factor  $g$ , and that GMR, which is responsible in parts of brain for attention and/or memory, is connected to RAPM results. All 8 participants were reported to have significantly improved their performances when playing Tetris, after the practice phase, by 69.45% (an average of the whole group). The discussion states that the higher the intelligence quotient, the greater the reduction in GMR level is, which was proved in all the participants. It concludes that learning and intelligence share the same factor  $g$ , and that  $g$  is not localized in the brain although the working memory and  $g$  are highly connected and greatly contribute to individual differences when solving RAPM tests. Also, after practicing Tetris, the only significant change in the brain occurs in the hippocampus (primary area for memory), which shows increased GMR. That means that there is an inverse correlation between GMR and PIQ (visual-spatial abilities) since Tetris requires attention and speed, however, it is not an adequate tool for researching working memory (which is highly connected to  $g$  factor).

Pioneer studies researching the relation between cognition and video games have low to medium correlation values and most often have narrow character in the questioning methodology. Some of the reasons for their probably flawed, however not insignificant results, are insufficient number of participants as well as insufficient

homogeneity in favor of one sex, unautomated performance measurements which could lead to less precise results. There is also the fact that, although the video games back in the day were very popular, they were not as intuitive, realistic, mechanically and physically advanced as they are today, and the console control itself could present a great mental effort.

## 2.2 Constructs

The term refers to computer tasks and games made or constructed with the aim of measuring and testing cognitive performance. In this sense, the constructs are tests similar to computer games that measure specific aspects of cognitive abilities such as Gs (Space Code) or WM (Space Matrix) or VSNA (Ventura et al.) to examine the connection between visuospatial abilities and students' success in STEM fields.

Guided by the new studies that research Gs (Processing Speed) and WM (working memory), which continues the thesis that these two domains are the most responsible for complex cognitive tasks and the proposition that the Gs and WM measuring tools could be constructed by using verbal, numerical and spatial stimuli which can be presented visually and auditory, as well as that Gs and WM measures can greatly be confused with psychological effects such as anxiousness and weakened motivation, Jason McPherson and Nicholas R. Burns, together with other researchers suggest that computer tasks or games can provide an ambient that causes less anxiety and encourages motivation in people who get tested, what is particularly important with children who are usually familiar with computers and control them easily, as well as because of the experience they have with video games [6]. Further on, they explain how computer games can embody a whole range of specific features that stir motivation, such as instant positive or negative response (using graphics, sound and results), as well as a feeling of progress through levels.

McPherson and Burns designed Space Code game using DSST (Digit Symbol Substitution Test) reference for Gs and Space Matrix (2008) for WM and Gf (fluid intelligence). The first experiment included 70 psychology students, 19.6 years old, from the University of Adelaide; 20 participants male, and 40 female. Participants solved tests in a particular order; Space Code, Space Matrix, Visual Matching, Picture Swaps, APM-DF, Space Code, Space Matrix. The order was chosen to maintain participants' motivation and allow as much time distance as possible between the first and second playing of the Space Matrix and Space Code games.

Space Matrix game is an "improved" version of the Space Code game from 2008, where the player must destroy the spaceship and at the same time memorize the space "sector" in which the enemy operates. This sector was presented as a dot placed on  $5 \times 5$  network, similar as in Dot Matrix task. Space Code game showed median correlation values (between 0.45 and 0.60) but had no correlations with visual processing results (Gv).

The second experiment included 94 participants out of which 42 male and 52 female. The experiment aimed to use Space Matrix and Space Code games for predicting school achievements using Gs and WM measures. It is especially

intended for subjects such as English language, Mathematics and Science. More accurate results were predicted for grades in English language for Gs than for Mathematics and Science; Gf measures for Mathematics were higher than for English and Science. GW measures should refer to general cognitive abilities. The experiment is based on an extensive study in which Gs and Wm measures could predict academic success of an individual equally successfully as Gs (crystallized intelligence) and Gf (fluid intelligence). However, the primary goal was to establish a direct comparison of external validity and reliability that tests similar to computer games have. Mean measuring values for Space Matrix and Space Code were very high. In both experiments, Space Matrix showed more consistent psychometric characteristics and a higher degree of similarity to traditional WM and Gf measures. On the other hand, it determined that Space Code probably requires abilities for mixed measures, and not primary for Gs as intended, since it leaned more on Gf, and to a certain degree on Gv. Correlation was set up between Space Matrix and RAPM test (taking data from both experiments) from 0.44 to 0.53 for Gf. Potential was shown for correlation with g. Additionally, taking into account the results and experience of the subjects in both experiments, the conclusion can be made that computer cognitive abilities tests with gamified elements are more accurate for students with gaming experience, which is true for both Gf /WM and Gs.

Ventura et al. [7] created a video game for virtual spatial navigation assessment (VSNA) in which the participants had to navigate four virtual spaces in search for jewels. The link between the time it took to collect all the objects and the different spatial abilities ranged from 0.18 to 0.37. Moreover, indoor video game spaces correlated with STEM categories containing self-assessing measures of spatial-temporal abilities.

Based on some other previous studies, which shows that spatial abilities can be a significant predictor of a degree of achievement in STEM field, and arguing that playing 3D games can improve spatial abilities, Ventura et al. [7] want to set up correlation connections in an experiment between VSNA, cognitive abilities and success in STEM field. Other encouraging references included in this study refer to the following: Feng et al. [8] discovered that playing action video games improves performances and abilities of mental rotation tasks; Uttal et al. [9] in their meta-analysis containing 206 papers, found a total of 24 papers that are video-game based. On the other hand, there is research that came across results that lacked transfer effects between playing action video games and basic cognitive functions and skills [10].

Research [11] discover that the experience with video games correlates with the ability of a person to plan routes for autonomous vehicles in 3D virtual simulations. Schuster et al. put forward a hypothesis that more frequent video game playing leads to better spatial abilities. Ventura et al. put together 323 volunteers (129 male and 194 female), all psychology students. The participants solved tests while playing games: SBSOD - Santa Barbara Sense of direction scale [12]; SOT - Spatial orientation test [13] for evaluation

of perspective abilities, MRT - Mental rotation test [14] for figural abilities, and a questionnaire on general experience with video games, and experience with games that share similarities with VSNA space. The results showed high reliability for SBSOD (0.89), MRT (0.76) and SOT (0.87). A correlation was found between indoor performance and STEM performance (10.13), between indoor VSNA spaces and SBSOD of 0.37, between VSNA and MRT (0.24), and between VSNA and SOT (0.18). The first set hypothesis (more correlations between VSNA and SBSOD) was confirmed by concluding that VSNA could be used as a measurement of spatial abilities (more for indoor and less for outdoor virtual spaces). The second hypothesis was also confirmed since VSNA results had higher correlations with mathematical than with verbal skills. The third STEM-related hypothesis was only partially confirmed as well as the fourth (playing video games improves spatial abilities at all levels), since no significant correlations were found between VDSNA and SAT for outdoor spaces, only for the indoor ones.

### 2.3 Commercial Video Games

By arguing that exposing an organism to changing visual environments often results in modifications in the visual system, and that the field of perceptual learning offers many examples of increased performance due to learning, Green and Bavelier [15] explain that perceptual learning tends to remain task-specific and can rarely be generalized or transferred to new tasks or other fields. They conducted 4 experiments in order to prove the hypothesis. People who took the test were placed into one of 2 groups.

The first group video game players (VGP) who played a set of video games for the previous 6 months a minimum of one hour per day, 4 days a week; GTA3, Half-Life, Counter Strike, Crazy Taxi, Team Fortress Classic, 007, Spider-Man, Halo, Marvel vs Capcom, Rogue Spear, and Super Mario Cart.

The second group was composed of people who preferably had no or very little experience playing similar games (non video game players - nVGP), and they were instructed not to play games during the determined time. The participants were between 18 and 23 years old. The first out of four conducted experiments used the "flanker compatibility" effect, a standard experimental paradigm in attention studies (Fig. 1, up). The task confirming the effect consisted of 6 circles and a minimum of 1 distractor. The participants were asked to confirm compatibility of the requested and given shapes, where the distractor element can but does not have to be compatible with the one that was displayed.

An interesting fact is that the more difficult the task and the more distractors it has, the more processing speed increases. This is because the more difficult the task, the fewer mental resources are provided to the distractor. In the second experiment, two groups had to answer the questions on how many square outlines they saw on a briefly presented image. The first group had an accuracy of 78% while the average accuracy in the second group was 65%.

Although these two experiments indicate that playing video games could increase attention capacity at least in the "training" area, it does not answer the question whether frequent game playing is responsible for processing beyond the range of the trained task. In order to test the possibilities, the results of two groups were compared in the task "useful field of view" (Fig. 1) for distribution of visual attention on three locations; one within the training range (0 degrees), the second at the border (20 degrees), and the third outside the training range (30 degrees). This test does not correlate well with standardized tests for visual acuity. However, it provides a measure of attention resources and their spatial distribution. The participants had to localize the target (a triangle within a circle outline) on a given screen location. VGP group showed improvement in localization abilities in the tasks outside the training range (30 degrees), which proves that spatial attention in this population is not limited only to the training tasks, at least not in this case.

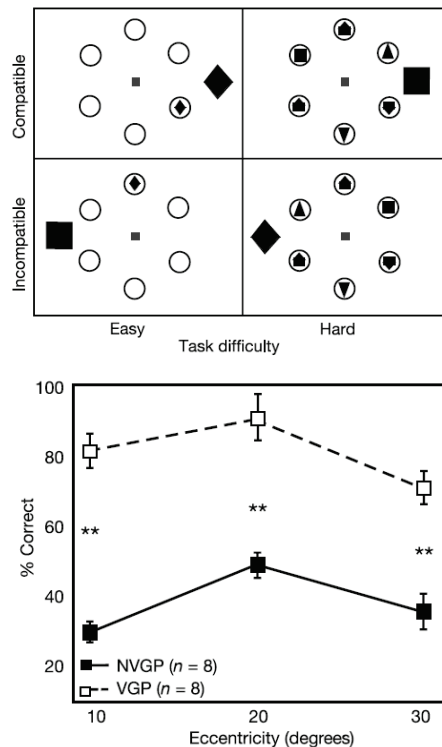


Figure 1 Testing Flanker compatibility effect (up) useful field of view (down)

The fourth experiment measured attention over time using a "blink" test in which the participants were shown consecutive multiple images in a very short time period. The possibility to forget the content of the first image after the second was shown was being checked. The test enabled visual attention distribution over time. In the beginning, the VGP group showed better results; however, after training and repetition, those results leveled with the second group (nVGP). This proves that attention over time can be trained.

Baniqued et al. [16] chose twenty casual videogames and compare the achieved performances with twenty-five psychometric tests, where correlation similarities were determined from 0.19 and 0.65 between the games and

different psychometric tests. The connection between the games and latent factors varied between 0.17 and 0.65. Heterogeneity in their performance measurements may represent different aspects of mental abilities.

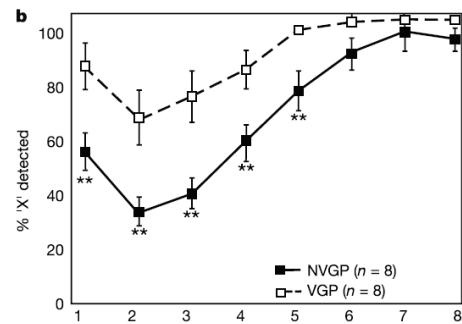


Figure 2 Results of blink test for VGP and nVGP group

Baniqued decided to find out whether commercial games could influence cognitive aspects, and whether they require more advanced cognitive abilities. Up to that point, it has been proven that cognitive training protocols can improve visual attention, inhibition or attention related to conflict, working memory and general judgment. However, these abilities are limited to specific tasks and rarely applicable in a wider range of cognitive abilities. Additionally, many similar programs have methodological issues such as [17] and are unsuccessful in replications [18].

Encouraged by the earlier study, Baniqued et al. [16] set a similar hypothesis stating that maintaining challenges and motivation through "cross-training" can produce greater gains in targeted abilities, and that greater diversity in process integration can lead to larger improvements in cognitive abilities; perhaps even in executive functions necessary in daily life, school, and the workplace. A total of 209 young adults (18 to 30 years old) who participated in the study were paid 10 dollars per session and were "motivated" by the fact they would be paid twice less per session if they failed to perform the tasks. The average age was 21.7, with 33% of participants being male. Out of all the examinees who firstly responded to participate in the study, all those that played games for 10 hours or more per week were excluded, as well as those with mental or psychological conditions. This was done in order to homogenize the group.

The protocol consisted of three cognitive testing sessions, which included: (1) fluid intelligence, spatial reasoning, processing speed, episodic memory and vocabulary, (2) ANT, VSTM (Visual Short Term Memory), task switching and Stroop test, and (3) AB (Attentional blink), n-back, SPWM, Digit Span and Trail Making. The participants played a total of 20 casual video games divided in 5 sessions, all of which were freely available on the web: (1) Silversphere, Filler, Memotri, Digital Switch; (2) Crashdown, Simon Says, Blaxorz, Enigmata, (3) Dodge, Sushi-Go-Round, 25 Boxes, Memocubes, (4) Round Table, Phange Wars, Cathode, Blobs; (5) Music Catch, Two Three, AlphaAttack, Oddball. Each session was done on different days, and each game playing time was limited to 20 minutes. Mutual correlations were calculated for all games at all 5 levels. Connections were also established between the levels - a connection was found between working memory and

perceptual speed of 0.295, between working memory and fluid intelligence of 0.5, between perceptual speed and fluid intelligence 0.19, between fluid intelligence and episodic memory 0.17; no correlation was found between these four categories and cognitive attention. Further on, the following values were obtained among these 5 components in video games and factor tasks: from 0.24 to 0.59 for working memory (with the highest correlations in working memory, spatial reasoning and object tracking), from 0.27 to 0.65 for fluid intelligence, from 0.23 to 0.36 for perceptual speed, and low significance correlations in episodic memory and ANT.

Quiroga et al. [19], conduct research in 2019 in which they want to confirm the correlations between intelligence and video games (the first research was conducted in 2009). They additionally want to prove that genre does not influence the correlations between the gaming performance and the results of intelligence standardized tests. There were 134 people, all students from the Faculty of Psychology in Madrid (105 female and 29 male) in an age range between 18 - 30, who initially played all games up to a certain level for training purposes (the number of levels varied depending on the complexity of the game). After that, in the testing phase, they had to solve as many levels as possible in a given time period. For each of the video games, reliability coefficients were calculated referring to either the number of levels completed, or the number of deaths or errors (depending on the game) that ranged from 0.77 to 0.92. Three positive correlations were found between video game performance quality and cognitive tests. Lower correlation was found with video games in Gs tests than in Gf and Gv tests. This was unexpected as most games required response speed and taking action. However, speed is a multifaceted construct with four aspects: psychomotor speed, decision speed, cognitive speed and search fluidity. Therefore, it is understandable that the speed expected in psychomotor tests may differ from the speed required in a particular game. AT - AR (abstract reasoning) was the only test with positive correlations in all games (from 0.19 to 0.60). This suggests that all these games require intelligence since DAT - AR holds a higher coefficient for g factor. Overall results suggest that even simple games require intelligence to some extent. In order to solve problems effectively, the ability to quickly adapt to a new environment is needed. The main goal was to analyze the potential of games to measure intelligence, which was confirmed with positive correlations. Commercial video games have the potential to measure certain aspects of cognitive abilities and intelligence. This study is very relevant, not only because it is a more recent one, but also because the authors have researched the same topic several times over the years (2009 and 2016). The calculations are clearer, with extensive descriptive statistics, factor models and a variety of reference games than in previous research by same and different authors.

### 3 INFLUENCE OF VIDEO GAMES ON COGNITIVE ABILITIES AND INTELLIGENCE

StarCraft is a strategy game developed by Blizzard Entertainment studio. It does not only require forward thinking but also a lot of remembering and memorizing of multiple units and structures, multi-tasking and high

attention and concentration levels. Compared to chess, the "playing field" can never be seen at one time since it is so big. In order to be successful in the game and win, the person who plays should constantly check what is happening on the map. All this suggests that this game definitely requires general intelligence, in addition to processing speed, general memory and fluid intelligence, at least from the logical point of view.

However, this argument lacks empirical statical data evidence, which is understandable given how difficult it would be to conduct such a study. Still, in 2013 a study was conducted in which Korean scientists used MRI to scan the brains of 23 experienced and successful, professional StarCraft players, and came to an interesting conclusion. The brain is a flexible organ prone to the formation and physical growth of certain more stimulated areas. As a result, thickenings were observed in certain parts of frontal cortex responsible for decision making and the parietal lobe responsible for redirecting attention. The research was conducted in association with Chung-Ang University Medical Centre in Korea. All the participants were members of KeSPa (Korea eSports Association). None of the participants suffered from depression, brain trauma, hyperactivity or drug abuse. The daily group average number of hours of playing StarCraft was 9.2.

The results showed positive correlations between career length and cortical thickness in three brain regions: superior frontal gyrus, parietal gyrus, and precentral gyrus, all to the right of the frontal lobe. Additionally, increased cortex thickness in prefrontal cortex correlated with professional league's victory rates. These thickenings were also associated with higher performance in the WCST (Wisconsin Card Sorting Test) test.



**Figure 3** Brain region associated with professional career length in eSport; A: Right superior frontal gyrus, B: Right superior precentral gyrus and C: Right precentral gyrus

The correlations between cortical thickness and career length of the pro-gamers were 0.57 for A, 0.67 for B, and 0.63 for C. Considering not everyone in the group played StarCraft professionally or unprofessionally for the same length of time, it was determined that the right medial frontal cortex was thicker in professional gamers with longer careers and higher winning rather than losing odds. This particular region is associated with attention span change, executive functions and inhibitory action control. The parietal cortex is responsible for movement control and is associated with spatial attention. The superior parietal cortex is responsible for working memory (it was previously mentioned that working memory is largely associated with general intelligence). Hyun et al. [20] concluded that long-term,

online game playing of this type (without addiction) increases cortical thickness.

Lewis et al. [21] developed a referent partial taxonomy of games so they could compare StarCraft with other types of games using 4 characteristics; stochasticity, incomplete information, unlimited opportunity and asymmetry. They argued stochastic games might restrict player actions based on the outcome of random events; incomplete information enable assumption since they do not give the player full information on state of game or situation of the opponent; unlimited opportunities allow constant modification of the game state through action (bringing decisions); asymmetry provides players with distinct materials, action repertoires, and higher territory variability. According to this classification, the representation of all characteristics in a particular game determines its difficulty, and it also requires optimal distribution of one's attention through tasks with different criteria. Accordingly, StarCraft resonates better than most other games to all the four criteria. It holds its place in a unique branch of game taxonomy, and the game complexity can be compared to real-world situations such as undergoing and managing a crisis situation.

Games & Tasks	Stochastic	Incomplete Information	Unlimited Opportunity	Asymmetry
Chess				
Backgammon	✓			
H.H. Hippos	✓		✓	
Mastermind	✓	✓		
Poker	✓	✓		✓
Tennis	✓		✓	✓
Starcraft	✓	✓	✓	✓
Disaster Management	✓	✓	✓	✓
Air Traffic Control	✓	✓	✓	✓
Military Command	✓	✓	✓	✓

Figure 4 A representation of strategic game taxonomy

Relationship between the measure of reaction speed and spatial variance of action was taken into account. It was concluded that quick reactions and quick attention distribution are characteristic for efficient cognitive abilities. Showing those abilities can play a role in predicting whether a player will lose or win. The question that arises whether people with a natural ability to distribute attention are simply inclined and attracted to demanding games such as StarCraft, or can games really "train the brain" and make an individual more intelligent by extending their cognitive abilities beyond genetic innateness. What was crucial for successfulness of the analysis is the replay file, a StarCraft feature that allows users to re-watch games after they have concluded playing.

Regarding methodology, the following was recorded: APM number (Action per Minute), SVA (Spatial Variance of

Action) - moving units and placing objects, (3) Macro action count (production and building), (4) Micro action count - a total number of actions connected to managing units during battle, scouting or positioning, and (5) Win state, 1 or 0 depending on whether the player won. It was determined that the players who can perform an action quicker (have higher APM) have a higher tendency of winning.

It was determined for SVA to be an indirect measure of the distribution of attention, for scouting opponent's base, gathering resources from the other part of the map, all which leads to success-winning actions. This indicates better multi-tasking abilities and attention distribution that can provide a good insight into the learning processes. APM and SVA numbers are not useful and do not correlate with winning/losing rates in less stochastic games without unlimited opportunities (for example, chess). It was concluded that in undergoing a crisis situation, a high APM can lead to increased success in maintaining stability in real-world situation.

Unsworth et al. [22] conducted 2 experiments in 2015. In the first experiment they reanalyzed their own results from an unpublished study conducted a year earlier [23], which included typical inconsistencies: lack of information on previous experience of playing video games, giving financial awards to participants, dismissing the participants who did not complete all the cognitive ability tests, and so on. There were 252 subjects (recruited for the Oregon University), 18 to 35 years old, who were group tested in 6 sessions lasting 2 hours max. According to the results, VGP group outperformed the second group on some working memory tests (symmetry span), all the fluid intelligence tests, and some of the attention-control tests. Better WM results were not all that significant, although the results were still better and in favor of the VGP group. The same testing was repeated in the second phase, but with 198 participants where VGP did not include first-person shooter players but other genre players. This experiment of applying different statistical methods showed how relative and susceptible to manipulation the results obtained for the purpose of getting higher correlations can be. Although none of these studies were methodologically inaccurate, where Quiroga et al. [19] produced the most extensive study proving correlations on a latent level, this experiment only showed that extreme groups always show greater correlations in favor of the desired hypothesis.

In order to correct the limitations from the first experiment, Unsworth et. al. conducted a second experiment where they reanalyzed the data from research done by Redick [24] with the purpose of expanding the results from experiment 1. A total of 586 subjects (226 male and 354 female), between the ages of 18 and 30, were tested at four different universities. It was concluded that more research and experiments were needed for determining to what extent video games could enhance cognitive abilities, giving a recommendation to use higher and full range of participants and research the established relationships through constructs that include latent variables.

The research from 2018 [25] used behavioral and electrophysiological measures for examining the plasticity of

Visual Selective Attention (VSA) linked to action video games and effects they have on VSA after one hour of practicing. The research included both VGP and nVGP so that a comparison within a group could be made. All the participants were students of the University of Electronic Science and Technology of China (UESTC). The group with gaming experience included  $n = 15$  participants, and the group without gaming experience included  $n = 14$  participants.

Research results indicated to: (a) improvement in response time in both groups after one hour of LOL playing, (b) improvement in neurological plasticity in the second group after one hour of playing: short-term effect, and (c) long-term effect of playing this type of game on neurological plasticity which was proved by cross comparing the results in the two groups.

Stojanoski et al. [26] conducted research aimed at denying the claims that video games enhanced cognitive functions that can be transferred to other tasks. There were 72 participants, some students from the University of Ontario and others workers in Amazon Mechanical Turk, separated into two groups. The results showed that extensive repetition of the gamified task improved the outcome in the performance test group by 18% on average. However, there was no evidence that subjects performed significantly better on cognitive tests (after the training phase) in some other tasks.

Stojanoski et al. also conducted a second experiment using a similar procedure with 24 new participants for the test group and the same group of people for the control group. Performances improved up to 60% after the training phase, but there was no improvement in transfer of acquired knowledge on special and new tasks.

West et al. [27] managed to prove, in their 2017 research, the negative effects first person shooting-games have on brain, such as reducing grey matter within the hippocampus, which brings increased risk of Alzheimer disease, in participants using non-spatial memory strategies, i.e. the mechanisms that are not hippocampus-dependent.

Reynaldo et al. [28] showed that there are several types of games (RPG, RTS, FPS) that could influence different cognitive categories. They have analyzed 27 experimental and literature review articles with the conclusions that video games do improve cognitive skills and decision-making.

In the case of mentally disabled individuals, Suárez-Iglesias et al. [29] have shown that some type of games (exergaming vs sedentary) could stimulate cognitive functions. They have analyzed 17 cases and concluded that videogames can improve health-related outcomes in people with intellectual disabilities.

Also Franceschini et al. [30] have conducted an experiment on visual perception, sensorimotor and reading skills in children with developmental coordination disorder and dyslexia. They used shooting and puzzle video-games and came to interesting conclusions that any type of videogame can be a useful clinical tool for the prevention and treatment of multiple cognitive disorders.

## 4 DISCUSSION AND CONCLUSION

Although it could sound pretentious to conclude that video games can make us smarter and expand our cognitive abilities, given the results of the referenced research described, such a claim cannot be denied. Since there is a small amount of empirical evidence, it can only be concluded with certainty that video games definitely have huge potential for further research on the topic as well as that they have, as proven in several studies, the potential to be used for medical, educational and research purposes. It is also a fact that certain games, or the mechanisms within, can determine individual differences in cognitive abilities between individuals, perhaps not to the same extent that intelligence tests do, but to a certain degree they can. This is understandable since it would not be realistic to expect that something which was not primarily designed as a tool for measuring cognitive abilities could match the intelligence tests that have been developed for decades. What games could do in future is to extend the classic tests to spheres, which cannot be measured.

While some of these studies support the hypothesis, others fail to find significant correlations between improving cognitive ability and playing video games. Some of the reasons are the use of different methodologies, too small participant groups, the use of games that are not demanding enough or simply do not relate to the required cognitive abilities. One of the reasons could be using too simple, or at the other end, too aggressive and stressful games. From all the above-mentioned research, the best results were shown by emotionally neutral or positive video games. This especially refers to certain strategy, action and puzzle games. The research that carries the most weight is probably that including changes in the hippocampus and frontal cortex after training, especially in professional and experienced players. Taking the assumption that intelligence can be expanded, video games should never replace physical activity, as well as no other form of cognitive training, healthy eating and other basic prerequisites for proper brain function. Instead, video games should be considered as a possible tool for developing cognitive flexibility with great potential in sharpening processing speed, multi-tasking, fluid intelligence, visual-spatial capabilities and working memory (which is  $u_f G_f$  in high correlation with the  $g$  factor).

This paper does not include all the research that exists on the topic, but only that which is methodologically accurate and most elaborate. One relatively certain conclusion can be made: different games, depending on the genre, can have influence in both directions in terms of improving cognitive abilities. Therefore, aggressive games can definitely have a negative psychological influence, and subsequently a cognitive or neurological one. We believe that further research should not pose the question "Do video games have an influence on the enhancement of cognitive abilities?" Future research should focus on finding specific mechanisms in video game design that have short-term and long-term effects on intelligence and cognition, which, after sufficient evidence, could consequently be projected onto game developments with the aim of (a) measuring intelligence, and (b) increasing certain  $g$  factor branches. The paper does not

describe serious video games, as they involve increased crystallized intelligence (learning new information) or specific ability trainings (not necessarily cognitive).

## 5 REFERENCES

- [1] ESA, E. (2020). Essential facts about the video game industry.
- [2] Bouchard Jr, T. J., Lykken, D. T., McGue, M., Segal, N. L., & Tellegen, A. (1990). Sources of human psychological differences: The Minnesota study of twins reared apart. *Science*, 250(4978), 223-228. <https://doi.org/10.1126/science.2218526>
- [3] Jones, M. B., Dunlap, W. P., & Bilodeau, I. M. (1986). Comparison of video game and conventional test performance. *Simulation & Games*, 17(4), 435-446. <https://doi.org/10.1177/0037550086174001>
- [4] Rabbitt, P., Banerji, N., & Szymanski, A. (1989). Space Fortress as an IQ test? Predictions of learning and of practised performance in a complex interactive video-game. *Acta psychologica*, 71(1-3), 243-257. [https://doi.org/10.1016/0001-6918\(89\)90011-5](https://doi.org/10.1016/0001-6918(89)90011-5)
- [5] Haier, R. J., Siegel, B., Tang, C., Abel, L., & Buchsbaum, M. S. (1992). Intelligence and changes in regional cerebral glucose metabolic rate following learning. *Intelligence*, 16(3-4), 415-426. [https://doi.org/10.1016/0160-2896\(92\)90018-M](https://doi.org/10.1016/0160-2896(92)90018-M)
- [6] McPherson, J. & Burns, N. R. (2008). Assessing the validity of computer-game-like tests of processing speed and working memory. *Behavior Research Methods*, 40(4), 969-981. <https://doi.org/10.3758/BRM.40.4.969>
- [7] Ventura, M., Shute, V., Wright, T. J., & Zhao, W. (2013). An investigation of the validity of the virtual spatial navigation assessment. *Frontiers in psychology*, 4, 852. <https://doi.org/10.3389/fpsyg.2013.00852>
- [8] Feng, J., Spence, I., & Pratt, J. (2007). Playing an action video game reduces gender differences in spatial cognition. *Psychological science*, 18(10), 850-855. <https://doi.org/10.1111/j.1467-9280.2007.01990.x>
- [9] Uttal, D. H., & Cohen, C. A. (2012). Spatial thinking and STEM education: When, why, and how? *Psychology of Learning and Motivation*, 57, 147-181. <https://doi.org/10.1016/B978-0-12-394293-7.00004-2>
- [10] Boot, W. R., Kramer, A. F., Simons, D. J., Fabiani, M., & Gratton, G. (2008). The effects of video game playing on attention, memory, and executive control. *Acta psychologica*, 129(3), 387-398. <https://doi.org/10.1016/j.actpsy.2008.09.005>
- [11] Richardson, M., Abraham, C., & Bond, R. (2012). Psychological correlates of university students' academic performance: a systematic review and meta-analysis. *Psychological bulletin*, 138(2), 353. <https://doi.org/10.1037/a0026838>
- [12] Hegarty, M., Richardson, A. E., Montello, D. R., Lovelace, K., & Subbiah, I. (2002). Development of a self-report measure of environmental spatial ability. *Intelligence*, 30(5), 425-447. [https://doi.org/10.1016/S0160-2896\(02\)00116-2](https://doi.org/10.1016/S0160-2896(02)00116-2)
- [13] Waller, D., Montello, D. R., Richardson, A. E., & Hegarty, M. (2002). Orientation specificity and spatial updating of memories for layouts. *Journal of experimental psychology: Learning, Memory, and Cognition*, 28(6), 1051. <https://doi.org/10.1037/0278-7393.28.6.1051>
- [14] Vandenberg, S. G. & Kuse, A. R. (1978). Mental rotations, a group test of three-dimensional spatial visualization. *Perceptual and motor skills*, 47(2), 599-604. <https://doi.org/10.2466/pms.1978.47.2.599>
- [15] Green, C. S., & Bavelier, D. (2003). Action video game modifies visual selective attention. *Nature*, 423(6939), 534-537. <https://doi.org/10.1038/nature01647>
- [16] Baniqued, P. L., Lee, H., Voss, M. W., Basak, C., Cosman, J. D., DeSouza, S., ... & Kramer, A. F. (2013). Selling points: What cognitive abilities are tapped by casual video games?. *Acta psychologica*, 142(1), 74-86. <https://doi.org/10.1016/j.actpsy.2012.11.009>
- [17] Boot, W. R., Blakely, D. P., & Simons, D. J. (2011). Do action video games improve perception and cognition?. *Frontiers in psychology*, 2, 226. <https://doi.org/10.3389/fpsyg.2011.00226>
- [18] Chooi, W. T. & Thompson, L. A. (2012). Working memory training does not improve intelligence in healthy young adults. *Intelligence*, 40(6), 531-542. <https://doi.org/10.1016/j.intell.2012.07.004>
- [19] Quiroga, M. A., Diaz, A., Roman, F. J., Privado, J., & Colom, R. (2019). Intelligence and video games: Beyond "brain-games". *Intelligence*, 75, 85-94. <https://doi.org/10.1016/j.intell.2019.05.001>
- [20] Hyun, G. J., Shin, Y. W., Kim, B. N., Cheong, J. H., Jin, S. N., & Han, D. H. (2013). Increased cortical thickness in professional on-line gamers. *Psychiatry Investigation*, 10(4), 388. <https://doi.org/10.4306/pi.2013.10.4.388>
- [21] Lewis, J., Trinh, P., & Kirsh, D. (2011). A corpus analysis of strategy video game play in starcraft: Brood war. *Proceedings of the Annual Meeting of the Cognitive Science Society*, 33(33).
- [22] Unsworth, N., Redick, T. S., McMillan, B. D., Hambrick, D. Z., Kane, M. J., & Engle, R. W. (2015). Is playing video games related to cognitive abilities? *Psychological science*, 26(6), 759-774. <https://doi.org/10.1177/0956797615570367>
- [23] Unsworth, N., & McMillan, B. D. (2014). Similarities and differences between mind-wandering and external distraction: A latent variable analysis of lapses of attention and their relation to cognitive abilities. *Acta psychologica*, 150, 14-25. <https://doi.org/10.1016/j.actpsy.2014.04.001>
- [24] Redick, T. S. (2014). Cognitive control in context: Working memory capacity and proactive control. *Acta psychologica*, 145, 1-9. <https://doi.org/10.1016/j.actpsy.2013.10.010>
- [25] Qiu, N., Ma, W., Fan, X., Zhang, Y., Li, Y., Yan, Y., ... & Yao, D. (2018). Rapid improvement in visual selective attention related to action video gaming experience. *Frontiers in human neuroscience*, 47. <https://doi.org/10.3389/fnhum.2018.00047>
- [26] Stojanoski, B., Lyons, K. M., Pearce, A. A., & Owen, A. M. (2018). Targeted training: Converging evidence against the transferable benefits of online brain training on cognitive function. *Neuropsychologia*, 117, 541-550. <https://doi.org/10.1016/j.neuropsychologia.2018.07.013>
- [27] West, G. L., Konishi, K., Diarra, M., Benady-Chorney, J., Drisdelle, B. L., Dahmani, L., ... & Bohbot, V. D. (2018). Impact of video games on plasticity of the hippocampus. *Molecular psychiatry*, 23(7), 1566-1574. <https://doi.org/10.1038/mp.2017.155>
- [28] Reynaldo, C., Christian, R., Hosea, H., & Gunawan, A. A. (2021). Using video games to improve capabilities in decision making and cognitive skill: a literature review. *Procedia Computer Science*, 179, 211-221. <https://doi.org/10.1016/j.procs.2020.12.027>
- [29] Suárez-Iglesias, D., Martínez-de-Quel, Ó., Marin Moldes, J. R., & Ayan Perez, C. (2021). Effects of videogaming on the physical, mental health, and cognitive function of people with intellectual disability: a systematic review of randomized controlled trials. *Games for Health Journal*, 10(5), 295-313.
- [30] Franceschini, S., Bertoni, S., Lulli, M., Pievani, T., & Facoetti, A. (2022). Short-term effects of video-games on cognitive

enhancement: The role of positive emotions. *Journal of Cognitive Enhancement*, 6(1), 29-46.  
<https://doi.org/10.1007/s41465-021-00220-9>

**Authors' contacts:**

**Dorja Hatlak**, mag. ing. techn. graph.  
University North,  
104. brigade 1, 42000 Varazdin, Croatia  
[dahatlak@unin.hr](mailto:dahatlak@unin.hr)

**Andrija Bernik**, PhD, Assistant Professor  
University North,  
104. brigade 1, 42000 Varazdin, Croatia  
[andrija.bernik@unin.hr](mailto:andrija.bernik@unin.hr)

**Igor Tomičić**, PhD, Assistant Professor  
Faculty of Organization and Informatics,  
Pavlinska ul. 2, 42000 Varazdin, Croatia  
[tomicic.igor@gmail.com](mailto:tomicic.igor@gmail.com)

# Deep Learning Based Models for Detection of Diabetic Retinopathy

İsmail Akgül\*, Ömer Çağrı Yavuz, Uğur Yavuz

**Abstract:** Diabetic retinopathy (DR) is an important disease that occurs because of damage to the retinal blood vessels in the human eye due to diabetes and causes blindness. If diagnosed correctly, the treatments to be applied increase the possibility of preventing vision loss or blindness. This study aims to present an evaluation of deep learning methods to detect diabetic retinopathy from retinal images. In this direction, the VGG16 model was considered, and two different versions of this model were obtained by making improvements. Besides, a model has been proposed, the first layers are dense, the next layers have decreasing convolution, and have fewer layers. According to the results, the VGG16 model, which reached 75.48% accuracy, reached 76.57% accuracy due to the dropout layer added to the classification layers, and 77.11% accuracy due to the dropout layer added to all blocks. The highest accuracy was obtained in the proposed model with 81.74%.

**Keywords:** artificial intelligence; deep learning; detection; diabetic retinopathy

## 1 INTRODUCTION

Diabetic retinopathy (DR) is a diabetic disease in which the retinal blood vessels of the human eye are damaged, causing blindness [1]. Diabetic retinopathy, the most common diabetic eye disease in the world, is the leading cause of blindness [2]. Defining the DR stage, which is considered one of the most dangerous complications of diabetes, is a complex task and needs to be interpreted by experts. If left untreated, it can cause permanent blindness [3]. Assessment of the severity and extent of retinopathy is currently performed by medical professionals based on fundus retinal images of the patient's eyes [4].

Diabetes is a serious and long-term condition that has a major impact on the lives of people around the world. The prevalence of diabetes, which was estimated to be 463 million people in 2019, is estimated to increase to 578 million in 2030 and to 700 million in 2045 [5]. DR is a preventable eye disease, and its early symptoms can be detected by the specialist either by visual observation of the retina or by automatic examination mode. DR affects the person's vision, if not detected and treated, it may not be noticed until the disease progresses and can lead to blindness [6]. The best treatment options that should be applied to patients differ according to the stages of the disease. For patients without DR or mild DR, only regular screening is required, while for patients with moderate or worse DR, treatment options range from diffuse laser therapy to vitrectomy. Therefore, it is important to degree DR severity in the first degree to provide patients with appropriate treatment [7]. Early detection of DR formation can be very helpful for clinical treatment. Although several different feature extraction approaches have been proposed for this, the classification task for retinal images does not yet provide adequate assistance to clinical treatments. Recently, deep convolutional neural networks have shown superior performance in image classification compared to previous handcrafted feature-based image classification methods [8].

The term deep learning or deep neural network refers to multi-layer Artificial Neural Networks (ANN). This term has been recognized as one of the most powerful tools in the last

few decades and has become very popular in the literature as it can handle large amounts of data. The interest in having deeper hidden layers has recently begun to surpass classical method performance in different fields. One of the most popular deep neural networks is Convolutional Neural Network (CNN) [9]. Deep learning allows computational models consisting of multiple processing layers to learn representations of data with multiple levels of abstraction. These methods have significantly improved cutting-edge technology in many fields such as speech recognition, visual object recognition, object detection, drug discovery, and genomics. Deep learning explores complexity in large datasets by using the backpropagation algorithm to specify how a machine should change its internal parameters used to calculate the representation in each layer from the representation in the previous layer. While deep convolutional networks have revolutionized the processing of images, videos, speech, and audio, recursive networks have shed light on sequential data such as text and speech [10].

Supervised techniques, in which training data are used to develop a system, have become increasingly popular in medical image analysis. Applications of deep learning to medical image analysis have been increasing rapidly in recent years. Although it has been applied in many areas, it is still not fully represented in the most important areas such as retinal image [11]. Automatic grading of diabetic retinopathy has potential benefits such as increasing efficiency, reproducibility, and coverage of screening programs, reducing barriers to access, and improving patient outcomes by providing early detection and treatment [12]. Automated techniques to be applied for the diagnosis of diabetic retinopathy are very important to solve these problems. In general, deep learning achieves high validation accuracies for binary classification, while multistage classification results are less impressive, especially for early-stage disease [13]. Deep learning, a new branch of machine learning technology under the broad term artificial intelligence, has significant potential for healthcare. It allows us to determine which patients are most likely to have a certain disease among those with certain disorders, which

patients should be treated more severely, and the most appropriate specific treatments to be applied to patients [14].

Due to uncontrolled blood sugar levels in diabetics, there is a lack of blood flow and oxygen in the retina. If not detected early, when the tension in the blood vessels increases, it can cause fluid leakage in the blood vessels and loss of proper vision in the eye [15]. Patients who are usually asymptomatic in their early stages show different symptoms because of disease progression. Symptoms can include blurred vision, blind spots, distorted central vision, large floaters, and sometimes sudden vision loss. Therefore, it is important to accurately detect the disease in its early stages and determine at what stage it is to reduce the complications of the disease and the possibility of vision loss [16]. Although there are enough treatment procedures to cope with DR disease that occurs in people with diabetes for a long time, neglect, and failure of early diagnosis cause people's eyesight. Recent advances in digital image processing and machine learning are used in the detection of DR [17]. Computer-aided diagnostic systems significantly reduce the burden on ophthalmologists [18].

Diabetic retinopathy due to diabetes is an eye disease that can damage blood vessels and lead to blindness. Physicians have a great job because it is a difficult, laborious, and demanding task to detect this disease. Every day, as in many other fields, pre-diagnosis systems are developed to help physicians to detect the symptoms of the disease in this field. For this purpose, in this study, the VGG16 model, which is one of the deep learning methods, and two different modified versions of this model were used, and a new model was proposed, to detect diabetic retinopathy. A new dataset, Asia Pacific Tele-Ophthalmology Society (APTOS) 2019 Blindness Detection dataset, published in mid-2019, was used to test the performance of the models. The current work aims to contribute to the increasing knowledge about the use of deep learning methods in diabetic retinopathy by characterizing the detection performance of diabetic retinopathy, which can cause blindness, with deep learning methods.

The remainder of the study is structured as follows. In Section 2, relevant studies are given. In Section 3, the materials and methods used in deep learning are explained. In Section 4, the experimental results are discussed, and in Section 5, the results of the study are presented.

## 2 RELATED WORKS

In studies carried out by increasing data on the APTOS 2019 Blindness Detection dataset or approaching it with different classification and different image sizing:

Khalifa et al. (2019) conducted training by applying the data augmentation technique in the APTOS 2019 Blindness Detection dataset with AlexNet, Res-Net18, SqueezeNet, GoogleNet, VGG16, and VGG19 deep transfer models. The highest performance was achieved with the AlexNet model, which has the least number of layers among the models used in the study, at a rate of 97.9%. In another study using the data augmentation technique, Chaturvedi et al. (2020) [19] made changes to the pre-trained DenseNet121 network and

trained on the APTOS 2019 Blindness Detection dataset and obtained 96.51% accuracy.

Tymchenko et al. (2020) proposed a deep learning-based method for detecting DR from human retinal images with a multi-stage transfer learning approach. EfficientNet-B4, EfficientNet-B5, and SE-ResNeXt50 convolutional neural network models achieved 99% success in binary classification results with DR/no DR. Similarly, Narayanan et al. (2019) [20] examined the results provided by deep neural networks for the detection of two-class DR as well as different diseases. In their studies with GoogleNet and ResNet models, they reached 97.3% and 96.2% binary classification accuracy, respectively. Chetoui and Akhloufi (2020) proposed a deep learning architecture based on EfficientNet convolutional neural network to detect DR. As a result of the tests, they applied for the detection of transferable DR and sight-threatening DR on the APTOS 2019 Blindness Detection dataset, they achieved a classification rate of 96.60% and 99.80%, respectively.

Kassani et al. (2019) [21] presented a new feature extraction method for the diagnosis of DR disease, based on deep layer clustering, which combines multilevel features from different convolution layers of a modified Xception architecture. They evaluated the performance of their proposed approach with four deep feature extractors, including Inception V3, MobileNet, ResNet50, and the original Xception architecture. As a result of the experiments, they carried out on the images they sized as 600x600 pixels, different from the ones in our study, they determined that the model they proposed achieved higher success than the other models they used in their studies. They revealed that the modified Xception deep feature extractor improves DR classification with a classification accuracy of 79.59% versus 83.09% compared to the original Xception architecture.

Like our study, in studies that preprocess the APTOS 2019 Blindness Detection dataset and classify the dataset in the same way:

Dekhil et al. (2019) [22] presented a convolutional neural network-based computer-assisted diagnostic tool to classify diabetic retinopathy into one of five stages. They have reached a test accuracy of 77% with the alternative solution they offer so that ophthalmologists can automatically detect the disease. Bodapati et al. (2020) [23] blended by extracting features from retinal images with pre-trained VGG16-fc1, VGG16-fc2, and Xception models to detect DR. They conducted two studies by considering the dataset with both two classes and five classes. They achieved 80.96% success with the DNN model they trained to detect one of the five classes using representative blended features. Zhuang and Ettehadi (2020) [24] developed solutions for the DR classification problem. They used transfer learning to retrain the last modified layer of a very deep neural network, such as Efficientnet-B3 to improve the generalization of less frequent class's ability of their shallow neural network model. As a result of their training, they achieved the best test accuracy of 77.87%.

Dondeti et al. (2020) [25] created a NASNet model to automatically predict the severity level of DR based on retinal images of diabetics. Focusing on extracting suitable

features from retinal images, they stated that performance improves when projecting into t-SNE (T-distributed stochastic neighbor embedding) space to obtain lower-dimensional representations from the deep features extracted from the NASNet model. In their experiments on the APTOS 2019 Blindness Detection dataset, they emphasized that the proposed model became more powerful with the robustness of the SVM (Support Vector Machine) models. They observed that deep features transformed using T-SNE provided more distinctive representations of retinal images and helped to achieve 77.90% accuracy.

### 3 EXPERIMENTAL METHOD

#### 3.1 Dataset

In this study, Asia Pacific Tele-Ophthalmology Society (APTOS) Blindness Detection dataset published in mid-2019 was used. The dataset containing 3662 images consists of 5 classes No DR, Mild DR, Moderate DR, Severe DR, and Proliferate DR. There are 1805 images in the No DR class, 370 in the Mild DR class, 999 in the Moderate DR class, 193 in the Severe DR class, and 295 in the Proliferate DR class [26].

Each image in the dataset consisting of five classes was labeled and grouped under the class it belongs to, and then converted to  $224 \times 224$  pixel dimensions and grey format. In Fig. 1, sample images of each class in the APTOS 2019 Blindness Detection dataset are given.

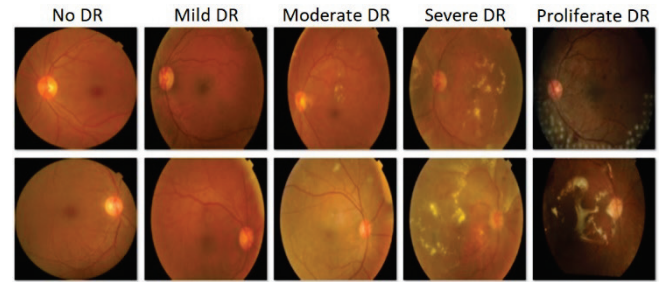


Figure 1 Example images of each class in the APTOS 2019 Blindness Detection dataset

#### 3.2 Convolutional Neural Network (CNN) Model

Convolutional Neural Networks (CNNs), a branch of deep learning, have an impressive track record for applications in image analysis and interpretation, including medical imaging [27]. Among the deep learning algorithms, especially convolutional networks have quickly become a preferred methodology for analysing medical images [11].

With the convolutional neural network method, which provides good success in deep learning, feature extraction and classification can be done well. There are many successful models such as AlexNet [28], VGGNet [29], GoogLeNet [30], and ResNet [31] developed using convolutional neural networks. The VGG16 model is one of these models.

Table 1 Model architectures

VGG16 - Original	VGG16 - Modified Version 1	VGG16 - Modified Version 2	Proposed Model
Input ( $224 \times 224 \times 1$ )			
Conv1 ( $3 \times 3$ ) – 64 Conv2 ( $3 \times 3$ ) – 64 MaxPool1 ( $2 \times 2$ )	Conv1 ( $3 \times 3$ ) – 64 Conv2 ( $3 \times 3$ ) – 64 MaxPool1 ( $2 \times 2$ )	Conv1 ( $3 \times 3$ ) – 64 Conv2 ( $3 \times 3$ ) – 64 MaxPool1 – ( $2 \times 2$ ) Dropout – 0.5	Conv1 ( $3 \times 3$ ) – 32 Conv2 ( $3 \times 3$ ) – 32 Conv3 ( $5 \times 5$ ) – 32 Conv4 ( $7 \times 7$ ) – 32 AvgPool1 ( $5 \times 5$ ) Dropout – 0.5
Conv3 ( $3 \times 3$ ) – 128 Conv4 ( $3 \times 3$ ) – 128 MaxPool2 ( $2 \times 2$ )	Conv3 ( $3 \times 3$ ) – 128 Conv4 ( $3 \times 3$ ) – 128 MaxPool2 ( $2 \times 2$ )	Conv3 ( $3 \times 3$ ) – 128 Conv4 ( $3 \times 3$ ) – 128 MaxPool2 ( $2 \times 2$ ) Dropout – 0.5	Conv5 ( $5 \times 5$ ) – 64 Conv6 ( $7 \times 7$ ) – 64 AvgPool2 ( $5 \times 5$ ) Dropout – 0.5
Conv5 ( $3 \times 3$ ) – 256 Conv6 ( $3 \times 3$ ) – 256 Conv7 ( $3 \times 3$ ) – 256 MaxPool3 ( $2 \times 2$ )	Conv5 ( $3 \times 3$ ) – 256 Conv6 ( $3 \times 3$ ) – 256 Conv7 ( $3 \times 3$ ) – 256 MaxPool3 ( $2 \times 2$ )	Conv5 ( $3 \times 3$ ) – 256 Conv6 ( $3 \times 3$ ) – 256 Conv7 ( $3 \times 3$ ) – 256 MaxPool3 ( $2 \times 2$ ) Dropout – 0.5	Conv7 ( $7 \times 7$ ) – 128 AvgPool3 ( $5 \times 5$ ) Dropout – 0.5
Conv8 ( $3 \times 3$ ) – 512 Conv9 ( $3 \times 3$ ) – 512 Conv10 ( $3 \times 3$ ) – 512 MaxPool4 ( $2 \times 2$ )	Conv8 ( $3 \times 3$ ) – 512 Conv9 ( $3 \times 3$ ) – 512 Conv10 ( $3 \times 3$ ) – 512 MaxPool4 ( $2 \times 2$ )	Conv8 ( $3 \times 3$ ) – 512 Conv9 ( $3 \times 3$ ) – 512 Conv10 ( $3 \times 3$ ) – 512 MaxPool4 ( $2 \times 2$ ) Dropout – 0.5	
Conv11 ( $3 \times 3$ ) – 512 Conv12 ( $3 \times 3$ ) – 512 Conv13 ( $3 \times 3$ ) – 512 MaxPool5 ( $2 \times 2$ )	Conv11 ( $3 \times 3$ ) – 512 Conv12 ( $3 \times 3$ ) – 512 Conv13 ( $3 \times 3$ ) – 512 MaxPool5 ( $2 \times 2$ )	Conv11 ( $3 \times 3$ ) – 512 Conv12 ( $3 \times 3$ ) – 512 Conv13 ( $3 \times 3$ ) – 512 MaxPool5 ( $2 \times 2$ ) Dropout – 0.5	
Flatten – 25088	Flatten – 25088	Flatten – 25088	Flatten – 128
FC1 – 4096	FC1 – 4096 Dropout – 0.5	FC1 – 4096 Dropout – 0.5	FC1 – 32 Dropout – 0.5
FC2 – 4096	FC2 – 4096 Dropout – 0.5	FC2 – 4096 Dropout – 0.5	
Output-5 (Softmax)			
134,279,877 params			743,269 params

The VGG16 model has an architecture consisting of 13 convolutional and 3 fully connected layers. The model has a total of 41 layers with Maxpooling, Fullconnected, ReLu, Dropout, and Softmax layers [29]. In our study, two different modified versions of the VGG16 model with the original were used and a new model was proposed. In Tab. 1, VGG16 original, VGG16 modified the first version, VGG16 modified the second version, and proposed model architectures are given. In Fig. 2, the block diagram of the proposed research is shown.

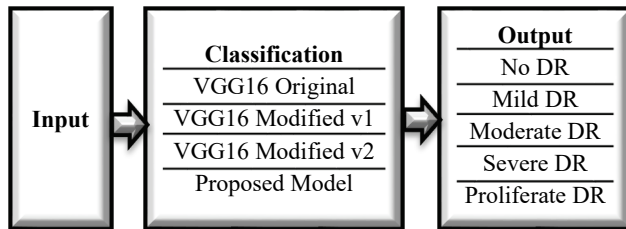


Figure 2 Block diagram of the proposed research

In Tab. 1, VGG16 modified version 1 was created by adding 0.5 dropout to the classification layers and VGG16 modified version 2 architectures were created by adding 0.5 dropout to all blocks of the VGG16 original architecture. In addition, a new model is proposed. Contrary to the VGG16 model, the proposed model is both a smaller model and has a denser convolution layer in the first layers and a decreasing convolution layer structure in the next layers. The proposed model contains fewer layers and fewer parameters than the VGG16 model. Besides, while maximum pooling is used in VGG16 architecture, average pooling is used in the proposed model. All models used in the study have a softmax layer with 5 classes in the output layer.

## 4 RESULTS AND DISCUSSION

Applied experiments for the detection of diabetic retinopathy with the models discussed in the study. It was made using the Python language with Jupyter Notebook in Google Colaboratory (CoLab).

The dataset is divided into three as 80% training, 10% validation, and 10% testing. There are 2928 images in the training set and 367 images in each of the validation and test sets. The parameters used during the training of VGG16 original, VGG16 modified version 1, VGG16 modified version 2 and the proposed model are given in Tab. 2.

Table 2 Model training parameters

Parameter	Value
Epoch	150
Mini Batch Size	16
Dropout	0,5
Activation Function	ReLU
Optimization Algorithm	Adamax

The training of the 4 models used in the study was repeated 5 times and the best accuracy and loss graph obtained for each model because of the training is given in Fig. 3. When the figure is examined, it is seen that the training

of the VGG16 original, VGG16 modified version 1 and VGG16 modified version 2 models are close to each other, and these three models initially started learning with a 49% training and validation rate. It is seen that learning takes place by reaching a rate of just over 70% of training and validation success until the first 30 iterations, and they reach a validation success of 70%-76% until 150 iterations. Like each other, these three models started training with a validation loss rate of 1,300 and showed a decrease in the loss rate in the first 30 iterations, and an increase in the loss rate because of the non-learning after 30 iterations. It is seen that the proposed model in the figure starts learning with 49% training and 65% validation rate, training and validation continues successfully until the 100th iteration, and learning continues after the 100th iteration, reaching 81.74% success accuracy because of 150 iterations. It is understood that learning takes place at every stage of the training of the proposed model. In addition, it is seen that the model, which started training with a validation loss rate of 1.018, reached a validation loss rate of 0.658 at the end of 150 iterations.

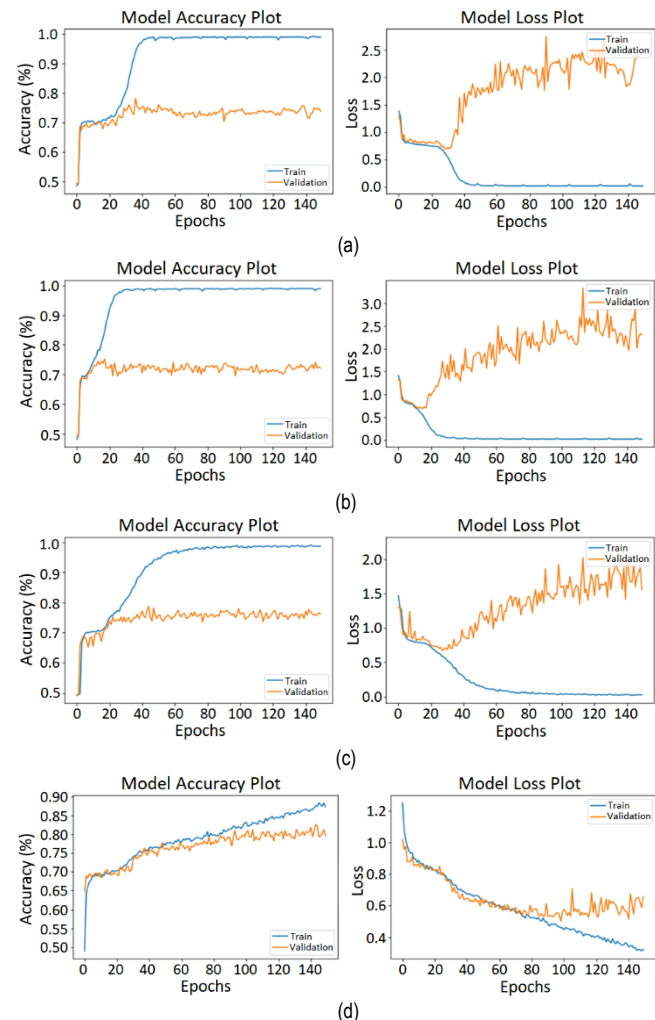


Figure 3 Accuracy and loss plots of the models: (a) VGG16 original, VGG16 modified version 1, (c) VGG16 modified version 2, (d) proposed model

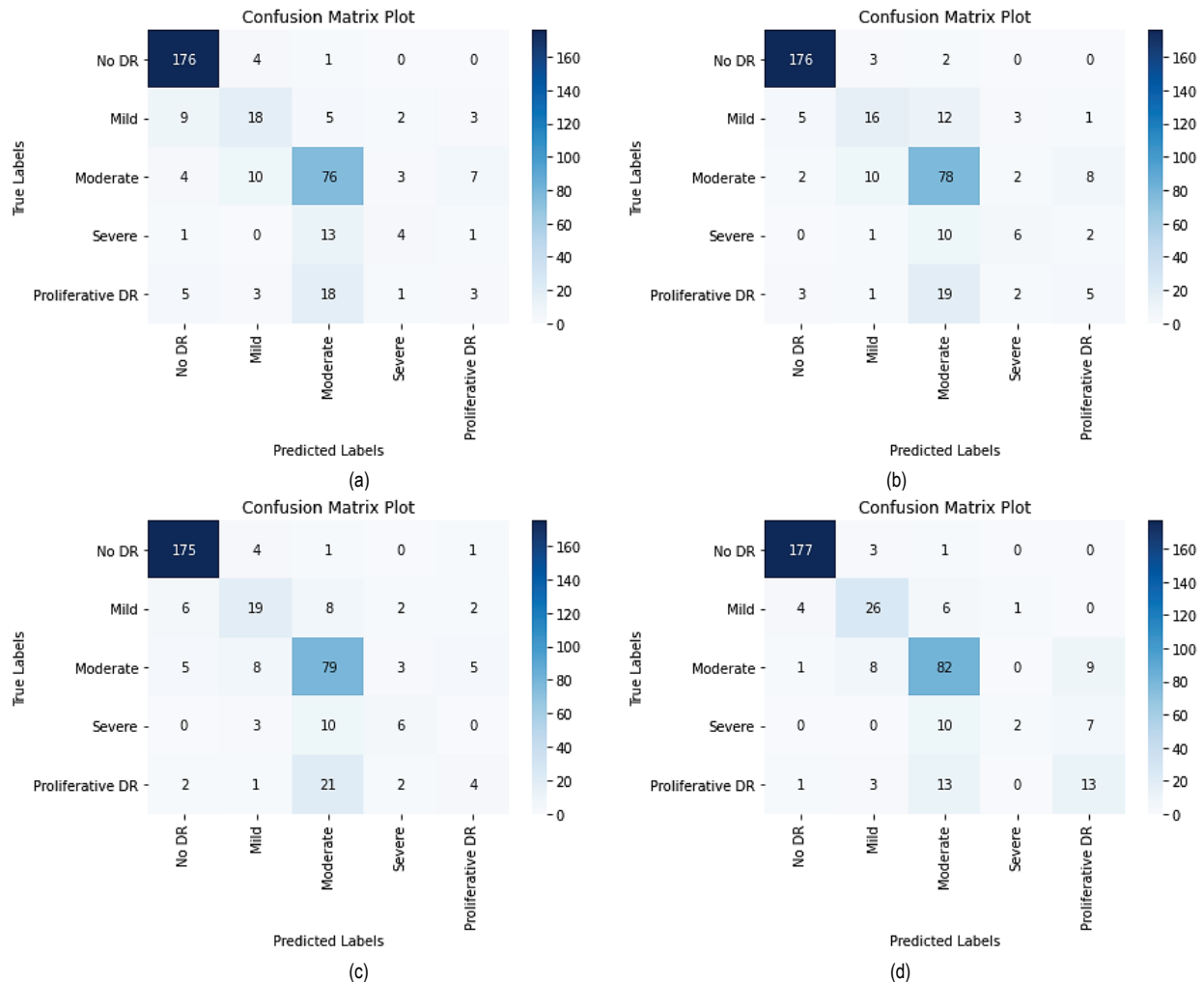
**Table 3** Accuracy and loss rate

Model	Accuracy (%)			Loss		
	Training	Validation	Test	Training	Validation	Test
VGG16 Original	98,91	73,84	75,48	0,012	2,465	2,696
VGG16 Modified Version 1	98,98	72,21	76,57	0,012	2,309	2,210
VGG16 Modified Version 2	98,67	76,29	77,11	0,026	1,558	1,793
Proposed Model	87,19	79,56	81,74	0,325	0,658	0,724

The results of the accuracy and loss rates obtained because of training the four models are given in Tab. 3. When the table is examined, it is seen that the success accuracy of the VGG16 original model is 75.47%, the VGG16 modified version 1 model which is obtained as a result of adding a 0.5 dropout layer to the classification layers of the VGG16 model is 76.57% and the VGG16 modified version 2 model which is obtained as a result of adding 0.5 dropout layer to all blocks of the VGG16 model is 77.11% on 367 images in the test dataset that are not included in the training. In parallel with the increase in test performance, the loss rates obtained in the test dataset have also decreased. The increase in the accuracy

rate and the decrease in the loss rate is because of the dropout layer. In addition, it is seen that the proposed model has a 0.5 dropout layer in all blocks and has more convolution in the first blocks and less convolution in the next blocks, reaching a high accuracy of 81.74%. In the proposed model, unlike the VGG16 model, the use of more convolutions in the first blocks significantly increased the learning success in this dataset consisting of few and disproportionate data.

The confusion matrix obtained from the test dataset consists of a total of 367 images created by taking 181, 37, 100, 19, and 30 images from the No DR, Mild DR, Moderate DR, Severe DR, and Proliferative DR classes respectively, is given in Fig. 4. When the figure is examined, it is seen that the highest performance in all four models is in the No DR and Moderate DR classes respectively, the lowest performance is in the Proliferative DR class in the VGG models used in the study and in the Severe DR class in the proposed model. It is noteworthy that in all four models, Severe DR and Proliferative DR classes are confused at most with the class Moderate DR images. Example images where Severe DR and Proliferative DR classes are confused with Moderate DR classes are given in Fig. 5. The fact that there are few images in the Severe DR class is seen as one of the obvious reasons for this situation.

**Figure 4** Confusion matrix of the models: (a) VGG16 original, VGG16 modified version 1, (c) VGG16 modified version 2, (d) proposed model

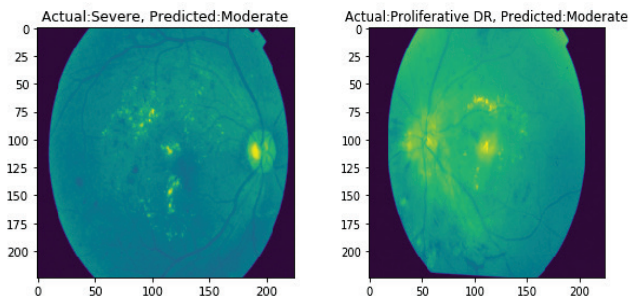


**Figure 5** Example images where the Severe DR and Proliferative DR classes are confused with the Moderate DR class

It would be beneficial to apply the proposed method, which is used in the detection of diabetic retinopathy with successful results, in areas such as Covid-19 detection and diagnosis [32, 33], fault diagnosis of electric impact drills [34], thermographic fault diagnosis of the shaft of a BLDC (Brushless Direct Current Electric) engine [35], and detection and classification of weapon types [36].

## 5 CONCLUSIONS

In this study, diabetic retinopathy disease was determined besides two different versions of the VGG16 model modified with the original, by making a new model proposed. To reveal the effect of the dropout layer, an alternative model was created by first adding the dropout layer to the classification layers of the original VGG16 model, and then another alternative model was created by adding the dropout layer at the end of all blocks of the VGG16 model. APTOS 2019 Blindness Detection dataset consisting of 5 classes and 3662 images was used to test the performance of the four models obtained with the proposed model.

According to the test results, the success rates of the VGG16 original, VGG16 modified version 1, VGG16 modified version 2, and the proposed model was 75.48%, 76.57%, 77.11%, and 81.74% respectively. An increase in test performance was observed with the effect of the dropout layer added to the VGG16 models. The highest classification success was achieved with the proposed model with an accuracy rate of 81.74%. This performance of the proposed model which is created with fewer layers is achieved by applying dense convolution in the first blocks and diluted convolution in the next blocks.

It has been observed that deep learning methods which provide successful results in the classification of images give good results in classifying diabetic retinopathy by being developed according to the dataset and the amount of data. As a result of our research, no study with better results than this study was found in the classification of diabetic retinopathy on this dataset. In cases where the number of data is low and disproportionate in the classes in the dataset, when classifying with deep learning, it is important to achieve higher performance by using models with denser first layers and decreasing convolution layers in the next layers. As a result, the proposed method will increase the diagnostic performance of specialists in the detection of diabetic

retinopathy, which occurs due to diabetes and can cause blindness. This study, which is thought to guide studies on similar datasets, is thought to be used on datasets with similar structures in different fields in future studies. In addition, our future studies will focus on the recognition of "No DR" images for diabetic retinopathy disease using different deep learning approaches.

## 6 REFERENCES

- [1] Soomro, T. A., Afifi, A. J., Zheng, L., Soomro, S., Gao, J., Hellwich, O., & Paul, M. (2019). Deep learning models for retinal blood vessels segmentation: a review. *IEEE Access*, 7, 71696-71717. <https://doi.org/10.1109/access.2019.2920616>
- [2] Khalifa, N. E. M., Loey, M., Taha, M. H. N., & Mohamed, H. N. E. T. (2019). Deep transfer learning models for medical diabetic retinopathy detection. *Acta Informatica Medica*, 27(5), 327. <https://doi.org/10.5455/aim.2019.27.327-332>
- [3] Tymchenko, B., Marchenko, P., & Spodarets, D. (2020). Deep learning approach to diabetic retinopathy detection. *arXiv preprint arXiv:2003.02261*. <https://doi.org/10.48550/arXiv.2003.02261>
- [4] Chetoui, M. & Akhloufi, M. A. (2020). Explainable diabetic retinopathy using EfficientNET. In *The 42<sup>nd</sup> Annual International Conference of the IEEE engineering in Medicine & Biology Society (EMBC)*, 1966-1969. <https://doi.org/10.1109/embc44109.2020.9175664>
- [5] Saeedi, P., Petersohn, I., Salpea, P., Malanda, B., Karuranga, S., Unwin, N., ... & IDF Diabetes Atlas Committee. (2019). Global and regional diabetes prevalence estimates for 2019 and projections for 2030 and 2045: Results from the International Diabetes Federation Diabetes Atlas. *Diabetes research and clinical practice*, 157, 107843. <https://doi.org/10.1016/j.diabres.2019.107843>
- [6] Ammal, M. A., & Gladis, D. (2021). Texture Feature Analysis in Fundus Image in Screening Diabetic Retinopathy. *Annals of the Romanian Society for Cell Biology*, 2139-2149.
- [7] Gao, Z., Li, J., Guo, J., Chen, Y., Yi, Z., & Zhong, J. (2018). Diagnosis of diabetic retinopathy using deep neural networks. *IEEE Access*, 7, 3360-3370. <https://doi.org/10.1109/access.2018.2888639>
- [8] Xu, K., Feng, D., & Mi, H. (2017). Deep convolutional neural network-based early automated detection of diabetic retinopathy using fundus image. *Molecules*, 22(12), 2054. <https://doi.org/10.3390/molecules22122054>
- [9] Albawi, S., Mohammed, T. A., & Al-Zawi, S. (2017). Understanding of a convolutional neural network. In *IEEE International Conference on Engineering and Technology (ICET)*, 1-6. <https://doi.org/10.1109/ICEngTechnol.2017.8308186>
- [10] LeCun, Y., Bengio, Y., & Hinton, G. (2015). Deep learning. *nature*, 521(7553), 436-444. <https://doi.org/10.1038/nature14539>
- [11] Litjens, G., Kooi, T., Bejnordi, B. E., Setio, A. A. A., Ciompi, F., Ghafoorian, M., ... & Sánchez, C. I. (2017). A survey on deep learning in medical image analysis. *Medical image analysis*, 42, 60-88. <https://doi.org/10.1016/j.media.2017.07.005>
- [12] Gulshan, V., Peng, L., Coram, M., Stumpe, M. C., Wu, D., Narayanaswamy, A., ... & Webster, D. R. (2016). Development and validation of a deep learning algorithm for detection of diabetic retinopathy in retinal fundus photographs. *Jama*, 316(22), 2402-2410. <https://doi.org/10.1001/jama.2016.17216>
- [13] Lam, C., Yi, D., Guo, M., & Lindsey, T. (2018). Automated detection of diabetic retinopathy using deep learning. *AMIA summits on translational science proceedings*, 2018, 147.

- [14] Wong, T. Y. & Bressler, N. M. (2016). Artificial intelligence with deep learning technology looks into diabetic retinopathy screening. *Jama*, 316(22), 2366-2367. <https://doi.org/10.1001/jama.2016.17563>
- [15] Sridhar, S. & Sanagavarapu, S. (2020, September). Detection and prognosis evaluation of diabetic retinopathy using ensemble deep convolutional neural networks. In *IEEE International Electronics Symposium (IES)*, 78-85. <https://doi.org/10.1109/IES50839.2020.9231789>
- [16] Shaban, M., Ogur, Z., Mahmoud, A., Switala, A., Shalaby, A., Abu Khalifeh, H., ... & El-Baz, A. S. (2020). A convolutional neural network for the screening and staging of diabetic retinopathy. *Plos one*, 15(6), e0233514. <https://doi.org/10.1371/journal.pone.0233514>
- [17] Sikder, N., Chowdhury, M. S., Arif, A. S. M., & Nahid, A. A. (2019, December). Early blindness detection based on retinal images using ensemble learning. In *The 22<sup>nd</sup> IEEE International Conference on Computer and Information Technology (ICCIT)*, 1-6. <https://doi.org/10.1109/ICCIT48885.2019.9038439>
- [18] Mookiah, M. R. K., Acharya, U. R., Chua, C. K., Lim, C. M., Ng, E. Y. K., & Laude, A. (2013). Computer-aided diagnosis of diabetic retinopathy: A review. *Computers in biology and medicine*, 43(12), 2136-2155. <https://doi.org/10.1016/j.combiomed.2013.10.007>
- [19] Chaturvedi, S. S., Gupta, K., Ninawe, V., & Prasad, P. S. (2020). Automated diabetic retinopathy grading using deep convolutional neural network. *arXiv preprint arXiv:2004.06334*. <https://doi.org/10.48550/arXiv.2004.06334>
- [20] Narayanan, B. N., De Silva, M. S., Hardie, R. C., Kueterman, N. K., & Ali, R. (2019). Understanding deep neural network predictions for medical imaging applications. *arXiv preprint arXiv:1912.09621*. <https://doi.org/10.48550/arXiv.1912.09621>
- [21] Kassani, S. H., Kassani, P. H., Khazaeinezhad, R., Wesolowski, M. J., Schneider, K. A., & Deters, R. (2019, December). Diabetic retinopathy classification using a modified xception architecture. In *2019 IEEE international symposium on signal processing and information technology (ISSPIT)*, 1-6. <https://doi.org/10.1109/ISSPIT47144.2019.9001846>
- [22] Dekhil, O., Naglah, A., Shaban, M., Ghazal, M., Taher, F., & Elbaz, A. (2019, December). Deep learning based method for computer aided diagnosis of diabetic retinopathy. In *IEEE International Conference on Imaging Systems and Techniques (IST)*, 1-4. <https://doi.org/10.1109/IST48021.2019.9010333>
- [23] Bodapati, J. D., Naralasetti, V., Shareef, S. N., Hakak, S., Bilal, M., Maddikunta, P. K. R., & Jo, O. (2020). Blended multi-modal deep convnet features for diabetic retinopathy severity prediction. *Electronics*, 9(6), 914. <https://doi.org/10.3390/electronics9060914>
- [24] Zhuang, H. & Ettehadi, N. (2020). Classification of diabetic retinopathy via fundus photography: Utilization of deep learning approaches to speed up disease detection. *arXiv preprint arXiv:2007.09478*. <https://doi.org/10.48550/arXiv.2007.09478>
- [25] Dondeti, V., Bodapati, J. D., Shareef, S. N., & Veeranjanyulu, N. (2020). Deep Convolution Features in Non-linear Embedding Space for Fundus Image Classification. *Revue d'Intelligence Artificielle*, 34(3), 307-313. <https://doi.org/10.18280/ria.340308>
- [26] APTOS 2019 blindness detection dataset. <https://www.kaggle.com/c/aptos2019-blindness-detection/data> (Accessed: February 10, 2021)
- [27] Pratt, H., Coenen, F., Broadbent, D. M., Harding, S. P., & Zheng, Y. (2016). Convolutional neural networks for diabetic retinopathy. *Procedia computer science*, 90, 200-205. <https://doi.org/10.1016/j.procs.2016.07.014>
- [28] Krizhevsky, A., Sutskever, I., & Hinton, G. E. (2012). Imagenet classification with deep convolutional neural networks. In: *Advances in neural information processing systems*, 1097-1105.
- [29] Simonyan, K. & Zisserman, A. (2014). Very deep convolutional networks for large-scale image recognition. *arXiv preprint arXiv:1409.1556*. <https://doi.org/10.48550/arXiv.1409.1556>
- [30] Szegedy, C., Liu, W., Jia, Y., Sermanet, P., Reed, S., Anguelov, D., ... & Rabinovich, A. (2015). Going deeper with convolutions. In *Proceedings of the IEEE conference on computer vision and pattern recognition*, 1-9. <https://doi.org/10.1109/cvpr.2015.7298594>
- [31] He, K., Zhang, X., Ren, S., & Sun, J. (2016). Deep residual learning for image recognition. In *Proceedings of the IEEE conference on computer vision and pattern recognition*, 770-778. <https://doi.org/10.1109/cvpr.2016.90>
- [32] Irfan, M., Iftikhar, M. A., Yasin, S., Draz, U., Ali, T., Hussain, S., ... & Althobiani, F. (2021). Role of hybrid deep neural networks (HDNNs), computed tomography, and chest X-rays for the detection of COVID-19. *International Journal of Environmental Research and Public Health*, 18(6), 3056. <https://doi.org/10.3390/ijerph18063056>
- [33] Almalki, Y. E., Qayyum, A., Irfan, M., Haider, N., Glowacz, A., Alshehri, F. M., ... & Rahman, S. (2021, May). A novel method for COVID-19 diagnosis using artificial intelligence in chest X-ray images. *Healthcare*, 9(5), p. 522. Multidisciplinary Digital Publishing Institute.
- [34] Glowacz, A. (2021). Fault diagnosis of electric impact drills using thermal imaging. *Measurement*, 171, 108815. <https://doi.org/10.1016/j.measurement.2020.108815>
- [35] Glowacz, A. (2022). Thermographic fault diagnosis of shaft of BLDC motor. *Sensors*, 22(21), 8537. <https://doi.org/10.3390/s22218537>
- [36] Kaya, V., Tuncer, S., & Baran, A. (2021). Detection and classification of different weapon types using deep learning. *Applied Sciences*, 11(16), 7535. <https://doi.org/10.3390/app11167535>

#### Authors' contacts:

**İsmail Akgül**, Assist. Prof.  
(Corresponding author)  
Department of Computer Engineering,  
Faculty of Engineering and Architecture,  
Erzincan Binali Yıldırım University, Erzincan, Turkey  
+904462240088; iakgul@erzincan.edu.tr

**Ömer Çağrı Yavuz**, Research Assistant  
Management Information Systems,  
Faculty of Economics and Administrative Sciences,  
Karadeniz Technical University, Trabzon, Turkey  
omercagriyavuz@ktu.edu.tr

**Uğur Yavuz**, Prof.  
Management Information Systems,  
Faculty of Economics and Administrative Sciences,  
Atatürk University, Erzurum, Turkey  
+904422312117; ugur@atauni.edu.tr

# Multicopter UAV Design and Development – Case Study

Nino Krznar, Petar Piljek\*, Zdenka Keran

**Abstract:** This paper proposes the development and production of multicopter UAV parts using additive manufacturing. A new smart design approach is needed to take advantage of additive manufacturing in terms of reducing the product weight and making the product more customizable and specific purpose-oriented while also reducing the time and cost of product development and production. This paper provides a brief overview of three additive technologies: fused deposition modelling, stereolithography, and selective laser sintering. Two different UAV modules, the avionics module and GPS holder assembly, are described and produced. Also, some design ideas and approaches are explained, such as snap-fit joints and thread joints using hex bolt pockets and metal screws. The goal of this paper is to develop and manufacture special purpose UAV parts that are durable, sustainable, and low cost. For this purpose, the additive manufacturing process is proposed and described, from the idea to the final product.

**Keywords:** additive manufacturing; fused deposition modelling; multicopter UAV; selective laser sintering; stereolithography

## 1 INTRODUCTION

Unmanned aerial vehicles (UAVs) are used in various branches of civil and military operations mostly because of their versatility and low cost [1]. Three main reasons why UAVs are more applicable in some kind of missions than piloted vehicles are: a) absence of a pilot, b) simpler design due to the no need for life support systems like temperature, pressure, and oxygen control, c) simpler and cheaper production [2]. UAV multicopters are getting more popular for use in various kinds of missions that can be dull, dirty, or dangerous for human pilots [3–5]. Despite the relatively short range and flight time, multicopter UAVs find good use in applications like video and photo capturing [1], surveillance [3], crop inspection [1], fire detection [1], agricultural crop control [6], disaster monitoring [4–6], item delivery [1], robotics and education [7], military missions [8], even space missions [9]. Some of the advantages of UAV multicopters are vertical take-off, versatile design, ability to hover [1, 2].

When it comes to multicopters, their design is often not overly complex. However, because of UAV's rapid development, product development engineers need cheap and fast production technologies for rapid prototyping and fast product development [10]. Additive manufacturing allows quick testing of new designs in real life and has widely contributed to the fast development of multicopter UAVs [11]. In addition to being reliable, multicopters must also be lightweight, configured for specific purposes (specialized), and often of unconventional design to achieve longer flight times [12]. Additive manufacturing technologies offer valuable tools for UAV development and production [3–5]. Multicopter UAVs can come in different configurations regarding the number of rotors (propellers) [7]. The most common multicopter configurations are with four [13, 14], six [7], or eight [7] rotors, as shown in Fig. 1. Furthermore, UAVs can have tilted rotors that enable fully actuated control therefore, such configurations can move in a horizontal plane without tilting [7]. Due to the simplicity of design and straightforward operation, there is an enormous growth of multicopters in the market [1]. They can be controlled remotely or fly autonomously.

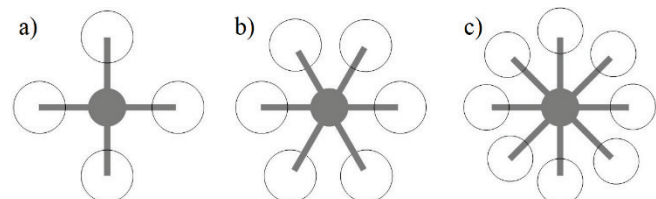


Figure 1 Multicopter configurations: a) 4 rotors, b) 6 rotors, c) 8 rotors

Multicopter parts are exposed to many different kinds of loads, thrust forces of propellers, wind forces, impacts, and weight of mounted objects [1]. Different multicopter modules must be designed in such way that it ensures structural stability under static and dynamic loads. Regarding the mechanical properties of 3D printed multicopter parts, several parameters to be considered, but the most important ones are the 3D printing direction and the orientation of object during printing [1]. In the design and development of multicopters amongst other production techniques, additive technologies often find very good use [6, 15]. Rapid prototyping technologies are also suitable for the production of special purpose multicopters as this type of aircraft usually requires individual production or the production of only a few aircraft [8, 16]. One of the most popular additive manufacturing technologies is Fused Deposition Modelling (FDM) due to its simplicity and low cost [1]. In addition, Selective Laser Sintering (SLS) and Stereolithography (SLA), can also be used for the production and development of UAV parts [17, 18].

Additive manufacturing can offer a new approach to design which can lead to innovative designs and also cut the time of the process from idea to final product [18, 19]. By shortening the time for the development of parts or whole products, the costs of the product can be reduced significantly [20]. Therefore, additive technologies are increasingly used for the development and production of UAVs [11]. In this work test parts for UAV multicopter have been designed and developed for additive manufacturing. Additive manufacturing technologies are used to produce several multicopter parts. The only parts not produced with additive

manufacturing technologies are prefabricated low-cost standardized carbon fibre tubes, bolts, screws, propellers, motors, batteries, and onboard electronics. All multirotor parts produced by additive manufacturing can easily be scaled, resized, modified, and customized by adding features, holes, and slots for electronic parts.

## 2 ADDITIVE MANUFACTURING

Additive manufacturing (AM) processes are useful for rapid prototyping and product development, particularly for UAVs [11, 15]. The use of additive technologies can cut the development time significantly which reduces the costs and the price of the final product as well [11, 16]. The time required to get from the developer's idea to the finished product is reduced since it is possible to produce test parts faster with AM than using conventional manufacturing technologies which often include additional costs for tooling, moulding, machining, and other [17,21]. Also, AM allows the production of parts directly from a solid CAD model [11, 17]. Today, AM is commonly used to produce UAV parts and users can easily produce UAV replacement parts on low-budget 3D printers available on the market [9]. Thus, in the case of damage or breakage of individual parts due to the crash of the UAV, AM is suitable for the production of spare parts, which may include even propellers [18]. Additive manufacturing is a broad term that encompasses multiple additive manufacturing technologies [19–21]. Commonly used additive manufacturing technologies are:

- FDM – Fused Deposition Modelling,
- SLS – Selective Laser Sintering,
- SLA – Stereolithography.

There is a wide range of materials used in 3D printing, from metals, composites, and ceramics to hard and soft polymers [22, 23]. These softer materials are suitable for "soft robotics". Robots are usually constructed from hard materials like metal and hard plastics. To create parts of the robot that are more like soft materials found in nature, like skin and muscles, materials like rubber, hydrogels, and silicones are used. Additive technologies give us a possibility to produce parts with these softer materials which have Young's modulus around  $10^4$ – $10^9$  Pa [23].

### 2.1 Fused Deposition Modelling

FDM (Fused Deposition Modelling) is manufacturing technology where objects are created by extruding a thermoplastic filament through a heated nozzle [6]. The whole process starts with creating a 3D CAD model and exporting it into an STL format [22]. The model is then cut into horizontal slices in the CAM software [17]. Nozzle paths are calculated by the software according to parameters set by the user. In this technique, the polymer filaments are fed to an extruder and then deposited on a platform through a nozzle moving in the XY plane, layer by layer [24]. Semi-melted thermoplastic material is pushed through a nozzle to be merged with the material from the previous layer on the part. When one layer is done, the entire platform will move

vertically and apply a new layer to the previous one. Part is being built from the bottom to the top by moving the nozzle in the XY plane and by moving the platform in Z-direction [25]. Slices are usually thick between 0.1 mm and 0.3 mm [11]. Fig. 2 shows a working mechanism of the FDM process.

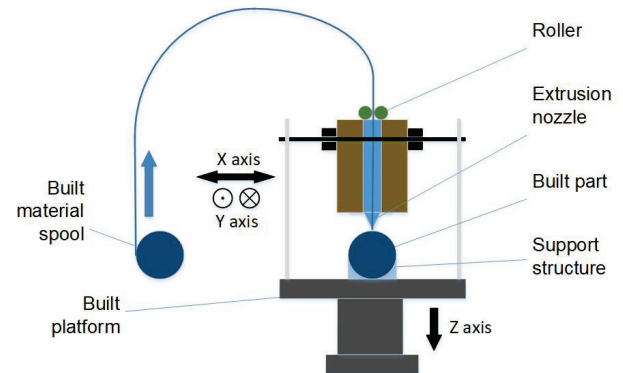


Figure 2 FMD working mechanism [1]

Various parameters can be set in the FDM process, such as layer thickness and height, number of shells (number of layers in the outer wall), infill percentage and geometry, built platform temperature, nozzle temperature and extrusion speed [1, 9]. These parameters are set in machine software after loading and positioning the STL file. The software then generates all the trajectories of the machine axes, extrusion speed, temperature, and behaviour of the machine according to the parameters set by the user [26]. Most common materials used in FDM are ABS (Acrylonitrile Butadiene Styrene), PLA (Polylactic Acid), PC (Polycarbonate), ASA (Acrylic Styrene Acrylonitrile), PPSF/PPSU (Polyphenylsulfone), ULTEM (trade name for a PEI (polyetherimide) variant), PE-HD/PH-HD (High-density Polyethylene), PE-LD (Low-density Polyethylene), PET (Polyethylene Terephthalate), and others [1, 11]. Also, it's possible to use composite materials in the FDM process [15, 27]. On the market, FDM 3D printers are available from low-cost desktop printers to more expensive industrial machines [1].

### 2.2 Selective Laser Sintering

SLS (Selective Laser Sintering) is a technology more suitable for industrial applications than other 3D printing methods [18]. SLS building material is available in powder form which is sintered using lasers to create the desired geometry [6, 28]. The powder is fed to the building chamber using rollers and piston and then is very accurately fused using laser beams [28]. This process does not require a support structure, since the unsintered powder provides the support for the object in the making [1]. With SLS is possible to make more complex plastic, metal, and ceramic parts that do not require a support structure [28]. Depending on the building material, the power of the laser system varies. To achieve certain mechanical properties of finish quality, further processing of part is needed, such as machining and/or heat treatment or coating [28]. Fig. 3 is showing the working mechanism of SLS.

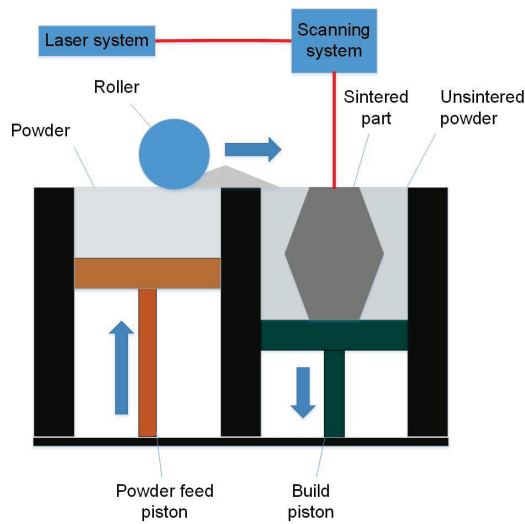


Figure 3 SLS working mechanism [1]

### 2.3 Stereolithography

Stereolithography (SLA) is an AM process in which objects are created by curing a polymer resin, using a UV laser beam in certain coordinates, layer by layer respectfully to the CAD model [6]. When one layer is cured by the laser, the built platform moves in the Z-direction and the new layer can be cured [28]. Materials for SLA are liquid form photosensitive thermoset polymers. With this procedure, it is possible to achieve high accuracy and smooth surface and it is the most cost-effective AM technology [6, 28]. In SLA laser is being focused with the mirror scanning system that cures the polymer resin with very high accuracy, which creates a smooth surface of the built object [1, 28]. However, SLA parts do not have particularly good mechanical properties compared to other AM technologies, so the use of SLA for UAVs is limited for the structural parts of the UAV, but it is very useful for rapid prototyping and development [1]. SLA is the first AM technology developed in 1986 by 3D Systems and it is first commercially available AM technology [6, 28]. Fig. 4 shows a working mechanism of the SLA process.

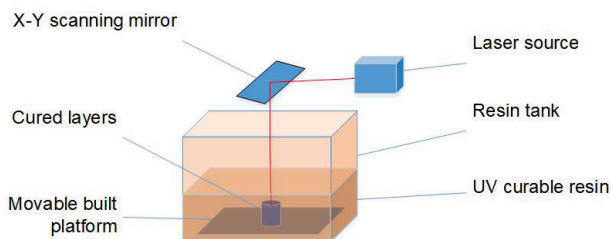


Figure 4 SLA working mechanism [1]

## 3 UAV DESIGN PROCES FOR ADDITIVE MANUFACTURING

AM technologies have certain advantages over conventional manufacturing technologies regarding design and production [17]. AM enables a new approach to 3D design without restrictions of conventional production

techniques. Regarding manufacturing, AM offers low-cost production for smaller series without costs of tooling, moulding and machining [11]. In 3D design for AM, certain elements of the part need to be considered, such as requirements and use of 3D printed parts [29]. Engineers should take into consideration the thickness of the part, infill density and possibly add ribs and profiles for reinforcements [1, 9]. AM works very well in combination with low-cost standardized parts like screws and bolts for tight joints. For example, instead of 3D modelling and printing of threads, a hexagon pocket is made in part with the metal bolt to get a quality thread joint [30]. This kind of joint is commonly used in additive manufactured products because it's simplicity and low cost, as shown in Fig. 5. Another type of joint to be considered is the "snap-fit" joint, where one part fits and snaps to another creating a tight joint until physically separated, which is shown in Fig. 6 [19].

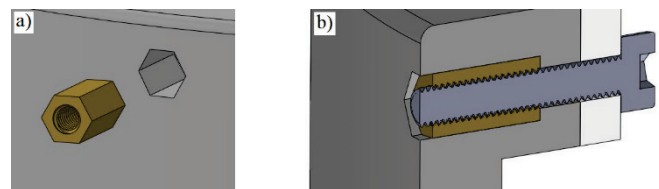


Figure 5 Thread joint: a) Pocket for Hex bolt, b) Cross-section of thread joint

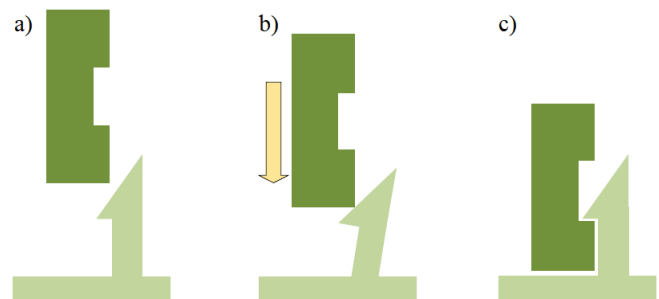


Figure 6 Snap-Fit Joint: a) separated, b) joining process, c) assembled

Snap-fit joints give the possibility to eliminate the use of screws and bolts which can decrease the mass of UAVs and enable easier and faster assembly and disassembly [18, 19]. Very few design instructions and guidelines of 3D design for AM have been published so the process of design can be a challenge, but with the liberty of layer-by-layer production, the 3D design process can result in very innovative designs and solutions [29, 31]. Another thing to consider is machine parameters set by the user in machine software. User can define the number of shells which means a number of outer solid layers of solid material, and infill density which affects the mass and mechanical properties of the product [6, 22]. There are many different infill patterns possible to use which also affect the mechanical properties of the product. Different infill patterns are used to achieve high-strength and low-weight structures for UAV parts. Also using different infill patterns can improve material usage efficiency [29, 32, 33]. Fig. 7 shows some of the possible infill patterns in 3D printing.

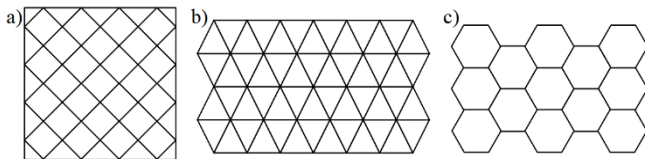


Figure 7 Infill patterns: a) square, b) triangle, c) honeycomb

User can also define parameters of the printing process such as printing bed and nozzle temperature, printing speed, support material usage and more [15, 17]. Fig. 8 is showing the entire process from the idea to the final product.

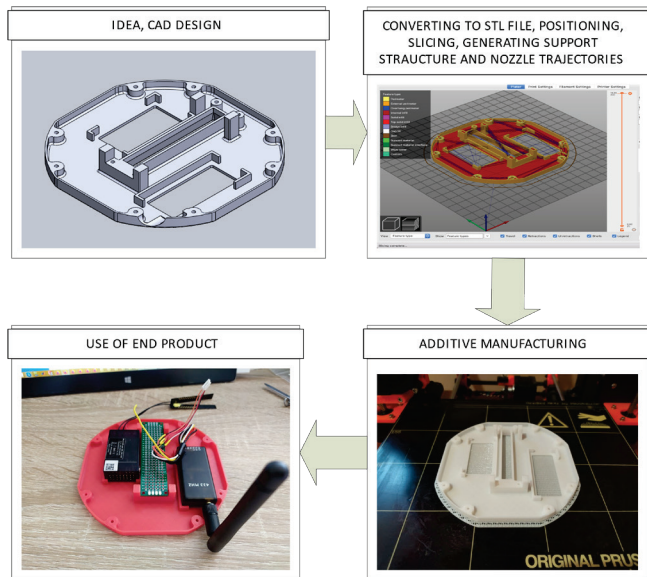


Figure 8 From idea to final product

There are a few requirements for the UAV test parts: structures should be lightweight, durable, and have a modular design (UAV systems and subsystems) [29]. Multirotors today are built mostly using conventional production technologies like injection moulding for plastic parts and using sheet materials cut into the desired shape. For smaller series, personalized products, and special purpose UAVs, AM technologies are more suitable if desired requirements are met [19]. Lightweight carbon fibre parts have good mechanical properties, therefore, are practical to use in combination with 3D printed parts for UAV assemblies [20].

## 4 DEVELOPMENT OF MULTIROTOR UAV MODULES

UAV consists of several systems and sub-systems or modules. The final assembly is divided into smaller modules some of which are: avionics, propulsion system, and electronics. All these modules work together in the final assembly as a harmonious system. The following section will detail components for two different UAV sub-systems fabricated using FDM additive technology.

### 4.1 Avionics

The avionics module housing provides housing and support for the electronics of the UAV. AM allow a specific

housing design to fit specific electronic components particular for this UAV version. As this part of UAV will not be subjected to any mechanical load during use and the surface quality is not critical factor for functionality, the layer thickness was only considered for achieving satisfactory dimensional accuracy to ensure tight fit during electronic components assembly, resulting in a layer thickness of 0.2 mm. The infill pattern used for housing is also not critical factor since relatively thin walls require little or no infill making any infill pattern sufficient. The material used was PET-G, which provides high UV resistance and some flexibility before breaking, enabling it to handle tight fits during electronic component assembly. Fig. 9 shows the assembly model of the avionics housing part with visible openings and pockets designed to fit electronic components and to provide rigid and non-movable support. Assembly has two parts which are connected by screws and hex bolts. Inside of housing are 3D shapes that hold electronic parts and cables securely in place. The production time for all the parts related to this avionics module housing was approximately 4.5 hours.

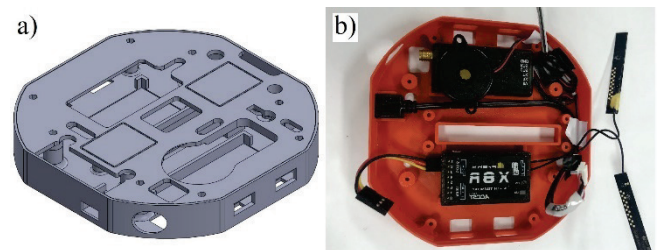


Figure 9 Avionics housing module: a) CAD model, b) 3D printed assembly

### 4.2 Foldable GPS Holder

3D CAD models and 3D printed GPS holder parts are shown in Fig. 10. The base part is connected to the avionics module by screw and bolt joints. Screws and bolts are also used to connect the rotary joint. Due to the rotary joint, the GPS holder can be folded when not in use. To ensure good mechanical properties, high dimensional accuracy, and smooth operation of holder folding and sliding of locking brackets, a layer thickness was 0.01 mm. The rods are printed using honeycomb infill to ensure required strength and lightness. To achieve good strength and sliding properties together with UV resistance, Nylon was chosen as the printing material. Furthermore, it is crucial to determine the correct orientation of the part on the printing bed to achieve desired mechanical properties. The strength will be improved in planes parallel to the printing bed, and the best sliding properties are achieved in the direction along the printed thread. The time required to fabricate all the parts necessary for the foldable GPS holder was approximately 7 hours. Low-cost additive technology allows more iterations of printing and design which is often the product development process when using AM. The GPS module can fit perfectly into the holder because it is 3D designed especially for this GPS element and produced with low-cost FDM additive technology. All parts are designed especially for use on this

UAV and can be modified and produced with any AM technology with low production and development costs.

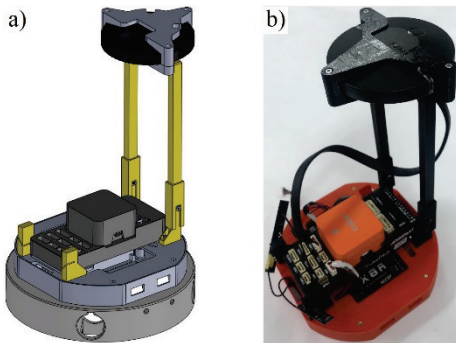


Figure 10 GPS holder: a) CAD model, b) 3D printed assembly

## 5 CONCLUSION

Additive technologies offer new possibilities in the manufacturing and rapid prototyping of products. New approaches in design for AM enable the faster creation of lighter UAVs that are easy to assemble. That is desirable for product development and design of UAV parts using trial and error methods.

The paper discusses various low-cost and effective joint techniques commonly used in 3D printing and some solutions for part reinforcement. These options are presented to overview the options available in the 3D printing world. The paper lists the materials and printing parameters utilized to fabricate the showcased UAV parts (avionics housing and foldable GPS holder). However, the determination of the appropriate material, adjustment of printing parameters required to achieve successful printing, desired dimensional accuracy, and mechanical properties of the parts, are not further discussed and are beyond the scope of this paper. For future work, other AM procedures will be conducted using different build materials and parameters. 3D printing of composite materials could offer better mechanical properties of parts and with little or no increase in mass, especially with different approaches in the design of UAVs.

The use of AM in the production and development of UAVs is an addition to advances in electronics and materials science which widely contribute to the growing use of UAVs in different fields of applications. AM is not only useful in rapid prototyping but also for the production of specific parts and small series of UAVs. Using AM engineers have the ability to create complex geometries without using expensive traditional technologies, tooling and machining, which is especially useful for the production of UAV parts that are mostly in small series and very specific from product to product. Thanks to AM, the production of parts has moved from factories to office desktops, homes, and development departments, resulting in the rapid development of UAVs.

## Acknowledgements

This research was funded by European Regional Development Fund, Operational programme competitiveness

and cohesion 2014–2020, grant number KK.01.1.1.04.0092 and the APC was funded by KK.01.1.1.04.0092.

## 6 REFERENCES

- [1] Piljek, P., Krznar, N., Krznar, M., & Kotarski, D. (2022). Framework for Design and Additive Manufacturing of Specialised Multirotor UAV Parts. In Răzvan Păcurar (Ed.), Trends and Opportunities of Rapid Prototyping Technologies [Working Title]. IntechOpen. <https://doi.org/10.5772/intechopen.102781>
- [2] Ferro, C. G., Mazza, A., Belmonte, D., Secli, C., & Maggiore, P. (2017). A Comparison between 3D Printing and Milling Process for a Spar Cap Fitting (Wing-fuselage) of UAV Aircraft. *Procedia CIRP*, 62, 487-493. <https://doi.org/10.1016/j.procir.2016.06.028>
- [3] Hell, P. M. & Varga, P. J. (2019). Drone Systems for Factory Security and Surveillance. *Interdisciplinary Description of Complex Systems*, 17, 458-467. <https://doi.org/10.7906/indcs.17.3.4>
- [4] Kiss-Leizer, G. K. & Tokody, D. (2017). Radiofrequency Identification by using Drones in Railway Accidents and Disaster Situations. *Interdisciplinary Description of Complex Systems*, 15, 114-132. <https://doi.org/10.7906/indcs.15.2.1>
- [5] Kiss-Leizer, G. K. (2018). Possible Areas of Application of Drones in Waste Management during Rail Accidents and Disasters. *Interdisciplinary Description of Complex Systems*, 16, 360-368. <https://doi.org/10.7906/indcs.16.3.8>
- [6] Goh, G. D., Agarwala, S., Goh, G. L., Dikshit, V., Sing, S. L., & Yeong, W. Y. (2017). Additive manufacturing in unmanned aerial vehicles (UAVs): Challenges and potential. *Aerospace Science and Technology*, 63, 140-151. <https://doi.org/10.1016/j.ast.2016.12.019>
- [7] Kotarski, D., Piljek, P., Pranjić, M., Grlj, C. G., & Kasac, J. (2021). A Modular Multirotor Unmanned Aerial Vehicle Design Approach for Development of an Engineering Education Platform. *Sensors*, 21(8), 2737. <https://doi.org/10.3390/s21082737>
- [8] Udayagiri, C., Kulkarni, M., Balasubramanian, E., Pakiriswamy, S., & Yang, L. J. (2016). Experimental studies on 3D printed parts for rapid prototyping of micro aerial vehicles. *Journal of Applied Science and Engineering*, 19, 17-22. <https://doi.org/10.6180/jase.2016.19.1.03>
- [9] Dordolova, C. (2020). A Design for Qualification Framework for the Development of Additive Manufacturing Components—A Case Study from the Space Industry. *Aerospace*, 7(3), 25. <https://doi.org/10.3390/aerospace7030025>
- [10] Bai, W., Fang, H., Wang, Y., Zeng, Q., Hu, G., Bao, G., & Wan, Y. (2011). Academic Insights and Perspectives in 3D Printing: A Bibliometric Review. *Applied Sciences*, 11(18), 8298. <https://doi.org/10.3390/app11188298>
- [11] Ferro, C., Grassi, R., Secli, C., & Maggiore, P. (2016). Additive Manufacturing Offers New Opportunities in UAV Research. *Procedia CIRP*, 41, 1004-1010. <https://doi.org/10.1016/j.procir.2015.12.104>
- [12] Balasubramanian, E., Sagar, N. V. S. S., Chandrasekhar, U., & Salunkhe, S. (2019). Development of light weight multi-rotor UAV structures through synergistic application of design analysis and fused deposition modelling. *International Journal of Materials and Product Technology*, 59(3), (2019) 229-238. <https://doi.org/10.1504/IJMPT.2019.102933>
- [13] Kotarski, D., Benic, Z., & Krznar, M. (2016). Control Design for Unmanned Aerial Vehicles with Four Rotors. *Interdisciplinary Description of Complex Systems*, 14(2), 236-245. <https://doi.org/10.7906/indcs.14.2.12>

- [14] Benic, Z., Piljek, P., & Kotarski, D. (2016). Mathematical Modelling of Unmanned Aerial Vehicles with Four Rotors. *Interdisciplinary Description of Complex Systems*, 14(1), 88-100. <https://doi.org/10.7906/index.14.1.9>
- [15] Galatas, A., Hassanin, H., Zweiri, Y., & Seneviratne, L. (2018). Additive Manufactured Sandwich Composite/ABS Parts for Unmanned Aerial Vehicle Applications. *Polymers*, 10(11), 1262. <https://doi.org/10.3390/polym10111262>
- [16] Aktas, Y. O., Ozdemir, U., Dereli, Y., Tarhan, A. F., Cetin, A., Vuruskan, A., Yuksek, B., Cengiz, H., Basdemir, S., Ucar, M., Gencav, M., Yukselen, A., Ozkol, I., Kaya, M. O., & Inalhan, G. (2016) Rapid Prototyping of a Fixed-Wing VTOL UAV for Design Testing. *Journal of Intelligent and Robotic Systems*, 84, 639-664. <https://doi.org/10.1007/s10846-015-0328-6>
- [17] Scott, J. A., Gupta, N., Wember, C., Newsom, S., Wohlers, T., & Caffrey, T. (2012). Additive Manufacturing: Status and Opportunities. *Science and Technology Policy Institute*, Washington, DC, 1-29. Retrieved from <https://www.researchgate.net/publication/312153354>
- [18] Klahn, C., Leutenecker, B., & Meboldt, M. (2014) Design for Additive Manufacturing – Supporting the Substitution of Components in Series Products. *Procedia CIRP*, 21, 138-143. <https://doi.org/10.1016/j.procir.2014.03.145>
- [19] Klahn, C., Singer, D., & Meboldt, M. (2016) Design Guidelines for Additive Manufactured Snap-Fit Joints. *Procedia CIRP*, 50, 264-269. <https://doi.org/10.1016/j.procir.2016.04.130>
- [20] Vaneker, T. H. J. (2017). The Role of Design for Additive Manufacturing in the Successful Economical Introduction of AM. *Procedia CIRP*, 60, 181-186. <https://doi.org/10.1016/j.procir.2017.02.012>
- [21] Jung, S. & Simpson, T. W. (2018). Product family redesign using additive manufacturing. In *44th Design Automation Conference (Proceedings of the ASME Design Engineering Technical Conference; Vol. 2B-2018)*. American Society of Mechanical Engineers (ASME). <https://doi.org/10.1115/DETC2018-85627>
- [22] Krznar, N., Kos, J., & Pilipovic, A. (2015). Application of reverse engineering in the development of polymer products for manufacturing by additive technologies. In *15th International Scientific conference on production engineering – CIM2015*, 10.-13.06.2015., Vodice, Croatia. Retrieved from <https://www.researchgate.net/publication/280717310>
- [23] Curkovic, P. & Jambrecic, A. (2020) Improving Structural Design of Soft Actuators Using Finite Element Method Analysis. *Interdisciplinary Description of Complex Systems*, 18(4), 490-500. <https://doi.org/10.7906/index.18.4.8>
- [24] Sanchez Ramirez, A., Islán Marcos, M. E., Blaya Haro, F., D'Amato, R., Sant, R., & Porras, J. (2019). Application of FDM technology to reduce aerodynamic drag. *Rapid Prototyping Journal*, 25(4), 781-791. <https://doi.org/10.1108/RPJ-09-2018-0251>
- [25] Pascariu, I. S. & Zaharia, S. M. (2020). Design and Testing of an Unmanned Aerial Vehicle Manufactured by Fused Deposition Modeling. *Journal of Aerospace Engineering*, 33(4), 06020002. [https://doi.org/10.1061/\(ASCE\)AS.1943-5525.0001154](https://doi.org/10.1061/(ASCE)AS.1943-5525.0001154)
- [26] Stucker, B. (2012). Additive manufacturing technologies: technology introduction and business implications. In *Frontiers of Engineering: Reports on Leading-Edge Engineering From the 2011 Symposium*, National Academies Press, Washington, DC, 5-14. Retrieved from <https://nap.nationalacademies.org/read/13274/chapter/4>
- [27] Azarov, A. V., Antonov, F. K., Golubev, M. V., Khaziev, A. R., & Ushanov, S. A. (2019). Composite 3D printing for the small size unmanned aerial vehicle structure. *Composites Part B: Engineering*, 169, 157-163. <https://doi.org/10.1016/j.compositesb.2019.03.073>
- [28] Grames, E. (2019). SLA vs SLS: The Differences – Simply Explained. Retrieved from <https://all3dp.com/2/sla-vs-sls-3d-printing-technology-shootout/>
- [29] Moon, S. K., Tan, Y. E., Hwang, J., & Yoon, Y. J. (2014). Application of 3D printing technology for designing light-weight unmanned aerial vehicle wing structures. *International Journal of Precision Engineering and Manufacturing - Green Technology*, 1, 223-228. <https://doi.org/10.1007/s40684-014-0028-x>
- [30] Krznar, N., Pilipovic, A., & Serce, M., (2016). Additive Manufacturing of Fixture for Automated 3D Scanning – Case Study. *Procedia Engineering*, 149, 197-202. <https://doi.org/10.1016/j.proeng.2016.06.656>
- [31] Booth, J. W., Alperovich, J., Chawla, P., Ma, J., Reid, T. N., & Ramani, K. (2017). The Design for Additive Manufacturing Worksheet. *ASME Journal of Mechanical Design*, 139(10), 100904. <https://doi.org/10.1115/1.4037251>
- [32] Alejandrino, J. D., Concepcion, R. S., Lauguico, S. C., Tobias, R. R., Venancio, L., Macasaet, D., Bandala, A. A., & Dadios, E. P. (2020). A machine learning approach of lattice infill pattern for increasing material efficiency in additive manufacturing processes. *International Journal of Mechanical Engineering and Robotics Research*, 9(9), 1253-1263. <https://doi.org/10.18178/ijmerr.9.9.1253-1263>
- [33] Hoang, V. N., Tran, P., Nguyen, N. L., Hackl, K., & Nguyen-Xuan, H. (2020). Adaptive Concurrent Topology Optimization of Coated Structures with Nonperiodic Infill for Additive Manufacturing. *Computer-Aided Design*, 129, 102918. <https://doi.org/10.1016/j.cad.2020.102918>

#### Authors' contacts:

**Nino Krznar**, MSc

University of Zagreb, Faculty of Mechanical Engineering and Naval Architecture,  
Ivana Lučića 5, 10002 Zagreb, Croatia  
nino.krznar@fsb.hr

**Petar Piljek**, PhD, Assistant Professor

(Corresponding author)

University of Zagreb, Faculty of Mechanical Engineering and Naval Architecture,  
Ivana Lučića 5, 10002 Zagreb, Croatia  
petar.piljek@fsb.hr

**Zdenka Keran**, PhD, Associate Professor

University of Zagreb, Faculty of Mechanical Engineering and Naval Architecture,  
Ivana Lučića 5, 10002 Zagreb, Croatia  
zdenka.keran@fsb.hr

# Allocating Safety Cost using in Construction Site

Yong-woo Kim, Sangchul Kim\*

**Abstract:** Environments, Health, and Safety (EHS) activities are strongly linked to the concept of sustainability in the current construction industry and consequently absorb more financial and managerial attention. One of major obstacles in EHS costing is that most EHS costs are buried in general overhead costs. Therefore, EHS costs lacks transparency, making it hard to allocate EHS costs to relevant construction projects. This paper present a recent study in which a method of activity-based costing (ABC) has been applied to safety costs at a contractor's home office. The list of safety activities, their cost drivers as well as their cost information on one of Korean general contractor is provided. The authors expect that the application of ABC will improve transparency in costing EHS costs as well as allocating EHS costs to projects.

**Keywords:** budget; safety accident; safety management; safety law

## 1 INTRODUCTION

Environments, Health, and Safety (EHS) activities are strongly linked to the concept of sustainability in the current construction industry and consequently absorb more financial and managerial attention. EHS activities can be carried out for a variety of purposes, from activities related to preventing safety accidents to administrative activities responding to an accident when it occurs. EHS activities are perceived critical activities that affects sustainability for the next generation. However, it is challenging to quantify the costs of EHS activities.

One of major obstacles in EHS costing is that most EHS costs are buried in general overhead costs, but none of them directly attempt to capture the full scope of measures taken to meet/exceed environmental, health, or safety standards. Therefore, EHS costs lacks transparency, making it hard to allocate EHS costs to relevant construction projects.

For the most part, the job is entirely performed by subcontractors. So general contractor (GC) don't see line items for EHS cost, such as "safety costs" or "fall prevention costs". For example, the framer's contract will have just a few schedule of value (SOV) line items, and when they bill GC the SOV will list a % complete for framing on levels 1, 2, 3, or 4. Some costs are more obvious to capture. And another example is that GC had to hire a third party testing agency to perform an air barrier test to conform to the design specification. These costs were considered soft costs though, so those billings were routed through the ownership entity accounting rather than the GC's accounting.

If GC really wanted to track this closer, GC would include separate line items in every contract that forced the subcontractor to bill GC for EHS work done. The problem is that makes the billings too complicated, which consumes a lot of our time on the back end correcting billing statements before GC send it to the lender to get funded. And few publications exist on methodology for tracking the overhead costs associated with environmental, health and safety initiatives on projects.

Generally a general contractor estimate EHS costs by assigning a certain percentage of total construction costs since it is challenging to accurately estimate the EHS costs. However, such practice remains potential financial risks

since a general contractor does not know accurate EHS costs. In this paper, we chose safety costs in general overhead costs for the case study. Given that contractors pay more safety costs than before, it is important for contractors to accurately measure safety costs on each project. While project safety costs can be easily tracked, it is hard to measure how much safety costs of general overhead costs is spent on each project.

The purpose of this research paper is to show how allocating safety overhead costs to construction projects can be distorted using traditional volume-based allocation method, and propose adopting activity-based costing which allows for accurate allocation of safety overhead costs. We also addressed the potential benefits along with the case study.

## 2 SAFETY COSTS

Safety cost could be defined as "the cost of the resources, goods and services employed in order to improve working conditions and to reduce the accident rate". Safety costs can be grouped into prevention costs and evaluation and monitoring costs [1]. The guideline to calculate safety costs in Korea is in contract regulation by the Ministry of Strategy and Finance [2]. The cost of safety on each project is calculated by a percentage of project direct cost. The standard of safety cost is stipulated by the Occupation Safety and Health Act by the Ministry of Employment and Labor [3].

**Table 1** Safety cost based on construction type and cost (Unit: \$) [4]

Type	Cost			
	Under 0.5 mil (X)	Over 0.5 mil to Under 5mil (C)	Over 5 mil (X)	
General (1)	2.93%	1.86%	5,349	1.97%
General (2): Lift, cable car etc.	3.09%	1.99%	5,499	2.10%
Heavy civil	3.43%	2.35%	5,400	2.44%
Rail and track	2.45%	1.57%	4,411	1.66%
Unique and etc.	1.85%	1.20%	3,250	1.27%
Safety cost	Direct cost $\times X$	Direct $\times X + C$		Direct cost $\times X$

Details on the method of calculating safety costs are presented in above Tab. 1. As seen in Tab. 1, different

percentage of project types is applied [4]. In general, a general contractor determines safety costs by multiplying construction costs by a certain percentage as seen in Tab. 1.

However, a research team note that many general contractors deliberately underestimate construction project costs overall in order to win bids, therefore, they underestimate safety and environmental costs the most [5].

Though the guideline differentiates the project types, it does not reflect the project context that each project has. Some project needs more resources in managing safety while some do not. Without accurately measuring safety costs of each project, contractors have difficulty in improving processes associated with safety management.

### 3 ACTIVITY-BASED COSTING

According to previous research [6], overhead cost management tool serves two roles: (1) it should offer precise quotation on cost objects; and (2) it should come up with decreasing total costs without losing its worth. Precise distribution of overall overhead costs to projects is vital for two reasons. First, exact distribution of the overall overhead costs offers the overall supplier with precise information on profits for each project. Second, exact cost information on each project allows the overall contractor to guess the costs on the forthcoming projects more correctly, putting him or her in a superior location in bidding for a future job.

Activity-based costing (ABC), a new accounting technique, has been created as a means of resolving the issues with traditional cost accounting, including (1) its failure to contribute to the reduction of overall costs and (2) cost distortion brought on by the incorrect allocation of overhead costs. A production system or organization's activities can be identified using the accounting methodology known as "activity-based costing" [7].

An ABC system has the following characteristics:

- 1) ABC uses two-stage costing Using resource cost drivers, general ledger accounts (i.e., resource costing) are linked in the right proportion to different activities (e.g., time or area). Using activity cost drivers, activity costs are subsequently allocated to final cost objects [8].
- 2) ABC System Recognizes Different Types of Activities (Hierarchy): The product unit level, the cluster level, the product sustaining level, and the provision sustaining level are the four standard levels of operations in the ABC system used in manufacturing [9-11]. ABC systems are frequently used in the building industry to benefit from a cost hierarchy with many levels of activities, including work division level, project level, and organization level [6, 12].

## 4 CASE STUDY

### 4.1 Background

This research deals with the overall overhead costs of an overall contractor in Korea. The sample business had 2021 sales of more than \$9 billion USD [13] and was listed among the top 30 builders in Engineering News-ranking Record's of the Top 250 International Contractors for 2021 [14]. The

sample contractor, XYZ, has five business sections: infrastructure, power, plant, architecture, and miscellaneous department.

Company XYZ spends about 1% of its sales revenue on on-site safety management expenses; the same amount of 1% is spent on the headquarters team for on-site support. Therefore, about 2% of sales revenue is being spent as a safety cost. The study focuses only on safety costs out of general overhead costs.

### 4.2 System Objectives and Cost Objects

The ABC system has twelve projects, each of which is cost object. Twelve projects are categorized into three business sectors: residential construction, commercial construction, and heavy civil construction. Therefore, we can use three business sectors by configuring overhead costs allocated to each project.

### 4.3 Data Collection Method

Interview and survey were employed for collection. The research team used open-ended questions for the interviews with key personnel of the safety department of XYZ. The questions included organizational structure, communication channels, and key activities of the department. Interview responses helped the research team develop a list of the activity centers and the activity. Once activities is identified, the research team used a time-effort way [15] in which a survey was used to identify every staff in the department to identify % of the staff's time consumed on each activity.

Table 2 Activity List

Activity Center	Activity ID	Activity
Safety Training	S-1-01	Plan Training
	S-1-02	Develop/Update Training Materials
	S-1-03	Execute Training
Safety Planning	S-2-01	Develop/Update Corporate Safety Manual
	S-2-02	Review/Approve Site Safety Plan
	S-2-03	Review/Approve Site Safety Budget
	S-2-04	Develop/Update Internal Safety Policy
Safety Auditing	S-3-01	Develop Auditing Plan
	S-3-02	Execute Site Safety Audits
	S-3-03	Document/Follow-up Auditing Results
Insurance/ Indemnification	S-4-01	Investigate Accidents
	S-4-02	Indemnify Safety Claims
	S-4-03	Process Worker's Compensation
	S-4-04	Renew Worker's Compensation Policy
	S-4-05	Renew Site Insurances

### 4.4 Activities

The research team used a series of interviews with each staff of safety department of XYZ's home office. Activities are grouped into activity centers. Through the interviews with staffs, 15 (fifteen) activities were identified and categorized into five activity centers. Each activity has its own activity ID number is presented in Tab. 2.

#### 4.5 Costs of Activities using Time-Effort Method

Each employee in the department (in this case, the safety department) that will be polled must identify the typical proportion of time spent on each activity. The result of survey using time-effort method is shown in Tab. 3. The following formula can be used to quickly determine each activity's cost [13].

$$\text{Activity Costs} = \sum (\text{Employee Salary} \times \text{Time-effort Percentage}). \quad (1)$$

#### 4.6 Cost Drivers

Any factor that changes the way other products, suppliers, or customers engage in an activity is referred to as a cost driver [12, 13]. In effect, the aspects that exhibits an equivalent connection with an activity cost is referred to be an activity cost driver [12, 15]. A factor whose volume rises as an activity cost does is known as a driver of activity cost. There are three types of cost drivers in construction ABC system: the budget cost driver, the duration cost driver, and the transactional cost driver [15]. The research team used two types of cost drivers: budget cost driver and transactional cost driver. The team determined a cost driver for each activity taking into account the behavior of each activity cost as well as the simplicity of tracking the capacity of each cost driver. The list of cost driver is shown in Tab. 4.

**Table 3** Time-Effort Survey Result (unit : %)

Activity Center	Activity	Staff 01	Staff 02	Staff 03	Staff 04	Staff 05	Staff 06	Staff 07
Safety Training	Plan Training	90	5					
	Develop/Update Training Materials	5	60					
	Execute Training	5	35					
Safety Planning	Update Corporate Safety Manual			60	30			
	Review/Approve Site Safety Plan			40	20			
	Review/Approve Site Safety Budget				30			
	Develop/Update Internal Safety Policy				20			
Safety Auditing	Develop Auditing Plan					20	40	
	Execute Site Safety Audits					30	40	
	Document/Follow-up Auditing Results					50	20	
Insurance/Indemnification	Investigate Accidents							20
	Indemnify Safety Claims							30
	Process Worker's Compensation							25
	Renew Worker's Compensation Policy							10
	Renew Site Insurances							15
Total		100	100	100	100	100	100	100

**Table 4** Cost Driver List

Activity Center	Activity	Cost Driver	Type
Safety Training	Plan Training	The number of training	Transaction
	Develop/Update Training Materials	The number of training	Transaction
	Execute Training	The number of training	Transaction
Safety Planning	Update Corporate Safety Manual	Budget ratio	Budget
	Review/Approve Site Safety Plan	Budget ratio	Budget
	Review/Approve Site Safety Budget	Budget ratio	Budget
	Develop/Update Internal Safety Policy	Budget ratio	Budget
Safety Auditing	Develop Auditing Plan	The number of audits	Transaction
	Execute Site Safety Audits	The number of audits	Transaction
	Document/Follow-up Auditing Results	The number of failures	Transaction
Insurance/Indemnification	Investigate Accidents	The number of accidents	Transaction
	Indemnify Safety Claims	The number of accidents	Transaction
	Process Worker's Compensation	The number of accidents	Transaction
	Renew Worker's Compensation Policy	Budget ratio	Budget
	Renew Site Insurances	Budget ratio	Budget

#### 4.7 Costs of Cost Objects

The unit rate of activity costs should be used to assign activity costs to cost items. The following definitions can be used to determine an activity cost's unit rate [15-17]:

$$\text{Unit Rate of Activity Costs} = \frac{\text{Activity Costs}}{\text{Total Volume of a Cost Driver}}. \quad (2)$$

The cost-allocation base was the unit rate of an activity's cost. This case study shows the research team measured two-month average of cost drivers' volume. The result of cost allocation using ABC can be seen in Tab. 5.

## 5 DISCUSSION AND CONCLUSION

While traditional cost accounting assigns overhead costs to numerous projects in proportion to each project's revenue

or contract amount, ABC does overhead costs on the consumption of cost drivers. Tab. 5 shows the result of overhead assignment using traditional method and its comparison with ABC.

**Table 5** Overhead assignment between traditional method and ABC

Activity	P1	P2	P3	Note
Overhead allocated, Trad \$	4,295.31	4,286.66	4,203.26	(1)
Overhead allocated, ABC \$	3,718.06	4,819.59	1,200.93	(2)
Difference	577.24	-532.93	3,002.33	
Difference %	16%	-11%	250%	
Over of Under-charged	Over	Under	Over	
Activity	P4	P5	P6	
Overhead allocated, Trad \$	2,337.49	3,655.94	4,234.37	(3)
Overhead allocated, ABC \$	6,788.69	1,044.55	3,700.65	(4)
Difference	-4,451.20	2,611.38	533.72	
Difference %	-66%	250%	14%	
Over of Under-charged	Under	Over	Over	
Activity	P7	P8	P9	
Overhead allocated, Trad \$	3,144.30	3,421.77	2,785.19	(5)
Overhead allocated, ABC \$	3,665.21	926.22	6,640.60	(6)
Difference	-520.90	2,315.55	-3,555.41	
Difference %	-14%	250%	-58%	
Over of Under-charged	Under	Over	Under	
Activity	P10	P11	P12	
Overhead allocated, Trad \$	3,073.12	3,589.45	3,150.14	(7)
Overhead allocated, ABC \$	2,312.23	3,516.39	3,666.87	(8)
Difference	763.90	73.06	-516.74	
Difference %	33%	2%	-14%	
Over of Under-charged	Over	Over	Under	
(1)+(3)+(5)+(7) = 42,000.00				
(2)+(4)+(6)+(8) = 42,000.00				

As seen in Tab. 5, the projects that was overcharged or undercharged more than 30% under traditional costing system are as follows:

- Overcharged Projects: Project 3, Project 5, Project 8, and Project 10
- Undercharged Projects: Project 4 and Project 9.

Provided that accurate cost information on safety costs of the general overhead, a company is able to measure the costs of safety. As seen in the case, ABC helps to prevent cost distortion that may occur under traditional costing system. In this regard, contractors can make their bidding numbers more competitive when ABC is adopted.

## Acknowledgements

A research grant from Hankyong National University for a 2022 academic exchange program helped to fund this work.

## 6 REFERENCES

- [1] López-Alonso, M., Ibarrondo-Dávila, M. P., & Rubio, M. C. (2016). Safety cost management in construction companies: A proposal classification. *Work*, 54(3), 617-630. <https://doi.org/10.3233/WOR-162319>
- [2] Revision and enforcement of contract rules of the Ministry of Strategy and Finance (2016.12.30.) Retrieved from [http://www.mosf.go.kr/lw/denm/detailTbDenmView.do?searchBbsId1=MOSFBBS\\_000000000119&searchNttId1=MOSF\\_00000000007082&menuNo=7020000](http://www.mosf.go.kr/lw/denm/detailTbDenmView.do?searchBbsId1=MOSFBBS_000000000119&searchNttId1=MOSF_00000000007082&menuNo=7020000)
- [3] National Law Information Center. (2020). Occupational Safety and Health Act, Retrieved from <https://www.law.go.kr/engLsSc.do?menuId=1&subMenuId=21&tabMenuId=117&query=%EC%82%B0%EC%97%85%EC%95%88%EC%A0%84%EB%B3%B4%EA%B1%B4%EB%B2%95#>
- [4] National Law Information Center. (2020). Calculation and usage standards for occupational safety and health management expenses in the construction industry, Retrieved from <https://www.law.go.kr/admRulInfoP.do?admRulSeq=2100000211668>
- [5] Flyvbjerg, B., Holm, M. S., & Buhl, S. (2002). Underestimating costs in public works projects: Error or lie? *Journal of the American planning association*, 68(3), 279-295. <https://doi.org/10.1080/01944360208976273>
- [6] Kim, Y. W. (2017). *Activity Based Costing for Construction Companies*. John Wiley & Sons. <https://doi.org/10.1002/9781119194705>
- [7] Johnson, T. (1992). Relevance regained: From top-down control to control to bottom-up.
- [8] Kim, Y. W. (2002). *The implications of a new production paradigm for project cost control*. University of California, Berkeley.
- [9] Cooper, R. (1988). The rise of activity-based costing - Part two: When do I need on activity-based cost system? *Journal of cost management*, 41-48.
- [10] Cooper, R., & Kaplan, R. S. (1992). Activity-based systems: Measuring the costs of resource usage. *Accounting horizons*, 6(3), 1-13.
- [11] Horngren, C., Foster, G., & Datar, S. (1999). *Cost Accounting*, 10th edition, Prentice Hall, Upper Saddle River, NJ.
- [12] Kim, Y. W. & Ballard, G. (2005). Profit-point analysis: A tool for general contractors to measure and compare costs of management time expended on different subcontractors. *Canadian Journal of Civil Engineering*, 32(4), 712-718. <https://doi.org/10.1139/I05-021>
- [13] GS Construction Company. (2021). Annual report, Retrieved from [https://www.gsenc.com/en/IR/Financial/Financial\\_02.aspx](https://www.gsenc.com/en/IR/Financial/Financial_02.aspx)
- [14] ENR (2022). Top 250 International contractors, Retrieved from <https://www.enr.com/toplists/2021-Top-250-International-Contractors-1>
- [15] Kim, Y. W. (2017). *Activity Based Costing for Construction Companies*. John Wiley & Sons. <https://doi.org/10.1002/9781119194705>
- [16] Cokins, G. (1996). *Activity-based cost management making it work: a manager's guide to implementing and sustaining an effective ABC system*. Irwin Professional Pub.
- [17] Norm, R. (1991). Glossary of Activity-Based Management. *The Journal of Cost Management*, 58.

## Authors' contacts:

**Yong-woo Kim**, Full professor  
Koon Endowed Professor of Construction Management  
College of Built Environments, University of Washington,  
Seattle, WA, USA, 98115  
206.616.1916, yongkim@uw.edu

**Sangchul Kim**, Full professor  
(Corresponding author)  
School of Architecture, Hankyong National University,  
Anseong-si, Kyonggi-Do, South Korea, 17579  
031.670.5277, sckim08@hknu.ac.kr

# A Study on the Improvement of Security Image Analysis Capability Using Artificial Intelligence

Seng-Phil Hong, Debnath Bhattacharyya\*

**Abstract:** The mining of patient data in the health care industry is becoming an increasingly important field because of the direct effect it has on the lives of patients. In the field of medicine, one use of data mining is the early diagnosis of medical diagnostic conditions. However, extracting information from medical records is a laborious process that involves a lot of time and effort. Communities that are dominated by females have an elevated risk of developing breast cancer. Even though mammography is one of the most common ways to use computer-assisted diagnostics, there is still a chance that breast cancer will not be found even if it is one of the most common ways to find and screen for the disease. This indicates that just thirty percent of breast cancers are diagnosed at the appropriate time. Digital image pre-processing includes grayscale-to-binary conversion, noise reduction, and character separation. Most picture recognition algorithms employ statistical, syntactic, and template matching. Neural networks and support vector machines have enabled recent photo identification advances. This article discusses the second stage of the pre-processing procedure, which is adding a filter to the image after it has been segmented in order to make it seem more appealing. It works to identify the area of interest and improve the image by removing the breast border in order to apply filtering algorithms. The breast image's edge is reconstructed using morphological processes in the segmentation method that has been proposed, and breast masses are found by subtracting the two images. In addition, a modified bi-level histogram and homomorphic filters were used in order to improve the image's quality by reducing noise and enhancing contrast.

**Keywords:** bilateral subtraction; cancer; deep learning; enhancement filter; image segmentation; image security; mammography

## 1 INTRODUCTION

The sophisticated image processing techniques, such as segmentation and enhancement, are the primary emphasis of this study's investigation [1]. The strategy entails finding the area of interest, masking off the breast border, and then applying various filtering algorithms to the image in order to improve it. The suggested method for image segmentation includes many components [2-3], including breast image edge restoration via the use of morphological processes, as well as breast mass identification through the use of bilateral image subtraction. A modified bi-level histogram and homomorphic filters were applied to the image that had previously been processed in order to find noise and boost the contrast level.

In Sections 2 and 3, we discuss the principles of algorithms for image segmentation [4], border detection, and contrast enhancement. These topics are covered in more detail below. In the article's fourth and final part, a discussion of how the problem may be fixed is presented. A summary of the proposed approach is provided in the third section of this article. In Section 6, we demonstrate how to segment images with mathematical morphological operations, improved morphological border recognition, and bilateral subtraction. In Section 7, we provide a comprehensive explanation of the suggested approach to improving contrast, which makes use of a modified bi-level histogram and a homomorphic filter (MBH-HF). The experimental analysis is the subject of the eighth part of the research, and it covers a wide range of issues, including the assessment measures, the datasets that were employed, and the interpretation of the results. The findings of the investigation are detailed in Section 13 of the report in this package.

The Major Contributions of the research article are as follows:

- In order to classify the current state of artificial intelligence application and the difficulties that are linked with it, this essay takes a case study method.
- The authors of the study investigate several ideas and methods for applying AI to the creation of unique goods in a variety of industries.

## 2 MEDICAL IMAGE SEGMENTATION WITH BOUNDARY DETECTION

Mammography is by far the most successful way of screening for breast cancer due to the fact that it produces an image of the breasts inside. The fact that these images are hard to understand because of the high degree of distortion and disruption they include [5] contributes to the difficulty of finding malignant tumors early in their development, which already presents a challenge in and of itself. Image pre-processing is an important approach that should be used whenever there is a need to improve the accuracy of the classification of malignant tissues. This is due to the fact that it improves the image by getting rid of unimportant factors that might otherwise have an effect on the genuine positive rate. Before the underlying photo can be digitally processed, all of the labels, markers, the pectoral muscle [6] and the background need to be removed. The digital image is used to generate a histogram, which is then applied to the image in order to modify it and normalize it.

### 2.1 Contrast Enhancement

The histogram of an image is often a graphical representation of the different gray-level intensities as well as a description of how the image looks. It is possible to utilize histogram methods in order to increase the overall quality of an image as well as its look. Utilizing the histogram

in conjunction [7] with the histogram equalization technique is a common method for increasing contrast and improving the overall image quality. When equalization is accomplished, the needed intensity is converted into a constant intensity that is spread over the whole image in a manner that is consistent [8]. Retaining the brightness of the light Bi-Histogram Histogram equalization was used so that the situation might be improved upon (BBHE). The histogram of the input image is divided into two sub-histograms based on the average intensity value, and then each sub-histogram is equalized on its own to keep the image bright.

## 2.2 Histogram Equalization

The technique for histogram equalization places a greater emphasis on the total amount of data than it does on any other consideration. This served as the impetus for the development of a method known as adaptive histogram equalization (AHE), which makes adjustments for alterations in the local context of an image rather than the context of the image as a whole. However, the approach results in an unhealthy increase in contrast and modifies the image's component parts in undesirable ways. CLAHE [9], which stands for contrast level adaptive equalization, is a revolutionary method that decreases the contrast level by raising it (CLAHE).

Histograms of colours display the distribution of colours across pixels in an image. The red, green, and blue components of a picture cannot each have their own histogram equalisation performed on them separately without having a significant impact on the image's colour balance. If the image is converted to the HSL/HSV colour space, the technique may be used to adjust either the brightness or value channel of the picture without affecting the hue or saturation.

## 2.3 Contrast Limited Adaptive Histogram Equalization (CLAHE)

Unsharp During the masking-based image enhancement process, a low pass filter is used. If you remove the filter from the original photo, you will be able to get an image that is more pleasing to the eye. It emphasizes the most distinguishable aspects of an otherwise straightforward image. However, the mistake that occurs the most often is the excessive amplification of contrast regions, which just helps to enhance the background noise.

The contrast-limited adaptive histogram equalisation (CLAHE) algorithm was used to chest CT scans for the purpose of this investigation. In a matter of seconds, a machine may solve CLAHE. A parallel engine that is built from off-the-shelf components can calculate CLAHE in under four seconds, after an initial loading period of five seconds. Because of differences in how different observers calibrate their equipment, agreement tests are unable to prove that the processing is successful for a variety of medical pictures.

## 2.4 Unsharp Masking (US)

In order to get the best possible results, equalization based on the histogram is used. The mapping component from the prior technique is included into this new approach, and a modified histogram is also included. After the facts have been gathered, the technique organizes them in a manner that enhances the value of the local area [10].

## 2.5 Histogram Modified – Local Contrast Enhancement (HMLCE)

The contrast of the image will be enhanced. Another method called the Bi-level Histogram Modification-Adaptive Nonlinear Filter (BHM-ANF) [11] is capable of producing results that are similar to those of the first method. In this method, the filter technique is responsible for improving the local contrast, while the bi-level histogram is responsible for improving the overall contrast.

## 3 LITERATURE REVIEW

Even before you segment an image, you get rid of the distracting background and bring the most important parts to the front. This makes it easier for the viewer to understand the image. In a nutshell, the process involves cutting the image into many small images, called "pixels," so that patterns can be searched for based on a set of rules. Several methods, such as thresholding [12, 13], filtering [14, 15], area expansion [15], statistical models [16, 17], convolutional networks [18, 19], and clustering [18, 19], are used to break the image into pieces that are easier to understand.

[16] Protocols for finding breast cancer were written down in great detail. Mammograms and MRIs are both good ways to find out if someone has breast cancer. Mammograms may help find breast cancer, but MRIs are better. Several different methods, such as edge detection and threshold-based approaches, were used to separate the tumors that could be seen in the image. Several operators worked on the final image, and the entropy of the images they made afterward was looked at to see how well they did their jobs [17] showed a way to find and get rid of the border that was based on how the intensity of the data changed. This was done by using a spatial averaging filter to smooth the image and then a gradient-based histogram thresholding algorithm to separate the image into its parts.

## 4 PROPOSED METHODOLOGIES

New prospects for study have opened up thanks to developments in machine learning and image processing methods. Extracting and analysing visual data is now a capability of machine learning. It's possible that machine learning and image processing may make security even better. Image processing contributes to both online and offline security. Examples of these types of applications include homeland security, surveillance software, ID verification, and physical security programmes. Protecting data is essential to ensuring digital safety. There are a few

ways to protect digital data, including steganography, network security, and digital watermarking.

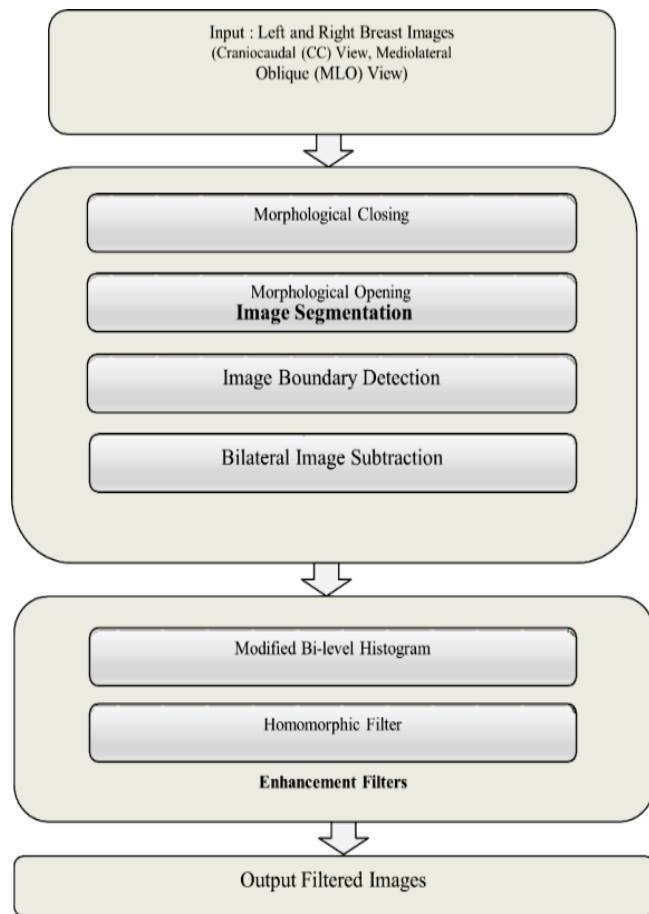


Figure 1 Showing the work flow of the proposed methodology

## 5 MEDICAL IMAGE SEGMENTATION FOR SECURITY

When preparing a photo for segmentation, the unneeded background is first eliminated, and then the main elements are brought to the front. This helps to improve the overall understanding of the image. In a nutshell, what it includes is dividing the image into numerous separate images ("pixels") so that patterns may be looked for using a certain set of criteria that has been specified beforehand. There are a variety of methods that may be used to simplify the image, including: thresholding [12, 13], filtering [14, 15], enlarging the area [15] using statistical models [16, 17] convolutional networks [18, 19] and clustering [18, 19].

There is a comprehensive record of the processes involved in breast cancer detection [16, 20, 21]. It's possible that breast cancer may be diagnosed with the use of mammograms as well as magnetic resonance imaging (MRI). Despite the fact that mammograms may be helpful in the identification of breast cancer, magnetic resonance imaging scans are far more accurate. Several different methods, such as threshold-based algorithms and edge detection, were used in order to isolate the tumors present in the image. The final image was created by a number of different operators, and the performance of those operators was judged based on the

entropy of succeeding images they generated. Changes in the data intensity were used in order to detect the border and then remove it [17]. To achieve this, a spatial averaging filter was employed to generate a uniform backdrop, and a gradient-based histogram thresholding approach was used to remove individual items from the resulting image. Both of these techniques are described in the following paragraphs.

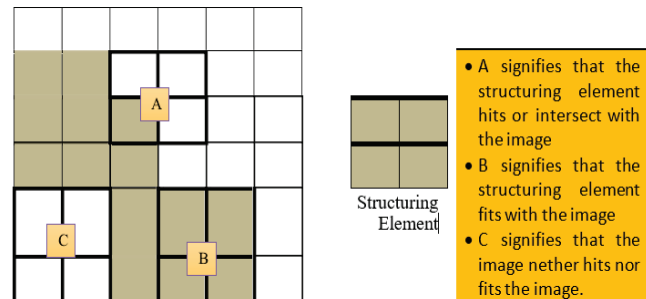


Figure 2 Probing of the binary image for the security in medical image analysis

In the event that the test is successful, the result of the morphological operations carried out on the binary image should be another binary image with the same size and a value of 1. This method makes it possible to conduct an examination of the shape of the image as well as to modify its features while still preserving the data and defining traits that it has. Erosion and expansion are two of the most basic morphological processes, and they may be seen almost everywhere. The dilation method often results in an increase in the number of pixels located at the image's borders. In order to produce an image denoted by the letter  $g$ , an image denoted by the letter  $f$  must first be subjected to a dilation operation, which is represented by the equation  $g = f \times s$ . By comparing the values of the pixels to the structuring element one may get a technique for obtaining the final image.

When, these are the coordinates that are input  $(x, y)$ . This process is repeated several times for each individual pixel. In addition, the number of additional pixels that are added to the image that is being used as the basis for the output image is determined by the size and shape of the structuring element. Since the margins of objects do not often need a great deal of attention, it is possible for them to "erode" away over time. Assuming that we started with an image denoted  $f$  and then added a structural element denoted  $s$  by a process known as erosion, the resulting image, denoted  $g$ , may be mathematically expressed as  $g = f + s$ . The answer, which is denoted by the equation, is the letter  $g$  in the image.

Once the pixel coordinates have been entered  $(x, y)$ . This process is repeated several times for each individual pixel. To generate the output image from the source image, a certain number of pixels will need to be extracted, and this number is determined not only by the size of the structuring element but also by its shape. The binary image may be seen as a result of using a method that involves both erosion and dilation [17]. In the end, morphological openness brings to a rounding off of the image's corners, a weakening of linkages, and the removal of any minute projections or relationships between things. On the basis of the whole structure, the

boring zone has been removed. This strategy, denoted by the equal sign ( $=$ ), is the fairest of the other options.

In order to improve the visibility of the image under the surface, it has been suggested that a bi-level histogram, in combination with a homomorphic filter, be used. There are two separate levels in this building. Increasing the image's contrast is the primary objective of the first step of the process, during which the bi-level histogram is modified. To achieve more clarity, step two's processing makes use of the homomorphic filter.

## 6 PROPOSED CONTRAST ENHANCEMENT USING MODIFIED BI-LEVEL HISTOGRAM WITH HOMOMORPHIC FILTER (MBH-HF)

Increasing contrast may be accomplished in a number of ways, the one that is the most common and easy being the adjustment and levelling of the image's intensities. Equalization of the histogram's intensity levels is accomplished according to the notion that intensity levels should be dispersed evenly over the graph. The fact that there is no opportunity for the user to modify the amount of contrast in the image is the most significant drawback of this strategy. This is because the level of contrast is automatically applied owing to the uniform distribution. The process of developing the framework for the new and improved histogram. The histogram of the original image is altered by these two methods in such a way that it resembles the uniform histogram in a greater degree. Now is the moment to make any necessary adjustments to the histogram so that the image's brightness may be maintained while the contrast is increased. The histogram is cut in half using this method, with each section corresponding to one half of the image's mean intensity value (Imean) [11]. Histogram, abbreviated as  $H$ , and uniform histogram, abbreviated as  $H_u$ , are both terms that refer to the same thing. The primary histogram may be subdivided into two sub histograms, which are denoted by the names  $H_{lower}$  and  $H_{upper}$  respectively. It is advised that the chosen histogram have an intensity value that is lower than the mean intensity value of the other histograms. Histogram  $H_{upper}$  is the one in which the intensity values are greater than the value that is considered to be the norm for the intensity values (Histogram Imean).

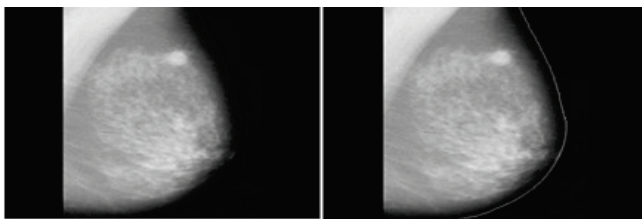


Figure 3 Breast border extraction for the image

$$H_{higher} = (1 - \alpha) \cdot H_{lower} + \alpha H_u, \quad (1)$$

Where  $0 \leq \alpha \leq 1$ . When we use the equations that were just discussed, we are able to understand that calculating the value of  $\alpha$  is the most difficult part of the process. When this

function is told to create  $H_u$ , a uniform histogram with increased contrast, setting it to  $= 1$  has this effect. A decrease in  $H$  may be thought of as the opposite of what occurs when  $= 0$ . In Eq. (1), the function returns the input  $H_{upper}$  when the parameter  $= 1$ ; however, when the parameter  $= 0$ , the function returns the uniform histogram  $H_u$ . The significance of the number 0.55 was highest among all of those that we tested. As a consequence of this, 0.55 has been decided to be the best possible value for the new histogram. (Agarwal et al.). The final modified histogram, denoted by the symbol  $H'$ , is obtained by adding the values of the altered sub-histograms, denoted by the symbols  $H'_{lower}$  and  $H'_{higher}$ .

Table 1 Comparison of breast boundary extraction methods

Breast border extraction methods	Number of images used in the study	Detection Rate
Intensity Gradient Based	322	89%
Region Growing	40	100%
Adaptive Histogram	320	98%
Active Contour	84	96%
Morphology	322	98.75%
Enhanced Morphological based boundary detection	100	99%

As a consequence of this, the strategy that was described ends up producing a histogram that is quite similar to the standard histogram. A modified bi-level histogram is used in Phase I for the purpose of improving contrast.

## 7 RESULTS AND DISCUSSIONS

The technique that is described in this chapter has been tested experimentally before being included here. In order to evaluate how successful, the suggested technique is, we make use of the database maintained by the Mammographic Image Analysis Society (MIAS). It has been shown that the one-of-a-kind way for locating the breast's margins and improving the overall image is more effective than the methods that have been used in the past. A database of digital mammograms has been established by the Mammographic Image Analysis Society (MIAS) in response to the requirements of research groups in the UK. The films from the UK National Breast Screening Programme are digitized to a pixel edge of 50 microns, and the database is used to evaluate the approach. A Joyce-Loebl scanning micro densitometer is one tool that may be used for the purpose of digitizing the 8-bitword of a pixel. The archive contains 161 pairs of images of the right and left breasts of the same patient, as well as 322 digitalized films and comments from the radiologist describing where and what was wrong.

In order to test the boundary extraction by image segmentation approach, we picked 100 breast images at random from the MIAS database for the purpose of this experiment. The strategy that is advocated makes use of openness and closure approaches that are derived from the study of morphology. The suggested method was applied to a total of one hundred images drawn from the MIAS image database in order to test its efficacy. Using the technique that was proposed, the borders of ninety-nine images were completely restored, while the border of the one remaining

photo was only partially restored. A knowledgeable radiologist performs a manual check at the method-generated border to ensure its accuracy. The reference that was utilized to generate the sample boundary for the breast image does not appear in Fig. 4.

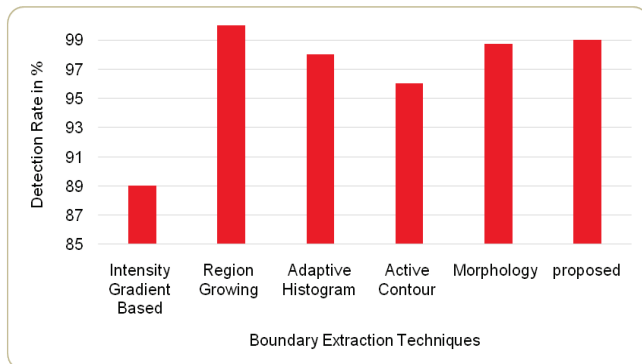


Figure 4 Comparison of boundary extraction techniques

Comparison to other approaches that are currently being used demonstrates that the suggested technique is more successful. Tab. 2 provides an illustration of the difference. The novel technique, which is based on morphology, is evaluated in comparison to the existing methods of Intensity Gradient Based Threshold with Region Growing, Active Contour, and Morphology.

The technique that has been suggested has a success record of 99 percent. The region-expanding strategy, which yields a result of 100% and requires an input size of forty, produces the greatest possible outcome. However, when

applied to a set of one hundred images, the augmented morphological technique is shown to be quite successful. This study examines the effectiveness of the suggested method by applying it to 14 mammograms taken from the MIAS dataset, which include both normal and cancerous tissue. The calculated EME value for the original image is 16,563, and the same calculation is performed on both the original image and the suggested method. You may see the results in their entirety in Tab. 2. On the other hand, the values of the average EME for the HE, BBHE, US, and HM-LCE methods are, respectively, 5.896, 13.581, 8.125, and 14.25. These values are less than the average EME value of the original photos, and they are undesirable since they are unable to improve the information that is being hidden from view. The average EME for CLAHE is 26.501, which is fairly high and obscures some of the more subtle aspects of the image. The average EME values are extremely high when considering the MBH-HF and BHM-ANF methods that have been recommended. Therefore, MBH-HF is superior to the methods that we are now aware of. AMBE is a different approach of determining whether or not an image has been successfully modified. The purpose of this exercise is to see how various techniques compare and contrast with one another.

In the Tab. 3, the value of entropy that is the lowest indicates that the image enhancement was effective. As can be seen in table 4.6, the original image has an entropy value that is around 4,818 on average. Entropy values on average ranged from 5.050 for CLAHE to 4.939 for HM-LCE to 4.828 for the US to 4.715 for BHM-ANF to 4.611 for BBHE.

Table 2 Comparison of EME values various enhancement techniques

File Name	Original	HE	BBHE	CLAHE	US	HM-LCE	BHM-ANF	MBH-HF
mdb005	5.141	6.885	13.657	25.542	08.456	15.069	18.912	18.514
mdb023	14.652	7.979	14.152	28.389	12.268	15.744	17.652	17.054
mdb025	19.433	6.897	14.647	28.376	8.856	16.245	22.433	21.145
mdb028	17.610	6.136	12.489	25.840	10.808	13.140	20.610	19.450
mdb058	18.813	4.970	14.109	27.187	03.554	14.118	21.813	21.254
mdb063	15.469	3.685	12.457	26.197	04.811	12.156	18.469	17.654
mdb069	15.463	7.388	15.577	30.435	08.919	18.084	21.663	20.456
mdb178	16.561	1.533	09.034	17.266	04.179	05.672	19.561	18.245
mdb184	18.968	5.892	12.072	25.073	06.312	15.024	22.908	21.458
mdb186	19.826	2.802	10.954	20.240	11.633	07.544	22.826	21.698
mdb190	15.282	7.990	18.933	29.666	09.796	17.312	18.282	18.112
mdb193	19.830	6.606	12.999	30.325	06.720	16.653	22.830	22.150
mdb204	17.417	6.761	12.995	24.711	10.097	17.686	20.417	19.123
mdb206	17.412	7.014	16.058	31.767	07.348	15.046	20.412	19.452
Average	16.563	5.896	13.581	26.501	8.125	14.250	20.628	19.698

Table 3 Comparison of AMBE values various enhancement techniques

File Name	HE	BBHE	CLAHE	US	HM-LCE	BHM-ANF	MBH-HF
mdb005	85.071	34.296	20.126	0.091	48.047	16.054	09.874
mdb023	80.075	23.24	17.984	0.069	82.975	17.153	10.214
mdb025	90.501	33.813	18.624	0.058	50.551	16.56	09.745
mdb028	91.299	32.842	19.065	0.034	88.816	18.441	10.879
mdb058	111.726	30.982	22.185	0.049	62.74	20.554	11.475
mdb063	122.218	28.553	18.064	0.071	91.596	16.705	09.874
mdb069	92.974	31.167	14.094	0.052	91.396	15.771	09.945
mdb178	155.884	24.961	13.724	0.041	71.357	7.913	05.241
mdb184	86.604	31.618	19.738	0.047	79.865	18.405	10.425
mdb186	137.29	22.384	14.285	0.039	46.299	10.382	06.785

**Table 4** Showing the various performance measure, the proposed method consistently provides better performance and thus the proposed method is proved to be efficient

File Name	Original	HE	BBHE	CLAHE	US	HM-LCE	BHM-ANF	MBH-HF
mdb005	5.176	3.966	4.124	5.417	5.188	5.433	5.189	4.287
mdb023	5.104	4.044	4.564	5.548	5.154	5.607	4.964	3.887
mdb025	5.410	3.987	5.009	5.542	5.415	5.562	5.009	4.125
mdb028	5.580	4.220	4.907	5.691	5.59	5.651	4.907	4.245
mdb058	4.232	3.052	4.122	4.406	4.235	4.396	4.122	3.945
mdb063	4.119	2.896	6.998	4.409	4.118	4.163	4.033	3.245
mdb069	5.519	4.280	4.868	5.662	5.514	5.629	5.868	4.124
mdb178	3.085	2.028	2.985	3.203	3.086	2.924	3.685	3.526
mdb184	4.900	3.673	4.618	5.163	4.909	5.101	4.668	3.887
mdb186	3.536	2.659	3.481	3.778	3.583	3.441	3.481	3.114
mdb190	5.135	4.049	4.574	5.454	5.133	5.374	4.874	3.458
mdb193	5.195	3.953	4.995	5.447	5.195	5.314	4.995	3.214
mdb204	5.422	4.263	4.587	5.683	5.433	5.599	5.487	3.914
mdb206	5.035	3.822	4.722	5.296	5.035	4.947	4.722	3.452
Average	4.818	3.635	4.611	5.05	4.828	4.939	4.715	3.745

The value of the suggested technique is 9.907, which places it in second place among the many ways to make improvements, behind only the US method, which has a value of 0.053. The CEM method is the third strategy that may be used to evaluate how well improvement projects are operating. The CEM values for each of the fourteen images that were produced utilizing a variety of tried-and-true and innovative processes are listed in the table that follows. In the last step, the entropy of an image is evaluated to determine the degree to which it has been enhanced. Tab. 4 displays the entropy values for the initial image, the improved image that was made using the traditional procedures, and the enhanced image that was created using the new methodology.

The strategy that was suggested has the average entropy value of 3,744, which places it in second place. With an average entropy value of 3.635%, HE has the lowest value among the various enhancement techniques when compared to the others was shown in the Tab. 4.

As a consequence of this, the technique that was recommended often results in improved performance across a range of performance metrics, which demonstrates that it is effective.

## 8 CONCLUSION AND FUTURE WORK

Investigation is being done on various image enhancement and segmentation algorithms. After the noise from the pre-processed image has been eliminated, the images are segmented using the method that has been supplied in order to get the Region of Interest and image border. By removing the breast border, the method that has been suggested draws more attention to the primary subject of the image. In the suggested method of breast image segmentation, the image borders of the breast are reconstructed through the use of morphological processes, and breast masses are eliminated via the use of bilateral image subtraction. We used a modified bi-level histogram in combination with homomorphic filters in order to find noise and increase the contrast of the pre-processed image. A method that is based on morphological opening and closing procedures was created and analysed in order to extract boundaries from the MIAS image database of mammograms. This was done by using the methodology. The recommended

technique searches for the target in a manner that is both more exhaustive and accurate (99.9% of the time). In addition to this, we explore and evaluate the suggested method for improving images (MBH-HF). Several distinct parameters, such as expected mean benefit (EME), average mean benefit (AMBE), maximum mean benefit (CME), and entropy, are used to conduct an analysis of the method's efficacy. The results show that it is superior to a number of other approaches that are already in use, with values of 19.7, 9.1, 1.28, and 3.75 respectively. The primary focus of future research will be on identifying and using fresh mammography imaging datasets and real-time images, in addition to deploying a variety of models for accurate diagnosis at the population level.

## 9 REFERENCES

- [1] Ritchie, H. & Roser, M. Causes of death. Published online at Our World in Data.org. Retrieved from: <https://ourworldindata.org/causes-of-death>
- [2] Akbari, M. E. (2008). Iran cancer report. Cancer Research Center, *Shahid Beheshti University of Medical Science*, First Edition.
- [3] Liou, D. M. & Chang, W. P. (2015). (2015). Applying Data Mining for the Analysis of Breast Cancer Data. In: Fernández-Llatas, C., García-Gómez, J. (eds) *Data Mining in Clinical Medicine. Methods in Molecular Biology*, 1246. Humana Press, New York, NY. [https://doi.org/10.1007/978-1-4939-1985-7\\_12](https://doi.org/10.1007/978-1-4939-1985-7_12)
- [4] National Research Council. (2001). Mammography and beyond: Developing technologies for the early detection of breast cancer. *National Academies Press*, edited by S. J. Nass, I. C. Henderson, and J. C. Lashof
- [5] Debra M. Ikeda, St. Louis, MO: Mosby. (2011). Breast imaging: The requisites. Second Edition, 448
- [6] Wang, C. (2016). Anove land automatic pectoral muscle dentification algorithm form ediolateral oblique (MLO) view mammograms using image jar. Xiv preprint ar Xiv:1603.01056
- [7] Wu, S., Zhu, Q., Yang, Y., & Xie, Y. (2013). Feature and contrast enhancement of mammographic image based on multiscale analysis and morphology. *IEEE International Conference on Information and Automation (ICIA)*, Yinchuan, China, 521-526. <https://doi.org/10.1109/ICInfA.2013.6720354>
- [8] Hum, Y. C., Lai, K. W., & Mohamad Salim, M. I. (2014). Multi objectives bihistogram equalization for image contrast enhancement. *complexity*, 20(2), 22-36.

- <https://doi.org/10.1002/cplx.21499>
- [9] Pisano, E. D., Zong, S., Hemminger, B. M., DeLuca, M., Johnston, R. E., Muller, K., Braeuning, M. P., & Pizer, S. M. (1998). Contrast limited adaptive histogram equalization image processing to improve the detection of simulated spiculations in dense mammograms. *Journal of Digital Imaging*, 11(4), 193. <https://doi.org/10.1007/BF03178082>
  - [10] Sundaram, M., Ramar, K., Arumugam, N., & Prabin, G. (2011). Histogram modified local contrast enhancement for mammogram images. *Applied Soft Computing*, 11(8), 5809-5816. <https://doi.org/10.1016/j.asoc.2011.05.003>
  - [11] Hazarikaand, M. & Mahanta, L. B. (2018). A new breast border extraction and contrast enhancement technique with digital mammogram images for improved detection of breast cancer. *Asian Pacific Journal of Cancer Prevention: APJCP*, 19(8), 2141.
  - [12] Ojala, T., Nappi, J., & Nevalainen, O. (2011). Accurate segmentation of the breast region from digitized mammograms. *Comput. Med. Imaging Graphics: The official J. of the Comput. Med. Imaging Soc.*, 25, 47-59. [https://doi.org/10.1016/S0895-6111\(00\)00036-7](https://doi.org/10.1016/S0895-6111(00)00036-7)
  - [13] Chen, X. & Zwiggelaar, R. (2010). Segmentation of the breast region with pectoral muscle removal in mammograms. *Medical Image Understanding and Analysis*, 71-76
  - [14] Ragupathy, U. S. & Saranya, T. (2012). Gabor wavelet-based detection of architectural distortion and mass in mammographic images and classification using adaptive neuro fuzzy inference system. *International Journal of Computer Applications*, 46(22), 0975-8887
  - [15] Priya, D. S. & Sarojini, B. (2013). Breast cancer detection in mammogram images using region-growing and contour based segmentation techniques. *International Journal of Computer & Organization Trends*, 3(8), 54-57
  - [16] Ramirez-Villegas, J. F. & Ramirez-Moreno, D. F. (2012). Wavelet packet energy, Tsall is entropy and statistical parameterization for support vector-based and neural-based classification of mammographic regions. *Neuro Computing*, 77(1), 82-100. <https://doi.org/10.1016/j.neucom.2011.08.015>
  - [17] Zhu, W., Xiang, X., Tran, T. D., & Xie, X. (2016). Adversarial deep structural networks for mammographic mass segmentation, arXiv preprint arXiv: 1612.05970. <https://doi.org/10.1101/095786>
  - [18] Liu, X. & Tang, J. (2014). Mass classification in mammograms using selected geometry and texture features, and a new SVM-based feature selection method. *IEEE Systems Journal*, 8(3), 910-920. <https://doi.org/10.1109/JSYST.2013.2286539>
  - [19] Kooi, T., Gubern-Merida, A., Mordang, J. J., Mann, R., Pijnappel, R., Schuur, K., den Heeten, A., & Karssemeijer, N. (2016). A comparison between a deep convolutional neural network and radiologists for classifying regions of interest in mammography. In: Tingberg, A., Lång, K., Timberg, P. (eds) *Breast Imaging, IWDM 2016, Lecture Notes in Computer Science*, 9699. Springer, Cham. [https://doi.org/10.1007/978-3-319-41546-8\\_7](https://doi.org/10.1007/978-3-319-41546-8_7)
  - [20] Fathi Islam S., Ali, A. M., Makhlof M. A., & Osman E. A. (2021). Compression techniques of biomedical signals in remote healthcare monitoring systems: A comparative study. *International Journal of Hybrid Information Technologies*, 1(1). <https://doi.org/10.21742/ijhit.2653-309X.2021.1.1.03>
  - [21] Mohammed, S., & Fiaidhi, J. (2022). Extending the power of problem oriented medical record with disease association discovery: The case study of empowering QL4POMR with OpenTargets. *International Journal of Hybrid Information Technology*, 2(1), 1-12. <https://doi.org/10.21742/ijhit.2653-309X.2022.2.1.01>

**Authors' contacts:****Seng-Phil Hong, Prof.**

Head professor of AI Advanced School,  
aSSiST (a Seoul School of Integrated Science & Technologies),  
46 Ewhayeodae 2-gil, Fintower, Sinchon-ro, Seodaemun-gu, Seoul, 03767, Korea  
sphong@assist.ac.kr

**Debnath Bhattacharyya, Prof.**

(Corresponding author)  
Department of Computer Science and Engineering, Koneru Lakshmaiah Education  
Foundation, Vaddeswaram, Guntur 522302, India  
debnathb@gmail.com

# Air Quality Supervision System using the IoT Platform

Marinko Stojkov, Goran Delija, Ivan Đuračić\*, Tomislav Alinjak

**Abstract:** This paper presents the idea of the Internet of Things (IoT) platform, which is demonstrated by creating a device that measures air quality, collects and processes real-time data, and presents it in a web application. The device comprises a microcontroller board called Wemos D1 Mini, which is powered by an ESP8266 microchip. It also consists of two sensors, CCS811, which measures air particle quantity, and BME280, which measures air temperature, pressure, and humidity. The device is wirelessly connected to an MQTT broker using a Wi-Fi network and the MQTT protocol. The paper also provides detailed information on the functioning and usage of the MQTT protocol along with guidelines for programming and configuring the MQTT broker for both Wemos D1 and Raspberry Pi.

**Keywords:** air quality control; IoT; Raspberry Pi; web application; Wemos D1 Mini

## 1 INTRODUCTION

Over the past few years, the term *Internet of Things* (IoT) can often be heard in the media. Devices for which until recently it was unthinkable to be connected to the Internet, such as household appliances and cars, are now advertised by their manufacturers as *smart*, and it is difficult to find a product that does not have an IoT version [1, 2]. Significant coverage by high-speed mobile networks, as well as the price of electronic components, which has decreased to a very low level, have enabled enthusiasts and hobbyists to make their own versions of such smart devices at a very low cost. Low prices make it possible to turn almost any device into a part of the IoT, giving it a kind of digital intelligence and the possibility of automatic data exchange between two devices, the so-called M2M (*Machine to Machine*) communication, without the need for human intervention [3-6].

The *Internet of Things* was initially most interesting and useful to large companies and manufacturers, where it was primarily used for communication between devices (M2M) and for tracking expensive equipment and tools in production using RFID (*Radio Frequency identification*) tags. Recently, the focus has increasingly shifted to transforming our homes and offices into "*smart spaces*" [7-8]. A device that performs trivial things such as turning off the lights and ordering groceries, gives the user more time to deal with more important things which contribute to stress reduction [9].

Industrial IoT architectures, which in recent years began to use the best data centers for data processing, have consequently received improvements in the form of increased production productivity, reduction of unplanned downtime in production as a result of failures, and reduction of electricity consumption [10-14].

In March 2019, the *Global mobile Suppliers Association* (GSA) announced that more than 100 mobile operators have NB-IoT (*Narrowband Internet of Things*) or LTE-M networks. By September 2019, this number had risen to 142 developed/started networks [10]. NB-IoT is best suited for IoT applications that require more frequent communication and data transmission because it operates on a licensed frequency spectrum and has no work cycle limitations [15, 16].

The basic idea for this work was to create an IoT sensor that will be able to run on batteries, so it will not have restrictions on the place of installation, and that will wirelessly send the measured values to a device connected to the Internet. Users are then able to check the sensor values at any time using a web application, for example using their smartphone.

The making of a sensor for air quality control, which also measures the amount of various particles in the air, was chosen. Such a sensor could have a wide application in mechanical engineering: companies engaged in, for example, metal processing could have insight into the air quality in their production halls at any time, in order to be sure of the safety of their employees. In the event that a process pollutes the air above a recommended level, the system could notify the responsible person, who could then take some action, such as ventilating the hall or removing workers from them.

As the main sensor unit, a development board based on the ESP8266 microcontroller, Wemos D1 Mini, was selected, to which the CCS811 air quality sensor and the BME280 atmospheric sensor were connected via the I<sup>2</sup>C (*Inter – Integrated Circuit*) bus. A Raspberry Pi 3B minicomputer was chosen to receive data from the development board. A few years ago, the Raspberry Pi made a real revolution because despite its small dimensions (it is the size of a credit card) it contains all the parts like an ordinary personal computer, of course much weaker, but still with enough power to start and perform many tasks related to the use of microcontrollers and sensors.

In the second chapter of this work, there is a description of the components of the air quality monitoring system, the setting of the MQTT protocol and the setting of the Python script to display the results. In the third chapter, the results of air quality measurements in real conditions are presented. The conclusion of this paper is given in chapter four.

## 2 DESCRIPTION

With the development of the IoT industry over the past few years, some new forms of wireless communication between devices have emerged. Some of the protocols for wireless communication were created on the basis of wireless technologies that were used many years before IoT as a

concept was even created, for example BLE (*Bluetooth Low Energy*) which arose from *Bluetooth Classic technology* that was primarily used to connect audio devices with computers or mobile phones.

The choice of protocol depends on the purpose of the IoT project. The basic selection criteria are consumption, range and bandwidth. Since IoT devices often do not have the ability to be powered by the power grid, they use batteries. In this case, it is important that the consumption of the device is as low as possible, so that its autonomy and service life are as long as possible. An autonomy of several years is often stated as a requirement for many IoT devices. As for the range, it can be from a few meters inside the building (e.g. Wi-Fi, BLE) to several kilometers in open space (e.g. LoRa – Long Range). Most often, as the range increases, the bandwidth, i.e. the amount of data sent by the IoT device, decreases, in order to keep the consumption as low as possible.

A brief description of the most commonly used wireless IoT protocols:

- **Wi-Fi** – the most common standard used in homes and businesses is 802.11n. It works on frequencies of 2.4 GHz and 5 GHz with a range of up to 50 meters. Data transfer speeds are a maximum of 600 Mbps depending on the channel frequency and the number of antennas (the latest 802.11-ac standard should offer 500 Mbps to 1 Gbps) [17],
- **NB-IoT** - *Narrowband Internet of Things* is a standard of radio technology, *Low Power Wide Area Network* (LPWAN), developed by 3GPP, the consortium in charge of network standards, for use in mobile devices and services [15, 16].
- **BLE** (*Bluetooth Low Energy*) – it is primarily intended as an upgrade of *Bluetooth Classic technology* for use in IoT devices. It is mostly used in devices in the health sector (constant control and measurements, for example: heart rate, glucose level, blood pressure, etc.), fitness, transmitters (beacon), security and home entertainment industry [18]. The bandwidth of BLE is usually in the range from 150 kbps to 1 Mbps [19],
- **LoRa** (*Long Range*) – it has the possibility of geolocation with a theoretical range greater than 10 km under ideal conditions [20].

## 2.1 Air Quality Supervising System Components

The device, the construction of which is explained in this paper, reads the quality of the air in the room, i.e. the proportion of carbon dioxide and the level of metal oxides, and at the same time measures the temperature, pressure and humidity of the air. CCS811 and BME280 sensors are used for the above and they represent the first layer of the IoT architecture. Wi-Fi was chosen as the communication technology. Data collection from sensors is done by Wemos D1 Mini, a development board based on the ESP8266 module, which sends data via Wi-Fi to a server built on a Raspberry Pi computer. Raspberry Pi contains a database in which sensor data is saved, as well as a *Web application* for displaying measurement results in text and graphic form.

The CCS811 (Fig. 1 and Fig. 2) was selected as the main sensor of the air quality control system. It is a very low-consumption digital gas sensor that detects a wide range of *Total Volatile Organic Compounds* (TVOC), including carbon dioxide equivalent (eCO<sub>2</sub>) and metal oxides (MOX) levels. Volatile organic gases are often categorized as air pollutants and/or compounds that irritate the senses, and can appear as a result of evaporation from various building materials such as paints, as well as the result of the operation of photocopiers and the presence of people (e.g. breathing, smoking).

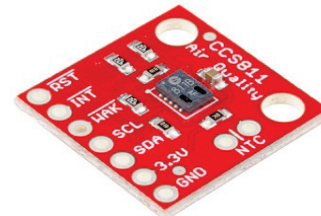


Figure 1 CCS811 sensor [21]

This sensor is intended for use in closed spaces, and is used in smart devices such as smartphones and smartwatches, or in home automation systems. This paper will use the sensor design on a separate printed circuit board, which uses a standard I<sup>2</sup>C bus for communication. The unique I<sup>2</sup>C address is 0x5A<sub>HEX</sub>.

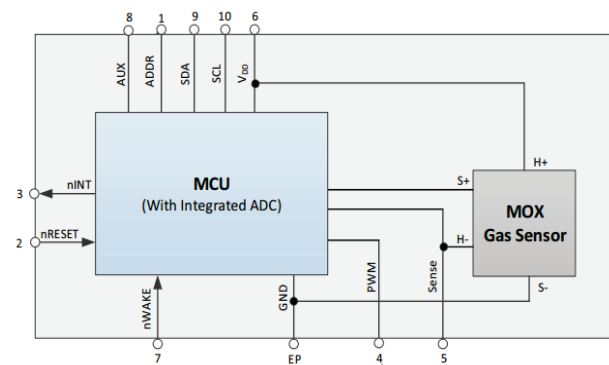


Figure 2 CCS811 Air quality sensor Block Diagram [22]

Tab. 1 shows the characteristics of the CCS811 sensor according to [23].

Table 1 Characteristics of the CCS811 sensor

Power supply:	1,8 V – 3,6 V
Current strength:	30 mA
Power Consumption:	60 mW (max)
Logic Level Voltage:	3,3 V – 5 V

I<sup>2</sup>C is a type of communication bus that enables the connection of *master* (control) and *slave* (peripheral) devices. As already explained, it uses two lines for communication: *Serial Data Line* (SDA) for sending and receiving data and *Serial Clock Line* (SCL) for sending *clock*. Connecting multiple *slave* devices using the same lines is possible because each device has a unique address.

All peripherals listen to the SDA line and monitor whether its address has been sent. The *master* sends the first data packet containing the start bit and the corresponding address of the peripheral device with which it wishes to communicate. The peripheral device responds to the sent request for communication, after which the *master* sends sending data. In order to achieve communication with several *slave* devices, a *pull-up* resistor is used. *Pull-up* is the name for a resistor that has the task of "pulling" both SCL and SDA lines to 5 V, i.e. into the logic unit [24].

In order to simplify the programming process and avoid writing complex algorithms, the *Adafruit\_CCS811* library is used for programming the CCS811 sensor, according to [25].



Figure 3 BME280 sensor [26]

In addition to the CCS811, a BME280 sensor is also used (Fig. 3 and Fig. 4). It is a combined sensor for measuring temperature, relative humidity and barometric air pressure. It has very small dimensions, low power consumption and is often used for home automation, in portable GPS modules or in smartwatches. It has high precision, so based on the pressure reading, it is possible to calculate the approximate altitude. As with the CCS811 sensor, a sensor design on a separate circuit board will be used. The standard I<sup>2</sup>C bus is also used for communication. The unique I<sup>2</sup>C address is 0x76<sub>HEX</sub>.

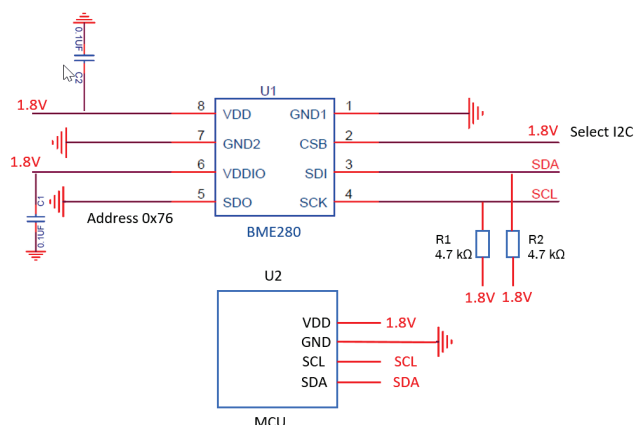


Figure 4 BME280 sensor electronics scheme [27]

The sensor characteristics are listed in Tab. 2 according to [28].

In order to simplify the programming process and avoid writing complex algorithms, the *Adafruit BME280* library is used to program the CCS811 sensor, according to [29].

Table 2 Characteristics of the BME280 sensor

Power supply:	1,71 V – 3,6 V
Current strength:	< 1 mA
Logic Level Voltage:	3,3 V – 5 V
Temperature range:	–40 °C - 85 °C (± 1 °C)
Humidity range:	0 - 100 % (± 3 %)
Pressure range:	300 hPa- 1100 hPa (± 1 hPa)
Altitude range:	0 m - 9000 m (± 1 m)

The ESP8266 (Fig. 5 and Fig. 6) is a very low-cost 32-bit Wi-Fi microcontroller from *Espressif Systems* that fully supports the TCP/IP protocol. It contains a microprocessor running at 80 MHz or 160 MHz clock. It has a memory of 32 KiB for management commands and 80 KiB for user data. The operating voltage and the logic level voltage are 3.3 V and have 16 input/output pins. It can be used as a microcontroller or as a separate Wi-Fi module to supplement another microcontroller. It supports the IEEE 802.11 b/g/n Wi-Fi protocol [30].



Figure 5 ESP8266 – 12E [31]

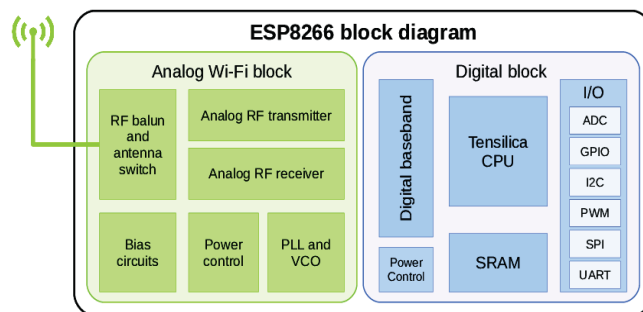


Figure 6 ESP8266 block diagram [32]

Since the ESP8266 microcontroller is intended for SMD (*Surface Mount Device*) soldering and operates at 3.3 V, in order to facilitate connection with a computer and simplify programming, in this work we use the Wemos D1 Mini development board (in the latest revision named Lolin). This board is based on the ESP-12 version of the ESP8266 chip and enables easy connection to a computer via a USB port and programming in the *Arduino IDE* development environment. Due to the combination of microcontroller and Wi-Fi connectivity, it is an excellent choice for demonstrating the capabilities of the IoT platform.

The processor with a frequency of 80 MHz on the Wemos board has at its disposal an increased memory capacity for saving program code, with a capacity of 1 MB, of which 0.8 MB is available, and 0.2 MB is reserved for the bootloader, and working memory with a capacity of 82 kB, of which 49 kB available to the user. Wemos D1 Mini has support for I<sup>2</sup>C, *Serial Peripheral interface* (SPI) and serial

communication, contains nine digital input/output pins, all of which support *Pulse with modulation* (PWM) control and one analog input pin. In addition to all of the above, the board uses CH340 as a USB 2.0 interface, contains a 3.3 V regulator and four LED indicators. Before saving the program code, Wemos performs an automatic hardware reset [33].

In this work, the Wemos chip will collect data from the sensors and send them wirelessly to the Raspberry Pi via Wi-Fi, using the MQTT (*Message Queuing Telemetry Transport*) protocol. The Wemos board and his Pins are shown in Fig. 7 and Fig. 8.



Figure 7 Wemos (Lolin) D1 Mini development board [34]

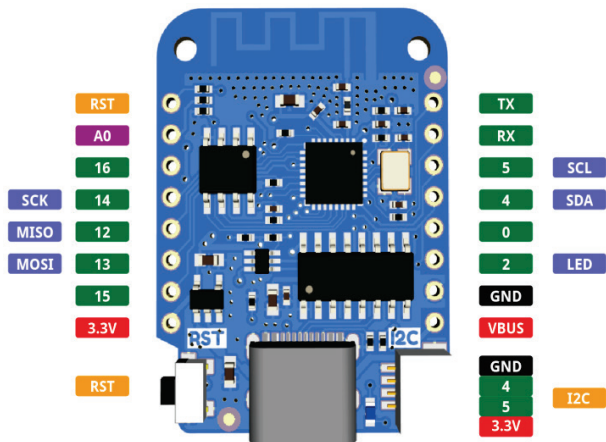


Figure 8 Wemos (Lolin) D1 Mini Pins [34]

Raspberry Pi is a minicomputer developed by "The Raspberry Pi Foundation", and it is designed as a cheap and accessible tool for hobbyists, enthusiasts, and for the needs of learning programming in schools, especially in less developed countries. It has very small dimensions, the size of a credit card, and all components are located on one circuit board. It contains ports and connectors for connecting an external power supply, mouse/keyboard, and video outputs for connecting a monitor. The operating system is stored on a microSD card, and in this work, the Raspbian operating system, based on Linux, is used.

Fig. 9 shows the connection scheme of sensors CCS811 and BME280 with Wemos D1 Mini using an experimental board.

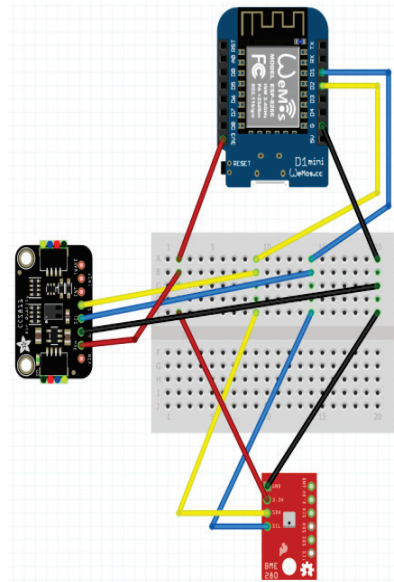


Figure 9 Scheme of connection of Wemos D1 and sensor in the "Fritzing" program

Fig. 10 shows the layout of the board with soldered sensors and Wemos D1.

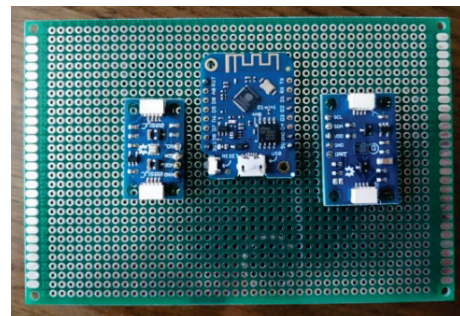


Figure 10 Wemos D1 sensors soldered on the board

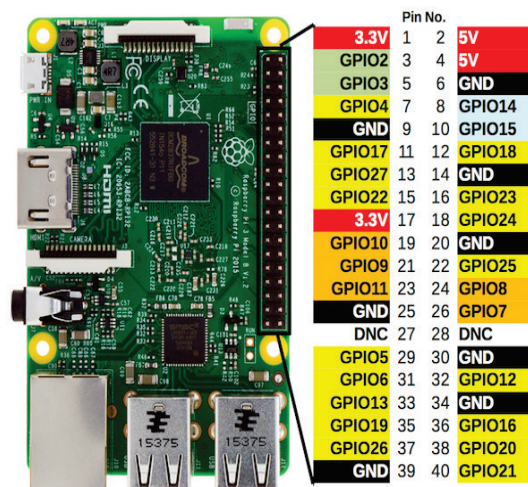


Figure 11 Layout of GPIO pins on the Raspberry Pi board

The Raspberry Pi 3B used in this work, contains forty General Input Output Pins (GPIO). GPIO pins are divided into pins with a constant voltage of 5.0 V, with a constant voltage of 3.3 V, pins for grounding (Ground - GND), pins

with an adjustable voltage and pins to which nothing is connected (Do Not Connect – DNC), according to [35].

Fig. 11 shows the arrangement of GPIO pins on the circuit board of the Raspberry Pi computer [36].

The Mosquitto MQTT broker and server will be configured on the Raspberry Pi minicomputer, which will enable local access to the Web application for displaying sensor readings.

## 2.2 MQTT Protocol Setup

MQTT is a communication protocol often used in IoT projects. It is responsible for data transfer management and is based on the *publish/subscribe* principle of operation. It is used when transmitting a small amount of data in remote locations, or in cases where a low bandwidth of wireless data transmission is available. It is simple and designed to be easily implemented [37]. It usually works over the existing TCP/IP protocol, but as a basis, it can also use other two-way protocols with loss protection (UDP protocol) [38].

Arlen Nipper and Andy Stanford-Clark created the first version of the MQTT protocol in 1999 [39, 40]. IBM released the next version (v3.1) in 2013, and then v3.1.1, which became the OASIS (*Organization for the Advancement of Structured Information Standards*) standard. The MQTT protocol started using the ISO standard in 2016 (ISO/IEC PRF 20922).

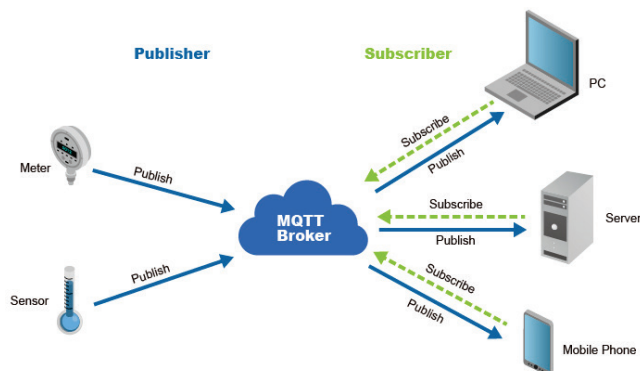


Figure 12 The working principle of the MQTT protocol [42]

Fig. 12 shows the basic principle of operation of the MQTT protocol. The MQTT *broker* communicates with all *clients* (devices). On the left side are clients that measure certain values and publish this data, and on the right side are clients that process the data to which they are subscribed. The MQTT protocol works on the publish/subscribe principle [41]. Sensors that measure some physical quantities publish measurement results on a certain topic. Clients to whom information needs to be delivered are subscribed to that same topic. When a message is published on a certain topic, it is received by all clients who have subscribed to that topic.

The MQTT broker performs the task of "intermediator" between clients and thus is the central part of the whole publish/subscribe mechanism. The main tasks of the MQTT broker are: receiving messages from all clients who publish on a certain topic, filtering messages, deciding whether to

forward specific messages and sending messages to subscribed clients.

The job of an MQTT *broker* can be performed by any computer whose specifications are powerful enough for the chosen *broker*, whether it is based on a Windows or Linux operating system. Today there are a large number of such programs. Some of the most used free MQTT *brokers* are Mosquitto, Emqtt, Hive MQ, MOSCA. In this paper, Mosquitto is used as a *broker*, which is configured on a Raspberry Pi 3B computer.

MQTT *clients* include subscribers and publishers. The MQTT client can simultaneously function as a subscriber (a client subscribed to a topic) and a publisher (a client publishes a message on a topic). The MQTT *client* task can be performed by a wide range of devices, from microcontrollers to personal computers, that is, any device that has implemented support for working with the MQTT protocol (MQTT libraries). MQTT libraries are available for a large number of programming languages: Java, JavaScript, C, C++, C#, as well as for the iOS and .NET platforms.

As an MQTT client, this paper uses a Web application made in NodeJS technology, which can be accessed in a local network, and is located in a server configured also on a Raspberry Pi computer.

*Quality of Service* (QoS) is an agreement between the publisher and subscriber of a message that defines the security of message delivery, depending on the level of the agreement.

In MQTT protocol, three levels of agreement are defined [43]:

- level 0: At most once – the message was sent only once, neither the client nor the broker perform any additional checks to see if the message was successfully received,
- level 1: At least once – the message is sent until the client confirms its receipt,
- level 2: Exactly once – the broker and the client exchange messages in two levels (two level handshake), in order to make sure that the message reaches the client exactly once.

Before installing Mosquitto, a software upgrade of the Raspberry Pi will be performed [44, 45].

```
sudo apt - get update
sudo apt - get upgrade
```

After that, Mosquitto and its associated client package are installed.

```
sudo apt-get install mosquitto -y
sudo apt-get install mosquitto-clients -y
```

After installing these two packages, it is necessary to configure the broker. The Mosquitto broker configuration file is located at `/etc/mosquitto/mosquitto.conf`.

```
sudo nano /etc/mosquitto/mosquitto.conf
```

```
// A function to connect Wemos to an MQTT broker
void connect_MQTT() {

  Serial.print("Connecting to ");
  Serial.println(ssid);

  // Connect to Wi-Fi
  WiFi.begin(ssid, wifi_password);

  // Waiting until a Wi-Fi connection is established before continue the
  program

  while (WiFi.status() != WL_CONNECTED) {
    delay(500);
    Serial.print(".");
  }

  // Debugging - printing the IP address of Wemos D1

  Serial.println("WiFi connected ");
  Serial.print("IP address: ");
  Serial.println(WiFi.localIP());

  // Connection to MQTT broker

  if (client.connect(clientID, mqtt_username, mqtt_password)) {
    Serial.println("Successful connection to MQTT broker!");
  }
  else {
    Serial.println("Failed to connect to MQTT broker...");
  }
}
```

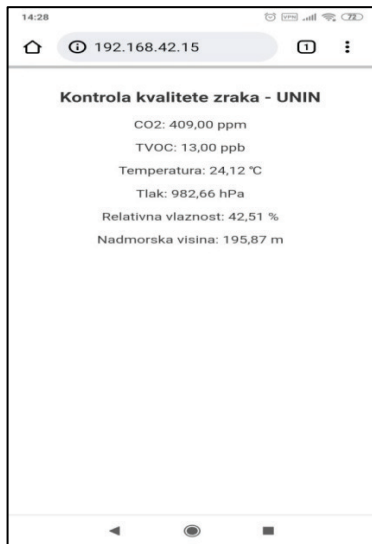


Figure 13 Web application opened on a smartphone

At the bottom of the file is the line:

```
include_dir /etc/mosquitto/conf.d
```

It will be deleted and these three lines will be added, telling Mosquitto that only clients with the correct username and password can subscribe to its topics, and that Mosquitto listens for messages on port 1883:

```
allow_anonymous false
password_file /etc/mosquitto/pwfile
listener 1883
```

If the user does not want the broker to require a username and password from the subscriber clients, he omits the first two lines. The changes to the file are saved and the file is closed. After that, it is necessary to specify a username and password. Enter the following command: - replacing username, where username is the desired username. Then the desired password is entered and the Raspberry Pi is restarted with the command:

```
sudo reboot
```

The Mosquitto MQTT broker is now configured and ready to receive messages from the Wemos D1 microcontroller board.

### 2.3 Python Script for Displaying the Results

To display the values from the sensors, which the Raspberry Pi receives from Wemos via the MQTT protocol, a Python script was created that displays the results in a Web application (Fig. 13), which can be accessed within the local network. The web application has a simple design, adapted for display on smartphones. The function responsible for generating the Web application is according to [46].

At the beginning of the program code, we enter the libraries for using the CCS811 and BME280 sensors, as well as the *PubSubClient.h* library for using the MQTT protocol on the Wemos D1 board. The *ESP8266WiFi.h* library allows Wemos to connect to a Wi-Fi network. The topics that will be sent via MQTT are defined, as well as the username and password, which must correspond to those configured in the Mosquitto broker on the Raspberry Pi.

Function for connecting Wemos D1 to MQTT broker and sending data. The previously defined username and password are used. In case of an inability to connect, it returns a warning to the user.

MQTT can only send data in string form (character). Therefore, it is first necessary to convert the measured values from the sensor from the real (float) form into character notation. Then the value is sent (Publish) to the MQTT broker. At the end of the code, disconnection from the MQTT topic is performed.

## 3 MEASUREMENT OF AIR QUALITY IN REAL CONDITIONS

Using the developed device, air measurements were made in three different environments:

- an office room,
- an underground garage,
- an industrial welding hall.

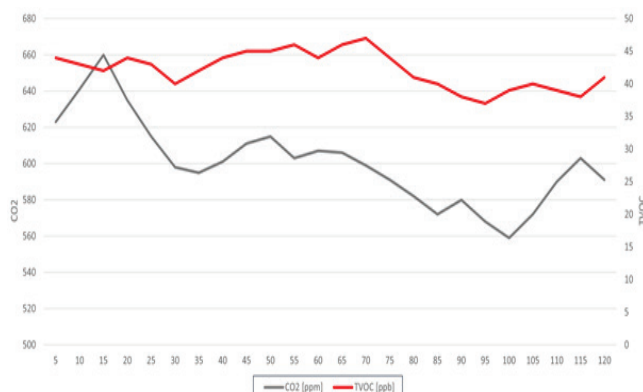
The sensor read values every five minutes for two hours, and before starting the measurement, it worked for one hour to make the measurement as accurate as possible (in the CCS811 sensor documentation, at least half an hour of "warm-up time" is recommended).

The values of the quantities measured by the CCS811 sensor and their impact on people are shown in Tab. 3.

**Table 3** Characteristics of the BME280 sensor

Concentration CO <sub>2</sub> (ppm)	Impact on people	Concentration TVOC-a (ppb)	Impact on people
< 500	normal	< 50	normal
500 - 1000	a little uncomfortable	50 - 750	uncomfortable, anxiety
1000 - 2500	tiredness	750 - 6000	headache, depression
2500 - 5000	harmful to health	> 6000	headache, harmful to the nervous system

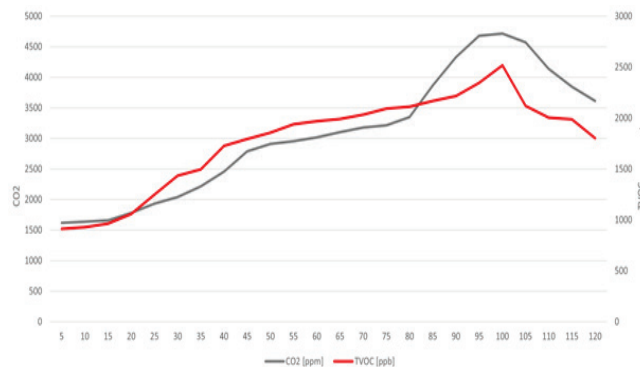
The first measurement was made in an office room with twenty employees. The CO<sub>2</sub> value ranged from 300 ppm to 550 ppm, while the TVOC value ranged from 10 ppb to 45 ppb. After 45 minutes from the beginning of the measurement, the window was opened and the room was ventilated, which contributed to the reduction of the concentration of both quantities. The measured concentrations are within normal limits and do not cause any disturbance or discomfort to people (Fig. 14).

**Figure 14** Measured air quality in the office room**Figure 15** Measured air quality in the underground garage

The second measurement was made on the second level of an underground garage (Fig. 15). The CO<sub>2</sub> value ranged from 560 ppm to 660 ppm, while the TVOC concentration ranged from 40 ppb to 45 ppb all the time. The CO<sub>2</sub> value is slightly above normal, but still did not cause any disturbances, while the TVOC value is within normal limits. The concentrations were at a similar level all the time due to the constant forced air exchange in the underground garage.

The third measurement was carried out in an industrial hall where five welders and two other employees work in

other jobs (e.g. drilling, cutting, grinding metal). CO<sub>2</sub> concentration ranged from 1500 ppm to 4750 ppm, while TVOC values were between 900 ppb and 2500 ppb. The measured concentrations are very high due to jobs that bring a large amount of metal particles into the air, as well as lubricants, paints and solvents (Fig. 16). This kind of working environment requires the use of protective breathing masks (respirators), because this high concentration of substances in the air is very harmful to the health of employees.

**Figure 16** Measured air quality in the welding hall

By performing the measurements, an idea was obtained for a possible improvement of the device, which is the automatic sending of an e-mail message or SMS to the responsible person in the company when the concentrations of CO<sub>2</sub> and TVOC exceed a certain value, in order to ventilate the hall.

## 4 CONCLUSION

The concept of the *Internet of Things* is explained using the example of an air quality sensor. Since IoT is a relatively new concept and platform, it can be assumed that in the near future most products on the market will become part of this platform, and that they will have the ability to monitor or manage some of their parameters. IoT as an industry has a huge potential for development.

The processed air quality control device has a wide potential application, from industrial plants to home automation systems. Relatively cheap and easily available parts enable the control and processing of various sizes, and their storage in a database for the possibility of checking values in a past period of time and comparing them with today. Thus, for example, a comparison could be made as to whether a change in the production process of a company contributed to the improvement of indoor air quality, resulting in a more pleasant workplace for employees and a reduction in the harmful impact on their health.

The development of smart devices is facilitated by the use of development boards based on various microcontrollers, such as the used Wemos D1 Mini. Such development boards already contain many connectors and pins that facilitate experimentation and testing with various sensors and other electronics. Of course, mass-produced devices use only microcontrollers and those electronic components that are necessary, but for enthusiasts and those

who want to learn about electronics and programming, development boards are a great solution.

It was shown how cheap mini-computers like Raspberry Pi have enough power to run servers that control smaller IoT systems. Such computers come every year with better specifications and a lower price, and it is difficult to predict how far they will go in a few years and what they will be able to run.

Air measurements were made in three different environments: an office room, an underground garage and in industrial welding hall. Measured concentrations in an office room are within normal limits and do not cause any disturbance or discomfort to people. The concentrations in the underground garage were at a similar level all the time due to the constant forced air exchange. The measured concentrations in industrial welding hall are very high due to jobs that bring a large amount of metal particles into the air, as well as lubricants, paints and solvents.

Future research could explore the effectiveness of the processed air quality control device in different industrial and home settings and assess its impact on indoor air pollution levels, employee health, and overall productivity. Future research could also explore the economic feasibility of implementing the device in various contexts, and evaluate alternative designs and features to improve its performance and ease of use. In addition, further research may be needed to assess the potential benefits and limitations of integrating the device with other smart home technologies and environmental monitoring systems, and to explore new applications and markets for processed air quality control devices.

## Acknowledgement

This work was funded by the European Union through the European Regional Development Fund, under the project "Smart Sticker for measuring and monitoring storage and transportation conditions of products" KK.01.1.1.04.0116.

## 5 REFERENCES

- [1] Delija, G. (2021). Kontrola kvalitete zraka korištenjem IoT platform. *Master's thesis*, University North, Croatia. <https://urn.nsk.hr/urn:nbn:hr:122:241977>, (in Croatian) (Accessed 1/18/2023)
- [2] Al-Fuqaha, A., Guizani, M., Mohammadi, M., Aledhari, M., & Ayyash, M. (2015). Internet of things: A survey on enabling technologies, protocols, and applications. *IEEE Communications Surveys & Tutorials*, 17(4), 2347-2376. <https://doi.org/10.1109/COMST.2015.2444095>
- [3] Amodu, O. A. & Othman, M. (2018). Machine-to-Machine Communication: An Overview of Opportunities. *Computer Networks*, 145, 255-276. <https://doi.org/10.1016/j.comnet.2018.09.001>
- [4] Uzair, M., Al-Kafrawi, S. Y., Al-Janadi, K. M., & Al-Bulushi, I. A. (2022). A Low-Cost IoT Based Buildings Management System (BMS) Using Arduino Mega 2560 and Raspberry Pi 4 for Smart Monitoring and Automation. *IJECE*, 13(3), 219-236. <https://doi.org/10.32985/ijeces.13.3.7>
- [5] Yassein, M. B., Shatnawi, M. Q., Aljwarneh, S., & Al-Hatmi, R. (2017). Internet of Things: Survey and open No s of MQTT protocol. *Proceedings of the International Conference on Engineering & MIS (ICEMIS)*, Monastir, Tunisia, 1-6. <https://doi.org/10.1109/ICEMIS.2017.8273112>
- [6] Hedi, I., Špeh, I., & Šarabok, A. (2017). IoT network protocols comparison for the purpose of IoT constrained networks. *Proceedings of the 40<sup>th</sup> International Convention on Information and Communication Technology, Electronics and Microelectronics*, Opatija, Croatia, 22-26 May 2017, 501-505. <https://doi.org/10.23919/MIPRO.2017.7973477>
- [7] Shafiq, M., Gu, Z., Cheikhrouhou, O., Alhakami, W., & Hamam, H. (2022). The Rise of "Internet of Things": Review and Open Research Issues Related to Detection and Prevention of IoT-Based Security Attacks. *Wireless Communications and Mobile Computing*, e8669348. <https://doi.org/10.1155/2022/8669348>
- [8] Crnjac-Milić, D., Dujmenović, I., & Peko, M. (2023). An Approach to the Application of the Internet of Things in Logistics. *Tehnički glasnik*, 17(1), 134-140. <https://doi.org/10.31803/tg-20220609190233>
- [9] Medium.com. The internet of things (IoT). <https://medium.com/zeux/the-internet-of-things-5-reasons-why-the-world-needs-it-125fe71195cc> (Accessed 1/18/2023)
- [10] Ahire, B. A. & Sakhare, S. R. (2021). Sound Prohibited Zone for Smart Cities using IoT. *Tehnički glasnik*, 15(1), 92-97. <https://doi.org/10.31803/tg-20210205091148>
- [11] Terroso-Saenz, F., González-Vidal, A., Ramallo-González, A. P., & Skarmeta, A. F. (2019). An open IoT platform for the management and analysis of energy data. *Future Generation Computer Systems*, 92(2), 1066-1079. <https://doi.org/10.1016/j.future.2017.08.046>
- [12] Sadhu, V., Zhao, X., & Pompili, D. (2020). Energy-Efficient Analog Sensing for Large-Scale and High-Density Persistent Wireless Monitoring. *IEEE Internet of Things Journal*, 7(8), 544-559. <https://doi.org/10.1109/JIOT.2020.2984484>
- [13] Casado-Vara, R., Martin-del Rey, A., Affes, S., Prieto, J., & Corchado, J. M. (2020). IoT network slicing on virtual layers of homogeneous data for improved algorithm operation in smart buildings. *Future Generation Computer Systems*, 102, 965-977. <https://doi.org/10.1016/j.future.2019.09.042>
- [14] Yang, C. H., Lee, K. C., & Li, S. E. (2020). A mixed activity-based costing and resource constraint optimal decision model for IoT-oriented intelligent building management system portfolios. *Sustainable Cities and Society*, 60(3), 655-671. <https://doi.org/10.1016/j.scs.2020.102142>
- [15] ShareTechnote. 4G/LTE – NB IoT Operation Mode. [https://www.sharetechnote.com/html/Handbook\\_LTE\\_NB\\_LTE.html](https://www.sharetechnote.com/html/Handbook_LTE_NB_LTE.html) (Accessed 1/18/2023)
- [16] Avsystem. What is Narrowband IoT? NB-IoT overview. <https://www.avsystem.com/blog/narrowband-iot/> (Accessed 1/18/2023)
- [17] IoT for all. The role of WiFi in IoT. <https://www.iotforall.com/wifi-role-iot> (Accessed 1/18/2023)
- [18] Link Labs. Bluetooth Low Energy M2M and IoT Applications. <https://www.link-labs.com/blog/bluetooth-vs-bluetooth-low-energy> (Accessed 1/18/2023)
- [19] Gomez, C., Oller, J., & Paradells, J. (2012). Overview and Evaluation of Bluetooth Low Energy: An Emerging Low-Power Wireless Technology. *Sensors*, 12(9), 11734-11753. <https://doi.org/10.3390/s120911734>
- [20] Adelantado, F., Vilajosana, X., Tuset-Peiro, P., Martinez, B., Melia, J., & Watteyne, T. (2017). Understanding the limits of LoRaWAN. *IEEE Communications Magazine*, 55(9), 34-40. <https://doi.org/10.1109/MCOM.2017.1600613>
- [21] SparkFun. Air Quality Breakout - CCS811. <https://www.sparkfun.com/products/14193> (Accessed 1/19/2023)

- [22] InnovatorsGuru. AMS - Ultra Low Power Digital Gas Sensor for Monitoring Indoor Air Quality, General Description, Block diagram from the manual, page 3. [https://innovatorsguru.com/wp-content/uploads/2020/01/CCS811\\_Datasheet-DS000459.pdf](https://innovatorsguru.com/wp-content/uploads/2020/01/CCS811_Datasheet-DS000459.pdf) (Accessed 1/20/2023)
- [23] SparkFun. Characteristics of the CCS811 sensor. [https://cdn.sparkfun.com/assets/learn\\_tutorials/1/4/3/CCS811\\_Datasheet-DS000459.pdf](https://cdn.sparkfun.com/assets/learn_tutorials/1/4/3/CCS811_Datasheet-DS000459.pdf) (Accessed 1/18/2023)
- [24] NXP. I<sup>2</sup>C-bus specification and user manual. <https://web.archive.org/web/20210426060837/https://www.nxp.com/docs/en/user-guide/UM10204.pdf> (Accessed 1/18/2023)
- [25] GitHub. Arduino library for the CCS811. <https://github.com/maarten-pennings/CCS811> (Accessed 1/18/2023)
- [26] Distrelecwebshop images. BME280 sensor picture. [https://www.distrelec.biz/Web/WebShopImages/landscape\\_large/2-/01/Adafruit-2652-30091192-01.jpg](https://www.distrelec.biz/Web/WebShopImages/landscape_large/2-/01/Adafruit-2652-30091192-01.jpg) (Accessed 1/18/2023)
- [27] Bosch. Complete schematic of typical BME280 use-case. <https://community.bosch-sensortec.com/t5/Knowledge-base/BME280-series-humidity-sensor-design-guide/ta-p/7385> (Accessed 1/18/2023)
- [28] Bosch. Technical data of the sensor BME280. <https://www.bosch-sensortec.com/products/environmental-sensors/humidity-sensors-bme280/> (Accessed 1/20/2023)
- [29] Last minute engineers. Arduino library manager. <https://lastminuteengineers.com/bme280-arduino-tutorial/> (Accessed 1/20/2023)
- [30] Espressif. ESP8266 overview. <https://www.espressif.com/en/products/socs/esp8266> (Accessed 1/20/2023)
- [31] Auscomtech. ESP8266MOD picture. <https://www.auscomtech.com.au/wp-content/uploads/2018/12/AD483-2.jpg> (Accessed 1/20/2023)
- [32] Orellana, C., Macías, M., González-Velasco, H., Manso, A., & Gallardo-Caballero, R. (2019). Low-Power and Low-Cost Environmental IoT Electronic Nose Using Initial Action Period Measurements. *Sensors*, 19(14), 3183. <https://doi.org/10.3390/s19143183>
- [33] Asinelli, M. G., Serra, M. S., Marimon, J. M., & Espauella, J. S. (2018). The smARTS\_Museum\_V1: An open Hardware device for remote monitoring of Cultural Heritage indoor environments. *HardwareX*, 4, e00028. <https://doi.org/10.1016/j.ohx.2018.e00028>
- [34] Wemos.cc. Wemos D1 mini board. [https://www.wemos.cc/en/latest/d1/d1\\_mini.html](https://www.wemos.cc/en/latest/d1/d1_mini.html) (Accessed 1/20/2023)
- [35] RaspberryPi. Specification of the Raspberry Pi. <https://www.raspberrypi.org/products/raspberry-pi-3-model-b/> (Accessed 1/20/2023)
- [36] Bigmessowires. Raspberry GPIO. <https://www.bigmessowires.com/wp-content/uploads/2018/05/Raspberry-GPIO.jpg> (Accessed 1/20/2023) [https://doi.org/10.1007/978-1-4842-3948-3\\_1](https://doi.org/10.1007/978-1-4842-3948-3_1)
- [37] Tareq, R. W. & Khaleel, T. A. (2021). Implementation of MQTT Protocol in Health Care Based on IoT Systems: A Study. *IJECE*, 12(4), 215-223. <https://doi.org/10.32985/ijece.12.4.5>
- [38] U-blox. MQTT explained. <https://www.u-blox.com/en/blogs/insights/mqtt-beginners-guide> (Accessed 1/22/2023)
- [39] Sugumar, K. (2020). MQTT-aLightweight Communication Protocol Relative Study. *Author Preprints*, 1-5. <https://doi.org/10.22541/au.159076954.48540044>
- [40] Mishra, B. (2018). TMCAS: An MQTT based collision avoidance system for railway networks. *Proceeding of the 18<sup>th</sup> International Conference on Computational Science and Applications*, Melbourne, VIC, Australia, 2-5 July 2018, 1-6. <https://doi.org/10.1109/ICCSA.2018.8439562>
- [41] Jaloudi, S. (2019). Communication protocols of an industrial internet of things environment: A comparative study. *Future Internet*, 11(3), p. 66. <https://doi.org/10.3390/fi11030066>
- [42] Oringnet. The working principle of the MQTT protocol. [https://oringnet.com/upload/media/Technology/MQTT/MQT\\_T\\_1091217-01.jpg](https://oringnet.com/upload/media/Technology/MQTT/MQT_T_1091217-01.jpg) (Accessed 1/25/2023)
- [43] Toldinas, J., Lozinskis, B., Baranauskas, E., & Dobrovolskis, A. (2019). MQTT Quality of Service versus Energy Consumption. *Proceedings of the 23<sup>rd</sup> International Conference Electronics*, Palanga, Lithuania, 17-19 June 2019, 1-4. <https://doi.org/10.1109/ELECTRONICS.2019.8765692>
- [44] Self Hosted Home. Setting up MQTT Broker for DIY Home Assistant Sensors. <https://selfhostedhome.com/setting-up-mqtt-broker-for-diy-home-assistant-sensors/> (Accessed 1/25/2023)
- [45] PiMyLifeUp. Installing the Mosquitto MQTT Server to the Raspberry Pi. <https://pimylifeup.com/raspberry-pi-mosquitto-mqtt-server/> (Accessed 1/25/2023)
- [46] Random nerd tutorials. MQTT Libraries. <https://randomnerdtutorials.com/esp8266-nodemcu-mqtt-publish-dht11-dht22-arduino/> (Accessed 1/25/2023)

#### Authors' contacts:

**Marinko Stojkov, PhD**, Full Professor  
University of Slavonski Brod,  
Trg Ivane Brlic Mazuranic 2, 35000 Slavonski Brod, Croatia  
mstojkov@unib.hr

**Goran Delija**, student  
University Center Varaždin, Mechanical Engineering Department,  
Jurja Križanića 31b, 42000 Varaždin, Croatia  
goran.delija1@gmail.com

**Ivan Đuračić**, PhD student  
(Corresponding author)  
University of Slavonski Brod,  
Trg Ivane Brlic Mazuranic 2, 35000 Slavonski Brod, Croatia  
idjuracic@gmail.com

**Tomislav Alinjak**, PhD  
Elektra Slavonski Brod,  
Petra Krešimira IV 11, 35000 Slavonski Brod, Croatia  
tomislav.alinjak@hep.hr

# Rewarding Scientific Productivity of University North Employees

Anica Hunjet\*, Marin Milković, Nikolina Topolko Špoljar

**Abstract:** Scientific productivity makes for an important indicator to all scientific institutions and professionally recognized scientists. Scientific activity is of particular interest to Republic of Croatia, as it holds a special place in the international (and particularly European) scientific domain. Scientists are known for their reputation, i.e., their productivity is often recognized in magazines that publish their research papers. University North has recently established a special reward system for scientist, in order to ensure proper rewards for scientific accomplishments, i.e., for published research papers, citations of said papers, and an overall improved recognition of the institution that employs them. This system has certain rules and criteria for rewarding scientists. The rewards in and of themselves are contributing to popularization of science at the institution in question; furthermore, rewarding provides for a very good incentive for publishing many research papers with excellent indexing. Publishing research papers is also important to the institution the paper is referencing, as it adds to said institution's visibility and recognition in the European and international domain of research and science.

**Keywords:** h index; rewarding; scientific activity; Scopus; University North; WoS

## 1 INTRODUCTION

Scientific activity at University North has been regulated via the Act on Higher Education and Scientific Activity [1], the University Statute from November 7th, 2018 [2], the Regulation on Election into Scientific Professional Vocations [3] and the Regulation on Rewarding Published Research Papers, Scientist Visibility and Granted University North Patents [4]. The right to monetary rewards is reserved exclusively for University North employees [4].

Scientific productivity is mostly measured via quantitative indicators, which include bibliometric parameters of evaluation of scientists and scientific institutions [5]. The scientific productivity evaluation process includes various indicators, but mostly considers the number of published research papers and how many times they were cited. Quantitative evaluation of scientific productivity based on published research papers has become an inevitable factor to evaluation of scientific contribution for the Croatian academic and scientific community [6].

Scientists find it important to choose magazines that publish their research results. Universities prefer scientists who publish in reputable magazines, as it affects the reputation of the University itself [7].

According to the Regulation on Organization and Systematization of University North Workplaces [8], the Department of Science, Art and International Cooperation at North University is in charge of all matters regarding science and scientific activity, which also makes it in charge of the scientist reward system. Furthermore, the Department is in charge of all matters regarding popularization of science and improvement of the University's scientific recognition in the domain of European and international science and research. Scientific work is conducted by scientists with institutions such as universities, scientific institutes, and others. The Department is also in charge of facilitating integration and connections between various domains and fields of scientific and artistic work at University North [9].

The purpose and objective of this paper is to depict the process of rewarding scientists at University North, in accordance with the Regulation on Rewarding Published

Research Papers, Scientist Visibility and Granted University North Patents [4].

At University North, the scientist reward system is designed as follows: a scientific research paper is defined as any paper published in magazines indexed within scientific databases Web of Science and Scopus. Web of Science (WoS) is actually one of the products of Thomson Reuters' platform Web of Knowledge (WoK). WoK is a research platform that helps its users find, analyse and exchange information from all areas of science. Some of the products included within Wok are: Biosis Citation Index, CAB Abstracts, Conference Proceedings Citation Index, Current Contents Connect, Food Science Technology Abstracts, Global Health Inspect, Journal Citation Reports, Medline, Web of Science, and Zoological Record [6]. Apart from WoS, Elsevier's multidisciplinary, bibliographic and citation base Scopus has recently been gaining traction with regards to bibliometric and scientometric research. The database's name, Scopus, was inspired by the bird Hammerkop Scopus Umbrette, which is known for its extraordinary navigational abilities. WoS is the key database for all STEM papers (science, technology, engineering, and mathematics), whereas both WoS and Scopus make for key databases for papers related to other scientific fields. Furthermore, patents are also subject to rewards. Patents are inventions that offer new technical solutions with regards to a certain product, procedure, or application. Patents are granted by the State Intellectual Property Office of Republic of Croatia [4].

One must also mention the Hirsch index, which is used to measure and evaluate scientific productivity via the number of published research papers, as well as the effects of said papers (measured by how many times they were cited).

Once a year, University North invites employees to apply for monetary rewards for papers published by the University's scientists. One can usually apply in the following three or four weeks [4].

Monetary rewards are awarded for research papers from the previous year, a scientist's personal influence and visibility, and patents granted by the State Intellectual Property Office in the previous year. The request for a monetary reward cites the authors, research papers and bibliometric data pertaining to said papers. Scientific

databases WoS and Scopus have their own special set of rules with regards to determination of quartiles and indicators of citation frequency (via Journal Citation Reports (JCR) and Scientific Journal Rankings (SJR)) [4].

After the initial phase, Committee for Evaluation of Requests for Monetary Rewards for Published Research Papers, Scientist Visibility and Granted Patents is formed. The Committee examines whether the required criteria is met, analyses the submitted documentation, and decides on the amount of the monetary reward. Once the aforementioned process has been completed, the Committee submits their evaluation and the proposed decision to the Rector, who makes the final decision on the amount of monetary rewards [4].

## 2 REGULATION OF SCIENTIFIC ACTIVITY AT UNIVERSITY NORTH WITH REGARDS TO REWARDING SCIENTISTS

Based on the University North's Statute [2], the University Senate has adopted Regulations on Rewarding Published Research Papers, Scientist Visibility and Patents Granted to University North's Employees [4].

Monetary rewarding of research paper authors and patent authors/inventors is closely regulated by the Regulation on Rewarding Published Research Papers, Scientist Visibility and Patents Granted to University North's Employees. The right to a monetary reward is reserved for University North employees exclusively [4].

According to the Act on Higher Education and Scientific Activity, scientific activity is based on the following: freedom and autonomy of scientific creativity, open science, scientists' and teachers' ethics, availability of research results to the public, research aimed at developing innovations and technology in the European research space, interconnection with the educational system, international quality measures, incitement and acceptance of specificity of national content, intellectual property protection, and social responsibility of scientists [1].

University North's Department of Science, Art and International Cooperation is charged with conducting all organizational and supporting activities from the domains of artistic, scientific, and innovation-related work at University North. Furthermore, based on previous strategies and analyses, the Department of Science, Art, and International Cooperation suggests, publishes, and supervises the conduction and realization of scientific objectives. The Department is also in charge of all forms of popularization of science, supervision of scientists' success pertaining to scientific and artistic work, and improvement of scientific visibility of University North within the international framework. The Department is in charge of providing necessary help, such as assistance with the process of application, documentation collection and other related activities, to scientists who are applying with their scientific, artistic, and other projects. The Department must inform scientists in a timely manner about all events, conferences, rewards, available scientific subsidies, and other important information pertaining to scientists' possible career advancements [7].

In accordance with Article 2 of the Regulation on Scientific and Artistic Domains, Fields, and Branches [9], scientific and artistic fields are as follows: natural science, technical science, biomedicine and healthcare, biotechnical science, social science, human science, art, interdisciplinary scientific fields, and interdisciplinary artistic fields.

University North's strategy pertaining to scientific research and art for the time period from 2021 to 2027 is focused on the strategic objective of *Ensuring proper quality of scientific activity*. This strategic objective places great importance upon the efficiency and quality of the scientific research process, as it makes for one of the main prerequisites for ensuring high-quality scientific activity at University North [10].

The University cherishes principles of quality in the domain of scientific research and teaching, as well as principles of ethics, creativity, and transparency. Moreover, the University persists in its cooperation with other international and national scientific institutions of higher education and insists on the development and preservations of excellent academic and interpersonal relations.

The University incites critical thinking and creativity via its conception of new ideas and technological solutions, which makes it into one of the key initiators of economic and sustainable development. University North shall strive to be the bearer of society of knowledge, creativity, and strategic development of north-western Croatia.

### 2.1 Scientific Research Paper

According to the Act on Higher Education and Scientific Activity [1], scientific work pertaining to scientific research papers is conducted by scientists with institutions such as universities, scientific institutes, and others. Scientific work is also conducted by persons elected into associate positions at the aforementioned organizations, as well as other scientists who meet the criteria for performance of scientific activity.

Postgraduate university students and persons elected into professional positions in accordance with the aforementioned Act can also participate in scientific research papers. Furthermore, other students and participants in the scientific and educational process can also take part in the scientific research papers [1].

Prior to choosing the magazine that will publish their paper, it is recommended that authors check the scientific databases said magazine is indexed with in order to make sure that paper will count as credit toward their election into a scientific vocation [11].

### 2.2 Scientific Research Paper within the Context of Rewarding University North Scientists

In accordance with Article 3, Paragraph 1 of the Regulation on Rewarding Published Research Papers, Scientist Visibility and Patents Granted to University North's Employees [4], the term scientific research paper is defined as any paper published in magazines indexed within scientific data bases Web of Science [12] and Scopus [13].

WoS is the key database for all STEM papers, whereas both WoS and Scopus make for key databases for papers related to other scientific fields.

The STEM field consists of study programmes from the biotechnical, technical, biomedical, and natural domains of science, as well as study programmes that result in bachelor's degrees in the field of informatics, business informatics, informational science, informatology, and informational technologies, or a master's degree in informatics, informatology, informational sciences, and informational technology. Furthermore, this area also includes university specialist degrees in business informational systems and STEM teaching study programmes that have been issued a special permission to perform study programmes for future informatics teachers that result in a master's degree in informatics education [14].

WoS is a platform that offers available citation indexes and databases from all fields of science. The platform contains over 33.000 indexed magazines and almost a billion records of cited references. It includes articles, conference anthologies, reports, patents, and others [12].

Scopus is a bibliographic and citation database that indexes sources from all over the world and covers all areas of science [13].

### 2.3 Patent within the Context of Rewarding University North Scientists

In accordance with Article 3, Paragraph 2 of the Regulation on Rewarding Published Research Papers, Scientist Visibility and Patents Granted to University North's Employees, a patent is defined as an invention that offers a new technical solution pertaining to a certain product, procedure, or application. Patents are granted by the State Intellectual Property Office of Republic of Croatia [4]. According to the State Intellectual Property Office of Republic of Croatia, a patent is an exclusive right granted for an invention that offers a new solution to a technical problem. A patent can be granted for an invention pertaining to a product, procedure, or application [15].

## 3 THE HIRSCH INDEX

Physicist J. E. Hirsch recognized the need to improve upon the calculation of indicators necessary for scientists' productivity evaluation, the number of published research papers, the influence of said papers measured by the number of times they were cited, the average number of citations per paper, and the number of papers characterized by an above-average number of citations. Hirsch therefore introduced an indicator that can measure the broader influence and recognizable effects of papers written by individual scientists and also magazines [16].

He suggested only one number, called the 'h-index,' as a simpler and more useful way of characterizing scientific activity of researchers [16].

If an author's h-index amounts to 10, that particular author has published 10 or more papers, whereby 10 of the papers were cited at least 10 times, and the remaining papers

were cited less than 10 times. In this case, the total citation number has to amount to at least 100 [17].

The Hirsch index is used to compare scientists from the same field of science and of approximately equal work experience. This also applies to magazines [16].

For the sake of comparison, if two scientists have approximately the same work experience and a relatively equal number of published papers/similar number of citations, but their h-indexes differ, the scientist with a greater h-index is more recognizable than the other one [16].

## 4 THE PROCESS OF ANNOUNCING THE INVITATION TO APPLY FOR MONETARY REWARDS FOR PAPERS PUBLISHED BY UNIVERSITY NORTH SCIENTISTS

According to Article 7, Paragraph 1 and 2 of the Regulation on Rewarding Published Research Papers, Scientist Visibility and Patents Granted to University North's Employees [4], the invitation to apply for monetary rewards for published work (scientific research papers, patents, and the h-index) shall be extended once a year via the University North's webpage and the Notice Board. The invitation is usually valid for three or four weeks.

The invitation to apply for monetary rewards is officially extended by the University North's Rector, thus inviting all University North employees who meet the criteria defined by the Regulation on Rewarding to apply for monetary rewards for published research papers, scientist visibility, or granted patents. The invitation for monetary rewards pertains to the previous year – for example, if the invitation was extended in 2022, it pertains to all research papers and patents published and visible in scientific databases/registered with the patent office from January 1<sup>st</sup> to December 31<sup>st</sup>, 2021. If the invitation was extended in 2022, then the increase in scientist's recognizability (the h-index) must be recorded for the time period from 2020 to 2021 [4].

If a scientific research paper or a patent has more than one author, the monetary reward is equally split between co-authors.

Apart from the invitation to apply for monetary rewards, the rector also makes the decision about the gross amount of said reward. Monetary rewards are awarded in accordance with the Regulation on Rewarding as follows.

### 4.1 Scientific Research Papers Published in the Previous Year

The rector's decision about the amount of the gross base for monetary rewards serves to define the amount of basis for the final calculation.

The established basis is multiplied by:

- factor 2 if the magazine belongs in the first quartile (Q1)
- factor 1,6 if it belongs in the second quartile (Q2)
- factor 1,2 if it belongs in the third quartile (Q3)
- factor 1 if it belongs in the fourth quartile (Q4).

Scientific research papers must reference the North University as the institution where the scientist is employed.

If the magazine belongs to a greater number of scientific categories, the category the magazine belongs to in the lowest quartile is used as a reference point.

## 4.2 Personal Influence and Scientist Visibility (Paper Production and Citations)

The rector's decision about the amount of the gross base for monetary rewards serves to define the amount of basis for the final calculation:

- the established basis is multiplied by the factor 2 for every unit of increase of the scientist's h-index for the previous year
- newer papers by said scientist must refer to University North / name University North as their employer
- minimal initial value of the scientist's h index must be 1
- the h index is evaluated in accordance with the *WoS* or *Scopus* database [4].

## 4.3 Patents Granted by the Patent Office in the Previous Year

A patent is granted by an authorized institution, mostly based on examination of the patent application. The patent application describes the invention in a way that is prescribed by Law. The authorized institution can be a national patent office (State Intellectual Property Office in Republic of Croatia) or a regional patent office that examines the patent application for several countries within a region (for example, Republic of Croatia is a member of the European Patent Organization, so the authorized institution is the European Patent Office). A patent is granted in accordance with the principle of territoriality, i.e., it is only valid in the country or region it was granted in [15].

The rector's decision about the amount of the gross base for monetary rewards serves to define the amount of basis for the final calculation. The gross basis is multiplied by the factor 2 [4].

## 5 REQUEST FOR A MONETARY REWARD

Request for a monetary reward is comprised of:

- 1) Type of application
- a) Scientific research paper
- b) An increase in the h-index
- c) A granted patent.

If the application pertains to a scientific research paper, the author must enter the name of the paper, first and last name of the author, and the CROSBID ID of the paper.

If the application pertains to an increase in the h-index, the author must report the exact amount of said increase. Furthermore, the author must enter their first and last name and proof of the h-index increase.

If the application pertains to a patent, the author must enter the name of the patent and file all relevant accompanying documentation.

In order to provide complete documentation, the author is obliged to deliver the pertinent scientific research papers, as well as the Certificate of the bibliometric data obtained

from the National and University Library in Zagreb or the University Library of University North [4].

Attachment 1.

### REQUEST FOR A MONETARY AWARD

Application type

- a) Application of a scientific paper
- b) Report of h-index increase
- c) Patent application

Name of the scientific paper and CROSBID ID of the paper/ increase in the scientist's h-index / description and name of the patent

Name and surname of the author, or all authors in the case of multiple authors

Additional attachments/evidence (circle as applicable)

1. Decision on patent recognition from the State Institute for Intellectual Property
2. Qualification papers for awarding
3. Confirmation of the National and University Library in Zagreb (NSK) or the University Library of the University Sjever - bibliometric data (cited works, increase in h-index) according to Art. 5, paragraph 3.

Author's signature:

In Koprivnica/Varaždin, \_\_\_\_\_ (day, month, year).

Figure 1 Request for a monetary reward, University North

## 5.1 Certificate of Bibliometric Data

Bibliometric data are obtained once the paper is published in a magazine. Said data is based on the quantitative indicators that show how often the paper was used, read, and cited, i.e., it is based on the influence and effect said paper has had on the scientific community.

Bibliographic data can be found in scientific databases *WoS* and *Scopus*. Data about the citation frequency can also be found in said databases, which is very important to evaluation of papers published by certain scientists, the institution that employs them and the very publication that published them [4].

### 5.1.1 Web of Science (WoS)

Eugen Garfield, founder of the Institute for Scientific Information in Philadelphia, is also considered the founder of the citation database *Web of Science*. Back in the 60's, Garfield attempted to create a significant source of new scientific literature on an international level. Said source was supposed to facilitate easier navigation through an increasing number of publications. The multidisciplinary database, the Science Citation Index, encompassed exclusively magazines and later became a source for scientometric research [6].

The *WoS* database can be used via the webpage <http://baze.nsk.hr/baza/web-science/>.

The bottom of the webpage provides both the text and the link - Search Database: Web of Science. After a click on the link, the search bar of the database *WoS* pops up [12].

Remote access outside of the institution via the AAI@EduHr identity is enabled by the following link: *Proxy Journal Citation Reports (JCR)* is a citation database available in two editions:

- *Science Edition* – for natural sciences
- *Social Sciences Edition* – for social sciences.

*Journal Citation Reports (JCR)* enables evaluation of scientific magazines through the impact factor. It can also use quantitative indicators for measurement, evaluation, categorization, and comparison of several magazines to check whether a certain magazine is well represented in the *WoS* database [12].

*JCR* categorizes magazines into categories ranging from highest to lowest quartiles (Q1, Q2, Q3 and Q4) based on the data on citation frequency pertaining to magazines represented within the *WoS* database.

If a certain magazine belongs in the highest quartile (Q1), it means it belongs with the 25% of magazines with the highest influence factor in the pertinent field of science.

If a magazine belongs in the second quartile (Q2), it means its influence factor belongs between the first 25% and 50% of magazines in the pertinent area of science [12].

*JCR* usually publishes its annual data around June of the following year, as a certain time period needs to pass in order to record the frequency of citation of papers published in a certain magazine [12].

### 5.1.2 SCOPUS

The *Scopus* database can be accessed via the following webpage: <https://www.scopus.com/search/form.uri?display=basic#basic> [13].

The scientific database *Scopus* also evaluates representation and division into quartiles (Q1, Q2, Q3, Q4). *SCImago Journal Rank (SJR)* is a *Scopus* citation base that enables various searches of magazines represented within it. The magazines can be searched by their respective scientific field, country, region, publication type etc. [13].

The depiction below shows how easy it is to check the frequency of citation of a certain publication via the *SJR* webpage. For example, 'Podravina', a magazine that often publishes papers written by University North professors, has been entered into the search bar. One must only enter the name of the magazine (in this case, 'Podravina') into the search bar in order to obtain the requested results [13].

A webpage will then pop up, providing a display sorted by year, showing what quartile the magazine belongs in [13].

## 6 COMMITTEE FOR EVALUATION OF REQUESTS FOR MONETARY REWARDS FOR PUBLISHED RESEARCH PAPERS, SCIENTIST VISIBILITY AND GRANTED PATENTS

The University North's Rector names the members of the Committee for Evaluation of Requests for Monetary Rewards for Published Research Papers, Scientist Visibility and Granted Patents via a special Decision [4].

Some of the tasks of the Committee are collection of applications based on the extended invitation, examination of the criteria the applicants meet and examination of the pertinent documentation in accordance with the Regulation on Rewards, as well as creation of a record of conducted selection of candidates [4].

Once the Committee has finished its tasks, the rector makes a final decision on the amount of monetary rewards for published scientific papers, scientist visibility and granted patents for that year. Tab. 1 shows details about the annually conducted Monetary Rewards contests, with an exact number of published scientific papers, h-index increases and granted patents [4].

**Table 1** Monetary rewards from 2018 to 2021, University North

Year	Scientific Paper Applications	h-Index Applications	Patent Applications
2018	52	7	0
2019	127	17	0
2020	100	17	0
2021	183	34	0

The table shows that in the year 2018, applicants applied with 52 scientific papers and 7 h-index increases. In the year 2019, there were 127 scientific papers (75 more than the previous year) entered by University North employees, as well as 17 h-index increases (10 more than the previous year). In the year 2020, 100 papers were entered by the University North employees, as well as 17 h-index increases. In 2021, a record number of employees applied with their papers – 183. There was another increase in the h-index reports – 34, which is 100% more than the previous year.

## 7 CONCLUSION

Scientific productivity is an important indicator to any scientific institution or a recognized scientist. Scientific activity refers to all scientists active in a certain scientific field that are subject to certain rules and norms of operation.

Scientists are recognized by their scientific reputation, i.e., their productivity is recognized by the indexing of magazines that publish their scientific research papers. In order to reward the scientists for their accomplishments, published papers and the citations of said papers, as well as improved scientific recognition of the institution that employs them, University North has established a high-quality scientist reward system.

The reward system has certain rules and criteria for rewarding scientists. The rewards in and of themselves are contributing to popularization of science at the institution in question; furthermore, rewarding provides for a very good

incentive for publishing many research papers with excellent indexing. Publishing research papers is also important to the institution the paper is referencing, as it adds to said institution's visibility and recognition in the European and international domain of research and science.

Networking and incitement of scientific activity, as well as rewarding papers published in magazines and books characterized by significant international visibility directly contributes to an increased scientific productivity.

An increase in scientist and researcher visibility, as well as monetary rewards awarded to University North's employees, will contribute toward an increased recognition of University North in significant circles, scientific networks, and reputable research spaces.

## 8 REFERENCES

- [1] Act on Higher Education and Scientific Activity (NN 119/2022). <https://doi.org/10.4324/9781003312826-13>
- [2] University North's Statute, Koprivnica, [https://www.unin.hr/wp-content/uploads/Statut\\_izmjene-i-dopune\\_studeni-2018\\_pro%C4%8Di%C5%A1%C4%87eni-tekst.pdf](https://www.unin.hr/wp-content/uploads/Statut_izmjene-i-dopune_studeni-2018_pro%C4%8Di%C5%A1%C4%87eni-tekst.pdf)
- [3] Regulation on Election into Scientific Professional Vocations (NN 28/17, 72/19 and 21/21 and 111/22)
- [4] Regulation on Rewarding Published Research Papers, Scientist Visibility and Granted University North Patents (clarified text), [https://www.unin.hr/wp-content/uploads/Pravilnik-o-nagra%C4%91ivanju\\_znanstveni-radovi\\_vidljivost\\_patenti1.pdf](https://www.unin.hr/wp-content/uploads/Pravilnik-o-nagra%C4%91ivanju_znanstveni-radovi_vidljivost_patenti1.pdf)
- [5] Čadovska, I. & Mitrović, G. (2018). The Role of Libraries in the Evaluation of Scientific Productivity: The Example of the National and University Library in Zagreb. *Vjesnik bibliotekara Hrvatske*, 61(2), 179-198. <https://doi.org/10.30754/vbh.61.2.697>
- [6] Mitrović, G. (2013). Representation of Croatian Scientific and Professional Magazines in the Web of Science and Scopus Databases with a Review of Social and Human Sciences. *Vjesnik bibliotekara Hrvatske*, 56(4), 129-144.
- [7] Macan, B. & Petrak, J. (2015). Bibliometric Indicators for Evaluation of Quality of Scientific Magazines. *Croatian scientific magazines: experiences, viewpoints, possibilities*, Hebrang Grgić, Ivana (ed.). Zagreb: Školska knjiga, pg. 37-53.
- [8] Regulation on Organization and Systematization of University North Workplaces (clarified text), February of 2022, (Class: 602-04/21-02/08, Ur. number: 2137-0336-09-21-11), see: [https://www.unin.hr/wp-content/uploads/Pravilnik\\_o\\_ustroju\\_i\\_sistematizaciji\\_radnih\\_mjesta\\_Sveu%C4%8Di%C5%A1ta\\_Sjever\\_pro%C4%8Di%C5%A1%C4%87eni\\_tekst.pdf](https://www.unin.hr/wp-content/uploads/Pravilnik_o_ustroju_i_sistematizaciji_radnih_mjesta_Sveu%C4%8Di%C5%A1ta_Sjever_pro%C4%8Di%C5%A1%C4%87eni_tekst.pdf)
- [9] Regulation on Scientific and Artistic Domains, Fields, and Branches (Clarified text – NN, nr. 118/09, 82/12, 32/13 i 34/16 - unofficial), see: [http://www.rektorskizbor.hr/fileadmin/rektorat/O\\_Sveucilistu/Tijela\\_sluzbe/Rektorski\\_zbor/dokumenti/Pravilnik\\_o\\_znanstvenim\\_i\\_umjetnickim\\_podrucjima\\_poljima\\_i\\_granama.pdf](http://www.rektorskizbor.hr/fileadmin/rektorat/O_Sveucilistu/Tijela_sluzbe/Rektorski_zbor/dokumenti/Pravilnik_o_znanstvenim_i_umjetnickim_podrucjima_poljima_i_granama.pdf)
- [10] University North's Strategy Pertaining to Scientific Research and Art from 2021 to 2027, see: [https://www.unin.hr/wp-content/uploads/ZNANSTVENO-ISTRA%C5%BDIVA%C4%8CKA-I-UMJETNI%C4%8CKA-STRATEGIJA\\_2021.-2027..pdf](https://www.unin.hr/wp-content/uploads/ZNANSTVENO-ISTRA%C5%BDIVA%C4%8CKA-I-UMJETNI%C4%8CKA-STRATEGIJA_2021.-2027..pdf)
- [11] Konjevod, B. (2020). Analysis of Croatian Scientific and Professional Magazines from the Field of Economics in Web of Science and Scopus Databases. *Education for Entrepreneurship - E4: scientific – professional magazine on education and entrepreneurship*, 10(2).
- [12] Electronic Source Portal for the Croatian Academic and Scientific Community, see: <http://baze.nsk.hr/baza/web-science/>
- [13] Electronic Source Portal for the Croatian Academic and Scientific Community, see: <http://baze.nsk.hr/baza/scopus/>
- [14] Regulation on terms and conditions for obtaining a state scholarship for the STEM field for full-time students (NN 106/2022)
- [15] State Intellectual Property Office of Republic of Croatia. <https://www.dziv.hr/hr/o-zavodu/dziv/>
- [16] Jokić, M. (2009). H-Index as the New Scientometric Indicator. *Biochemia Medica*, 19(1), 5-9. <https://hrcak.srce.hr/file/51302>
- [17] Golenko, D. (2019). Guide to Publishing Research Papers in the European Research Space. [https://pravri.uniri.hr/files/ridoc/Vodi\\_za\\_objavljivanje\\_radova\\_u\\_EIP2019-12.pdf](https://pravri.uniri.hr/files/ridoc/Vodi_za_objavljivanje_radova_u_EIP2019-12.pdf)

### Authors' contacts:

**Anica Hunjet**, prof. dr. sc.  
University North,  
104. brigade 3, 42 000 Varaždin, Croatia  
[ahunjet@unin.hr](mailto:ahunjet@unin.hr)

**Marin Milković**, prof. dr. sc.  
University North,  
Križanićeva 31b, 42000 Varaždin, Croatia  
[mmilkovic@unin.hr](mailto:mmilkovic@unin.hr)

**Nikolina Topolko Špoljar**, mag. iur.  
University North,  
104. brigade 3, 42 000 Varaždin, Croatia  
[ntopolko@unin.hr](mailto:ntopolko@unin.hr)

# Investigation of Tribological Applications and Mechanical Properties of Zinc-Aluminium (ZA40)/Multi-Wall Carbon Nanotube (MWCNT) Composite Alloys

Emre Deniz Yalçın\*, Aykut Çanakçı

**Abstract:** In this study, ZA40/ MWCNT composites were produced by using powder metallurgy technique and hot press method by adding 0,5-1-1,5-2% wt. MWCNT to ZA40 alloy. Powders made with mechanical alloys were sintered by hot pressing for 3 hours under 500 °C and 800 MPa pressure. Wear tests were carried out under 5N and 10N loads in a dry friction environment using the ball-on-disk technique. Weight losses, average friction force, and wear rate of the samples were calculated after wear tests. Morphology, internal structure images, and examination of worn surfaces of the samples were investigated using scanning electron microscopy (SEM). The wear test results show the coefficient of friction of ZA40-2wt. % MWCNT was 0,18  $\mu$  (lower than the coefficient of friction of 0,66  $\mu$  for ZA40 alloy). The wear rate of ZA40 alloy was almost 6 times higher than ZA40-2 wt. % MWCNT composite.

**Keywords:** Multi-Wall Carbon Nanotube; Powder Metallurgy; Wear; ZA40

## 1 INTRODUCTION

Zinc-Aluminium alloys are used successfully in many engineering applications today. Especially ZA8-ZA12-ZA27 and ZA40 alloys; due to their many properties such as durability, good thermal conductivity, good sintering, and rigidity, it is preferred more than aluminium, and bronze alloys in many industrial applications [1]. Zn-Al alloys; have higher tribological effects with low melting temperature and low cost; compared to that of cast iron, brass and aluminium. Especially in 1960 and 1970, ZA8-ZA12-ZA27-ZA33-ZA40 and ZA48 series Zn-Al alloys were developed. These alloys have limited applications due to the deterioration of some of their mechanical properties at operating temperatures above 100 °C. Since Zn-Al alloys are one of the most important alloying elements, it is possible to produce new materials with advanced engineering properties by adding ceramic-based reinforcement materials at different rates [2].

The most important task of a lubricant is to minimize wear in the wear environment. A suitable oil film significantly reduces the wear of the various parts in contact with each other. Composite alloys with appropriate lubricant additives are used in many applications according to operating conditions, pressure, load, and temperature of the system.

MWCNTs have been used as lubricant additives in various alloys due to their wear-reducing properties and thermal and electrical conductivity [3].

Li et al. obtained promising results in mechanical properties by adding yttrium (Y) in different ratios to ZA27, ZA35, and ZA40 alloys. Especially with 4% Y reinforcement, they observed significant increases in the elongation stress and hardness values of the composites [4].

A recent study investigated the wear behavior and mechanical properties of ZA27/SiC/Gr hybrid composites under 20-40 and 60 N loads in a dry friction environment in a pin on disc wear device by adding 1,5% SiC and 0,5% graphite to the ZA27 matrix. According to the results, the microhardness and breaking stress values increased. In

addition, the weight losses in the samples after wear were less in hybrid composites than in the matrix material [5]. The composites formed by mechanical alloying (30 minutes) method by adding 2% MWCNT to AA 6061 aluminium matrix alloy were carried out with pin-on-disc (500, 1000 and 1600 m) wear tests in a dry environment with 5, 7 and 10 N loads. According to the results, it was seen that MWCNT reinforced composites have a lower wear rate, lower friction coefficient, and weight loss [6].

In a recent study, the wear behavior of the composites formed by strengthening the ZA27 matrix alloy SiC and Gr under different loads and at different sliding speeds in the dry friction environment was investigated. According to the results, it has been observed that SiC and Gr reinforcement have positive effects on the wear rate. [7]. Preethi et al. studied that mixtures reinforced with 500nm size of 1-1,5% and 2% CNT to Al6061 alloy produced by powder metallurgy technique with mechanical alloying at 150 rpm for 4 hours. The hardness value and wear data of the produced samples were examined under 10 N and 20 N loads, and according to the results obtained, an increase in hardness values, a decrease in density values occurred, and the best wear resistance was observed in the 2% CNT reinforced sample [8]. Aranke et al. investigated the wear behavior of composites formed by reinforcing 0,25-0,5-0,75 by % weight of multi-wall carbon nanotubes (MWCNT) to Al 7075 alloy under 20-40 N and 60 N loads at 200-300 and 450 rpm. The results showed that the best abrasion resistance was in 0.5 %wt. reinforced composite [9]. In a study, made with carbon nanotube, composites were formed by adding zircon, graphene and carbon nanotube to  $\text{Al}_2\text{O}_3$  alloy and sintering at 1600 °C. Composites were tested in ball on flat abrasion test setup and according to the results obtained, it has been observed that carbon nanotube reinforcement significantly reduces the wear rate and improves the wear resistance and mechanical properties of the composites [10].

This study, it was aimed to develop a new composite material with MWCNT reinforcement to ZA40 alloy and examine its microstructure, mechanical and tribological

properties. Since ZA40 alloy is zinc-based, the biggest factor limiting its use in industrial applications is that its mechanical and tribological properties are not at the desired level at temperatures above 100 °C. For this reason, the effect of MWCNT reinforcement added to the ZA40 alloy at different rates on the microstructure, mechanical and tribological properties of the produced composites was investigated and it was aimed to produce a new advanced engineering material.

## 2 EXPERIMENTAL PROCEDURE

ZA40 alloy powders were used as matrix and MWCNT powders were used as reinforcement material. ZA40 powders were obtained from İki-el Metal Powders Company in 63 µm size. MWCNT powders used as reinforcement material were 30 nm in diameter with a purity of 90% (Graphene Chemical Industries). The chemical composition of the ZA40 alloy is shown in Tab. 1. In addition, the reinforcement ratios and coding of the samples are given in Tab. 2. Composite powders were ground in a planet-type ball mill (Retsch PM 200) with a milling speed of 350 rpm and a milling time of 2 hours. The milling process was carried out under an argon atmosphere. In the milling process, tungsten carbide balls with a diameter of 10 mm were used and the ball: powder weight ratio was found to be 5:1. Powder mixtures were placed in a 30 mm wide mold made of 4140 steel material and subjected to hot pressing (hot press, Fig. 1) at 800 MPa and 500 °C for 3 hours. Before hot pressing, the samples were subjected to cold pre-pressing under 350 MPa pressure for 1 minute. Zinc stearate was used at 0,5% by weight to prevent agglomeration. Theoretical densities of the produced samples were determined by applying the mixture rule. Archimedes method was applied in experimental intensities. The dimensions of the samples are  $\pm 0,01$  mm after measuring with a caliper to an accuracy of  $\pm 0,01$  mm. The measurements were made by measuring with precision scales. The hardness measurements of the samples were made using a 2,5 mm diameter penetrating tip under a load of 31,25 kgf, 8 measurements were made with the Brinell hardness measurement method and the arithmetic average was taken. The surfaces of the composites prepared for the abrasion tests were sanded with 400, 800, 1000, 1200, 1500 and 2000 sandpapers to obtain as a smooth surface as possible. Ball on disc wear mechanism was used in wear resistance tests (Fig. 2). Abrasive balls 10 mm diameter balls made of H11 hot work tool steel were used. Abrasion tests were carried out under 5 and 10 N loads, at 250 rpm speed and 100 meters distance. Abrasion tests were carried out with 5 samples 10 times. Morphologies and internal structure analyses of the ground composite powders were examined using a ZEISS LS 10 scanning electron microscope (SEM). The distribution of the reinforcements in the matrix, the porosity and the interfacial examinations of the samples were made in detail by SEM analyses. In the EDS analysis of the samples, the distribution of the additives in the matrix was examined by using Aztec 3.3 SP1 program in the Oxford instrument x-act brand model device. After the wear tests in

SEM, the wear type, surface condition, and the damages on the wear surface were examined.

**Table 1** Composition of ZA40 (wt. %).

Al	Cu	Zn	Mg
43,29	1,92	54,79	0,01

**Table 2** Samples code and ratio of MWCNT

Sample code	ZA40 (wt. %)	MWCNT (wt. %)
ZA40	100	0
ZC-0.5	99,5	0,5
ZC-1	99	1
ZC-1.5	98,5	1,5
ZC-2	98	2



**Figure 1** Hot press

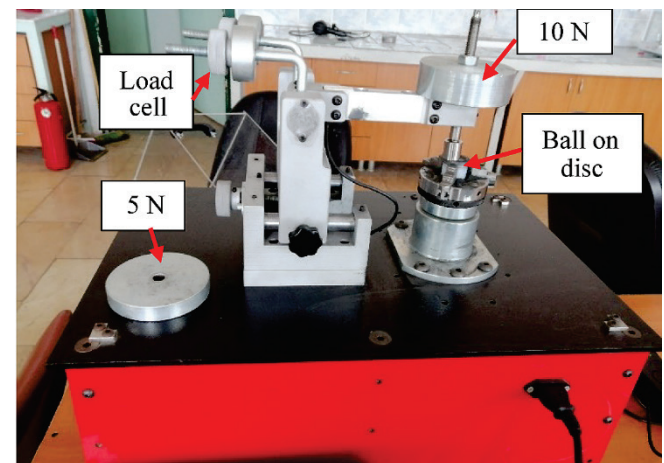


**Figure 2** Ball on disc wear tester

## 3 RESULTS AND DISCUSSION

The data obtained from the production of ZA40/MWCNT composite powders by T/M method and the microstructure, hardness, porosity, wear, friction and worn surface examinations are analysed and discussed below.

### 3.1 Microstructure

In ZA40/MWCNT composites, a milling time of 2 hours was determined to ensure that the MWCNT powders were homogeneously dispersed into the ZA40 matrix powders and at the same time sufficiently embedded. The distribution of MWCNT in the ZA40 matrix is seen at 500× magnification in Fig. 3a. To achieve high performance in ZA series composite materials, it is necessary to ensure a homogeneous distribution of the reinforcement particles in the matrix and to establish a good interfacial bond between the reinforcement particles and the matrix [11]. Fig. 3b clearly shows that the MWCNT particles are well embedded in the ZA40 matrix alloy. It was determined that MWCNT particles were heterogeneously dispersed in the matrix.

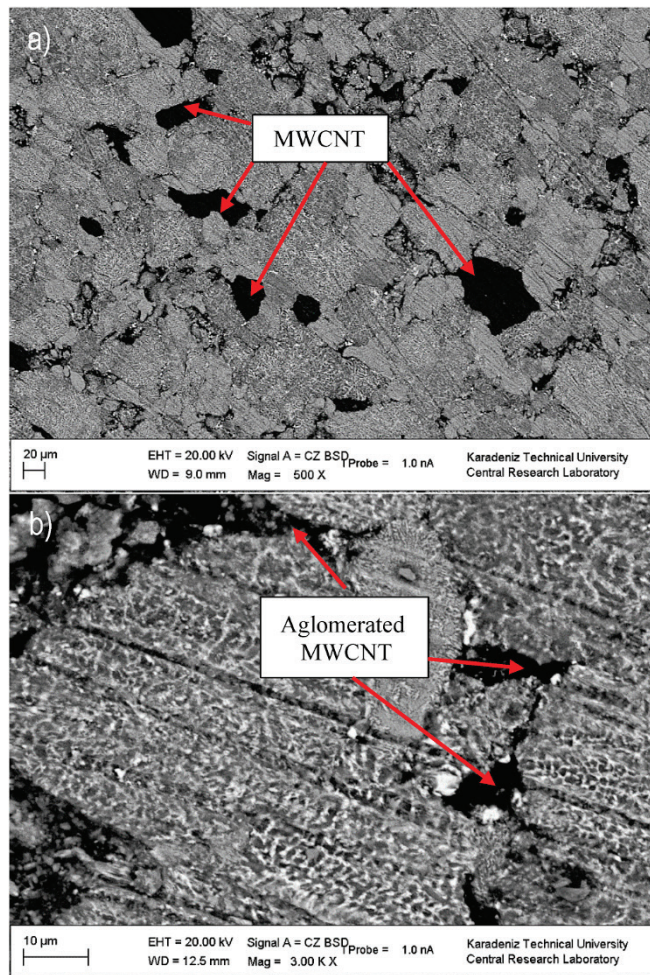


Figure 3 SEM image of ZC-2; a) at 500× magnification, b) at 3000× magnification.

An increase in MWCNT particle aggregation resulted in an increase in MWCNT agglomeration. As a result, the MWCNT distribution in the ZA40 matrix was not homogeneous. It can be concluded that more MWCNT particle aggregates would adversely affect the mechanical properties, wear and corrosion behavior of ZA40/MWCNT composites. In particular, the increase in the amount of reinforcement increased the agglomeration of the powders and led to the enlargement of the grain boundaries [12]. To

increase the homogeneity, the mechanical alloying time can be increased and the ball: powder ratio can be changed, but at this time, undesirable problems such as low hardness and poor wear resistance may occur in the mechanical and tribological properties of the composites [13]. In Figure 4, the element distributions of the SEM-EDS analysis of the composites are shown. The red, green, yellow and blue regions of these microstructures show the distribution of Zn, Al, C and Cu elements, respectively. It seems there is no adequate homogeneous distribution. It was observed that the C elements clustered towards the grain boundaries.

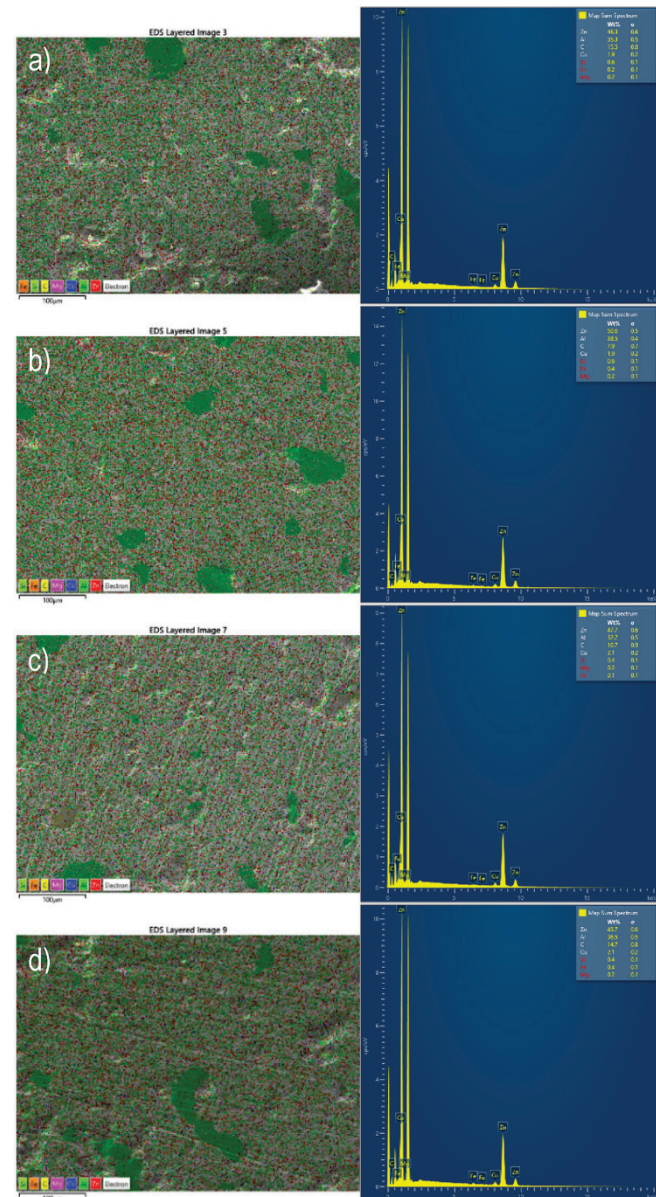


Figure 4 EDS mapping of composites a) ZC-0,5 b) ZC-1 c) ZC-1,5 d) ZC-2

### 3.2 Porosity and Hardness

As can be seen in Tab. 3 and Fig. 5, the porosity ratio between matrix and composites increased with the increase in MWCNT reinforcement. The highest porosity value was observed in the ZC-2 sample with 13,55 %. While the

porosity was measured as 11.19% in the ZA40 matrix, it immediately increased to 12.01% in the ZC-0,5 sample, and the ZC-0,5 sample had less agglutination in the composites. Here, the effect of the packing factor and the agglomeration of the powders to the grain boundaries and the growth of the grain boundaries increased the porosity. The densities decreased with the increase in the amount of reinforcement. It was determined that the hot press technique decreased the densities of the samples and increased the porosities.

Brinell hardness values of the samples are shown in Tab. 3 and Fig. 5 While the hardness value was measured at 150 HB in the matrix material, the lowest hardness value was measured in the ZC-2 sample with 92 HB with the increase in the amount of MWCNT. The most significant decrease was between ZC-1 and ZC-1,5. The addition of graphene-based particles such as MWCNT to the matrix reduced the hardness of the samples linearly. However, it improved the wear resistance and mechanical properties of the samples positively. Particularly, the 2-hour mechanical alloying time facilitated sintering and the distribution of MWCNT reinforcement in the matrix was an important factor in the reduction of hardness.

**Table 3** Porosity and hardness value of samples

Sample code	Porosity content (%)	Hardness Brinell (HB)
ZA40	11,19	150
ZC-0,5	12,01	148
ZC-1	12,21	142
ZC-1,5	12,28	113
ZC-2	13,55	92

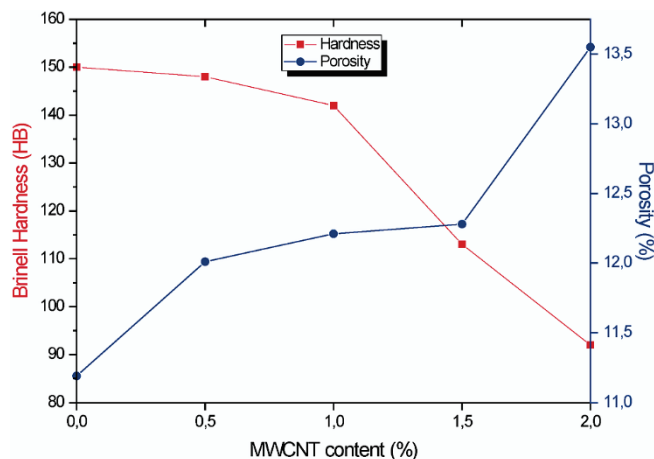


**Figure 5** ZA40 and its composites hardness and porosity values

### 3.3 Wear

The samples that have passed the wear tests are shown in Fig. 6 When the wear data is examined, in Tab. 4 and Fig. 7, the weight loss of 0,0529 mg in the matrix material under 5 N load was measured as 0,021 with the addition of 0,5% MWCNT. This can be explained by the lubricating property of MWCNT. While the weight loss of the matrix material was 0,1032 under 10 N load, the weight losses decreased with increasing MWCNT supplementation. However, it was minimized with 2% MWCNT supplementation. The least weight loss was observed in the ZC-2 sample under 5 N load.

In addition, it was observed that the weight losses of the composites under 5 N load were less than the matrix material. The most significant decrease under 10 N load occurred between ZC-1,5 and ZC-2 composites. The least weight loss occurred in ZC-2 composite in all composites and under all loads. These findings suggested that 2% MWCNT supplementation is the ideal rate. For metal matrix composites, one of the most important factors is the reinforcement content; because as the microstructure reinforcement content increases (% by weight), it transforms from metal to ceramic matrix [14]. Although the hardness of the composite samples decreased, their wear resistance increased. Because it is known that carbon-derived additives settled on the grain boundaries form a lubricating film on the surface with the effect of friction and reduce the contact of the abrasive ball with the material, and also fill the grooves formed on the surface of the sample during the wear test [15].



**Figure 6** Wear specimens

**Table 4** Weight loss of ZA40 and its composites

Sample Number	5 N Weight Loss (mg)	10 N Weight Loss (mg)
ZA40	0,0529	0,1032
ZC-0,5	0,021	0,0916
ZC-1	0,0181	0,0708
ZC-1,5	0,01	0,0588
ZC-2	0,005	0,0168

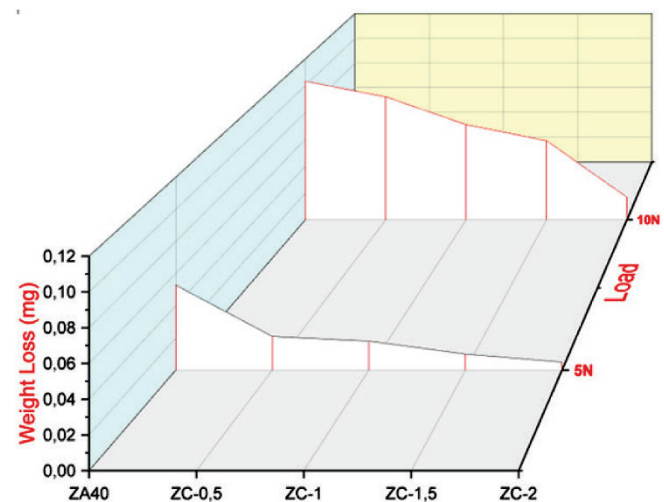


**Figure 7** Weight loss of ZA40 and its composites

### 3.4 Average Frictional Coefficient and Wear Rate

Yan et al. studied ZA27, ZA33, ZA40 and ZA48 zinc aluminium alloys in oily environments. Their results showed that ZA27 and ZA48 exhibited similar properties in friction coefficients in experiments carried out under a load of 400 to 1000 N, but the friction coefficient of ZA40 alloy decreased with increasing loads [2]. As can be seen in Tab. 5 and Fig. 8, the lowest average friction coefficient is seen in the ZC-2 sample under 5 N load. It is clearly seen that increasing MWCNT reinforcement decreases the friction coefficient value. The increased MWCNT reinforcement from 0,5 %wt. to 2 %wt. reduces the friction coefficient from 0,56  $\mu$  to 0,18  $\mu$  at 5N load and its lubricating property. The highest coefficient of friction was obtained in the ZA40 matrix material for each load. Also it was observed that 2% MWCNT reinforcement had a significant effect on the coefficient of friction at 5 N and 10 N loads. It can be concluded that better distribution of the MWCNTs in the ZA40 matrix causes a lower friction coefficient for the composites. Throughout wear, the friction between the hard ball and the ZA40-MWCNT composites was fewer due to the multilayer structure of the reinforcement, which offers a lubricating influence on the ZA40 matrix subsequent in a decreased friction coefficient [16].

**Table 5** Average friction coefficient of ZA40 and its composites

Sample Number	5 N Average Friction Coefficient ( $\mu$ )	10 N Average Friction Coefficient ( $\mu$ )
ZA40	0,66	0,62
ZC-0.5	0,56	0,58
ZC-1	0,52	0,56
ZC-1.5	0,37	0,33
ZC-2	0,18	0,28

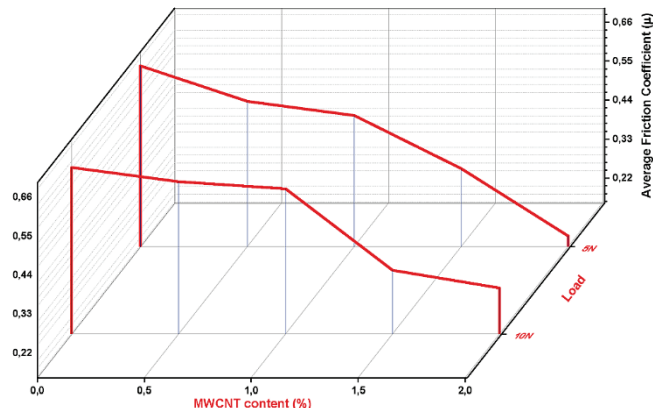


**Figure 8** Average friction coefficients of ZA40 and its composites

The results obtained in the wear tests showed that, the increased load and reinforcement rates changed the wear rate of the matrix alloy and composites. When Fig. 9 and Tab. 6 are examined, the lowest wear rate is seen in ZC-2 composite alloy under 5 and 10 N loads. In particular, a significant decrease in the wear rate between ZC-1,5 and ZC-2 under 10N load was noted. This decrease is in parallel with the decrease in weight loss between ZC-1,5 and ZC-2. The highest wear rate was seen in the unreinforced ZA40 alloy. These findings indicated that the MWCNT reinforcement

acts as a lubricant between the H11 ball and the surface during wear.

**Table 6** Wear rate of ZA40 and its composites

Sample Number	5 N Wear Rate ( $10^{-4} \text{ mm}^3/\text{N}\cdot\text{m}$ )	10 N Wear Rate ( $10^{-4} \text{ mm}^3/\text{N}\cdot\text{m}$ )
ZA40	1,391	2,71
ZC-0.5	0,559	2,438
ZC-1	0,484	1,894
ZC-1.5	0,267	1,574
ZC-2	0,136	0,458

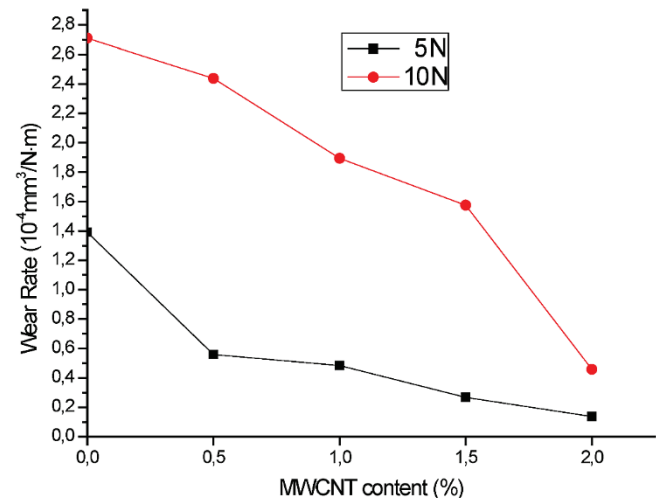


**Figure 9** Wear rate of ZA40 and its composites

### 3.5 Worn Surface Analysis

When the wear surfaces in Fig. 10 were examined, it was seen in the SEM pictures that there was adhesive and sliding wear in ZA40/MWCNT composites. Shear stresses are transferred to the material below the contact zone during wear testing for metal matrix composites. Wear particles are formed due to high deformation and wear in the surface area. A layer is mechanically formed between two sliding surfaces. During the wear test of ZA40/MWCNT composites, a plastic hardening matrix phase is formed on the surface with fine reinforcement particles on the inner surface. The brittle region breaks off from the matrix during the delamination process. The presence of reinforcement particles in the matrix increases its mechanical strength in micro-spaces with its homogeneous distribution [12]. Fig. 10k shows less wear. In the current study, it was found that MWCNT particles changed the wear mechanism to sliding wear, especially under 10 N load. The trace diameter formed on the sample surface of the 10 mm diameter H11 abrasive tip in the ball on disc wear device was measured. When Fig. 11 and Fig. 12 are examined, the trace diameter, which was measured as 3,254 mm in the ZA40 matrix material under 5N load, was found to be 1,640 mm in the ZC-2 sample. Likewise, when we reduced the load by 10 N, the trace diameter was measured as 3,331 mm in the ZA40 matrix material and 2,147 mm in the ZC-2 composite. As a result, the increase in load increased the scar diameter in the composites, as expected. Increasing the MWCNT ratio led to a decrease in the scar diameter of composites. In Fig. 11b and Fig. 12b, the

wear mark and wear were observed to be decreased with the lubricating property of MWCNT reinforcement.

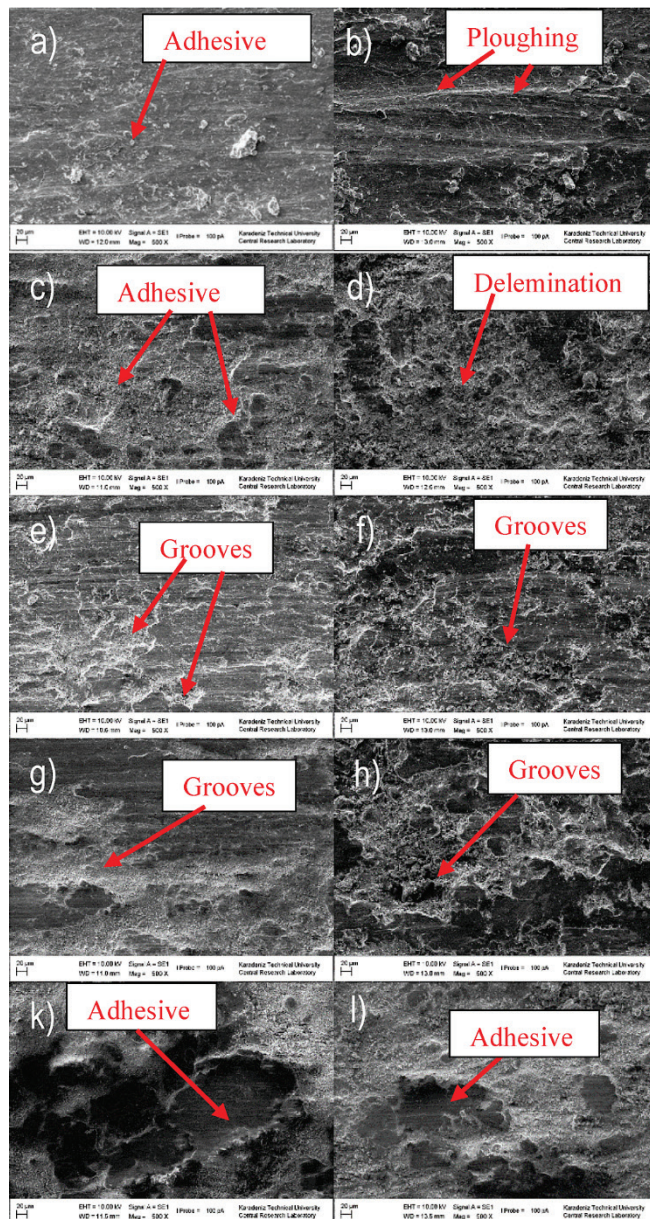


Figure 10 SEM of images ZA40/MWCNT composites (5-10 N): (a-b) ZA40; (c-d) ZC-0,5; (e-f) ZC-1; (g-h) ZC-1,5 and (k-l) ZC-2

#### 4 CONCLUSIONS

In this study, composite samples were produced using the powder metallurgy method by reinforcing ZA40 matrix material with MWCNT. The density, hardness, microstructure, wear and friction behaviours of the samples produced were investigated. The findings obtained can be listed as below:

- 1) MWCNT reinforced composite materials with ZA40 matrix were produced by the mechanical alloying and hot pressing method, which is a good technique in the powder metallurgy method.

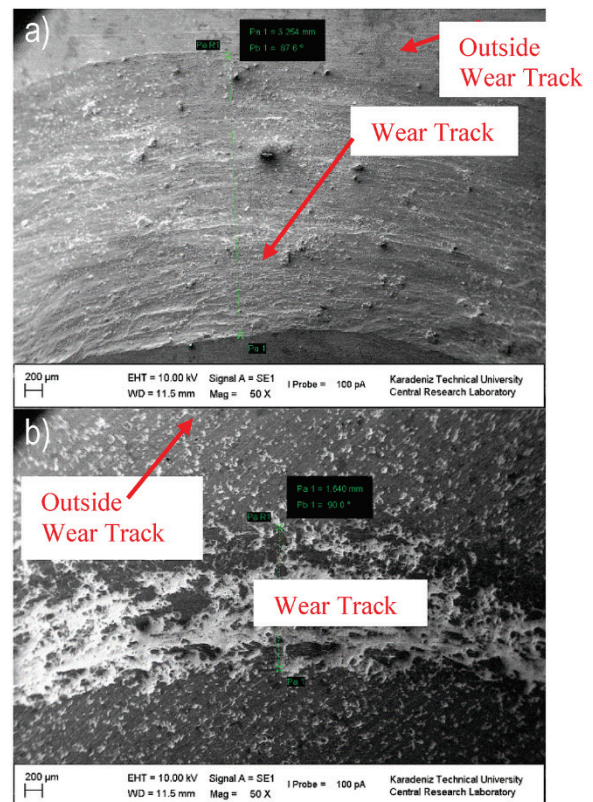


Figure 11 Wear scar diameter measurement under 5 N load at 50X magnification a) ZA40 and b) ZC-2

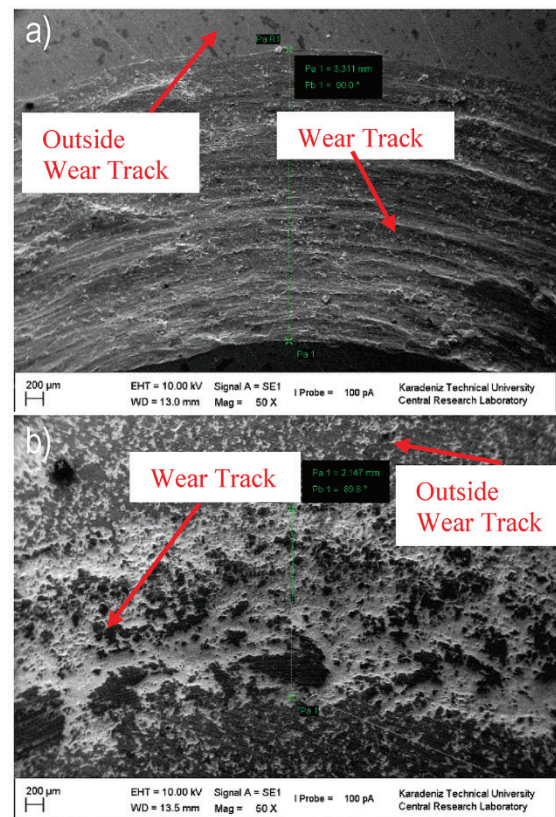


Figure 12 Wear scar diameter measurement under 10 N load at 50X magnification a) ZA40 and b) ZC-2

- 2) According to the characterization results of the microstructures of ZA40/MWCNT composite powders obtained after mechanical alloying, it can be concluded that the milling time during which the MWCNT particles were ideally dispersed in the ZA40 matrix was determined as 2 hours.
- 3) The density values of ZA40/MWCNT composites decreased with increasing reinforcement ratios, but the porosity ratio increased. The highest porosity ratio was seen in the ZC-2 sample containing the highest MWCNT supplement.
- 4) The hardness values of ZA40/MWCNT composites decreased with increasing reinforcement ratios, and the highest hardness value was measured in the ZA40 matrix sample with 150 HB, and the lowest hardness value was measured in the ZC-2 sample with 92 HB.
- 5) The wear mechanisms observed as a result of the ball-on-disc wear test for all composite materials were determined to be adhesive and abrasive wear. Wear losses increase with increasing load. The greatest weight losses were observed in wear tests under 10 N load. The highest weight loss; 0,1032 mg under 10 N load in ZA40 matrix material. The lowest weight loss is 0,005 mg under 5 N load in the ZC-2 sample was measured.
- 6) All composites showed a higher wear resistance than ZA40 matrix alloy.
- 7) A lower coefficient of friction was measured in all composite samples compared to the ZA40 alloy. The highest coefficient of friction was measured as  $\mu = 0,66$  in the ZA40 matrix alloy under 5 N load, while the lowest was measured as  $\mu = 0,18$  under 5 N in the ZC-2 composite. MWCNT reinforcement reduced friction in wear tests and lowered the coefficient of friction.
- 8) A lower wear rate was measured in all composite samples compared to the ZA40 alloy. The wear rate increased with increasing load and decreased with increasing MWCNT reinforcement. It has been clearly seen that MWCNT reinforcement reduces the wear rate in composites.

Based on the results of the study, the following recommendations can be tried:

- 1) In wear tests, wear behaviors can be examined more broadly by applying different speeds, different loads, different durations and longer travel distances.
- 2) Wear tests carried out in a dry friction environment can be performed in a full oil environment and intermittent oil environment, and the wear behaviour of materials can be examined from different angles.
- 3) The mechanical properties can be re-examined by applying various heat treatments to the produced samples.

## 5 REFERENCES

- [1] Ranganath, G., Sharma, S. C., & Krishna, M. (2001). Dry sliding wear of garnet reinforced zinc/aluminium metal matrix composites. *Wear*, 251(1-12), 1408-1413. [https://doi.org/10.1016/S0043-1648\(01\)00781-5](https://doi.org/10.1016/S0043-1648(01)00781-5)
- [2] Yan, S., Xie, J., Liu, Z., Wang, W., Wang, A., & Li, J. (2010). Influence of Different Al Contents on Microstructure, Tensile and Wear Properties of Zn-based Alloy. *J. Mater. Sci. Technol.*, 26(7), 648-652. <https://doi.org/10.1016/S1005-0302>
- [3] Pourpasha, H., Heris, S. Z., Mahian, O., & Wongwises, S. (2020). The effect of multi-wall carbon nanotubes/turbine meter oil nanofluid concentration on the thermophysical properties of lubricants. *Powder Technology*, 367, 133-142. <https://doi.org/10.1016/j.powtec.2020.03.037>
- [4] Li, M., Lu, S., Long, F. et al. (2015). Effect of Y Addition on the Mechanical Properties and Microstructure of Zn-Al Alloys. *JOM*, 67, 922-928. <https://doi.org/10.1007/s11837-014-1269-4>
- [5] Kumar, N. S. (2018). Mechanical and Wear Behavior of ZA-27/SiC/Gr Hybrid Metal Matrix Composites. *Materials Today: Proceedings*, 5(9, part 3), 19969-19975. <https://doi.org/10.1016/j.matpr.2018.06.363>
- [6] Jeyasimman, D., Gurunathan, K., & Narayanasamy, R. (2016). Dry sliding wear behaviour of AA 6061-MWCNT nanocomposites prepared by mechanical alloying. *IOSR Journal of Mechanical and Civil Engineering*, 13(4), 46-53. <https://doi.org/10.9790/1684-1304044653>
- [7] Miloradović, N., Vujanac, R., Stojanović, B., & Pavlović, A. (2021). Dry Sliding Wear Behaviour of ZA27/SiC/Gr Hybrid Composites with Taguchi Optimization. *Composite Structures*, 264, 113658. <https://doi.org/10.1016/j.compstruct.2021.113658>
- [8] Preeth, K., Raju, T. N., Shivappa, H. A., Shashidhar, S., & Nagral, M. (2021). Processing, microstructure, hardness and wear behavior of carbon nanotube particulates reinforced Al6061 alloy composites. *Materials Today: Proceedings*, 1-5. <https://doi.org/10.1016/j.matpr.2021.03.608>
- [9] Aranke, O., Gandhi, C., Dixit, N., & Kuppan, P. (2018). Influence of Multiwall Carbon Nanotubes (MWCNT) on Wear and Coefficient of Friction of Aluminium (Al 7075) Metal Matrix Composite. *Materials Today: Proceedings*, 5(2, part 2), 7748-7757. <https://doi.org/10.1016/j.matpr.2017.11.452>
- [10] Duntua, S. H., Eliasua A., Ahmadb I., Islamc, M. & Boakye-Yiadom, S. (2021) Synergistic effect of graphene and carbon nanotubes on wear behaviour of alumina-zirconia nanocomposites. *Materials Characterization*, 175, 111056. <https://doi.org/10.1016/j.matchar.2021.111056>
- [11] Savaşkan, T. & Azakli, Z. (2008). An investigation of lubricated friction and wear properties of Zn 40Al 2Cu 2Si alloy in comparison with SAE 65 bearing bronze. *Wear*, 264(11-12), 920-928. <https://doi.org/10.1016/j.wear.2007.06.008>
- [12] Aksöz, S., Bican, O., Çalın, R., & Bostan, B. (2014). Effect of T7 heat treatment on the dry sliding friction and wear properties of the SiC-reinforced AA 2014 aluminium matrix composites produced by vacuum infiltration. *Journal of Engineering Tribology*, 228(3), 312-319. <https://doi.org/10.1177/1350650113506570>
- [13] Folorunso, D. O. & Owocye, S. (2019). Influence of quarry dust-silicon carbide weight percentage on the mechanical properties and tribological behavior of stir cast ZA-27 alloy based hybrid composites. *Journal of King Saud University - Engineering Sciences*, 31, 280-285. <https://doi.org/10.1016/j.jksues.2017.07.003>
- [14] Savaskan, T., Hekimoglu, A. P., & Purcek, G., (2004). Effect of copper content on the mechanical and sliding wear properties of monotectoid-based zinc-aluminium-copper alloys. *Tribology International*, 37, 45-50. <https://doi.org/10.1016/S0301-679X>
- [15] Han, D., Yan, G., & Wang, C. (2022). Influence of multi-walled carbon nanotubes (MWCNTs) content on metal friction and wear in thermally cracked carbon black (CBp) formulation system during mixing. *Polymer Testing*, 113, 107674.

<https://doi.org/10.1016/j.polymertesting.2022.107674>

- [16] Al-Qutub A. M., Khalil, A., Saheba, N., & Hakeem, A. S. (2013). Wear and friction behavior of Al6061 alloy reinforced with carbon nanotubes. *Wear*, 297(1-2), 752-761. <https://doi.org/10.1016/j.wear.2012.10.006>

**Authors' contacts:**

**Emre Deniz Yalçın**, PhD  
(Corresponding Author)  
Karadeniz Technical University,  
Abdullah Kanca Vocational High School,  
61530, Sürmene, Trabzon, Türkiye  
Tel: +90 462 377 81 70  
E-mail: [emredenizyalcin@ktu.edu.tr](mailto:emredenizyalcin@ktu.edu.tr)

**Aykut Çanakçı**, Prof. PhD  
Karadeniz Technical University,  
Department of Metallurgical and Materials Engineering,  
61080, Ortahisar, Trabzon, Türkiye  
Tel: +90 462 377 27 90  
E-mail: [aykut@ktu.edu.tr](mailto:aykut@ktu.edu.tr)

# Analysis of Sewage Sludge Disposal Routes – Varazdin and Medimurje County

Domagoj Nakić\*, Ines Belalov Dovečer, Dražen Vouk, Bojan Đurin

**Abstract:** The aim of this paper is to analyse sewage sludge production at the level of Medimurje and Varazdin counties with economic analysis of acceptable technical/technological solutions for sludge management routes. The topic is very broad, so the focus was placed on four variants of sludge disposal, which were determined by preliminary analysis to be the most applicable for the area in question. These are: 1) disposal of sewage sludge in agriculture, 2) incineration of sludge in a central mono-incinerator, 3) composting for the area of Varazdin County and at the same time use of sludge reed beds for the area of Medimurje County, and 4) export of sludge outside the state borders. Based on the analysis carried out for the described four variants, sludge incineration in a regional mono-incinerator turned out as the economically most advantageous solution, while the variant that includes disposal of sludge in agriculture has showed as the most expensive one. The last one also showed the largest range of costs uncertainties, but the mentioned facts are greatly influenced by unfavourable legislation, the changes of which in a more rational direction would greatly contribute to the greater competitiveness of this variant. Overall, taking into account the lowest cost and uncertainties in the predicted unit costs, the sludge composting in the Varazdin County and the construction of a reed beds for the Medimurje County, turned out to be the optimal variant. This solution is also the one that was ultimately adopted in practice.

**Keywords:** composting; incineration; reed beds; sewage sludge treatment and disposal; use in agriculture

## 1 INTRODUCTION

The wastewater collected by the public drainage system is taken to the wastewater treatment plant (WWTP) and after reaching the required level of treatment, it is discharged into the recipient. The by-product of every technological process of municipal WWT is sewage sludge, which requires further processing and disposal in the most economical way, while considering its technical and ecological suitability. On average globally, generated unit quantities of daily sludge production amount to 35 - 85 g DM/PE (dry matter / population equivalent) [1]. The available data for Croatia, based on operational WWTP, show, this value amounts to 50 - 55 g DM/PE daily [2].

The aim of this paper is to analyze the sludge production for Medimurje and Varazdin counties and give analysis of economically acceptable technical and technological solutions for sludge treatment and disposal routes.

All conventional sludge treatment methods ultimately generate stabilized and dehydrated sludge that also requires further disposal. Also, additional sludge processing procedures result in either a new form of sludge or a new by-product of its processing: dried sludge, sewage sludge ash, compost (or sludge like compost within reed beds) etc. So, all these processes generate sludge, ash or compost that ultimately needs to be disposed of somewhere or used in some other applications [4].

According to EUROSTAT data, even at the EU level there are no unified strategies or guidelines for sludge disposal. Use in agriculture is dominant method in Ireland, Portugal, UK, Denmark, Spain and Luxembourg, while in the Baltic countries, as well as Finland, Slovakia, Hungary and Czech Republic, the use of sludge on non-agricultural lands prevails. On the other hand, in some of the most developed countries such as the Netherlands, Switzerland, Germany, Belgium and Austria, thermal treatment of sludge, primarily incineration, is the predominant method of its disposal. Although limited and for the most part even prohibited by EU

regulations, disposal of sludge in landfills is still the predominant method of disposal of sludge in Italy, Greece, Romania, but unfortunately also in Croatia [5].

According to Tarpani et al. [6] over 70% of generated sludge in Europe is treated thermally (incineration) or used as a fertilizer in agriculture. The best solution is to include the waste produced from wastewater treatment into the cycle of matter and energy, preferably as it happens in nature, but also in any other sustainable way. This is also the basis of Council Directive 91/271/EEC [7] which states: "Sludge from wastewater treatment will be reused whenever possible."

Since there are many acceptable methods of sludge treatment (thickening, stabilization, dehydration, thermal hydrolysis, drying, solidification, mono-incineration, pyrolysis, gasification, composting, grounding, etc.), combined with many acceptable methods of its final disposal and/or use (landfilling treated sludge, use of sludge in agriculture or on non-agricultural land, disposal of ash in specially arranged landfills for non-hazardous waste, use of sludge (ash) in construction, different types of co-incineration of sludge (e.g. with municipal solid waste or in cement kilns), export of dehydrated or dried sludge or sewage sludge ash outside the country in which it originated), the resulting number of different solutions for complete sludge management is even higher, which further complicates the process of finding the optimal solution. To select the optimal solution (or combination of solutions), it is usually necessary to apply a multi-criteria decision methodology, which involves defining the criterion structure and evaluating the variants according to the adopted criteria [8]. In the continuation of this paper, a technical-economic analysis of the selection of the optimal variant of sludge disposal for area of northern Croatia will be presented. Nevertheless, it is noted that within the framework of conducting a comprehensive analysis, as part of future steps, it is necessary to conduct an analysis of environmental and sociological

impacts, which would complete the whole in terms of the basic requirements of sustainable development.

The relevant input data for determining sewage sludge production was the projected capacity of the agglomerations (WWTPs) in the Medimurje and Varazdin counties defined as part of the Water Area Management Plan 2016-2021 [3] and corrected according to data obtained from the responsible utility companies Medimurske vode d.o.o. and Varkom d.o.o.

The analysis covers 7 agglomerations of more than 2,000 population equivalent (PE) in Medimurje County and 11 agglomerations in Varazdin County, as shown in Fig. 1.

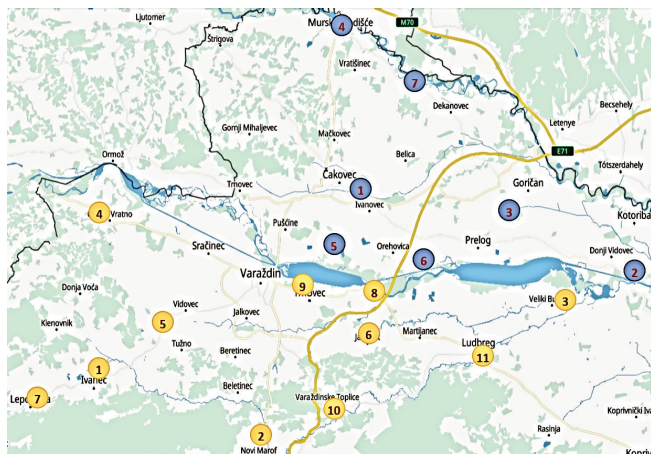


**Figure 1** Considered agglomerations in Varazdin County (yellow marks: 1 - Ivanec, 2 - Novi Marof, 3 - Veliki Bukovec, 4 - Cestica, 5 - Greda, 6 - Jalzabet, 7 - Lepoglava, 8 - Semovec, 9 - Varazdin, 10 - Varazdinske Toplice, 11 - Ludbreg) and Medimurje County (blue marks: 1 - Cakovec, 2 - Donja Dubrava, 3 - Donji Kraljevec, 4 - Mursko Središće, 5 - Novo Selo na Dravi, 6 - Podbrest, 7 - Podturen) [3]

## 2 COST ANALYSIS

For the considered WWTPs, the amounts of generated sewage sludge were calculated, as well as the production of dehydrated sludge with 23 and 33% DM and the amount of

generated dry sludge in the case of solar drying up to 75% DM (Tab. 1). Ash production (t/year) was also calculated in the case that the entire sludge is incinerated in a central mono-incinerator presumably located next to WWTP Varazdin, as by far the largest one within analyzed area. The starting point for determining sludge production was the predicted capacity of built and planned WWTPs. The capacities of the WWTPs considered were taken over as the planned capacities of the planned agglomerations from the Water Area Management Plan 2016-2021 year, corrected according to data obtained from the responsible utility companies Medimurske vode d.o.o. and Varkom d.o.o. Data on the unit costs of solar drying, transportation of dehydrated and dried sludge, sampling and analysis of sludge, transaction costs and premiums to farmers for disposal in agriculture, data on the costs of composting and reed beds, unit costs of sludge incineration in mono-incinerators and ash disposal, as well as the costs of sewage sludge export outside the country, were taken from the Action Plan for Sewage Sludge Disposal [9] and Vouk et. al. (2017) [10] and corrected to a certain extent considering the current situation and price movements on the market.

In the particular case, already by carrying out preliminary analyses, the most cost-effective solution was to build plants for sewage sludge solar drying in two locations, the largest WWTPs for each county. The location of WWTP Cakovec was chosen as the location of the central plant for solar drying of sludge in Medimurje County, and the location of WWTP Varazdin as the location of the central plant for solar drying of sludge in Varazdin County, considering that such an approach results in a lower unit price of total sludge treatment (solar drying including transportation costs). The calculated costs of sludge solar drying include the cost of building, operation, maintenance and depreciation of solar sludge drying plants and the cost of road transport of dehydrated sludge from individual WWTPs to the regional center in Cakovec or Varazdin, as shown in Tab. 2.

**Table 1** Calculation of the generated quantities of dehydrated and solar-dried sludge and the amount of ash in the case of sludge incineration

WWTP	PE	Sludge production	Quantities of dried (dewatered) sludge			Ash production
			75 % DM	33 % DM	22% DM	
		t DM/year	t/year			
Cakovec	84,123	1,647	2,196	4,990	7,485	815
Donja Dubrava	13,000	254	339	771	1,157	126
Donji Kraljevec	9,000	176	235	534	801	87
Mursko Središće	12,000	235	131	712	1,068	116
Novo Selo na Dravi	5,000	98	130	297	445	48
Podbrest	10,000	196	261	593	890	97
Podturen	17,600	345	459	1,044	1,566	170
Ivanec	11,806	231	308	700	1,050	114
Novi Marof	7,464	146	195	443	664	72
Veliki Bukovec	2,588	51	68	154	230	25
Cestica	4,111	80	107	244	366	40
Greda	5,162	101	135	306	459	50
Jalzabet	3,138	61	82	186	279	30
Lepoglava	6,894	135	180	409	613	67
Semovec	2,254	44	59	134	201	22
Varazdin	129,933	2,543	3,391	7,707	11,561	1,258
Varazdinske Toplice	5,423	106	142	322	483	53
Ludbreg	8,260	162	216	490	735	80
TOTAL:	337,756	6,611	8,815	20,034	30,052	3,271

**Table 2** The cost of construction and maintenance of a plant for solar drying of sewage sludge with included road transportation costs

WWTP	Cost of construction, operation and maintenance for solar drying		Regional center (RC)	Distance from the RC	The cost of road transport of dried sludge to the RC		Total cost
	€/tDM	€/year		km	€/t-km	€/year	€/year
Cakovec	50	82,333	Cakovec	0.2	0.65	973	83,306
Donja Dubrava	50	12,723		33	0.52	19,848	32,572
Donji Kraljevec	50	8,808		19	0.62	9,395	18,204
Mursko Središće	50	11,745		20	0.62	13,186	24,931
Novo Selo na Dravi	50	4,894		11	0.65	3,181	8,074
Podbrest	50	9,787		11	0.65	6,362	16,149
Podturen	50	17,225		18	0.62	17,406	34,631
Ivanec	45	10,399	Varazdin	30	0.55	17,411	27,810
Novi Marof	45	6,575		22	0.59	8,547	15,122
Veliki Bukovec	45	2,280		30	0.55	3,817	6,096
Cestica	45	3,621		25	0.59	5,349	8,971
Greda	45	4,547		20	0.62	5,672	10,219
Jalžabet	45	2,764		12	0.65	2,178	4,942
Lepoglava	45	6,073		40	0.49	11,961	18,034
Semovec	45	1,985		8	0.65	1,043	3,028
Varaždin	45	114,451		0.2	0.65	1,503	115,954
Varaždinske Toplice	45	4,777		16	0.62	4,767	9,544
Ludbreg	45	7,276		22	0.59	9,459	16,734
<b>TOTAL:</b>		312,263				142,057	454,321

The variant that includes composting of sludge in the Varazdin County and reed beds in the Medimurje County involves the construction of a composting plant in Varazdin and the transportation of sewage sludge from smaller WWTPs in the Varazdin County to the central composting plant and the construction of reed beds in Cakovec and the transportation of sludge from smaller WWTPs in the Medimurje County on the reed beds located by the Cakovec WWTP. The total cost includes the construction, operation, maintenance and depreciation of the composting plant in Varazdin and the cost of road transportation of dried sludge from smaller WWTPs to the composting plant, as well as the cost of reed beds construction, emptying and sludge removal,

sampling and the cost of road transportation of sludge from smaller WWTPs to the reed beds (Tab. 3).

In practice, the solution with the construction of reed beds in Cakovec and a composting plant in Varazdin was adopted. This includes collecting of sludge from smaller WWTPs in the area of Medimurje and Varazdin County, on two biggest central WWTPs, but it does not exclude the possibility that some of the smaller WWTPs will adopt a separate solution for sludge disposal. Sludge that is brought from smaller WWTPs to the reed beds in Cakovec is previously thickened and stabilized and contains around 3% DM in order to ensure a good distribution of liquid (non-dehydrated) sludge over the entire surface of the reed beds.

**Table 3** Total cost of sewage sludge composting in the area of Varazdin County and reed beds in the area of Medimurje County

WWTP	Distance from the composting plant (CP)	The cost of road transport of dried sludge to the CP		Cost of composting*		Total cost
	km	€/t-km	€/year	€/tDM	€/year	€/year
Ivanec	30	0.55	17,411	115	26,576	43,987
Novi Marof	22	0.59	8,547	115	16,802	25,349
Veliki Bukovec	30	0.55	3,817	115	5,826	9,642
Cestica	25	0.59	5,349	115	9,254	14,604
Greda	20	0.62	5,672	115	11,620	17,292
Jalžabet	12	0.65	2,178	115	7,064	9,242
Lepoglava	40	0.49	11,961	115	15,519	27,480
Semovec	8	0.65	1,043	115	5,074	6,117
Varazdin	0	0.65	1,503	115	292,486	293,989
Varaždinske Toplice	16	0.62	4,767	115	12,207	16,975
Ludbreg	22	0.59	9,459	115	18,594	28,052
<b>TOTAL 1:</b>			71,707		421,022	492,728
WWTP	Distance from the reed beds (RB)	The cost of road transport of fresh sludge to the RB		Cost of reed beds**		Total cost
	km	€/t-km	€/year	€/tDM	€/year	€/year
Cakovec	0.2	0.65	7,136	90	148,199	155,335
Donja Dubrava	33	0.52	145,555	90	22,902	168,457
Donji Kraljevec	19	0.62	68,897	90	15,855	84,752
Mursko Središće	20	0.62	96,698	90	21,140	117,838
Novo Selo na Dravi	11	0.65	23,326	90	8,808	32,135
Podbrest	11	0.65	46,652	90	17,617	64,269
Podturen	18	0.62	127,641	90	31,006	158,647
<b>TOTAL 2:</b>			515,905		265,528	781,433
<b>TOTAL (1+2):</b>						1,274,161

\*Including construction, operation, maintenance and depreciation

\*\*Including reed beds construction, emptying, sludge removal, sampling costs

**Table 4** Total cost of sludge disposal in agriculture

WWTP	Cost of transportation of dried sludge		Cost of sampling and analysis		Transaction costs	Premium for farmers	Total cost
	€/t	€/year	€/tDM	€/year	€/t	€/t	€/year
Cakovec	13	97,302	90	148,199	5	10	357,774
Donja Dubrava	13	15,037	90	22,902	5	10	55,289
Donji Kraljevec	13	10,410	90	15,855	5	10	38,277
Mursko Središće	13	13,880	90	21,140	5	10	51,036
Novo Selo na Dravi	13	5,783	90	8,808	5	10	21,265
Podbrest	13	11,567	90	17,617	5	10	42,530
Podturen	13	20,357	90	31,006	5	10	74,853
Ivanec	13	13,656	90	20,799	5	10	50,211
Novi Marof	13	8,633	90	13,149	5	10	31,744
Veliki Bukovec	13	2,993	90	4,559	5	10	11,007
Cestica	13	4,755	90	7,242	5	10	17,484
Greda	13	5,971	90	9,094	5	10	21,954
Jalžabet	13	3,630	90	5,528	5	10	13,346
Lepoglava	13	7,974	90	12,145	5	10	29,320
Semovec	13	2,607	90	3,971	5	10	9,586
Varazdin	13	150,290	90	228,902	5	10	552,603
Varazdinske Toplice	13	6,273	90	9,554	5	10	23,064
Ludbreg	13	9,554	90	14,552	5	10	35,130
TOTAL:		390,672		595,023			1,436,471

The variant with disposal of sludge in agriculture includes the cost of transporting dried sludge to agricultural areas without any restrictions, located within a radius of up to 50 km from any of the considered WWTP assumed following unit costs: the cost of 13 €/t for transportation within a radius of 10-50 km, the cost of sampling and analysis (for this analysis was assumed to be 90 €/t of dried sludge), transaction costs (5 €/t of dried sludge) and premium for farmers which take over sludge (10 €/t of dried sludge). This is shown in detail in Tab. 4.

The variant with sludge incineration in a mono-incinerator includes the construction of a mono-incinerator within the WWTP Varazdin perimeter and the collection of dried sewage sludge from two central plants for sludge solar

drying: in Cakovec and Varazdin. The central plant for solar drying in Cakovec is 21 km distant from the location of the mono-incineration plant, while the plant for solar drying in Varazdin is within the WWTP perimeter and in the immediate vicinity of the incinerator. The cost of incineration in a mono-incinerator includes the cost of solar drying, the cost of transporting sludge from central plants for sludge solar drying to the mono-incinerator, the cost of construction, operation, maintenance and depreciation of the mono-incinerator (with assumed incineration unit price at €65/t DM) and the cost of ash disposal (Tab. 5). It was assumed that the ash will be disposed of at an organized non-hazardous waste disposal site, close to the incinerator.

**Table 5** Total cost of sludge incineration and ash disposal

WWTP	The cost of solar drying	The cost of sludge transportation to the incinerator	Mass of sludge incinerated	Cost of incineration*	Ash production	Cost of ash disposal**	Total cost
	€/year	€/year	tDM/year	€/year	t/year	€/year	€/year
Cakovec	217,866	164,748	2,950	191,770	1,460	58,381	632,765
Donja Dubrava							
Donji Kraljevec							
Mursko Središće							
Novo Selo na Dravi							
Podbrest							
Podturen							
Ivanec	236,454	2,163	3,661	237,969	1,811	72,445	549,032
Novi Marof							
Veliki Bukovec							
Cestica							
Greda							
Jalžabet							
Lepoglava							
Semovec							
Varazdin							
Varazdinske Toplice							
Ludbreg							
TOTAL:	454,321	166,911	6,611	429,739	3,271	130,826	1,181,797

\*Cost of incineration (including construction, operation, maintenance and depreciation) = 65 €/tDM

\*\*Cost of ash disposal = 40 €/t

**Table 6** The total cost of export and disposal of sludge outside the state

WWTP	The cost of solar drying	Payment to a legal entity*	Total cost of export of dried sludge with 75% DM	Total cost of export of dewatered sludge with 33% DM	Total cost of export of dewatered sludge with 22% DM
	€/year	€/t	€/year	€/year	€/year
Cakovec	83,306	105	313,838	523,936	785,905
Donja Dubrava	32,572	105	68,197	80,967	121,450
Donji Kraljevec	18,204	105	42,867	56,054	84,081
Mursko Središće	24,931	105	57,816	74,739	112,108
Novo Selo na Dravi	8,074	105	21,777	31,141	46,712
Podbrest	16,149	105	43,553	62,282	93,423
Podturen	34,631	105	82,862	109,617	164,425
Ivanec	27,810	105	60,164	73,530	110,296
Novi Marof	15,122	105	35,576	46,487	69,731
Veliki Bukovec	6,096	105	13,188	16,119	24,178
Cestica	8,971	105	20,236	25,604	38,406
Greda	10,219	105	24,365	32,150	48,225
Jalžabet	4,942	105	13,541	19,544	29,316
Lepoglava	18,034	105	36,926	42,937	64,406
Semovec	3,028	105	9,205	14,038	21,058
Varazdin	115,954	105	472,025	809,251	1,213,877
Varazdinske Toplice	9,544	105	24,405	33,776	50,663
Ludbreg	16,734	105	39,370	51,445	77,168
<b>TOTAL:</b>	<b>312,263</b>		<b>1,379,913</b>	<b>2,103,618</b>	<b>3,155,427</b>

\* that transports and disposes of sludge outside the state

The solution that envisaged sewage sludge export outside the state assumes that a certain legal entity (company) will take over dried sludge (with around 75% DM) from the planned two locations of the sludge solar sludge plants and transport it over the border to Hungary where it will be disposed. In this variant, the cost of sludge solar drying and the cost of payment to a legal entity, which includes the cost of transportation and disposal of sludge outside the state, are included in total costs (Tab. 6). Given that the transportation represents the most significant component of the final price, solutions with the export of dehydrated sludge that excludes sludge solar drying (sludge with 22% and 33% DM) are not economically acceptable, since significantly larger total quantities of sludge would require transportation over significant distances. This would not only inevitably result in unreasonably high costs but would also have a negative impact on the environment (increased emissions from transport, etc.), ultimately resulting in the reduced overall sustainability of such a solution. It is noted here that the final method of disposal in the country to which the sludge is exported (in this case Hungary) is left to the choice of the legal entity (company) that took over the sludge and charged an adequate fee included in the presented analysis (assumed with the amount of 105 €/t as shown in Tab. 6). However, given that in this particular case receiving country is Hungary and taking into account the currently prevailing method of sludge disposal, it is to be expected that this sludge, in a certain way, would ultimately be disposed of in agriculture.

Based on the analyzes carried out for the described four variants (Fig. 2) in the area of Medimurje and Varazdin County, it is evident that sludge incineration in a regional mono-incinerator represents economically the most advantageous solution with the total cost estimated of €1.18 million/year. In the second place, slightly more expensive, is the variant with reed beds in the area of Medimurje County and composting of sludge in the area of Varazdin County, 7.81% more expensive than the variant with sludge

incineration. Although the variant with disposal of sludge in agriculture turns out to be economically the most unfavorable (47.97% more expensive than the variant with incineration), with the adoption of more rational legislation, i.e. by reducing the costs of sampling and analysis of sludge and soil, its better economic profitability could be expected. Export of sludge outside Croatia, although a more cost-effective variant than the use of processed sludge on the agricultural land (16.76% more expensive than the variant with sludge incineration), does not represent an acceptable solution. It is justified to use it only as a temporary solution until the establishment of an appropriate sludge management system in the region in question. Considering that all the presented results and rankings of individual variants are based on the assumed unit prices of individual processes, a kind of sensitivity analysis was carried out below.

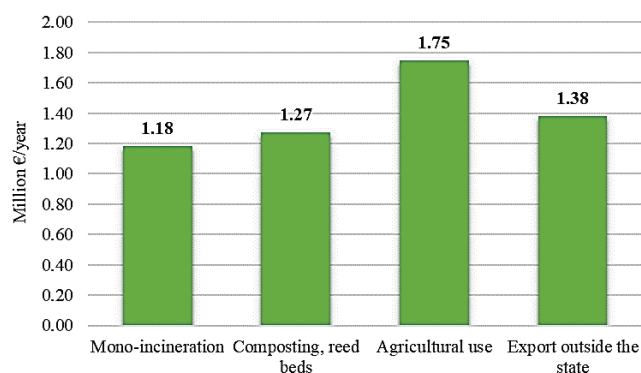


**Figure 2** Total costs of sludge disposal according to the variants considered in Medimurje and Varazdin counties

### 3 RISK ANALYSIS

Given that costs in sludge disposal analysis are variable, and of stochastic character, it is necessary to carry out additional risk analysis that determines dependence of the

final results on changes in assumed unit prices. Hereby, the ranges of possible total costs for each of analysed variants of sludge disposal were defined (Tab. 7).

Below are the results of the economic risk analysis, giving an indication of the possible ranges of total costs of the considered scenarios relation to the assumed fixed and variable inputs (unit costs). In the concrete example, the unit costs of the following parameters were varied: sludge solar drying total cost, the cost of sampling and analysis of sludge and soil (when it is used in agriculture), premium for farmers cost, total incineration costs, ash disposal costs, total cost of sludge export outside the country, total costs of reed beds and total composting costs were selected as stochastic parameters.

**Table 7** Ranges of unit prices of assumed variable input parameters

Parameter	Minimum value	The most probable (expected) value	Maximum value
The cost of solar drying	40/45 €/t DS*	45/50 €/t DS*	50/55 €/t DS*
Sampling and analysis of sludge and soil when sludge is used in agriculture cost	50 €/t DS	90 €/t DS	110 €/t DS
Premium for farmers	0 €/t	10 €/t	15 €/t
Transportation of dried sludge costs (when used in agriculture)	10 €/t	13 €/t	20 €/t
Incineration cost	60 €/t DS	65 €/t DS	130 €/t DS
Ash disposal cost	30 €/t	40 €/t	50 €/t
Sludge export and disposal outside the country – total cost	85 €/t	105 €/t	125 €/t
Reed beds cost	85 €/t DS	90 €/t DS	105 €/t DS
Composting cost	100 €/t DS	115 €/t DS	125 €/t DS

\* The cost of construction, operation and maintenance of a plant for solar drying of sludge - estimated regarding the capacity of the plant next to WWTP Varazdin (lower unit value) and WWTP Cakovec (higher unit value)

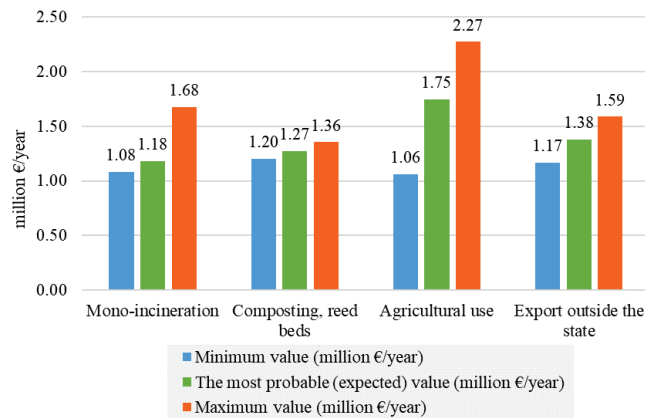


**Figure 3** Total costs of sludge disposal according to the variants considered in Medimurje and Varazdin counties

Tab. 7 shows the analyzed ranges of variable parameters considered through risk analysis. In the same way, it is possible to include other and additional parameters through risk analysis, e.g. the composition of the sludge generated, the capacities of selected WWTP, etc. The following values are defined for all the selected stochastic inputs: minimum, maximum and most likely value. Specific values were determined on the basis of collected literature data and actual

data characteristic of the analyzed geographical area. Fig. 3 shows the expected (possible) ranges of total costs for each of the four analyzed variants of sludge disposal.



**Figure 4** Constructed reed beds within WWTP Cakovec



**Figure 5** Constructed composting plant within WWTP Varazdin

Regarding the presented results of the performed risk analysis, the alternative where sludge is being composted in Varazdin County and sludge reed beds are used in Cakovec County proved to be the most acceptable. This solution is also the one that was ultimately adopted in practice (Fig. 4 and Fig. 5). At the same time solution with agricultural use of sludge shows the largest range of possible expected costs,

and thus risks. However, with the reduction of specific sampling and analysis costs when sludge is used in agriculture, a significant improvement in the profitability of this solution is to be expected. Incineration of sludge in central mono-incinerator located by the WWTP Varazdin, although the most favourable if only the most probable (expected) value is observed, shows somewhat larger deviations in the positive direction (possible increase of the total cost), which is why this variant is ultimately ranked behind the selected solution with composting and sludge reed beds.

However, it is necessary to emphasize that all analyses and evaluation of individual options refer exclusively to economic criteria. In reality, it is necessary to include other criteria, primarily environmental impacts, which in such cases are most often quantified using life cycle analysis (LCA) and models based on them [10]. With the eventual inclusion of additional criteria, such as sociological ones, the analysis can be extended by carrying out a multi-criteria analysis. Also, the sensitivity analysis can be expanded to additional parameters by varying the expected amount of sludge generated at each WWTP or its basic characteristics (such as moisture content) etc.

#### 4 CONCLUSION

Different sewage sludge disposal routes in the area of northern Croatia (Varazdin and Medimurje County) were analysed regarding technical and financial considerations. Four variants (solutions of sludge disposal) were considered: sludge incineration in central mono-incinerator, use of sewage sludge in agriculture, combination of reed beds and composting in two regional centres and export of the sludge outside the state.

The total capacity of all WWTPs (agglomerations) considered is 337.756 PE, i.e. 150.723 PE in the area of Medimurje County and 187.033 PE in the area of Varazdin County. Results show that the economically most favourable is to build 2 plants for sludge solar drying: by the WWTP Cakovec - central plant for Medimurje County, and by the WWTP Varazdin - central plant Varazdin County. Based on the analysis carried out, it is evident that sludge incineration in a regional mono-incinerator represents the economically most advantageous solution, at the total cost of €1.18 million/year. In second place is the variant with reed beds in the area of Medimurje County and composting of sludge in the area of Varazdin County, 7.81% more expensive than the variant with sludge incineration.

Even though the variant with sludge disposal in agriculture turned out to be the most economically unfavourable (as much as 47.97% more expensive than the variant with incineration), with the adoption of more rational legislation, i.e. by lowering the costs of sampling and analysis of sludge and soil, better economic profitability can be expected. Export of sludge outside of Croatia, does not represent an acceptable solution, and could be justified only as a temporary solution until the establishment of an appropriate sewage sludge management system in the region. Based on the results of the economic risk analysis, a solution with combination of reed beds in Medimurje County and composting in Varazdin County turned out to be the most

favourable regarding reliability of the analysis made and the obtained estimates of the total costs. Also, this is the solution that for the most part corresponds to the solution adopted in practice.

#### Acknowledgements

This work has been fully supported by Croatian Science Foundation under the project "IP2019-04-1169 - Use of treated oily wastewater and sewage sludge in brick industry - production of innovative brick products in the scope of circular economy".

#### 5 REFERENCES

- [1] Jamshidi, A., Mehrdadi, N., & Jamshidi, M. (2011). Application of sewage dry sludge as fine aggregate in concrete. *J. Environ. Stud.*, 37(59).
- [2] Vouk, D., Serdar, M., Nakic, D., & Anic-Vucinic, A. (2016). Use of sludge generated at WWTP in the production of cement mortar and concrete. *Civil Engineer.*, 68(3), 199-210.
- [3] Hrvatske vode, Plan upravljanja vodnim područjima 2016.-2021. NN 66/16. (in Croatian)
- [4] Fytli, D. & Zabaniotou, A. (2008) Utilization of sewage sludge in EU application of old and new methods – A review. *Renew. Sust. Energ. Rev.*, 12(1), 116-140. <https://doi.org/10.1016/j.rser.2006.05.014>
- [5] Eurostat. (2022) Sewage sludge production and disposal. [https://ec.europa.eu/eurostat/databrowser/view/ENV\\_WW\\_SPD\\_custom\\_863447/bookmark/table?lang=en&bookmarkId=5758a478-af17-400c-9e31-2c73b4cc6903](https://ec.europa.eu/eurostat/databrowser/view/ENV_WW_SPD_custom_863447/bookmark/table?lang=en&bookmarkId=5758a478-af17-400c-9e31-2c73b4cc6903) (Accessed 17 January 2023). (in Croatian)
- [6] Tarpani R.R.Z., Alfonsin C., Hospido A., Azapagic A, (2020), Life cycle environmental impacts of sewage sludge treatment methods for resource recovery considering ecotoxicity of heavy metals and pharmaceutical and personal care products. *Journal of Environmental Management*, 260, 109643, <https://doi.org/10.1016/j.jenvman.2019.109643>
- [7] EC Directive, (1991), Council Directive 91/271/EEC of 21 May 1991 concerning urban waste-water treatment, NoL135/40, *Official Journal of the European Communities*, 30.5.91. <https://eur-lex.europa.eu/legal-content/EN/TXT/?uri=CELEX%3A31991L0271>. (Accessed 17 January 2023).
- [8] Vouk, D., Nakic, D., Bubalo, A., & Bolanca, T. (2022) Environmental aspects in selecting optimum variant of sewage sludge management. *Environm. Eng. and Manag. J.*, 21(3), 443-456. <https://doi.org/10.30638/eemj.2022.042>
- [9] Akcijski plan za korištenje mulja iz uređaja za pročišćavanje otpadnih voda na pogodnim površinama, HIDROPROJEKT-ING Zagreb, Hidroing Osijek, Građevinski fakultet Sveučilišta u Zagrebu, Institut IGH, 2020. (in Croatian)
- [10] Vouk, D., Nakic, D., & Anic-Vucinic, A. (2017) Possibilities of sewage sludge disposal - Split-Dalmatia County. *Hrvatska vodoprivreda*, 219(2), 12-15.

#### Authors' contacts:

**Domagoj Nakić**, PhD, Assistant Professor  
(Corresponding author)  
University of Zagreb, Faculty of Civil Engineering,  
Kačićeva 26, 10000 Zagreb, Croatia  
University North, Civil Engineering Department,  
104. brigade 1, 42000 Varazdin, Croatia  
Tel. +385911839023  
E-mail: domagoj.nakic@grad.unizg.hr

**Ines Belalov Dovečer**, mag. ing. aedif.

Colas Hrvatska d.d.

Međimurska 26, 42000 Varaždin

Tel. +385995381550

E-mail: ines.belalovdovecer@colas.hr

**Dražen Vouk**, PhD, Associate Professor

University of Zagreb, Faculty of Civil Engineering,

Kačićeva 26, 10000 Zagreb, Croatia

Tel. +38514639213

E-mail: dvouk@grad.hr

**Bojan Đurin**, PhD, Associate Professor

University North, Civil Engineering Department,

104. brigade 1, 42000 Varaždin, Croatia

Tel. +385989749716

E-mail: bdjurin@unin.hr



## IMPORTANT DATES

**September 5, 2023**

Full Paper/Abstract submission deadline

**October 5, 2023**

Acceptance/Rejection Notification

**February 25, 2024**

Listener registration Deadline

## PROCEEDINGS

The accepted papers will be collected in the conference proceedings, which will be indexed by EI Compendex and Scopus.

## SUBMISSION

1. Language: English Only
2. For presentation only, only abstract is needed
3. For presentation and publication, full paper is needed
4. You can also send your paper directly to [aeic\\_conf@academic.net](mailto:aeic_conf@academic.net)
5. The manuscript should be edited strictly in accordance with the conference template.

Template download:

<http://aeic.net/files/Template.docx>

## CONTACT

Ali Yan

Email: [aeic\\_conf@academic.net](mailto:aeic_conf@academic.net)



Contact us on wechat  
AEIC2024+Paper ID

## SPONSOR



北京中控机智能科技研究院  
Beijing Institute of Control Robotics and Intelligent Technology

2024 International Conference on Automation Engineering and Intelligent Control (AEIC 2024), will be held in Milan, Italy on February 27-29, 2024.

AEIC aims to bring together top researchers around the world to exchange research results and address open issues in all aspects of automation engineering and intelligent control. Its mission is to foster automation engineering and intelligent control among researchers and practitioners working in a wide variety of scientific areas with a common interest in improving automation engineering and intelligent control related techniques.

## Conference Scope

Papers are solicited on all aspects of Automation Engineering and Intelligent Control, from the points of view of both theory and practice. This includes, but is not limited to, the following topics:

- Autonomous robots
- Behavioral decision making
- Classification
- Command and control systems
- Control system applications
- Data analysis, prediction and model identification
- Data fusion and mining
- Decision support systems
- Distributed decision making
- Dynamic systems modeling
- Fault diagnosis
- High speed communication
- Human factors in system design
- Hybrid systems
- Hyper network communication
- Image processing
- Image understanding
- Intelligent control systems
- Intelligent databases & information retrieval
- Intelligent information systems
- Parallel computing applications in identification & control
- Pattern recognition
- Prediction and time series analysis
- Qualitative and approximate-reasoning modeling
- Risk management
- Robot dynamics and control
- Robotics and automation
- Robotics and automation
- Applications
- Artificial intelligence
- Bayesian controllers
- Bayesian probability
- Characteristics of intelligent control systems
- Computing approaches
- Design concerns
- Evolutionary computation
- Expert control
- Foundations of intelligent control
- Fuzzy control
- Fuzzy control design
- Genetic algorithms
- Genetic operators
- Intelligence and intelligent control
- Intelligent and autonomous control
- Intelligent control
- Intelligent control systems
- Intelligent control techniques
- Machine learning
- Multilayer perceptrons
- Neural network controllers
- Neural networks
- Planning systems for control
- The population of individuals
- Signal processing
- System identification
- Transportation systems

## Organizing Committee

Conference Chairs

Jiansheng Dai, Southern University of Science and Technology, China (FREng, IEEE Fellow, ASME Fellow, RSA Fellow, IMechE Fellow)

Yongsheng Ma, Southern University of Science and Technology, China

Conference Co-Chairs

Dan Zhang, York University, Canada, (CAE Fellow, ASME Fellow, EIC Fellow, CSME Fellow)

Ian Walker, Clemson University, USA (IEEE Fellow, AIAA Senior Member)

Program Committee Chairs

Belkacem OULD BOUAMAMA, Ecole Polytechnique de Lille, France

Andras Horvath, Peter Pazmany Catholic University, Hungary

Zhongxue Gan, Fudan University, China

Xuanhao Duan, Xidian University, China

Lili Zhang, Beijing Institute of Control Robotics and Intelligent Technology, China

Program Committee Co-Chairs

David Branson, University of Nottingham, UK

Zhongbin Wang, China University of Mining and Technology, China

Wilson Wang, Lakehead University, Canada

Conference Website: <http://aeic.net/>

# Article Title Only in English (Style: Arial Narrow, Bold, 14pt)

Ivan Horvat, Thomas Johnson, Marko Marić (Style: Arial Narrow, Normal, 10pt)

**Abstract:** Article abstract contains maximum of 150 words and is written in the language of the article. The abstract should reflect the content of the article as precisely as possible. TECHNICAL JOURNAL is a trade journal that publishes scientific and professional papers from the domain(s) of mechanical engineering, electrical engineering, civil engineering, multimedia, logistics, etc., and their boundary areas. This document must be used as the template for writing articles so that all the articles have the same layout. (Style: Arial Narrow, 8pt)

**Keywords:** keywords in alphabetical order (5-6 key words). Keywords are generally taken from the article title and/or from the abstract. (Style: Arial Narrow, 8pt)

## 1 INTRODUCTION (Article Design)

(Style: Arial Narrow, Bold, 10pt)

(Tab 6 mm) The article is written in Latin script and Greek symbols can be used for labelling. The length of the article is limited to eight pages of international paper size of Letter (in accordance with the template with all the tables and figures included). When formatting the text the syllabification option is not to be used.

### 1.1 Subtitle 1 (Writing Instructions)

(Style: Arial Narrow, 10pt, Bold, Align Left)

The document format is Letter with margins in accordance with the template. A two column layout is used with the column spacing of 10 mm. The running text is written in Times New Roman with single line spacing, font size 10 pt, alignment justified.

Article title must clearly reflect the issues covered by the article (it should not contain more than 15 words).

Body of the text is divided into chapters and the chapters are divided into subchapters, if needed. Chapters are numbered with Arabic numerals (followed by a period). Subchapters, as a part of a chapter, are marked with two Arabic numerals i.e. 1.1, 1.2, 1.3, etc. Subchapters can be divided into even smaller units that are marked with three Arabic numerals i.e. 1.1.1, 1.1.2, etc. Further divisions are not to be made.

Titles of chapters are written in capital letters (uppercase) and are aligned in the centre. The titles of subchapters (and smaller units) are written in small letters (lowercase) and are aligned left. If the text in the title of the subchapter is longer than one line, no hanging indents.

Typographical symbols (bullets), which are being used for marking an item in a list or for enumeration, are placed at a beginning of a line. There is a spacing of 10pt following the last item:

- Item 1
- Item 2
- Item 3

The same rule is valid when items are numbered in a list:

- 1) Item 1
- 2) Item 2
- 3) Item 3

## 1.2 Formatting of Pictures, Tables and Equations

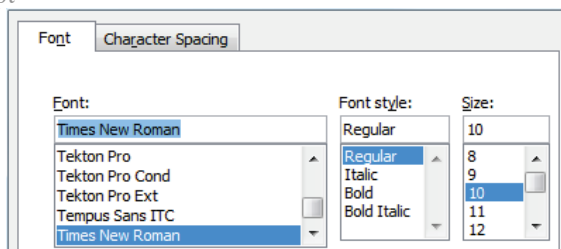
(Style: Arial Narrow, 10pt, Bold, Align Left)

Figures (drawings, diagrams, photographs) that are part of the content are embedded into the article and aligned in the centre. In order for the figure to always be in the same position in relation to the text, the following settings should be defined when importing it: text wrapping / in line with text.

Pictures must be formatted for graphic reproduction with minimal resolution of 300 dpi. Pictures downloaded from the internet in ratio 1:1 are not suitable for print reproduction because of unsatisfying quality.

Figure 1 Text under the figure [1]

(Style: Arial Narrow, 8pt, Align Centre)



The journal is printed in black ink and the figures have to be prepared accordingly so that bright tones are printed in a satisfactory manner and are readable. Figures are to be in colour for the purpose of digital format publishing. Figures in the article are numbered with Arabic numerals (followed by a period).

Text and other data in tables are formatted - Times New Roman, 8pt, Normal, Align Center.

When describing figures and tables, physical units and their factors are written in italics with Latin or Greek letters,

while the measuring values and numbers are written upright.

10pt

**Table 1** Table title aligned centre  
(Style: Arial Narrow, 8pt, Align Centre)

	1	2	3	4	5	6
ABC	ab	ab	ab	ab	ab	ab
DEF	cd	cd	cd	cd	cd	cd
GHI	ef	ef	ef	ef	ef	ef

10 pt

Equations in the text are numbered with Arabic numerals inside the round brackets on the right side of the text. Inside the text they are referred to with equation number inside the round brackets i.e. "... from Eq. (5) follows ...." (Create equations with MathType Equation Editor - some examples are given below).

10pt

$$F_{\text{avg}}(t, t_0) = \frac{1}{t} \int_{t_0}^{t_0+t} F[q(\tau), p(\tau)] d\tau, \quad (1)$$

$$\cos \alpha + \cos \beta = 2 \cos \frac{\alpha + \beta}{2} \cdot \cos \frac{\alpha - \beta}{2}, \quad (2)$$

$$(AB)^T = B^T A^T. \quad (3)$$

10pt

Variables that are used in equations and also in the text or tables of the article are formatted as *italics* in the same font size as the text.

10pt

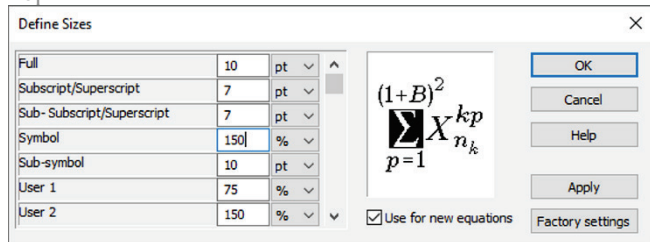


**Figure 2** The texts under figures  
(Style: Arial Narrow, 8pt, Align Centre)

10pt

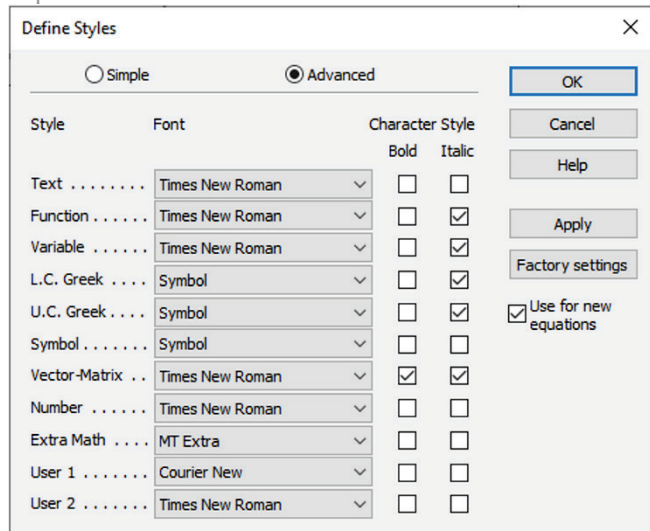


**Figure 3** The texts under figures  
(Style: Arial Narrow, 8pt, Align Centre)

Figures and tables that are a part of the article have to be mentioned inside the text and thus connected to the content i.e. "... as shown in Fig. 1..." or "data from Tab. 1..." and similar.

10pt

## 2 PRELIMINARY ANNOTATION

10pt

Article that is offered for publication cannot be published beforehand, be it in the same or similar form, and it cannot be offered at the same time to a different journal. Author or authors are solely responsible for the content of the article and the authenticity of information and statements written in the article.

Articles that are accepted for publishing are classified into four categories: original scientific papers, preliminary communications, subject reviews and professional papers.

**Original scientific papers** are articles that according to the reviewer and the editorial board contain original theoretical or practical results of research. These articles need to be written in such a way that based on the information given, the experiment can be repeated and the results described can be achieved together with the author's observations, theoretical statements or measurements.

**Preliminary communication** contains one or more pieces of new scientific information, but without details that allow recollection as in original scientific papers. Preliminary communication can give results of an experimental research, results of a shorter research or research in progress that is deemed useful for publishing.

**Subject review** contains a complete depiction of conditions and tendencies of a specific domain of theory, technology or application. Articles in this category have an overview character with a critical review and evaluation. Cited literature must be complete enough to allow a good insight and comprehension of the depicted domain.

**Professional paper** can contain a description of an original solution to a device, assembly or instrument, depiction of important practical solutions, and similar. The article need not be related to the original research, but it should contain a contribution to an application of known scientific results and their adaptation to practical needs, so it presents a contribution to spreading knowledge, etc.

Outside the mentioned categorization, the Editorial board of the journal will publish articles of interesting content in a special column. These articles provide descriptions of practical implementation and solutions from the area of production, experiences from device application, and similar.

10pt

## 3 WRITING AN ARTICLE

10pt

Article is written in the English language and the terminology and the measurement system should be adjusted to legal regulations, standards and the International System of Units (SI) (Quantities and Units: ISO 80 000 - from Part 1 to Part 14). The article should be written in third person.

**Introduction** contains the depiction of the problem and an account of important results that come from the articles that are listed in the cited literature.

**Main section of the article** can be divided into several parts or chapters. Mathematical statements that obstruct the reading of the article should be avoided. Mathematical statements that cannot be avoided can be written as one or more addendums, when needed. It is recommended to use an example when an experiment procedure, the use of the work in a concrete situation or an algorithm of the suggested method must be illustrated. In general, an analysis should be experimentally confirmed.

**Conclusion** is a part of the article where the results are being given and efficiency of the procedure used is emphasized. Possible procedure and domain constraints where the obtained results can be applied should be emphasized.

10pt

#### 4 RECAPITULATION ANNOTATION

10pt

In order for the articles to be formatted in the same manner as in this template, this document is recommended for use when writing the article. Finished articles written in MS Word for Windows and formatted according to this template must be submitted using our The Paper Submission Tool (PST) (<https://tehnickiglasnik.unin.hr/authors.php>) or eventually sent to the Editorial board of the Technical Journal to the following e-mail address: [tehnickiglasnik@unin.hr](mailto:tehnickiglasnik@unin.hr)

The editorial board reserves the right to minor redaction corrections of the article within the framework of prepress procedures. Articles that in any way do not follow these authors' instructions will be returned to the author by the editorial board. Should any questions arise, the editorial board contacts only the first author and accepts only the reflections given by the first author.

10pt

#### 5 REFERENCES (According to APA)

10pt

The literature is cited in the order it is used in the article. No more than 35 references are recommended. Individual references from the listed literature inside the text are addressed with the corresponding number inside square brackets i.e. "... in [7] is shown ...". If the literature references are web links, the hyperlink is to be removed as shown with the reference number 8. Also, the hyperlinks from the e-mail addresses of the authors are to be removed. In the literature list, each unit is marked with a number and listed according to the following examples (omit the subtitles over the references – they are here only to show possible types of references):

9pt

- [1] See <http://www.bibme.org/citation-guide/apa/>
- [2] See [http://sites.umuc.edu/library/libhow/apa\\_examples.cfm](http://sites.umuc.edu/library/libhow/apa_examples.cfm)
- [3] (Style: Times New Roman, 9pt, according to APA)
- [4] Amidzic, O., Riehle, H. J., & Elbert, T. (2006). Toward a psychophysiology of expertise: Focal magnetic gamma bursts as a signature of memory chunks and the aptitude of chess players. *Journal of Psychophysiology*, 20(4), 253-258.

<https://doi.org/10.1027/0269-8803.20.4.253>

- [5] Reitzes, D. C. & Mutran, E. J. (2004). The transition to retirement: Stages and factors that influence retirement adjustment. *International Journal of Aging and Human Development*, 59(1), 63-84. Retrieved from <http://www.baywood.com/journals/PreviewJournals.asp?Id=0091-4150>
- [6] Jans, N. (1993). *The last light breaking: Life among Alaska's Inupiat Eskimos*. Anchorage, AK: Alaska Northwest Books.
- [7] Miller, J. & Smith, T. (Eds.). (1996). *Cape Cod stories: Tales from Cape Cod, Nantucket, and Martha's Vineyard*. San Francisco, CA: Chronicle Books.
- [8] Chaffe-Stengel, P. & Stengel, D. (2012). *Working with sample data: Exploration and inference*. <https://doi.org/10.4128/9781606492147>
- [9] Freitas, N. (2015, January 6). People around the world are voluntarily submitting to China's Great Firewall. Why? Retrieved from [http://www.slate.com/blogs/future\\_tense/2015/01/06/tencent\\_s\\_wechat\\_worldwide\\_internet\\_users\\_are\\_voluntarily\\_submitting\\_to.html](http://www.slate.com/blogs/future_tense/2015/01/06/tencent_s_wechat_worldwide_internet_users_are_voluntarily_submitting_to.html)  
(Style: Times New Roman, 9pt, according to APA)

10pt

10pt

#### Authors' contacts:

8pt

**Full Name**, title  
Institution, company  
Address  
Tel./Fax, e-mail

8pt

**Full Name**, title  
Institution, company  
Address  
Tel./Fax, e-mail

**Note:** Gray text should be removed in the final version of the article because it is for guidance only.

# DESIGN2024

18<sup>TH</sup> INTERNATIONAL DESIGN CONFERENCE  
20–23 MAY 2024, CAVTAT – DUBROVNIK – CROATIA

## INVITATION

*By tradition, DESIGN Conference is a forum for discussion and further development of design knowledge from cognition and philosophy to methods and tools, from research theory to practice.*

The transition from known and comfortable to unknown and challenging is ubiquitous. It is challenging every aspect of our being. How can design research and practice respond to changes, influence wellness, ensure sustainable development, reimagine the future, rethink product design and development in new and emerging contexts?

How to improve design methodologies, tools, projects, and processes? How to develop products and services to make the world a healthier place? Which competencies, information, and communication technologies are needed? What is the impact on everyday design work? Which social and legal issues should be considered? How will we teach future designers, communicate ideas and share knowledge?

Applied, theoretical, and results-oriented papers from academia and industry,

based on thorough analysis or argumentation, will be considered for the conference programme. The submitted papers should fit into one of the proposed conference topics. It is expected that these specific topics are extensive and nonexhaustive.

A list of example keywords is added to illustrate the core topics. It is required explicitly from all contributors to show how they contribute to the overall research within these areas. A detailed description of topics and instructions for online submission is available at [www.designconference.org](http://www.designconference.org).

Programme chairs welcome the high-quality submissions covering substantial, original, and previously unpublished research.

Rigour academic research should provide designers with the next generation of methods and tools appropriate to the demands.

## PROGRAMME

*The DESIGN Conference provides an interactive environment where participants proactively create opportunities to share design knowledge and new cross-disciplinary research that leads to innovation.*

### PLENARY SESSIONS

The new ideas and visions will be presented by the keynote speakers.

### TOPIC-ORIENTED SESSIONS

Will host papers selected around common research questions in order to foster discussion.

### WORKSHOPS

DESIGN 2024 workshops will promote integration of different views, approaches and methods. Workshop coordinators could invite selected presentations and demonstrations in order to stimulate the debate as well as to propose any format of delivery that inspires interaction. The workshops will be organised on the 20th of May.

### PHD STUDENTS' FORUM

The forum will be a unique opportunity for younger researchers and PhD students to discuss their research questions and ideas with experienced researchers, practitioners and R&D managers in order to facilitate their research efforts.

### THE DESIGN DEBATE

The purpose of the design debate is to investigate in a forensic manner some key topics that affect the engineering design research community. Two opponents and the debate moderator will be distinguished key players in the community presenting evidence for or against a particular topic.

## REVIEWING POLICY

The papers will be accepted on the double-blind review basis made by the members of the Scientific Advisory Board.

The review criteria will be the novelty and level of contribution, validity of conclusions, industrial or application perspective and formal qualities of the contribution.

DESIGN Conference papers are published online with open access. All papers are indexed in SCOPUS and WOS - CPCI and referenced in CrossRef with DOI identifier.

# DESIGN 2024 TOPICS

## DESIGN THEORY AND RESEARCH METHODS

Multidisciplinary research approaches  
Design theories and models  
Experimental design research  
Design typology  
New paths in design research

## DESIGN ORGANISATION, COLLABORATION AND MANAGEMENT

Organisational processes for Industry 4.0  
Product development models and agile management  
Market and business implications  
Co-design and collaboration  
Design teams and communication  
Open/social innovation

## DESIGN INFORMATION AND KNOWLEDGE

Design representations of information and knowledge  
Decision-making rationale and support  
Knowledge-intensive design  
Knowledge-based engineering  
Emerging IT technologies

## DESIGN METHODS AND TOOLS

Product families and modularisation  
Prototyping methods and tools  
CAX/PDM/PLM  
Requirements and change management  
Usage and integration of supportive technologies

## HUMAN BEHAVIOUR AND DESIGN CREATIVITY

Human factors in design  
Designer's attitudes and skills  
Design thinking, cognition and problem-solving  
Cognitive processes in design creativity  
Supporting and assessment of design creativity  
Bioinspired design

## DESIGN FOR SUSTAINABILITY

Sustainability awareness  
Design for social equity and cohesion  
Design for the circular economy  
Technology and sustainable society  
Product-service systems  
Sustainable transition

## DESIGN FOR HEALTHCARE

Healthcare ecosystems  
Healthcare design  
Healthcare services  
Use of advanced technologies in healthcare  
Life sciences and design

## DESIGN FOR ADDITIVE MANUFACTURING

Design approaches for additive manufacturing  
Design digitalisation approaches  
Design optimisation frameworks  
Generative design and topological optimisation  
Architecting materials for additive manufacturing

## DESIGN FOR EXCELLENCE

Design for product improvement and quality  
Design for manufacturing and assembly  
Design for packaging and ergonomics  
Design for robustness and reliability  
Design for maintainability

## ARTIFICIAL INTELLIGENCE AND DATA-DRIVEN DESIGN

Artificial intelligence in product development  
Data-driven design process  
Knowledge discovery and data mining in design  
AI for smart product-service systems  
Digital twins  
Autonomous vehicles and electromobility

## INDUSTRIAL DESIGN

User-centred design  
Aesthetics and visual impressions  
Product semantics and perceptions  
Visual and haptic interactions  
User experience  
Social relationships and emotional design

## SYSTEMS ENGINEERING AND DESIGN

Architecting complex engineering systems  
Simulation within complex systems  
Model-based systems engineering (MBSE)  
Complex cyber-physical systems design  
Approaches to socio-technical systems design

## DESIGN EDUCATION

Competency and skills development  
Digital learning and ICT in education  
Project-based learning  
Adopting different teaching and learning environments  
Lifelong and organisational learning

## ENGINEERING DESIGN PRACTICE

Geometrical modelling and advanced CAX use cases  
Advanced visualisation and virtualisation  
Case studies of design methods application  
Best design practices from industry

## IMPORTANT DATES

**1** Full paper submission deadline  
**15 November 2023**

**2** Final acceptance of papers  
**31 January 2024**

**3** Publish-ready papers  
**23 February 2024**

**4** Final Conference programme  
**April 2024**

**5** DESIGN 2024 Conference  
**20-23 May 2024**

## PROGRAMME CHAIRS

**P. John Clarkson**  
*University of Cambridge, United Kingdom*

**Tim McAloone**  
*Technical University of Denmark, Denmark*

**Julie Stal-Le Cardinal**  
*CentraleSupélec, France*

**Sandro Wartzack**  
*Friedrich-Alexander-Universität  
Erlangen-Nürnberg, Germany*

**Mario Štorga**  
*University of Zagreb, Croatia*

**Stanko Škec**  
*University of Zagreb, Croatia*

## CONFERENCE VENUE

**Hotel Croatia Cavtat**  
Frankopanska ul. 10, 20210 Cavtat, Croatia

## ORGANISING SECRETARIAT

**Faculty of Mechanical Engineering  
and Naval Architecture**  
10000 Zagreb, I. Lučića 5, Croatia

**design2024@fsb.hr**  
**www.designconference.org**

the **Design Society**  
a worldwide community

**cad lab**

**FSB**  
**100**



TEHNIČKI GLASNIK / TECHNICAL JOURNAL – GODIŠTE / VOLUME 17 – BROJ / ISSUE 4

PROSINAC 2023 / DECEMBER 2023 – STRANICA / PAGES 479-635



Sveučilište  
Sjever

SVEUČILIŠTE SJEVER / UNIVERSITY NORTH – CROATIA – EUROPE

ISSN 1846-6168 (PRINT) / ISSN 1848-5588 (ONLINE)

TEHNICKIGLASNIK@UNIN.HR – [HTTP://TEHNICKIGLASNIK.UNIN.HR](http://tehnickiglasnik.unin.hr)